Determination of Ocean Continent Transition Structure, Continent Ocean Boundary Location and Magmatic Type at Rifted Continental Margins

UNIVERSITY OF LIVERPOOL

Thesis Submitted In Accordance With the Requirements of the University Of Liverpool for the Degree of Doctor in Philosophy

By: Leanne Cowie

July 2014

Acknowledgements

I would like to express my deepest gratitude to Professor Nick Kusznir, my supervisor, for his patient guidance, enthusiastic encouragement, his extremely useful critique of this research, and for keeping my progress on schedule.

My grateful thanks to Professor Gianreto Manatschal for his assistance and guidance throughout the more geological aspects of my PhD, and for some memorable time spent in the field.

I wish to thank Alan Roberts and the rest of the team at Badley Geoscience for their helpful advice and useful discussions.

This work would not have been possible without funding from the MM3 consortium, and special thanks to ION-GXT for providing invaluable seismic data.

Special thanks to Michael King for his unwavering support, as well as his grammatical expertise and his knowledge of Microsoft Word during the formatting of this thesis.

I would like to thank Ludovic Jeanniot for being a constant source of entertainment for the last 4 years. Without his 'European charm', my PhD experience would not have been the same.

A huge thank you to friends and colleagues at the University of Liverpool over the last 8 years who have made this time in my life truly unforgettable.

Finally, I would like to thank my parents and family for their support and encouragement throughout my PhD.

Abstract

Determination of Ocean Continent Transition Structure, Continent Ocean Boundary Location and Magmatic Type at Rifted Continental Margins.

Leanne Cowie

Knowledge of ocean continent transition (OCT) structure, continent ocean boundary (COB) location and magmatic type are of critical importance for understanding rifted continental margin formation and evolution, and in evaluating petroleum systems in deep-water frontier oil and gas exploration. A suite of quantitative analytical techniques have been developed in order to determine the structure of the OCT, the location of the COB and magmatic type at rifted continental margins; these techniques include the use of gravity anomaly inversion, residual depth anomaly (RDA) and subsidence analysis. Gravity anomaly inversion, incorporating a lithosphere thermal gravity anomaly correction, has been used to determine Moho depth, crustal basement thickness and continental lithosphere thinning. RDA analysis has been used to investigate OCT bathymetric anomalies with respect to expected oceanic bathymetries, and subsidence analysis has been used to determine the distribution of continental lithosphere thinning. These techniques have been applied to the Iberian, Gulf of Aden, northern Angolan, and south-eastern Brazilian rifted continental margins.

Integrated quantitative analysis results have been validated using ODP well data and magnetic anomalies along the Iberian rifted continental margin. Results identify a clearly defined zone of exhumed mantle on the Iberian profiles, which is also observed in the ODP well data.

In addition to the quantitative analysis techniques, a methodology for the joint inversion of deep long offset seismic data and gravity anomaly data has been developed in order to further constrain the OCT structure and COB location. The joint inversion method solves for coincident seismic and gravity Moho in the time domain and calculates the lateral variations in crustal basement densities and velocities along profile. Integrated quantitative analysis along the northern Angolan profile suggests that exhumed mantle, corresponding to a magma-poor margin, is absent beneath the allochthonous salt and that the thickness of earliest oceanic crust is approximately 7km. Integrated quantitative analysis along the south-eastern Brazilian profile predicts that the earliest oceanic crust is between 7km and 8km thick and that there is no evidence of exhumed mantle as suggested by Zalán et al. (2011).

The results from the integrated quantitative analysis have also been used together with post-breakup subsidence modelling to determine the palaeo-bathymetry of the base Loeme salt along northern Angolan profiles. The proximal autochthonous base salt restores to near sea level, but not the distal allochthonous salt. Our interpretation is that the distal salt formed during the late syn-rift while the crust under it was being actively thinned, resulting in additional tectonic subsidence.

Residual topography, which we attribute to mantle dynamic topography, has been determined using RDA analysis, with corrections for sediment loading and crustal basement thickness variations. Residual topography of -650m is measured along the Iberian Abyssal Plain; +400m in the Gulf of Aden, and +700m along the northern Angolan margin.

Table of Contents

Chapter 1

1. Introduction

1.1. Aims

The principle aims of this PhD thesis are to develop, apply and test methodologies used to determine the ocean continent transition (OCT) structure, continent ocean boundary (COB) location and magmatic type at rifted continental margins. Knowledge and understanding of the OCT structure, COB location and magmatic type are important for an understanding of the processes responsible for continental lithosphere thinning leading to breakup, rifted continental margin formation and evolution, and also for deep water oil and gas exploration. We have applied and tested these methodologies at four different rifted continental margins, locations shown in Figure 1.1(a); offshore Iberia (Figure 1.1(b)), the Gulf of Aden (Figure 1.1(c)), south-eastern Brazil (Figure 1.1(d)) and northern Angola (Figure 1.1(e)). These rifted continental margins provide ideal natural laboratories for studying the tectonic and magmatic processes involved in rifted continental margin formation and evolution. The case study areas vary by magmatic type and OCT structure, which has enabled us to fully test and validate the developed methodologies. While the majority of the work described within this thesis has focussed on the determination of the OCT structure, COB location and magmatic type, an extension of this work has examined the application of these methodologies to further understand subsidence histories at rifted continental margins.

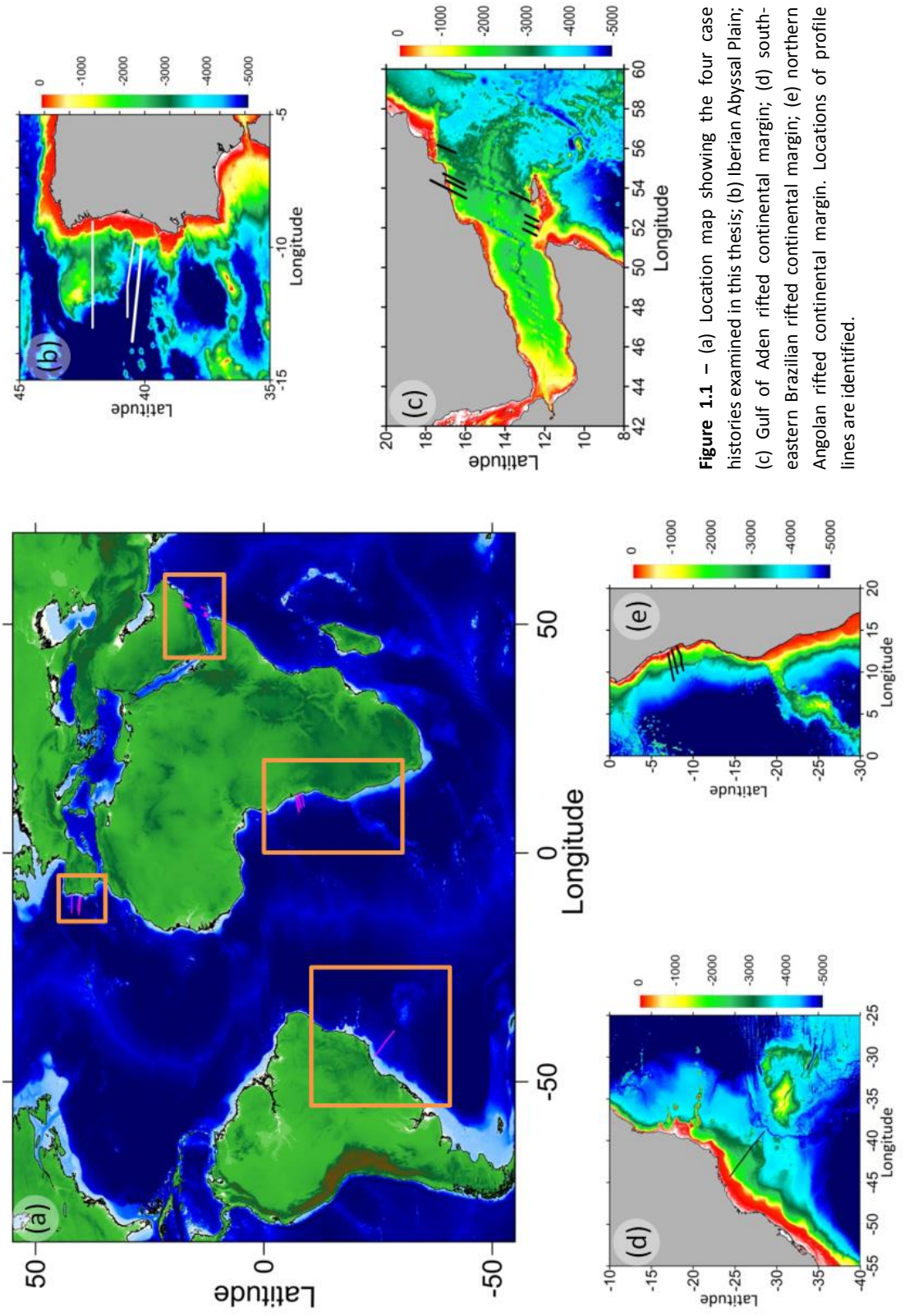

Figure 1.1 – (a) Location map showing the four case histories examined in this thesis; (b) Iberian Abyssal Plain; (c) Gulf of Aden rifted continental margin; (d) south-eastern Brazilian rifted continental margin; (e) northern Angolan rifted continental margin. Locations of profile lines are identified.

At rifted continental margins there is a transition from thick continental crust to thinner oceanic crust; a classical ('normal' magmatic) view of rifted continental margin is shown in Figure 1.2(a). This schematic model shows a rifted continental margin comprising fault controlled continental crustal basement, which has a syn-rift sedimentary cover that pinches out ocean-ward. A 'normal' magmatic rifted continental margin (Figure 1.2(a)) has magmatic addition, which results in oceanic crust of approximately 7km in thickness (White et al., 1992). In addition to 'normal' magmatic rifted continental margins, there are two end members: magma-poor margins (Figure 1.2(b)) and magma-rich margins (Figure 1.2(c)). Magma-poor rifted continental margins are often characterized by a wide OCT, extreme crustal thinning accompanied by normal faulting (Boillot et al., 1980; Manatschal, 2004; Reston, 2009) and anomalously small fractions of magmatism leading to mantle exhumation prior to oceanic spreading (Pérez-Gussinyé, 2012). Magma-rich margins are characterized by thick wedges of volcanic flows (Hinz, 1981), shown on seismic data as seaward dipping reflectors (SDRs), large amounts of syn-rift magmatic extrusives and intrusives (Coffin and Eldholm, 1994), high velocity lower crust seaboard of the continental rifted margin (Franke, 2013), and the crustal thinning may occur over a short distance. Within this thesis we present a methodology for the determination of the magmatic type of a rifted continental margin; that is the volume of magmatic addition, whether the margin is 'normal', magma-poor or magma-rich.

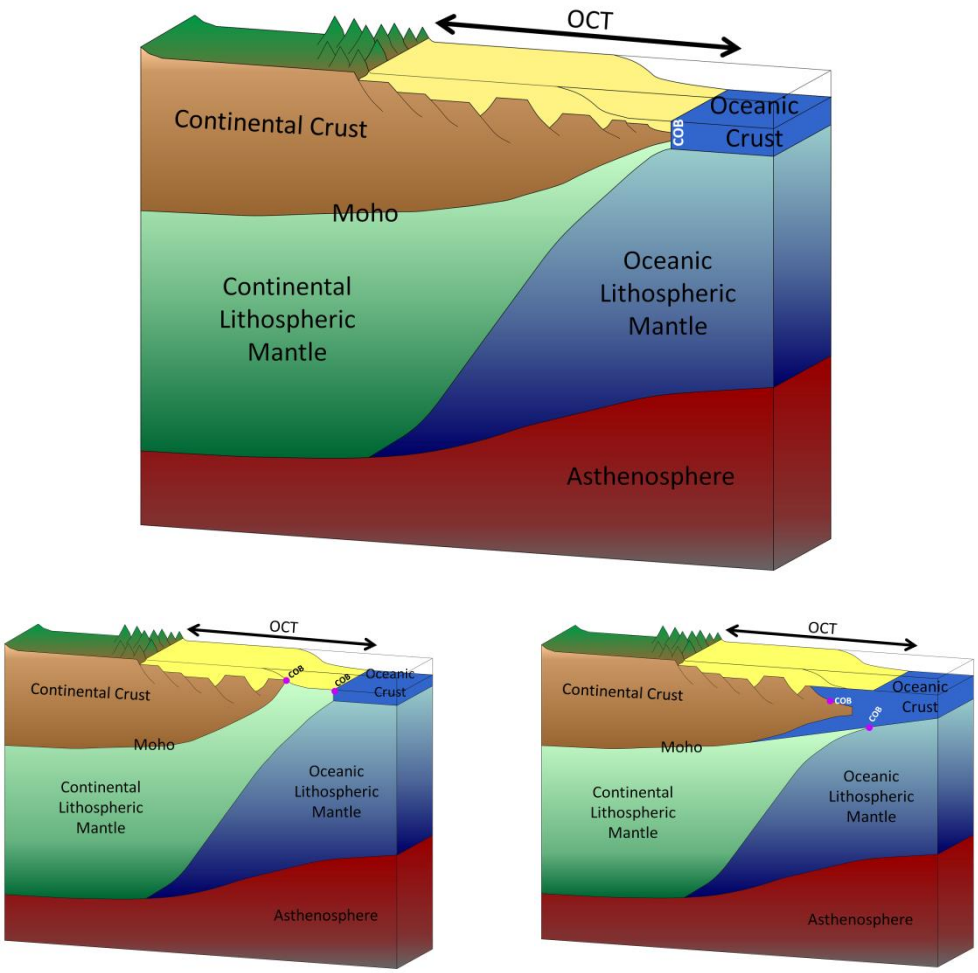

Figure 1.2 – Three schematic models showing continental rifted margin for (a) 'normal' magmatic (b) magma-poor and (c) magma-rich end members. The OCT and COB locations are identified in each model.

Within the literature there are a range of different definitions of the OCT and COB (e.g. Pèron-Pinvidic et al. (2007), Whitmarsh and Miles (1995), Manatschal et al. (2001), Dean et al. (2000), Manatschal et al. (2010) and Discovery 215 Working et al. (1998)). Within this thesis, however, we define the OCT as the region between unequivocal continental crust of 'normal' thickness and unequivocal oceanic crust; the continental lithosphere in this region is highly thinned, with complex tectonics, variable magmatism and possible mantle exhumation. We define the COB as the distal limit of unequivocal continental crust; however, determining the location of the COB is made difficult by the presence of exhumed mantle and complex tectonics.

Another important term used within this thesis is continental breakup age, which within this thesis is associated with the onset of seafloor spreading. Conceptually the term continental breakup may be used to either describe the point at which the continental crust ruptures and starts to separate, or when the divergent plate boundary is localised by the onset of decompression melting and seafloor spreading. Traditionally in classical models of continental breakup, rifting is immediately followed by seafloor spreading, which implies that continental breakup can be identified as a specific spatial and temporal boundary (Peron-Pinvidic et al., 2006). The timing and location of continental breakup is often defined by the first observation of a magnetic anomaly that is generated by magma erupted from the newly formed mid-ocean ridge (Bronner et al., 2011). There are many indicators for determining continental breakup, including magnetic anomalies, the breakup unconformity, the distribution of high-angle faults, and the presence of sedimentary wedges (Peron-Pinvidic et al., 2006). However, depending on the magmatic type of a margin, some (or all) of these indicators may not be reliable for identifying the age and location of breakup.

1.2. OCT Structure, COB Location and Magmatic Type

Detailed knowledge of rifted continental margins, in particular the structure of the OCT, the location of the COB and magmatic type, is a generic problem globally. Determining the distal extent of thinned continental crust outboard of the margin hinge and the structural architecture of the OCT are often hindered by the presence of a thick post-rift sedimentary cover and mobile salt. The existence of exhumed mantle (Boillot et al., 1989; Pickup et al., 1996), hyper-extended continental crust separating unequivocal oceanic and continental crust within the OCT (e.g. Contrucci et al. (2004), Hopper et al. (2006)), and isolated blocks of continental crust add further complications when studying rifted continental margins. An understanding of the OCT structure, COB location and magmatic type provides further

knowledge of the geodynamic, tectonic and magmatic processes responsible for continental lithosphere stretching and thinning leading to breakup, which is critical for evaluating rifted continental margin formation and evolution. For the hydrocarbon industry, rifted continental margins are key exploration frontiers, and knowledge of the OCT structure, COB location and magmatic type are important for deep-water frontier oil and gas exploration. OCT structure, COB location and magmatic type have significant consequences for petroleum systems in terms of source rocks, reservoirs and thermal maturation. The position of the COB (i.e. determining whether we are looking at thinned continental crust or oceanic crust) is particularly important for determining the thermal maturity of a petroleum system. Petroleum systems require heat during the maturation period; this heat, in part, comes from the radiogenic heat productivity within continental crust.

In recent years, new observations have forced the recognition of broad domains of exhumed mantle within the OCT (Brun and Beslier, 1996; Lavier and Manatschal, 2006; Péron-Pinvidic and Manatschal, 2008) and the observation of depth-dependent stretching and thinning of rifted continental margin lithosphere (Davis and Kusznir, 2004; Huismans and Beaumont, 2011; Kusznir et al., 2005; Reston, 2007). The newly available high quality refraction and reflection seismic data (Contrucci et al., 2004; Moulin et al., 2005; Unternehr et al., 2010), including deep long offset seismic reflection data acquired for the hydrocarbon exploration industry, and the recently identified geological analogues of orogenically exhumed rifted continental margins (e.g. Alpine-Tethys (Manatschal and Müntener, 2009)) have enabled more detailed analysis of rifted continental margins to be considered. These observations have forced the reconsideration of rifted continental margin evolution, formation processes and structure.

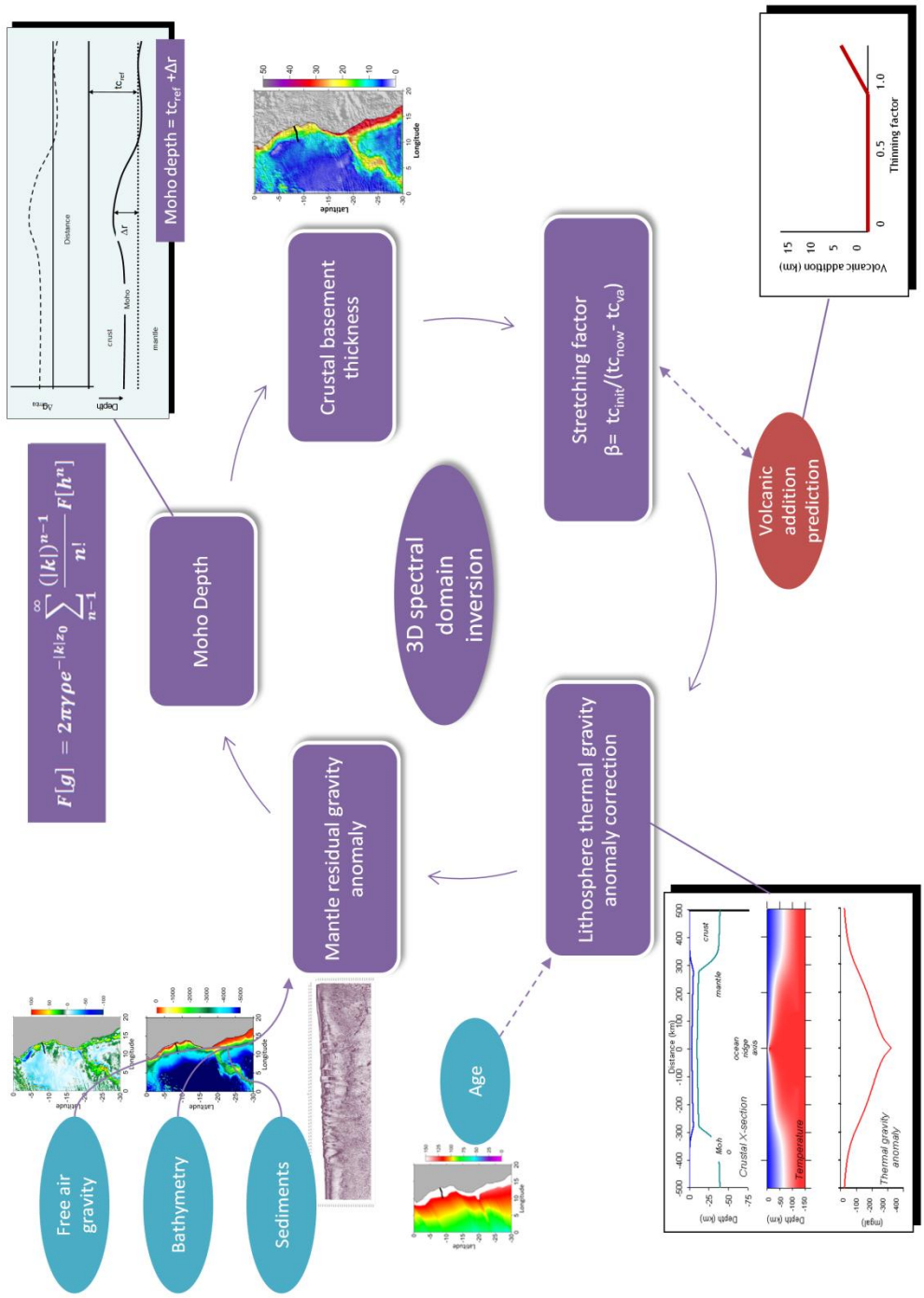

Figure 1.3 – Gravity anomaly inversion workflow, showing input data, the iterative cycle, corrections applied and the output results

A suite of quantitative analytical techniques have been developed in order to determine the structure of the OCT, the location of the COB and magmatic type at rifted continental margins; these techniques include the use of gravity anomaly inversion, residual depth anomaly (RDA) and subsidence analysis. Gravity anomaly inversion, incorporating a lithosphere thermal gravity anomaly correction, has been used to determine Moho depth (i.e. base of the crust), crustal basement thickness and continental lithosphere thinning. The gravity anomaly inversion workflow is summarised in Figure 1.3. RDA analysis has been used to investigate OCT bathymetric anomalies with respect to expected oceanic bathymetries, and subsidence analysis has been used to determine the distribution of continental lithosphere thinning; these methodologies are shown in Figure 1.4.

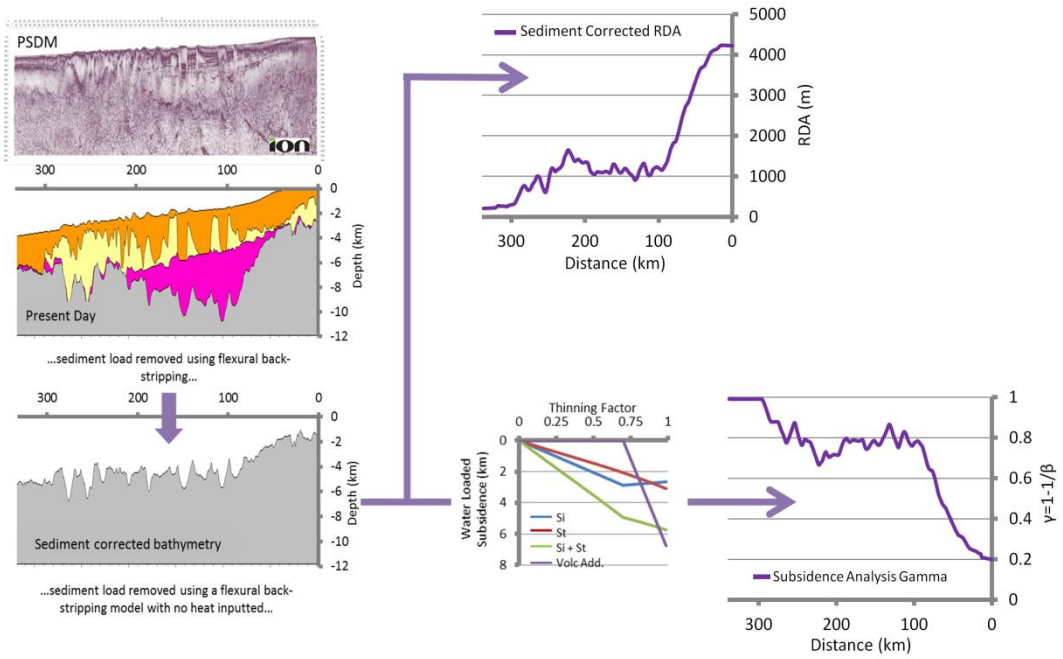

Figure 1.4 – Summary of the RDA and subsidence analysis workflow, showing 2D flexural backstripping to determine sediment corrected bathymetry. Within the RDA analysis the sediment corrected bathymetry is used to determine sediment corrected RDAs, whilst within the subsidence analysis workflow it is converted into continental lithosphere thinning factors.

In addition to the quantitative analysis techniques, a methodology for the joint inversion of deep long offset seismic data and gravity anomaly data has been developed in order to further constrain the structure of the OCT and the location of the COB. The joint inversion method solves for coincident seismic and gravity Moho, in the time domain, and calculates the lateral variations in crustal basement densities and seismic velocities. The quantitative analysis and joint inversion techniques have been applied to geological cross sections along the offshore Iberian (Figure 1.1(b)), the Gulf of Aden (Figure 1.1(c)) south-eastern Brazilian (Figure 1.1(d)) and northern Angolan (Figure 1.1(e)) rifted continental margins. The integrated use of all these techniques together is a new approach, which provides a more robust geological interpretation of the OCT structure, COB location and magmatic type at rifted continental margins. The integrated workflow is summarised in Figure 1.5.

Within the integrated quantitative analysis methodology a crustal basement density of 2850kgm^{-3} is assumed for both oceanic and continental crustal basement (Chappell & Kusznir 2008). Sensitivity tests of this value have been carried out within the range 2800kgm^{-3} to 2900kgm^{-3} and do not change the interpretation of the results presented within this thesis. Different values of oceanic and continental basement density are not used so as to avoid prejudicing the integrated quantitative analysis prediction of continent ocean boundary with *a priori* information.

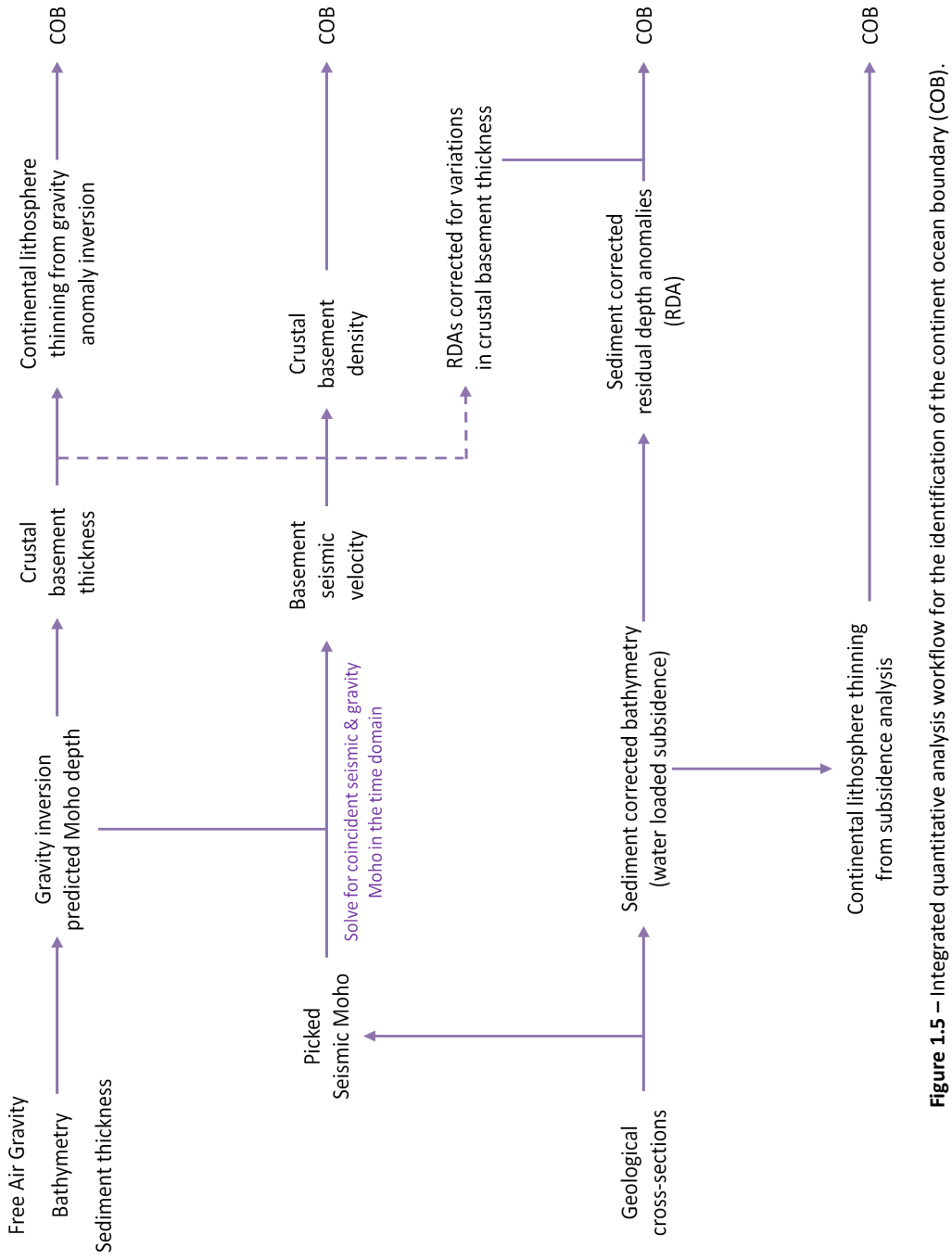

Figure 1.5 – Integrated quantitative analysis workflow for the identification of the continent ocean boundary (COB).

In order to determine the magmatic type of a margin, sensitivities to the amount of decompression melting have been considered (Figure 1.6). For a 'normal' magmatic margin, it is assumed that decompression melting begins at γ=0.7 and will produce a maximum magmatic addition of 7km at a thinning factor of 1.0 (for $\beta=\infty$). Magma-rich margins have more decompression melting and magmatic addition to the crust, with melt initiation occurring at γ=0.5 and a maximum magmatic addition of 10km at γ=1.0. We also consider the case of a magma-poor margin where no magmatic addition to the crust is generated. Within this thesis, crustal and lithosphere thinning are presented according to the depth-uniform stretching model.

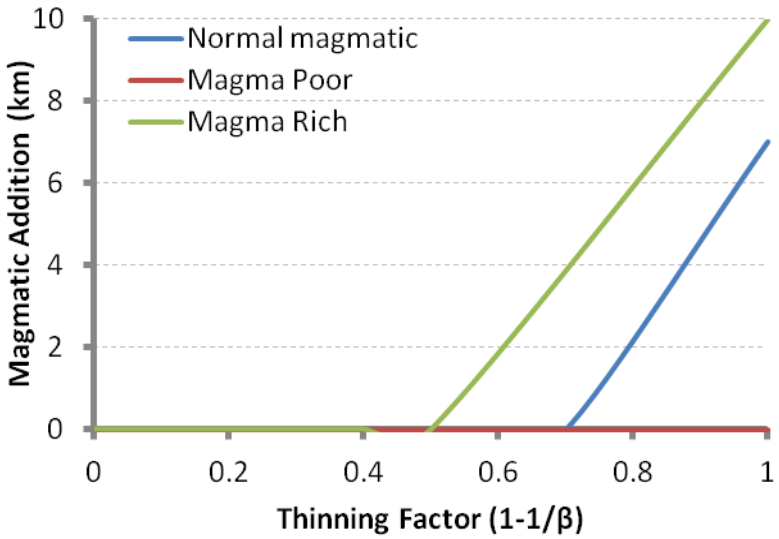

Figure 1.6 – Relationship between continental lithosphere thinning factor and magmatic addition, for three magmatic solutions: 'normal' magmatic, magma-poor and magma-rich. This plots shows when decompression melting begins and the maximum amount of magmatic addition for these three magmatic solutions.

1.3. Subsidence History at Rifted Continental Margins

It has been proposed (Davis and Kusznir, 2004; Lucazeau et al., 2008; Péron-Pinvidic and Manatschal, 2008; Unternehr et al., 2010) that some rifted continental margins have anomalous early subsidence histories, and that at breakup they were elevated at shallower bathymetries than the isostatic response of classical rift models (e.g. McKenzie (1978)) would predict. The existence of anomalous syn- or post-breakup subsidence of this form would have important implications for understanding the geodynamics of continental breakup, the subsidence history of the margin and the evolution of syn- and post-breakup depositional systems. In addition, an understanding of the syn- and post-breakup subsidence evolution and the resulting palaeo-bathymetries and depositional environments, are critical to deep-water hydrocarbon exploration at rifted continental margins.

The results from the integrated quantitative analysis, which have been used to determine the structure of the OCT, the location of the COB and magmatic type of rifted continental margins, have also been used to provide some constraints on margin subsidence history. The reports of anomalous subsidence at rifted continental margins may partly (or wholly) be attributed to mantle dynamic topography. We use RDAs corrected for sediment loading and crustal basement thickness variations to determine present day residual topography measurements for the offshore Iberian, northern Angolan and the Gulf of Aden rifted continental margins. We have compared residual topography extracts from global models (Crosby and McKenzie, 2009; Flament et al., 2013; Kaban et al., 2003; Steinberger, 2007) to our measurements of residual topography from RDA analysis.

The integrated quantitative analysis results have also been used to make predictions of palaeo-bathymetry, which we have applied to the northern Angolan rifted continental margin. Knowledge of the OCT structure and COB location, from integrated quantitative

analysis, have been used together with continental lithosphere thinning factors predicted from gravity anomaly inversion and reverse post-breakup subsidence modelling to determine the palaeo-bathymetry of the base Aptian salt and its context within the OCT structure.

1.4. Thesis Structure

The core of this thesis (chapters 2 – 5) is presented as a series of journal papers. Due to this format, some background material and key concepts are repeated and re-introduced in each chapter.

Chapter 2 is presented in the form of a paper, entitled "Determining the COB Location along the Iberian Margin and Galicia Bank from Gravity Anomaly Inversion, Residual Depth Anomaly and Subsidence Analysis". This paper describes the methodologies and applications of a suite of quantitative analytical techniques, which include gravity anomaly inversion, RDA and subsidence analysis, at the Iberian rifted continental margin. The work has focussed along three key profiles: ISE-01 along Galicia Bank and profiles IAM9 and Lusigal 12 (with the inclusion of the TGS extension) along the Iberian Abyssal Plain. Integrated quantitative analysis techniques have been used in order to determine the crustal structure of the OCT, locate the COB and determine magmatic type along the Iberian margin. The Iberian rifted continental margin is a natural laboratory, which has abundant observational data. As a consequence, we have used the Iberian margin to demonstrate and test the integrated quantitative analysis methodologies and techniques used in this thesis.

Chapter 3 is presented in the form of a paper, entitled "OCT Structure, COB Location and Magmatic Type of the Northern Angolan and South-eastern Brazilian Rifted Continental Margins". This paper uses the afore mentioned quantitative analysis techniques (gravity anomaly inversion, RDA and subsidence analysis) to determine the OCT structure, COB

location and magmatic type of the northern Angolan and south-eastern Brazilian rifted continental margins. In addition to the quantitative analysis techniques, a joint inversion technique using deep seismic reflection and gravity anomaly data has also been applied to these margins. The joint inversion method solves for coincident seismic and gravity Moho, in the time domain, and calculates the lateral variations in crustal basement densities and seismic velocities along profile, which provides further constraints on the OCT structure and COB location.

Chapter 4 is presented as a paper, entitled "The Palaeo-bathymetry of the Base Aptian Salt Deposition on the Angolan Rifted Margin: Constraints from Flexural Backstripping and Reverse Post-breakup Thermal Subsidence Modelling". The bathymetric datum with respect to global sea level for Aptian salt deposition in the South Atlantic is hotly debated. Some models propose that the salt was deposited in an isolated ocean basin in which local sea level was between 2km and 3km below the global level. In this paper we propose several interpretations of the palaeo-bathymetric results for the depositional environment of the salt along the northern Angolan margin.

Chapter 5 takes the form of a paper entitled "Residual Topography Predictions from Residual Depth Anomaly Analysis: Applications to the Iberian, Gulf of Aden and Northern Angolan Rifted Continental Margins". In this paper we measure present day residual topography for oceanic lithosphere at three rifted continental margins using RDA analysis, which makes isostatic corrections for sediment loading, crustal thickness variation and lithosphere thermal structure. Residual topography may be defined as the topography remaining after the isostatic contributions from sediments, ice, crust and lithosphere (including oceanic lithosphere cooling) are removed, which we attribute to mantle dynamic topography. While different global measurements of residual topography using independent approaches give a broadly similar pattern at long wavelengths, they differ substantially in predicted amplitude

and at shorter wavelengths. We compare our detailed measurements of residual topography made using RDA analysis for Iberia, Gulf of Aden and northern Angola with measurements extracted from these global models of residual topography.

Chapter 6 is a discussion and summary of the methodologies and results obtained in this thesis.

The work presented in this thesis is solely the work of the author unless otherwise referenced.

1.5. References

Boillot, G., Feraud, G., Recq, M., and Girardeau, J., 1989, Undercrusting by serpentinite beneath rifted margins: Nature, v. 341, no. 6242, p. 523 - 525.

Boillot, G., Grimaud, S., Mauffret, A., Mougenot, D., Kornprobst, J., Mergoil-Daniel, J., and Torrent, G., 1980, Ocean-continent boundary off the Iberian margin: A serpentinite diapir west of the Galicia Bank: Earth and Planetary Science Letters, v. 48, no. 1, p. 23-34.

Bronner, A., Sauter, D., Manatschal, G., Peron-Pinvidic, G., and Munschy, M., 2011, Magmatic breakup as an explanation for magnetic anomalies at magma-poor rifted margins, Nature Geoscience, Volume 4, Nature Publishing Group, a division of Macmillan Publishers Limited. All Rights Reserved., p. 5.

Brun, J. P., and Beslier, M. O., 1996, Mantle exhumation at passive margins: Earth and Planetary Science Letters, v. 142, no. 1–2, p. 161-173.

Coffin, M. F., and Eldholm, O., 1994, Large igneous provinces: Crustal structure, dimensions, and external consequences: Reviews of Geophysics, v. 32, no. 1, p. 1-36.

Contrucci, I., Matias, L., Moulin, M., Géli, L., Klingelhofer, F., Nouzé, H., Aslanian, D., Olivet, J.-L., Réhault, J.-P., and Sibuet, J.-C., 2004, Deep structure of the West African continental margin (Congo, Zaïre, Angola), between 5°S and 8°S, from reflection/refraction seismics and gravity data: Geophysical Journal International, v. 158, no. 2, p. 529-553.

Crosby, A. G., and McKenzie, D., 2009, An analysis of young ocean depth, gravity and global residual topography: Geophysical Journal International, v. 178, no. 3, p. 1198-1219.

Davis, M., and Kusznir, N., 2004, Depth Dependant lithospheric Stretching at Rifted Continental Margins, *in* Karner, G. D., Taylor, B., Driscoll, N. W., and Kohlstedt, D. L., eds., Rheology and Deformation of the Lithosphere at Continental Margins, Columbia University Press, p. 408.

Dean, S. M., Minshull, T. A., Whitmarsh, R. B., and Louden, K. E., 2000, Deep structure of the ocean-continent transition in the southern Iberia Abyssal Plain from seismic refraction profiles: The IAM-9 transect at 40°20'N: Journal of Geophysical Research: Solid Earth, v. 105, no. B3, p. 5859-5885.

Discovery 215 Working, G., Minshull, T. A., Dean, S. M., Whitmarsh, R. B., Russell, S. M., Louden, K. E., and Chian, D., 1998, Deep structure in the vicinity of the ocean-continent transition zone under the southern Iberia Abyssal Plain: Geology, v. 26, no. 8, p. 743-746.

Flament, N., Gurnis, M., and Müller, R. D., 2013, A review of observations and models of dynamic topography: Lithosphere, v. 5, no. 2, p. 189-210.

Franke, D., 2013, Rifting, lithosphere breakup and volcanism: Comparison of magma-poor and volcanic rifted margins: Marine and Petroleum Geology, v. 43, no. 0, p. 63-87.

Hinz, K., 1981, A hypothesis on terrestrial catastrophes: wedges of very thick oceanward dipping layers beneath passive continental margins - their origin and paleoenvironmental significance. : Geologisches Jahrbuch Reihe E, p. 3-28.

Hopper, J. R., Funck, T., Tucholke, B. E., Louden, K. E., Holbrook, W. S., and Christian Larsen, H., 2006, A deep seismic investigation of the Flemish Cap margin: implications for the origin of deep reflectivity and evidence for asymmetric break-up between Newfoundland and Iberia: Geophysical Journal International, v. 164, no. 3, p. 501-515.

Huismans, R., and Beaumont, C., 2011, Depth-dependent extension, two-stage breakup and cratonic underplating at rifted margins: Nature, v. 473, no. 7345, p. 74-78.

Kaban, M. K., Schwintzer, P., Artemieva, I. M., and Mooney, W. D., 2003, Density of the continental roots: compositional and thermal contributions: Earth and Planetary Science Letters, v. 209, no. 1–2, p. 53-69.

Kusznir, N. J., Hunsdale, R., Roberts, A. M., and i, S. T., 2005, Timing and magnitude of depth-dependent lithosphere stretching on the southern Lofoten and northern Vøring continental margins offshore mid-Norway: implications for subsidence and hydrocarbon maturation at volcanic rifted margins: Geological Society, London, Petroleum Geology Conference series, v. 6, p. 767-783.

Lavier, L. L., and Manatschal, G., 2006, A mechanism to thin the continental lithosphere at magma-poor margins: Nature, v. 440, no. 7082, p. 324-328.

Lucazeau, F., Leroy, S., Bonneville, A., Goutorbe, B., Rolandone, F., d'Acremont, E., Watremez, L., Düsünur, D., Tuchais, P., Huchon, P., Bellahsen, N., and Al-Toubi, K., 2008, Persistent thermal activity at the Eastern Gulf of Aden after continental break-up: Nature Geoscience, v. 1, no. 12, p. 854-858.

Manatschal, G., 2004, New models for evolution of magma-poor rifted margins based on a review of data and concepts from West Iberia and the Alps: International Journal of Earth Sciences, v. 93, no. 3.

Manatschal, G., Froitzheim, N., Rubenach, M., and Turrin, B. D., 2001, The role of detachment faulting in the formation of an ocean-continent transition: insights from the Iberia Abyssal Plain: Geological Society, London, Special Publications, v. 187, no. 1, p. 405-428.

Manatschal, G., and Müntener, O., 2009, A type sequence across an ancient magma-poor ocean–continent transition: the example of the western Alpine Tethys ophiolites: Tectonophysics, v. 473, no. 1–2, p. 4-19.

Manatschal, G., Sutra, E., and Péron-Pinvidic, G., The lesson from the Iberia-Newfoundland rifted margins: how applicable is it to other rifted margins?, *in* Proceedings 2nd Central & North Atlantic Conjugate Margins: Rediscovering the Atlantic, New Insights, New winds for an old sea2010, Volume 2, p. 27 - 37.

McKenzie, D., 1978, Some Remarks on the Development of Sedimentary Basins Earth and Planetary Science Letters, v. 40, p. 25-32.

Moulin, M., Aslanian, D., Olivet, J.-L., Contrucci, I., Matias, L., Géli, L., Klingelhoefer, F., Nouzé, H., Réhault, J.-P., and Unternehr, P., 2005, Geological constraints on the evolution of the Angolan margin based on reflection and refraction seismic data (ZaïAngo project): Geophysical Journal International, v. 162, no. 3, p. 793-810.

Pérez-Gussinyé, M., 2012, A tectonic model for hyperextension at magma-poor rifted margins: an example from the West Iberia–Newfoundland conjugate margins: Geological Society, London, Special Publications, v. 369.

Péron-Pinvidic, G., and Manatschal, G., 2008, The final rifting evolution at deep magma-poor passive margins from Iberia-Newfoundland: a new point of view: International Journal of Earth Sciences, v. 98, no. 7, p. 1581-1597.

Peron-Pinvidic, G., Manatschal, G., Minshull, T., and Sawyer, D., 2006, How is continental break-up recorded in magma-poor rifted margins?, American Geophysical Union, Fall Meeting: San Francisco, AGU.

Péron-Pinvidic, G., Manatschal, G., Minshull, T. A., and Sawyer, D. S., 2007, Tectonosedimentary evolution of the deep Iberia-Newfoundland margins: Evidence for a complex breakup history: Tectonics, v. 26, no. 2, p. TC2011.

Pickup, S. L. B., Whitmarsh, R. B., Fowler, C. M. R., and Reston, T. J., 1996, Insight into the nature of the ocean-continent transition off West Iberia from a deep multichannel seismic reflection profile: Geology, v. 24, no. 12, p. 1079-1082.

Reston, T., 2007, Extension discrepancy at North Atlantic nonvolcanic rifted margins: Depth-dependent stretching or unrecognized faulting?: Geology, v. 35, no. 4, p. 367-370.

Reston, T. J., 2009, The structure, evolution and symmetry of the magma-poor rifted margins of the North and Central Atlantic: A synthesis: Tectonophysics, v. 468, no. 1–4, p. 6-27.

Steinberger, B., 2007, Effects of latent heat release at phase boundaries on flow in the Earth's mantle, phase boundary topography and dynamic topography at the Earth's surface: Physics of the Earth and Planetary Interiors, v. 164, no. 1–2, p. 2-20.

Unternehr, P., Péron-Pinvidic, G., Manatschal, G., and Sutra, E., 2010, Hyper-extended crust in the South Atlantic: in search of a model: Petroleum Geoscience, v. 16, no. 3, p. 207-215.

White, R. S., McKenzie, D., and O'Nions, R. K., 1992, Oceanic Crustal Thickness From Seismic Measurements and Rare Earth Element Inversions: Journal of Geophysical Research, v. 97, no. B13, p. 19683-19715.

Whitmarsh, R. B., and Miles, P. R., 1995, Models of the development of the West Iberia rifted continental margin at 40°30'N deduced from surface and deep-tow magnetic anomalies: Journal of Geophysical Research: Solid Earth, v. 100, no. B3, p. 3789-3806.

Chapter 2

2. Determining the COB Location along the Iberian Margin and Galicia Bank from Gravity Anomaly Inversion, Residual Depth Anomaly and Subsidence Analysis

Preface

This chapter has been written in the form of a paper. Co-authors are N. J. Kusznir (University of Liverpool) and G. Manatschal (CNRS-EOST, Université de Strasbourg). Section headers, figures and page numbers have been renumbered to conform to the format of this thesis.

Abstract

Knowledge and understanding of the ocean continent transition (OCT) structure, continent-ocean boundary (COB) location and magmatic type are of critical importance in evaluating rifted continental margin formation and evolution. OCT structure, COB location and magmatic type also have important implications for the understanding of the geodynamics of continental breakup and in the evaluation of petroleum systems in deep-water frontier oil and gas exploration at rifted continental margins. Mapping the distribution of thinned continental crust and lithosphere, its distal extent and the start of unequivocal oceanic crust and hence determining the OCT structure and COB location at rifted continental margins is therefore a generic global problem. In order to determine the OCT structure and COB location, we present methodologies using gravity anomaly inversion, residual depth anomaly (RDA) analysis and subsidence analysis, which we apply to the Iberian rifted continental margin. The Iberian margin has one of the most complete data sets available for deep magma-poor rifted margins, so there are abundant data to which the results can be calibrated. Gravity anomaly inversion has been used to determine Moho depth, crustal basement thickness and continental lithosphere thinning; subsidence analysis has been used to determine the distribution of continental lithosphere thinning; and RDAs have been used to investigate the OCT bathymetric anomalies with respect to expected oceanic bathymetries at rifted continental margins. These quantitative analytical techniques have been applied to the Iberian rifted continental margin along profiles IAM9, Lusigal 12 (with the TGS-extension) and ISE-01. Our predictions of OCT structure, COB location and magmatic type (i.e. the volume of magmatic addition, whether the margin is 'normal' magmatic, magma-poor or magma-rich) have been tested and validated using ODP wells (Legs 103, 149 and 173), which provide observational constraints on the Iberian margin.

2.1. Introduction

Knowledge of the structure of the ocean continent transition (OCT), the location of the continent ocean boundary (COB), magmatic type (i.e. the volume of magmatic addition, whether the margin is 'normal' magmatic, magma-poor or magma-rich) and the distribution of oceanic and continental lithosphere are key to understanding present day rifted continental margin architecture and evolution. The determination of rifted continental margin magmatic type and OCT structure, which show great diversity globally, are important for understanding the geodynamic, tectonic and magmatic processes involved in rifted continental margin formation and their evolution to the present day. Understanding structure and formation processes of rifted continental margins is important, not only because they are a key component of the plate tectonic Wilson cycle (Wilson, 1966) but also for deep-water hydrocarbon exploration. In this chapter, we present a set of integrated quantitative analysis techniques for determining OCT structure, COB location and magmatic type at rifted continental margins, which have been applied and tested on the Iberian rifted continental margin, where independent observations from ODP wells are available for ground-truthing.

Numerous studies (e.g. Zalán et al. (2011); Autin et al. (2010); Unternehr et al. (2010); Reston (2009); White et al. (2008); D'Acremont et al. (2005); Contrucci et al. (2004); Hopper et al. (2004); Chian et al. (1999); Pickup et al. (1996); Whitmarsh and Miles (1995)) have used various approaches to determine OCT structure and COB location of rifted continental margins. Techniques that have been used include the analysis of: seismic reflection and refraction data, gravity and magnetic anomalies, bathymetric breaks and well data. The aims of these studies have focussed on: (i) distinguishing whether the OCT at a rifted continental margin is narrow or wide; (ii) determining the location of the distal extent of continental crust

and the presence of any isolated ribbons of thinned continental crust and (iii) determining the magmatic type of a rifted continental margin.

The Iberian rifted continental margin has abundant observational data; including seismic reflection and refraction surveys, magnetic anomalies and ODP well data. As a consequence it is a good natural laboratory for studying rifted continental margin evolution and has been used to demonstrate and test the methodologies and techniques used in this chapter to determine OCT structure, COB location and magmatic type. On the Iberian rifted continental margin, there have been many studies, which have addressed these and other questions. The application of seismic reflection and refraction data (e.g. Dean et al. (2000); Pickup et al. (1996); Whitmarsh et al. (1996)) and also seismic tomography (e.g. Zelt et al. (2003)) has focussed on the determination of the OCT structure and the identification of the inner and outer bounds of the OCT. Detailed seismic mapping and borehole data have also been applied in order to further constrain the crustal type (e.g. Péron-Pinvidic et al. (2007)), whilst magnetic anomalies have been used to tentatively locate the COB (e.g. Bronner et al. (2011)). The determination of the magmatic type of a margin has been further constrained using seismic reflection data, magnetic anomalies and ODP well data as discussed in Pickup et al. (1996).

In this study, we have applied an integrated quantitative analysis of gravity anomaly inversion, residual depth anomaly (RDA) analysis and subsidence analysis to the Iberian rifted continental margin. Gravity anomaly inversion, incorporating a lithosphere thermal gravity anomaly correction, has been used to determine crustal basement thickness, Moho depth and continental lithosphere thinning across the Iberian rifted continental margin. Sediment corrected RDAs have been used to calculate departures from standard oceanic water depths, as predicted by Crosby et al. (2006) and Stein and Stein (1992), whilst subsidence analysis has been used to give the distribution of continental lithosphere thinning. These techniques have

been interpreted individually and together to identify the distribution of oceanic and thinned continental crust, in order to determine the structure of the OCT and locate the COB.

The Iberian margin is the result of polyphase rifting and continental breakup between the North American and Iberian plates during the Late Triassic to Early Cretaceous (Manatschal, 2004; Manatschal et al., 2001; Péron-Pinvidic et al., 2007; Russell and Whitmarsh, 2003). The Iberian Abyssal Plain is part of the north-west magma-poor Iberian margin (Chian et al., 1999) and is considered to be a type example of a sediment-starved magma-poor rifted continental margin (Sutra and Manatschal, 2012). The Iberian margin is subdivided into three main sections: Galicia margin to the north, the Iberian Abyssal Plain in the middle and the Tagus Abyssal Plain to the south (Manatschal et al., 2001). This chapter focuses on three key profiles (IAM9, Lusigal 12 and ISE-01) along the Iberian Abyssal Plain and the Galicia margin highlighted in Figure 2.1(a). The Iberian rifted continental margin is, at present, considered to be one of the best studied rifted continental margins world-wide due to the abundant observational data available in the form of deep sea drilling (ODP Legs 103, 149 and 173) (Boillot et al., 1987; Sawyer et al., 1994; Tucholke et al., 2007; Whitmarsh et al., 1998; Whitmarsh and Sawyer, 1996) combined with seismic reflection and refraction surveys (Manatschal et al., 2010).

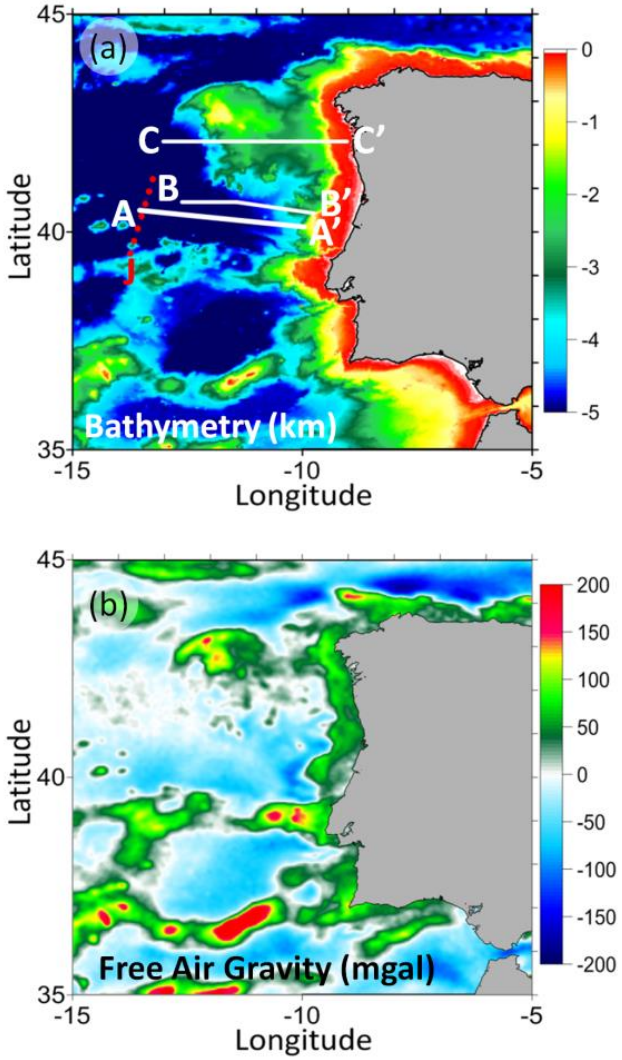

Figure 2.1 – Data used in the gravity anomaly inversion, RDA and subsidence analysis for the Iberian Abyssal Plain and Galicia Bank. (a) Bathymetry (km) (Amante and Eakins 2009). Locations of profiles IAM9 (A-A'), Lusigal 12 (with the TGS extension) (B-B') and ISE-01 (C-C') are indicated. The red dashed line indicates the location of the J anomaly (Bronner et al., 2011; Dean et al., 2000; Whitmarsh et al., 2001). (b) Free air gravity (mgal) (Sandwell and Smith 2009).

Within the literature there are a range of different definitions of the OCT and COB (e.g. Pèron-Pinvidic et al. (2007), Whitmarsh and Miles (1995), Manatschal et al. (2001), Dean et al. (2000), Manatschal et al. (2010) and Discovery 215 Working et al. (1998)). Within this chapter, however, we define the OCT as the region between unequivocal continental crust of 'normal' thickness and unequivocal oceanic crust; the continental lithosphere in this region is highly thinned, with complex tectonics, variable magmatism and possible mantle exhumation. We define the COB as the distal limit of unequivocal continental crust; however,

determining the location of the COB is made difficult by the presence of exhumed mantle and complex tectonics. Another important term used is continental breakup age, which within this chapter is associated with the onset of seafloor spreading. Conceptually the term continental breakup may be used to either describe the point at which the continental crust ruptures and starts to separate, or when plate boundaries are localised by the onset of decompression melting and the onset of seafloor spreading.

2.2. OCT Structure and COB Location: Profile IAM9

Integrated quantitative analysis has been used to determine OCT structure, COB location and magmatic type along profile IAM9 (A-A'). Profile IAM9 has been used to describe the gravity anomaly inversion, RDA analysis and subsidence analysis techniques in detail due to the availability of reliable seismic Moho depths (Dean et al., 2000), which are required for calibration of the reference Moho depth.

2.2.1. Crustal Basement Thickness and Continental Lithosphere Thinning along IAM9 from Gravity Anomaly Inversion

Gravity anomaly inversion has been used to determine crustal basement thickness, Moho depth and continental lithosphere thinning, which in turn give the distribution of oceanic and continental lithosphere. The data used within the gravity anomaly inversion are bathymetry (Amante and Eakins, 2009) (Figure 2.1(a)), satellite derived free air gravity (Sandwell and Smith, 2009) (Figure 2.1(b)), 2D sediment thickness from wide angle seismic data (Dean et al., 2000) (Figure 2.2(a)) and ocean age isochrons from Müller et al. (2008).

The gravity anomaly inversion method is carried out in the 3D spectral domain, using the scheme of Parker (1972) to predict Moho depth and hence determine crustal basement

thickness. As the gravity anomaly inversion has been applied to rifted continental margin lithosphere, a lithosphere thermal gravity anomaly correction is incorporated to account for the elevated geothermal gradient within oceanic and rifted continental margin lithosphere. Failure to include the correction for the lithosphere thermal gravity anomaly can lead to predictions of Moho depth and crustal basement thickness at rifted continental margins, which are substantially too great. The results from gravity anomaly inversion are dependent on the age of continental breakup due to the lithosphere thermal gravity anomaly correction being dependent on the lithosphere thermal re-equilibration time. Some papers consider the age of breakup for the Iberian margin to be at the Aptian-Albian boundary, 112Ma (Péron-Pinvidic et al., 2007); whereas others consider an older breakup age of 126Ma, (Manatschal, 2004; Russell and Whitmarsh, 2003). As the gravity anomaly inversion requires a definitive breakup age, a Cretaceous breakup age of 120Ma, which is within this proposed range, has been examined. Changing the breakup age used within the gravity anomaly inversion to the maximum breakup age proposed, 126Ma, or to the minimum breakup age proposed, 112Ma, has a small effect on the results, but does not substantially change the overall conclusions. A more detailed methodology of the gravity anomaly inversion technique is described in Cowie and Kusznir (2012), Alvey et al. (2008), Chappell and Kusznir (2008) and Greenhalgh and Kusznir (2007).

Within the gravity anomaly inversion the reference Moho depth is an important parameter that requires careful consideration and calibration. The long wavelength components of the Earth's gravity anomaly field are controlled by deep mantle dynamic processes and are not related to lithosphere and crustal structure. As a consequence the reference Moho depth varies globally. It is therefore necessary for the reference Moho depth to be determined by calibration against seismic refraction Moho depths to ensure the correct reference Moho depth is used within the gravity anomaly inversion (Cowie and Kusznir, 2012). A crustal

basement density of 2850kgm^{-3} (Carlson and Herrick, 1990; Christensen and Mooney, 1995) and a mantle density of 3300kgm^{-3} are used in the gravity anomaly inversion; sensitivity tests to these values have been made.

Reference Moho depths have been calibrated, for the oceanic domain, using profile IAM9, which has reliable seismic Moho depth estimates from the wide angle seismic data of Dean et al. (2000). Sensitivities to reference Moho depths of 35km, 37.5km, 40km and 42.5km have been examined for the IAM9 profile. Moho depths predicted from gravity anomaly inversion produced for these sensitivities to reference Moho depth are shown in Figure 2.2(b). Reference Moho depths of 35km and 37.5km are too small as they predict Moho depths, which are too shallow and in places plot shallower than the top basement and within the sedimentary layer. A larger reference Moho depth is required; both reference Moho depths of 40km and 42.5km predict a deeper Moho. Calibration gives a reference Moho depth of 41km (Figure 2.2(c)) in order to predict crustal basement thicknesses consistent with those seen in the wide-angle seismic data.

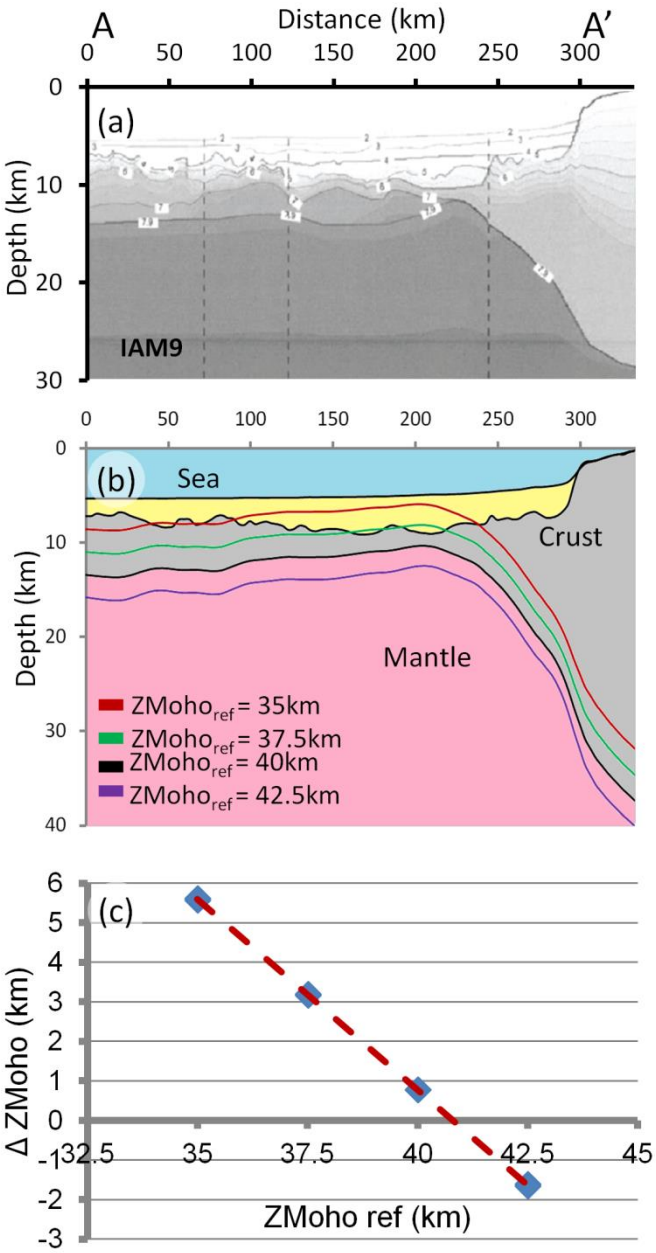

Figure 2.2 - Calibration of the reference Moho depth used in the gravity anomaly inversion along profile IAM9. (a) Wide-angle seismic data for IAM9 (Dean et al. 2000) showing Moho depth. (b) Moho depths predicted from gravity anomaly inversion have been calculated using reference Moho depths of 35km, 37.5km, 40km and 42.5km. (c) Calibration of the reference Moho depth for profile IAM9 shows that a reference Moho depth of 41km is required.

A crustal cross section (A-A') along profile IAM9 (Figure 2.3(a)), has been constructed using the bathymetry and 2D sediment thickness data (Dean et al., 2000) with the crustal basement thicknesses and Moho depths predicted from gravity anomaly inversion assuming the calibrated reference Moho depth of 41km. The crustal cross section along profile IAM9

(A-A') shows the distribution of oceanic and continental crust and hence the structure of the OCT. The red dashed line shows the 7.9kms^{-1} iso-velocity contour (Dean et al., 2000) representing the seismic Moho depth. There is a good correlation between the Moho depths predicted from gravity anomaly inversion, using the calibrated reference Moho depth of 41km, and the seismic Moho depths; crustal basement thicknesses between 5km and 7km are predicted at the western end of the profile. In the centre of the profile (between 100km and 200km) the crustal basement thicknesses predicted from gravity anomaly inversion thin considerably, to between approximately 1.5km and 2km, and the gravity anomaly inversion predicts a shallower Moho depth than predicted by the 7.9kms^{-1} iso-velocity contour. The start of the margin hinge region again shows a good correlation between the Moho depths predicted from gravity anomaly inversion and the seismic Moho depths. Under the continental crust inboard of the margin hinge there is a significant difference between the gravity anomaly inversion predicted Moho depths and the seismic Moho depths. This difference can be attributed to the poor seismic resolution and too thin estimate of sediment thicknesses in this region. A thicker sedimentary package at the continental end of the profile (A') would cause the Moho depths predicted from gravity anomaly inversion beneath the continental crust to become shallower. The difference could also be due to errors in the seismic Moho depth in this region, as there are no OBS stations this far inboard of the hinge.

The distribution of continental lithosphere thinning predicted from gravity anomaly inversion has also been used along the Iberian rifted continental margin. During continental rifting and breakup there can be a significant addition of magmatic material to the crust. The thickness of the crustal magmatic addition is estimated using the parameterization of decompression melting model of White & McKenzie (1989), from the lithosphere thinning factor (γ) determined from gravity anomaly inversion, where

$$\gamma = 1 - \frac{1}{\beta} \quad (1)$$

This parameterisation of decompression melting is described in detail in Chappell & Kusznir (2008). Decompression melting results in magmatic addition, which leads to the generation of oceanic crust and also magmatic under-plating and extrusives (e.g. seaward dipping reflectors (SDRs)) at many rifted continental margins; at the Iberian margin SDRs are not observed. 'Normal' decompression melting produces a 7km thick oceanic crust with the initiation of decompression melting occurring at γ=0.7 and a maximum magmatic addition of 7km at a thinning factor of 1.0 (for $\beta=\infty$). Magma-rich margins have more decompression melting and magmatic addition to the crust, with melt initiation occurring at γ=0.5 and a maximum magmatic addition of 10km at γ=1.0. We also consider the case of a magma-starved margin where no magmatic addition to the crust is generated. In the case of magma-starved margins, serpentinization of exhumed mantle occurs. Therefore, we also consider a solution for mantle serpentinization, applicable to magma-starved margins, in which serpentinization begins at approximately γ=0.7 (corresponding to approximately 10km thick crust) and at γ=1.0 generates a serpentinised mantle with a mass deficiency with respect to mantle equivalent to crustal basement of thickness 3km.

Continental lithosphere thinning factor (γ) estimates, for profile IAM9, derived from gravity anomaly inversion assuming three different solutions, shown in Figure 2.3(b). A magma-poor solution (Va=0 km); a 'normal' magmatic solution (Va=7 km) and a solution for serpentinized mantle have been examined. Continental lithosphere thinning factors of zero indicate that there has been no stretching or thinning of the continental lithosphere, whereas a continental lithosphere thinning factor of one indicates that there has been infinite stretching and thinning of the original continental lithosphere and there is no continental lithosphere (or crust) remaining. Changes in the continental lithosphere thinning factors, determined from gravity anomaly inversion, specifically changes from high thinning factors (between 0.8 and 1.0) to lower thinning factors, can be used to constrain the COB location along the profile lines. Along profile IAM9 (Figure 2.3(b)), the continental lithosphere thinning factors, from gravity anomaly inversion for 'normal' magmatic addition, are 1.0 outboard of the hinge. The continental lithosphere thinning factors for a magma-poor solution and a serpentinized mantle solution are similar in magnitude ranging between 0.85 and 1.0, with the main difference seen in the centre of the profile. This difference is expected as Dean et al. (2000) indicate that there are peridotite mantle ridges in this region, which would be better represented using the solution for serpentinized mantle.

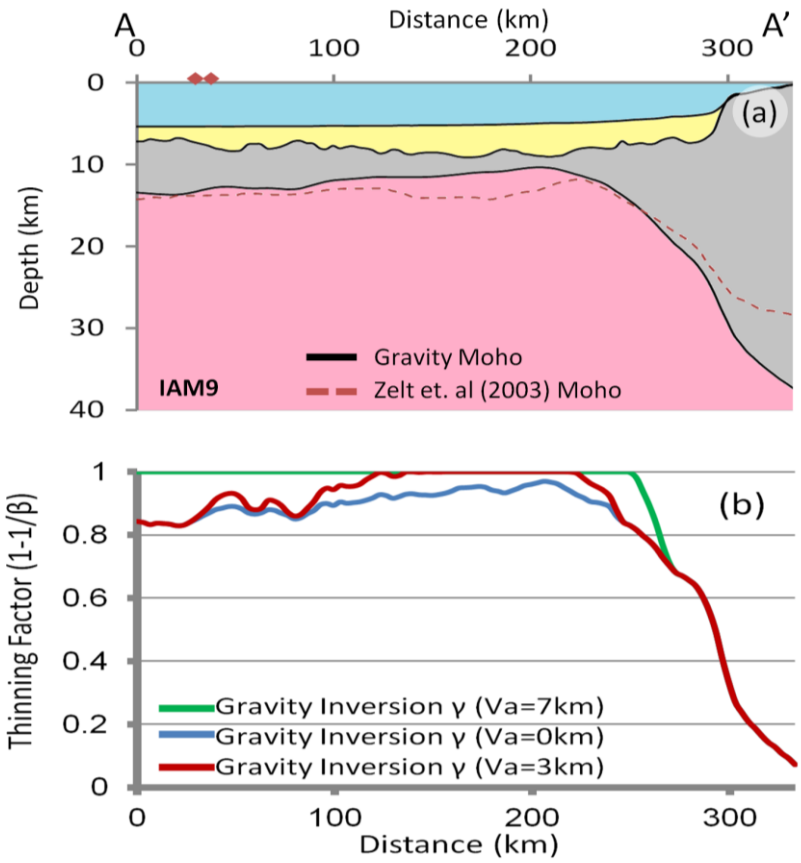

Figure 2.3 - (a) Crustal cross section (A-A') along profile IAM9 is constructed using bathymetry (Amante and Eakins 2009), 2D sediment thickness (Dean et al. 2000) and Moho depth from gravity anomaly inversion. The red dashed line shows the 7.9kms^{-1} iso-velocity contour (Dean et al. 2000) representing the seismic Moho depth. The red diamonds indicate the location of the Moho depths, in the oceanic domain, used for calibration. (b) Continental lithosphere thinning factors predicted from gravity anomaly inversion along profile IAM9. Sensitivities to a 'normal' magmatic solution (Va=7km), a magma-poor solution (Va=0km) and a solution for serpentinised mantle have been examined. A 'normal' magmatic solution predicts thinning factors of 1.0 between the oceanic region and the hinge, the solution for serpentinized mantle predicts thinning factors, which increase from 0.9 to 1.0 in this region.

2.3. Residual Depth Anomaly Analysis: Profile IAM9

2.3.1. Sediment Corrected RDA

Residual depth anomaly (RDA) analysis has been applied to the Iberian rifted continental margin in order to examine OCT bathymetric anomalies with respect to expected oceanic bathymetries at the rifted continental margin. A RDA for oceanic crust is the difference between observed (b_{obs}) and ocean age predicted bathymetry ($b_{predicted}$). Age predicted bathymetric anomalies have been calculated using the thermal plate model predictions from Crosby and McKenzie (2009). Sensitivities to the thermal plate model predictions from Parsons and Sclater (1977) and Stein and Stein (1992) have also been examined; RDA results computed using these different thermal plate model predictions do not vary significantly.

$$\mathrm{RDA} = \mathrm{b_{obs}} - \mathrm{b_{predicted}} \quad (2)$$

Changes in RDA signature are used to estimate the distal extent of continental crust and where unequivocal oceanic crust begins.

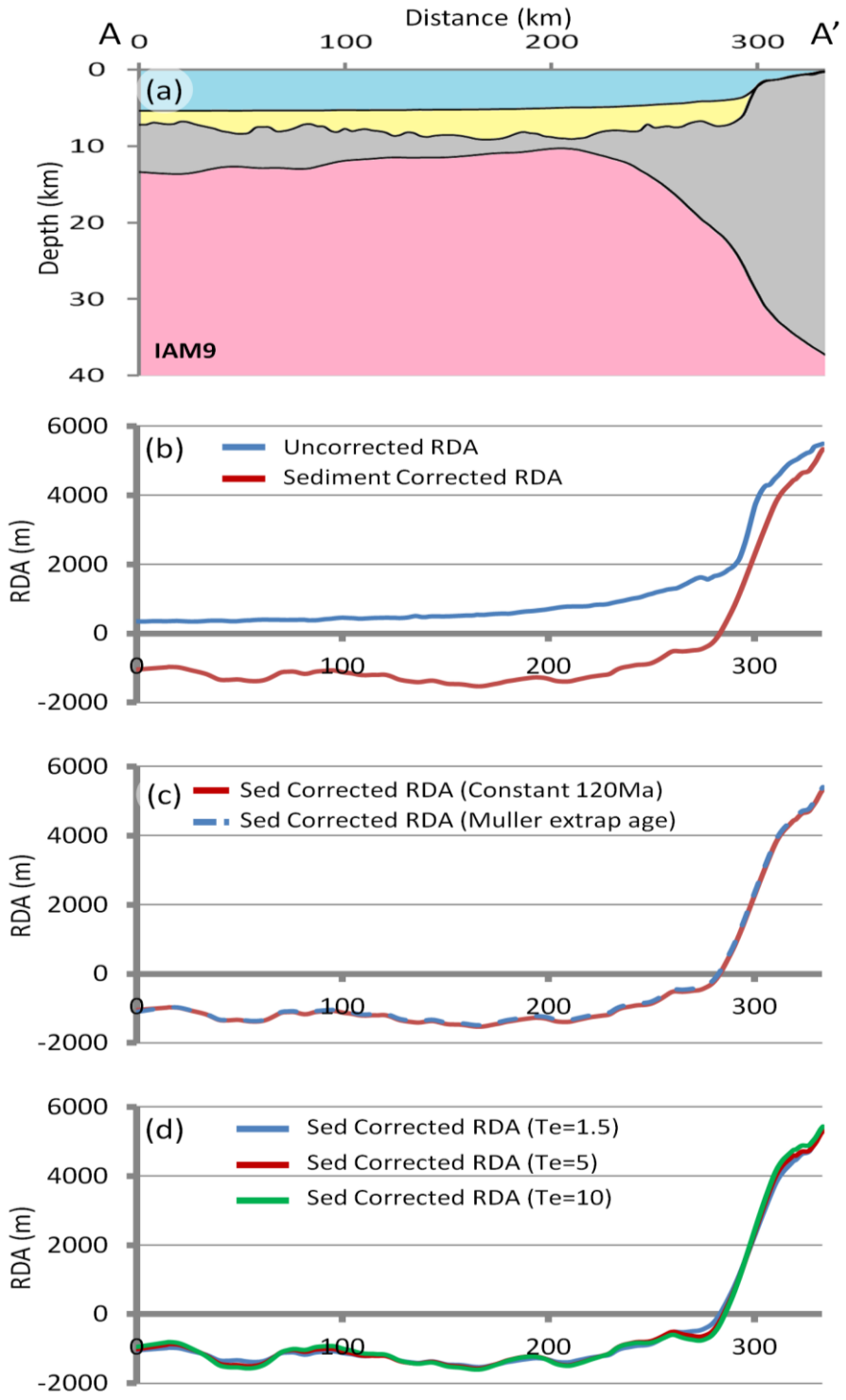

Figure 2.4 - (a) Crustal cross section along profile IAM9. (b) Comparison of uncorrected RDA results with the sediment corrected RDA results along IAM9. (c) The sensitivity to oceanic lithospheric age for sediment corrected RDA results has been examined using two approaches: the first uses a constant value of 120Ma for the profile, whilst the second uses Müller et al. (2008) age isochrons with their age gradient extrapolated inboard. (d) Sensitivities to the effective elastic thickness (Te) for the sediment corrected RDA results have been examined. Te's of 1.5km, 5km and 10km produce sediment corrected RDAs of similar magnitude.

Sediment corrected bathymetry, used to calculate RDAs corrected for sediment loading, has been determined using flexural backstripping and decompaction. Figure 2.4(a) shows a comparison of the uncorrected RDA and the sediment corrected RDA along profile IAM9. Correcting for the effect of sediment loading has a considerable effect on the RDA results; the difference between the uncorrected RDA and the sediment corrected RDA is approximately 1500m at the western end of the profile. Sediment corrected bathymetry has been calculated using flexural backstripping (Kusznir et al., 1995) and comprises the removal of the sedimentary load, allowing for the flexural isostatic response and decompaction of the remaining sediments. Figure 2.5(a) shows present day bathymetry and the depth to top basement, digitized from the IAM9 seismic profile (Dean et al., 2000) and Figure 2.5(b) shows the 'new' bathymetry and depth to top basement which have been corrected for sediment loading using flexural backstripping. Flexural backstripping and decompaction assumes shaly-sand compaction parameters during the removal of the sedimentary layer. Removal of the sedimentary layer along profile IAM9, results in a sediment corrected bathymetry that is approximately 1500m deeper than observations of present day bathymetry. The sediment corrected RDA along profile IAM9 (Figure 2.6(b)), is negative with a magnitude between -1000m and -1500m at the western end of the profile.

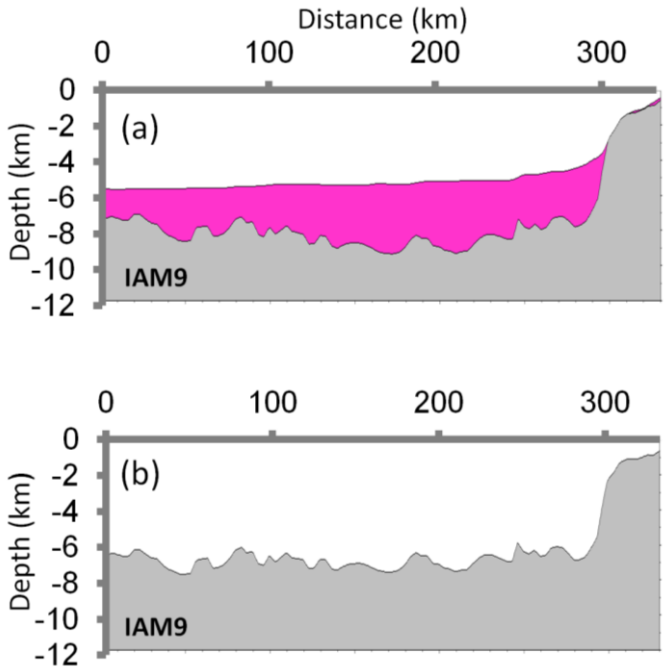

Figure 2.5 – 2D flexural backstripping comprises the successive removal of the sedimentary load and decompaction of the remaining sediments, considering the flexural isostatic response along profile IAM9. A Te=1.5km is assumed. (a) Present day depth section along the IAM9 profile, offshore Iberian Abyssal Plain. The sedimentary layer is highlighted in pink and the crust is in grey. (b) Flexurally backstripped to top basement with no thermal input to determine the sediment corrected bathymetry along IAM9.

Age predicted oceanic bathymetries, used to calculate the sediment corrected RDA, are dependent on the oceanic lithospheric age. The Müller et al. (2008) global ocean age isochrons do not extend the entire length of profile IAM9; it is therefore necessary to consider sensitivities to oceanic lithospheric age. Two approaches have been examined: the first uses a constant value of 120Ma for the profile, whilst the second uses Müller et al. (2008) age isochrons with their age gradient extrapolated inboard. A comparison and sensitivity of the sediment corrected RDA results to ocean age isochrons is shown in Figure 2.4(c), both approaches produce similar results.

The flexural backstripping process calculates the flexural isostatic response of the removed layer of sediments. Within this calculation the effective elastic thickness (Te) controlling the flexural strength of the lithosphere is considered. Te's between 1.5km and 5km have been

determined for syn-rift extensional settings (Roberts et al., 1998). Te depends on the bending stresses applied to the plate, the rate of stress application, the lithosphere composition and the geothermal gradient (Kusznir and Karner, 1985). The sensitivity to Te is shown for the Iberian Abyssal Plain sediment corrected RDA results in Figure 2.4(d); sensitivities to Te's of 1.5km, 5km and 10km have been examined. Te's of 1.5km, 5km and 10km produce sediment corrected RDAs of similar magnitude; a Te of 1.5km has been used due to the negligible difference in the magnitude of the sediment corrected RDAs.

2.3.2. RDA Component from Crustal Basement Thickness Variations (RDACT)

In addition to the RDA corrected for sediment loading, the RDA component from variations in crustal basement thickness (RDA_{CT}) has also been computed, which is the result of the presence of anomalously thick or thin crust. Crustal basement thicknesses from gravity anomaly inversion are used to predict departures from the average global oceanic crustal thickness of 7km (White et al., 1992). The RDA_{CT} has been computed using the difference between the gravity anomaly inversion predicted crustal basement thickness (tc_{grav}) and the average global oceanic crustal basement thickness (tc_{ref}) together with Airy isostasy. The local isostatic response to variation in gravity inverted non-continental crustal thickness, from the 7km global average oceanic crustal thickness (*tcref*) is given by:

$$\mathrm{RDA_{CT}} = \frac{(\mathrm{tc_{ref}} - \mathrm{tc_{grav}})(\rho_m - \rho_c)}{(\rho_m - \rho_{infil})} \quad (3)$$

where ρ_m is the density of the mantle (3300kgm^{-3}), ρ_c is the density of the crust (2850kgm^{-3}) and ρ_{infill} is the density of the water infill (1000kgm^{-3}). Crust, which is approximately 7km thick, will have a corresponding RDA_{CT} of zero. A positive RDA_{CT} reflects crust that is thicker than 7km, whereas if the RDA_{CT} is negative, this corresponds to crust that is thinner than 7km or the presence of exhumed mantle.

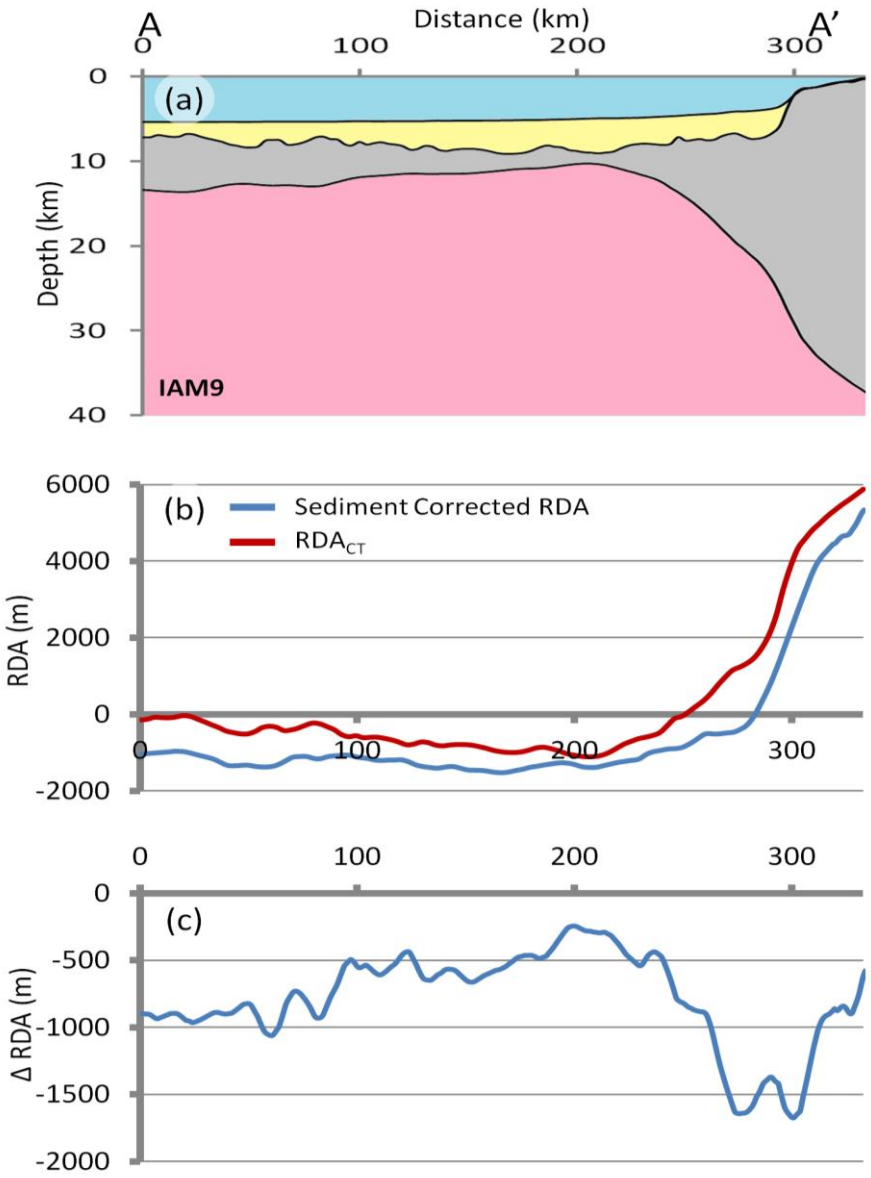

Figure 2.6 - (a) Crustal cross section A-A' along the IAM9 profile. (b) Sediment corrected RDA and the RDA component from crustal thickness variations (RDA_{CT}) along IAM9. Both the sediment corrected RDA and the RDA_{CT} are negative; the sediment corrected RDA ranges between -1500m and -1000m, whereas the RDA_{CT} ranges between -500m and zero. (c) The negative sediment corrected RDA, further corrected for variations in crustal basement thickness (ΔRDA), implies mantle dynamic subsidence.

The RDA_{CT} along profile IAM9 (Figure 2.6(b)) ranges between zero and approximately -800m at the western end and central region of the profile, and becomes more negative before increasing and becoming positive over the continental crust.

2.3.3. Sediment Corrected RDA Further Corrected for Crustal Basement Thickness Variations (ΔRDA)

Figure 2.6(b) shows the sediment corrected RDA and the RDA_{CT} along profile IAM9, with reference to the crustal cross-section (Figure 2.6(a)). In unequivocal oceanic regions it is expected that the RDA signal, from both the sediment corrected RDA and the RDA_{CT}, will be constant and near zero, whereas for regions of thicker continental crust it is expected that the RDA signals will show a positive trend. Changes in the RDA signal may be used to identify the change in crustal type and hence locate the COB. Figure 2.6(b) shows that at the western end of the profile and in the peridotite ridge region the sediment corrected RDA ranges between -1000m and -1500m, implying either the presence of crust which is thinner than 7km, or anomalous subsidence. The RDA_{CT} ranges between zero and -800m at the western end of the profile, which becomes more negative in the peridotite ridge region, between -800m and -1000m; the negative RDA_{CT} corresponds to either the presence of crust, which is thinner than 7km, or the presence of exhumed mantle. Both the sediment corrected RDA and the RDA_{CT} along profile IAM9 are negative in the western and central region and show the same general trend along the profile although they have different magnitudes.

The difference (ΔRDA) between the sediment corrected RDA and the RDA_{CT} has been computed in order to determine whether there is any anomalous subsidence or uplift along the Iberian rifted continental margin.

$$\Delta\mathrm{RDA} = \text{sediment corrected RDA} - \mathrm{RDA_{CT}} \quad (4)$$

This difference (ΔRDA) corresponds to the sediment corrected RDA further corrected for variations in crustal thickness. A ΔRDA of zero implies that there is no anomalous uplift or subsidence at the margin, whereas a positive ΔRDA implies anomalous uplift and a negative ΔRDA implies anomalous subsidence along a margin. The ΔRDA (Figure 2.6(c)) along IAM9 is

between -300m and -1000m at the western end of the profile, which is equated to mantle dynamic subsidence.

2.4. Continental Lithosphere Thinning from Subsidence Analysis

Subsidence analysis has been used to determine the distribution of continental lithosphere thinning and the distal extent of continental crust in order to locate the inner and outer bounds of the OCT. Subsidence analysis involves the conversion of water loaded subsidence into continental lithosphere thinning factors, assuming McKenzie (1978). Flexural backstripping is used to give the sediment corrected bathymetry to top pre-rift and top oceanic crust. It is assumed that the initial datum of original continental pre-rift surface was at or near to sea level; therefore the sediment corrected bathymetry can be equated to water loaded subsidence. Water loaded subsidence is interpreted as the sum of initial (Si) and thermal (St) subsidence in the context of the McKenzie (1978) intra-continental rift model. A correction for magmatic addition due to adiabatic decompression (White and McKenzie, 1989) during continental rifting and seafloor spreading has been included and uses the same scheme as described earlier in the gravity anomaly inversion section. Magmatic addition from decompression melting results in thicker crust due to volcanic intrusion and extrusion, which isostatically reduces the initial subsidence as predicted by McKenzie (1978) and corresponds to the formation of oceanic crust. Magmatic addition also increases the thickness of the crust thinned by lithosphere stretching.

Initial subsidence corresponds to the isostatic response of the crustal thinning and thermal loads at the time of rifting, which is assumed to be instantaneous; whilst total subsidence corresponds to the isostatic response of the crustal thinning and thermal loads after a defined time in the post-rift. The Iberian rifted continental margin is the result of polyphase rifting between the North American and Iberian plates (Manatschal et al., 2001; Péron-

Pinvidic et al., 2007). Sensitivity tests using upper and lower bounds of the time of breakup (126 and 112 Ma) have been examined and the results are not significantly different. The crustal thinning load is assumed to be constant after rifting, while the thermal subsidence varies with time due to the dissipation of the syn-rift lithosphere thermal anomaly. Instantaneous rifting is assumed, which allows the comparison of the numerically calculated total subsidence from flexural backstripping with that analytically calculated using McKenzie (1978) modified for magmatic additions. Magmatic additions due to decompression melting modify the predicted relationship between thinning factor (γ) and water loaded subsidence. Water loaded subsidence is inverted using the curves (Figure 2.7(a)) to give continental lithosphere thinning factors.

Continental lithosphere thinning factors from subsidence analysis along profile IAM9 are shown in Figure 2.7(c). For the Iberian margin, a 'normal' magmatic solution (Va=7km), a magma-poor solution (Va=0km) and a solution for serpentinized mantle are examined. A 'normal' magmatic solution (Va=7km) predicts continental thinning factors of 1.0 at the western end of the profile whilst a solution for serpentinized mantle predicts continental thinning factors that range between 0.9 and 1.0 in this region. Variations in the continental lithosphere thinning factors predicted by the three solutions indicate that it is possible to use the sensitivities to magmatic addition to locate the extent of the exhumed mantle.

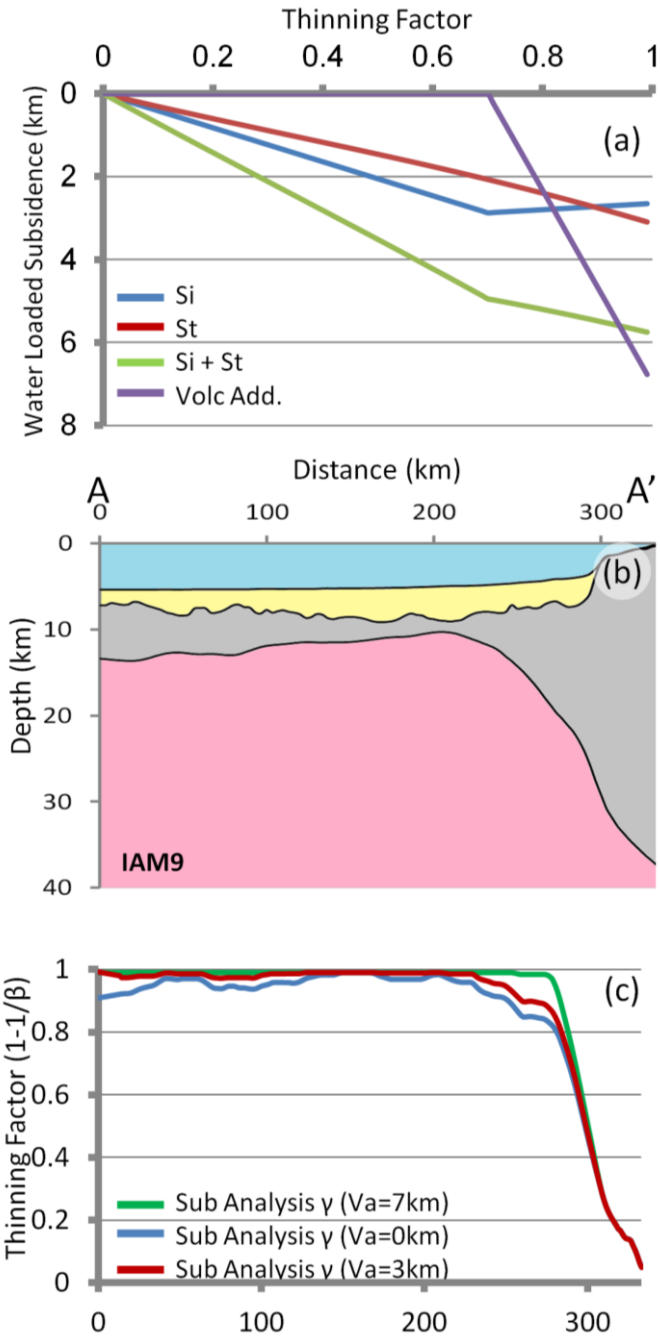

Figure 2.7 – Subsidence analysis involves the conversion of water loaded subsidence into continental lithosphere thinning factors, assuming McKenzie (1978), and is modified to incorporate the isostatic consequence of magmatic addition. (a) Water loaded subsidence as a function of lithosphere thinning factor (γ). Initial subsidence (Si) is shown in blue, the time dependent thermal subsidence (St) is shown in red, the combined total subsidence (Si+St) is shown in green and the sensitivity to magmatic addition (assuming a 'normal' magmatic solution) is shown in purple. (b) Crustal cross section along profile IAM9. (c) Continental lithosphere thinning factors from subsidence analysis along IAM9. Sensitivities to a 'normal' magmatic solution (Va=7km), a magma-poor solution (Va=0km) and a solution for serpentinised mantle have been examined.

Changes in continental lithosphere thinning factors calculated from subsidence analysis, from high thinning factors (between 0.8 and 1.0) to lower thinning factors can be used to determine the distribution of continental lithosphere thinning and further constrain the COB location along profile IAM9. The quantitative analytical method assumes depth uniform stretching and thinning, as a consequence thinning factors for continental lithosphere and crust are identical.

2.5. OCT Structure and COB Location along the Lusigal 12 Profile

2.5.1. Crustal Basement Thickness and Continental Lithosphere Thinning along Lusigal 12 from Gravity Anomaly Inversion

Gravity anomaly inversion has been applied to the Lusigal 12 profile (with the TGS-extension (Sutra and Manatschal, 2012)) in order to determine the crustal basement thickness, Moho depth and continental lithosphere thinning along profile. Within the gravity anomaly inversion the calibrated reference Moho depth of 41km, from IAM9, has been assumed to be applicable due to the proximity of Lusigal 12 to IAM9. Crustal cross section (B-B') along profile Lusigal 12 (Figure 2.8(b)) is constructed using bathymetry, sediment thickness (Sutra and Manatschal, 2012) (Figure 2.8(a)) and predicted Moho depths from gravity anomaly inversion. Using the calibrated reference Moho depth of 41km, the gravity anomaly inversion predicts thin crust between 2km and 4km at the western end of the profile.

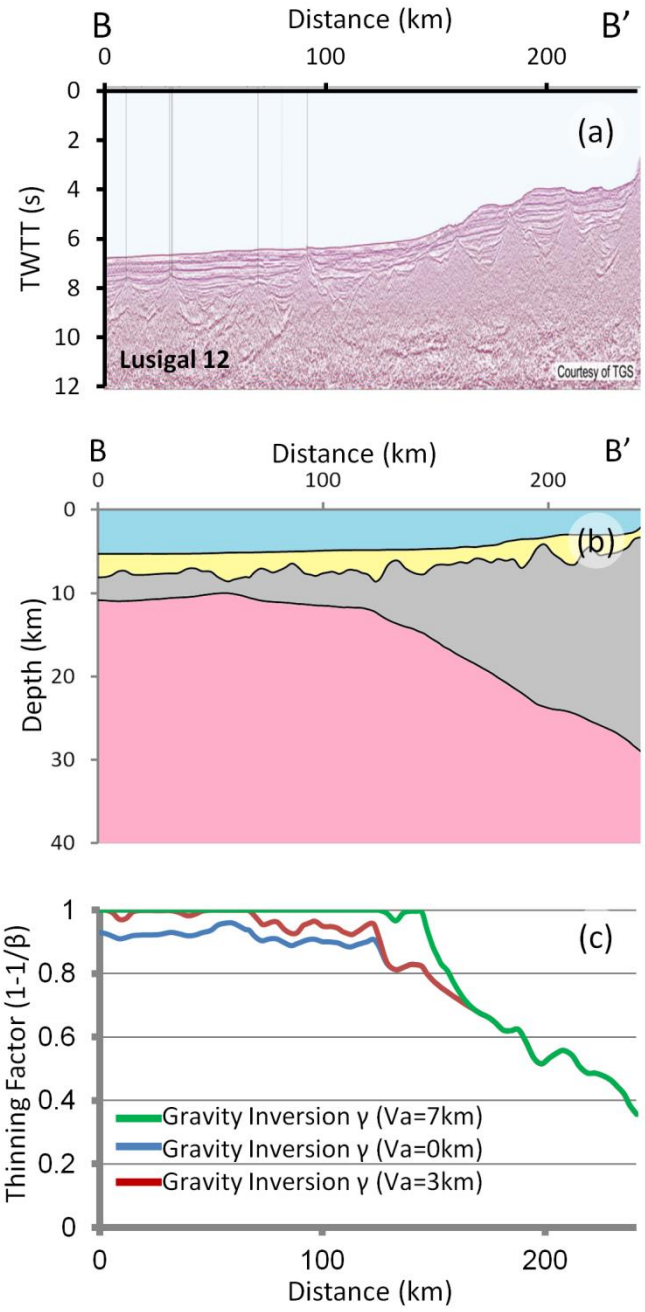

Figure 2.8 - (a) 2D seismic reflection profile (Sutra and Manatschal 2012) for Lusigal 12 (with the TGS extension). (b) Crustal cross section B-B' across Iberian Abyssal Plain, from gravity anomaly inversion. (c) Continental lithosphere thinning predicted from gravity anomaly inversion along Lusigal 12. Sensitivities to a 'normal' magmatic solution (Va=7km), a magma-poor solution (Va=0km) and a solution for serpentinised mantle have been examined. A 'normal' magmatic solution predicts thinning factors of 1.0 at the western end of the profile, the solution for serpentinized mantle predicts thinning factors that increase from 0.9 to 1.0 in this region, whereas a magma-poor solution predicts thinning factors of 0.8.

Continental lithosphere thinning factors (γ) predicted from gravity anomaly inversion are shown in Figure 2.8(c). Sensitivities to a magma-poor solution (Va=0 km), a 'normal' magmatic solution (Va=7 km) and a solution for serpentinized mantle have been examined. Continental lithosphere thinning factors from gravity anomaly inversion show high thinning factors for all three solutions at the western end of the profile. At the western end of the profile, the 'normal' magmatic solution and the serpentinized mantle solution predict continental lithosphere thinning factors of a similar magnitude (approximately 1.0) indicating no continental lithosphere remains, whereas the magma-poor solution predicts continental lithosphere thinning factors of 0.9 for the same region.

2.5.2. RDAs corrected for Sediment Loading and Crustal Basement Thickness Variations along Lusigal 12

Sediment corrected RDAs and RDA_{CT} have been computed along the Lusigal 12 profile as shown in Figure 2.9(a) and show the same general trend, however, with varying magnitudes. The sediment corrected RDA ranges between -500m and -1500m in the west, implying that the presence of crust which is thinner than 7km or anomalous subsidence. At the western end of the profile, the RDA_{CT} ranges between -800m and -1000m, corresponding to either the presence of crust which is thinner than 7km, or the presence of exhumed mantle. Figure 2.9(c) shows the ΔRDA plot for Lusigal 12, which illustrates the sediment corrected RDA further corrected for crustal basement thickness variations. The ΔRDA ranges between zero and -500m implying that there is anomalous subsidence along Lusigal 12, which is in agreement with the anomalous subsidence predicted by RDA analysis along profile IAM9, the other profile in the Iberian Abyssal Plain.

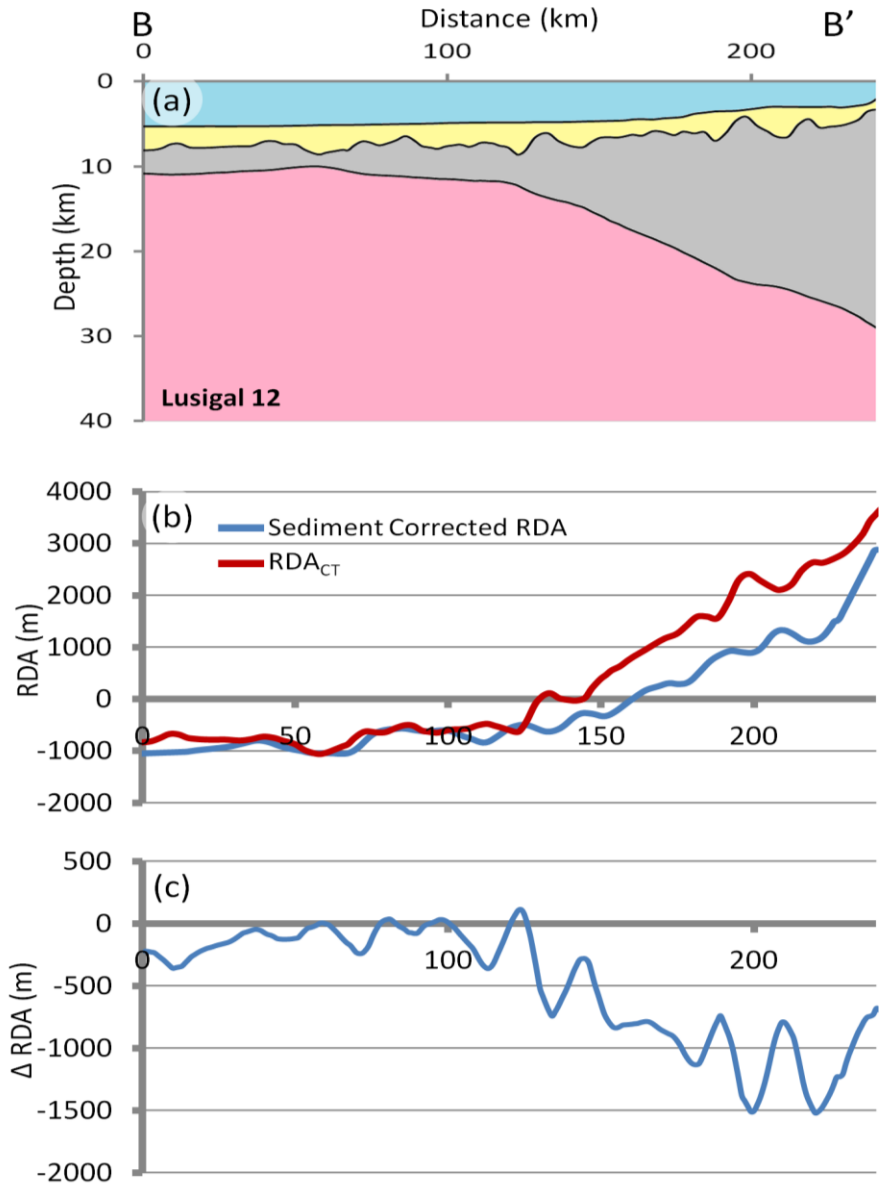

Figure 2.9 - (a) Crustal cross section B-B' along Lusigal 12. (b) Sediment corrected RDA and the RDA component from crustal thickness variations (RDA_{CT}) along Lusigal 12. Both the sediment corrected RDA and the RDA_{CT} are negative; the sediment corrected RDA ranges between -1500m and -500m, whereas the RDA_{CT} ranges between -1000m and -800. (c) The sediment corrected RDA, further corrected for variations in crustal basement thickness (ΔRDA), is negative implying mantle dynamic subsidence.

2.5.3. Continental Lithosphere Thinning from Subsidence Analysis along Lusigal 12

Continental lithosphere thinning factors determined from subsidence analysis are shown in Figure 2.10(b); at the western end of the Lusigal 12 profile, continental lithosphere thinning

factors from subsidence analysis are between 0.85 and 1.0, indicative of oceanic crust or possibly exhumed mantle. Sensitivities to the three magmatic solutions have been examined. Assuming a 'normal' magmatic solution, subsidence analysis predicts continental lithosphere thinning factors of 1.0 at the western end of the profile, indicating the presence of oceanic crust. The magma-poor (Va=0km) solution and the solution for serpentinized mantle are of similar magnitude, with negligible difference between them, and predict continental lithosphere thinning factors that range between 0.9 and 1.0. The negligible difference between the solution for serpentinized mantle and a magma-poor (Va=0km) solution implies the presence of exhumed mantle.

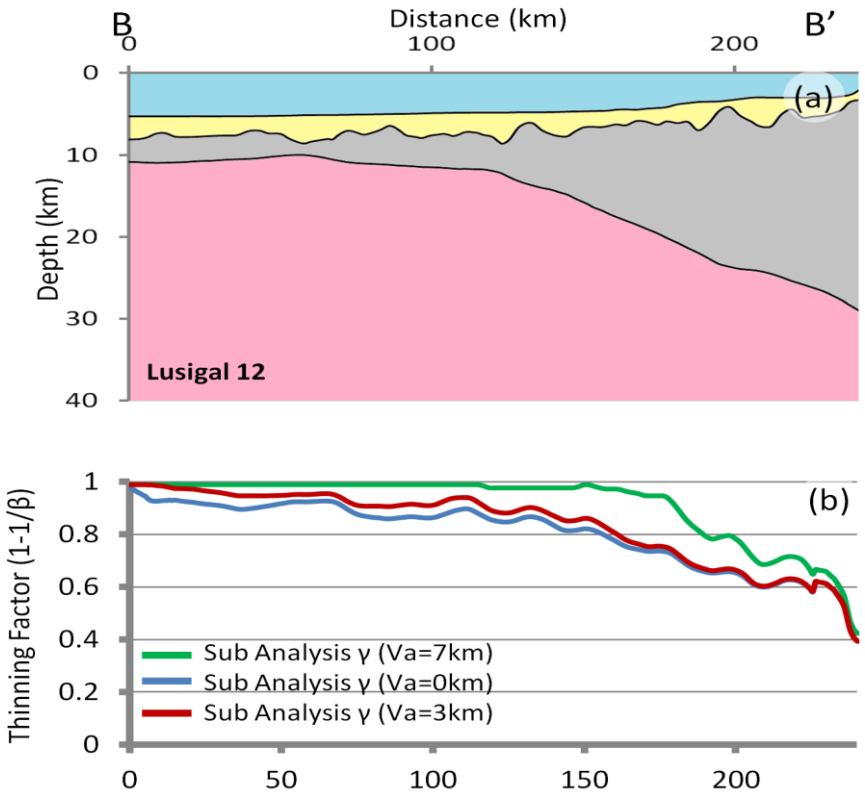

Figure 2.10 - (a) Crustal cross section along Lusigal 12. (b) Continental lithosphere thinning factors from subsidence analysis along Lusigal 12. Sensitivities to a 'normal' magmatic solution (Va=7km), a magma-poor solution (Va=0km) and a solution for serpentinised mantle have been examined. A 'normal' magmatic addition predicts thinning factors of 1.0 at the western end of the profile, the solution for serpentinized mantle and a magma-poor (Va=0km) solution predict thinning factors between 0.9 and 1.0 in this region.

2.6. OCT Structure and COB Location along Profile ISE-01

2.6.1. Crustal Basement Thickness and Continental Lithosphere Thinning along ISE-01 from Gravity Anomaly Inversion

Gravity anomaly inversion has been applied in order to determine crustal basement thickness, Moho depth and continental lithosphere thinning along profile ISE-01. Sediment thicknesses (Figure 2.11(a)) used in the gravity anomaly inversion are from Shipley et al. (2005). Sensitivities to reference Moho depths have been examined within the gravity anomaly inversion along profile ISE-01, reference Moho depth sensitivities of 35km, 37.5km and 40km are shown in Figure 2.11(b). A reference Moho depth of 35km is too small and predicts a Moho which is too shallow and comes up into the sediments at the start of the profile, whereas both reference Moho depths of 37.5km and 40km predict more sensible Moho depths; calibration of the reference Moho depth is therefore required. Zelt et al. (2003) uses two different methods in an attempt to determine the depth of the Moho along the ISE-01 profile, however, the Moho remains unresolved and the estimated Moho depths from Zelt et al. (2003) are very shallow under Galicia Bank and the Galicia Interior Basin, possibly indicating the presence of exhumed mantle. Calibration of Moho depths should only be done on unequivocal oceanic crust (or continental crust); ODP wells along ISE-01 do not observe oceanic crust, so calibration of the reference Moho depth along ISE-01 has not been possible. Crustal cross section (C-C') along ISE-01 (Figure 2.11(c)) is constructed using bathymetry, sediment thickness and Moho depths from gravity anomaly inversion. Using the calibrated reference Moho depth of 41km, from profile IAM9, the gravity anomaly inversion predicts thin crust, between 4km and 5km at the start of the profile.

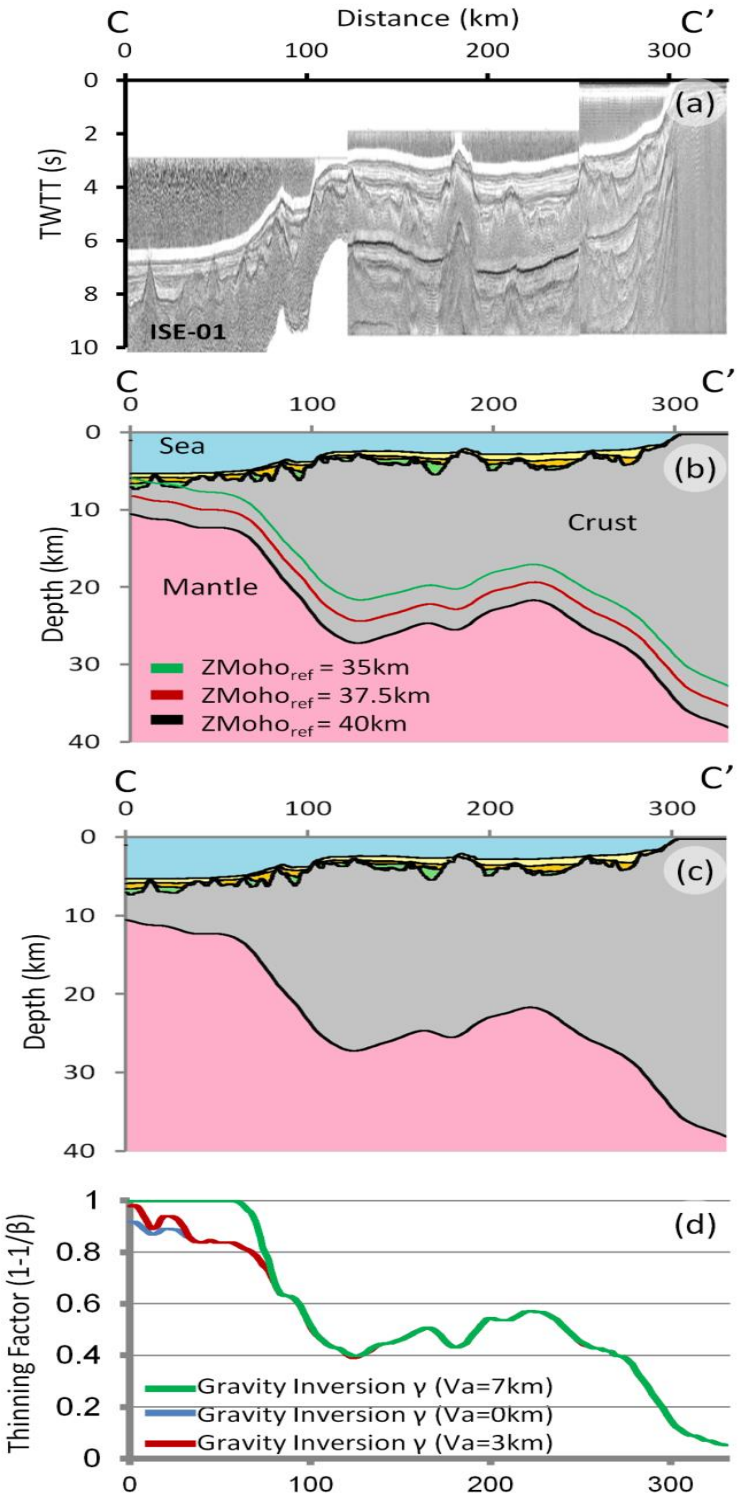

Figure 2.11 - (a) 2D seismic reflection data (Shipley et al. 2005) along profile ISE-01. (b) Crustal cross section (C-C') along ISE-01 showing Moho depths predicted from gravity anomaly inversion, using reference Moho depths of 35km, 37.5km and 40km. (c) Crustal cross section (C-C') along profile ISE-01 using the calibrated reference Moho depth of 41km. (d) Continental lithosphere thinning from gravity anomaly inversion along profile ISE-01. Sensitivities to a 'normal' magmatic solution (Va=7km), a magma-poor solution (Va=0km) and a solution serpentinised mantle have been examined. A 'normal' magmatic solution predicts thinning factors of 1.0 at the western end of the profile, using a solution for serpentinized mantle predicts thinning factors that increase from 0.8 to 1.0 in this region.

Figure 2.11(d) shows continental lithosphere thinning factor (γ) estimates from gravity anomaly inversion for profile ISE-01 assuming a magma-poor model (Va=0 km); a 'normal' magmatic solution (Va=7 km) and a solution for serpentinized mantle. Continental lithosphere thinning factors from gravity anomaly inversion show high values of thinning factors for all three magmatic solutions at the western end of the profile. A 'normal' magmatic solution (Va=7km) predicts thinning factors of 1.0 at the western end of the profile, whereas a solution for serpentinized mantle predicts thinning factors that increase from 0.8 to just less than 1.0 and a magma-poor solution predicts thinning factors that increase from 0.8 to 0.9 in the same region.

2.6.2. RDAs Corrected for Sediment Loading and Crustal Basement Thickness Variations along ISE-01

At the western end of the ISE-01 profile, the sediment corrected RDA ranges between zero and -800m (Figure 2.12(b)), which implies either the presence of crust, which is thinner than 7km or anomalous subsidence. The RDA_{CT} ranges between zero and -1000m (Figure 2.12(b)), which corresponds to the presence of crust, which is thinner than 7km, or the presence of exhumed mantle. The sediment corrected RDA and the RDA_{CT} along profile ISE-01 (Figure 2.12(b)) show the same general trend. The sediment corrected RDA further corrected for variations in crustal basement thickness (ΔRDA) (Figure 2.12(c)) is approximately zero implying that there is negligible anomalous subsidence or uplift at Galicia Bank.

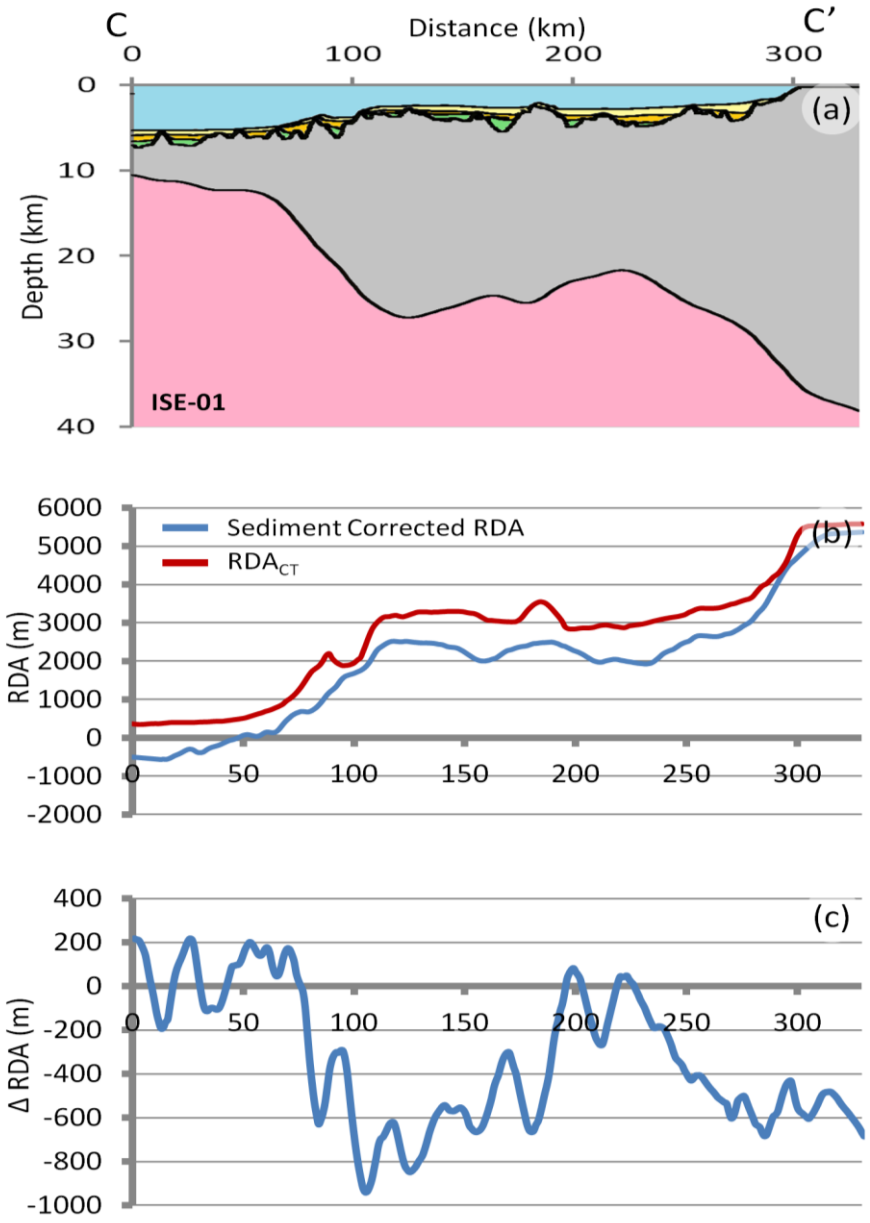

Figure 2.12 - (a) Crustal cross section C-C' along ISE-01. (b) Sediment corrected RDA and the RDA component from crustal thickness variations (RDA$_{CT}$) along ISE-01. Both the sediment corrected RDA and the RDA$_{CT}$ are negative; the sediment corrected RDA ranges between -800m and zero, whereas the RDA$_{CT}$ ranges between -1000m and zero. (c) The sediment corrected RDA, further corrected for variations in crustal basement thickness (ΔRDA), is zero at the western end of the profile implying that there is no mantle dynamic topography.

2.6.3. Continental Lithosphere Thinning from Subsidence Analysis along ISE-01

Continental lithosphere thinning factors determined from subsidence analysis (Figure 2.13(b)) range between 0.8 and 0.9 at the western end of the ISE-01 profile. Sensitivities to a 'normal' solution (Va=7km), a magma-poor solution (Va=0km) and a solution for

serpentinised mantle have been examined. A 'normal' magmatic solution predicts continental lithosphere thinning factors of 1.0 at the western end of the profile; the solution for serpentinized mantle and a magma-poor solution are of similar magnitude, with negligible difference between them, and predict thinning factors that range between 0.9 and just less than 1.0 in the west implying the presence of exhumed mantle.

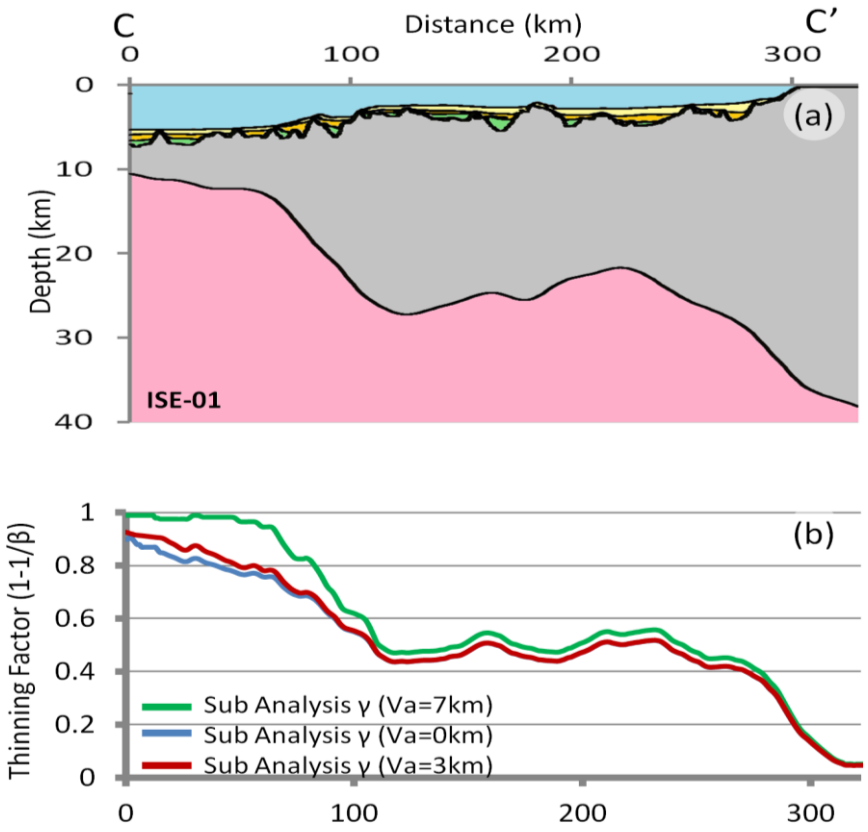

Figure 2.13 - (a) Crustal cross section along profile ISE-01. (b) Continental lithosphere thinning factors predicted from subsidence analysis, along profile ISE-01. Sensitivities to a 'normal' magmatic solution (Va=7km), a magma-poor solution (Va=0km) and a solution for serpentinised mantle have been examined. A 'normal' magmatic addition predicts thinning factors of 1.0 at the western end of the profile, the solution for serpentinized mantle and a magma-poor (Va=0km) solution predict thinning factors between 0.8 and 0.9 in this region.

2.7. Predicting OCT Structure and COB Location

The previous sections have shown the results from integrated quantitative analysis using gravity anomaly inversion, RDA and subsidence analysis, applied to IAM9 and Lusigal 12 in the Iberian Abyssal Plain and ISE-01 on Galicia Bank. Gravity anomaly inversion has been used to predict Moho depth and crustal basement thickness, whilst departures from the standard oceanic water depths are derived from RDA analysis. Continental lithosphere thinning factors are determined from both subsidence analysis and gravity anomaly inversion. These techniques may all be used to predict the transition from continental to oceanic crust. However, the results from each technique need to be examined together, to constrain our interpretation of the OCT structure, COB location and magmatic type of the Iberian margin. For each of the three profiles considered a composite analysis plot is used to summarize the results from gravity anomaly inversion, RDA analysis and subsidence analysis, as shown in Figures 2.14, 2.15 and 2.16. The composite analysis plot consists of (i) a crustal cross section from gravity anomaly inversion, (ii) sediment corrected RDA and RDA_{CT} along profile and (iii) a comparison of the continental lithosphere thinning factors predicted from gravity anomaly inversion and subsidence analysis. The analysis of the composite plot allows for an informative interpretation of the OCT structure, COB location and magmatic type to be made, when the crustal domains are clearly defined.

As previously mentioned the Iberian rifted continental margin is one of the most studied rifted continental margins world-wide due to the abundant observational data available in the form of seismic reflection and refraction surveys (Manatschal et al., 2010) and deep sea drilling (ODP Legs 103, 149 and 173) (Boillot et al., 1987; Sawyer et al., 1994; Tucholke et al., 2007; Whitmarsh et al., 1998; Whitmarsh and Sawyer, 1996). Using ODP wells, located along the Lusigal 12 and ISE-01 profiles, it has been possible to compare the predicted OCT

structure and COB location determined from integrated quantitative analysis with that inferred from direct well observations.

2.7.1. IAM9

The composite analysis plot for profile IAM9 in the Iberian Abyssal Plain (Figure 2.14) is interpreted as showing three distinct crustal zones: zone A - oceanic crust; zone B - serpentinised exhumed mantle; and zone C - thinned continental crust. The location of each of these three zones is based on crustal basement thickness from gravity anomaly inversion, variations in the RDA signal from the sediment corrected RDA and RDA_{CT}, and continental lithosphere thinning factors derived from subsidence analysis and gravity anomaly inversion.

We have examined the relationship between our interpretations of the boundaries between these three crustal zones to those proposed in the literature, in particular the J anomaly. The J anomaly is a structural ridge or step in the oceanic basement that lies beneath the J magnetic anomaly (Tucholke and Ludwig, 1982). Whilst the J anomaly and the interfaces between zones A and B and zones B and C are shown as sharp lines, in reality they are likely to be transitional boundaries. The J anomaly is identified at approximately 25km distance along the IAM9 profile (Figure 2.14(a)) (Bronner et al., 2011; Dean et al., 2000; Whitmarsh et al., 2001), and corresponds to inflection points in Moho depth, RDA signal and continental lithosphere thinning factors, determined assuming magma-poor solution, and is west of our interpreted COB.

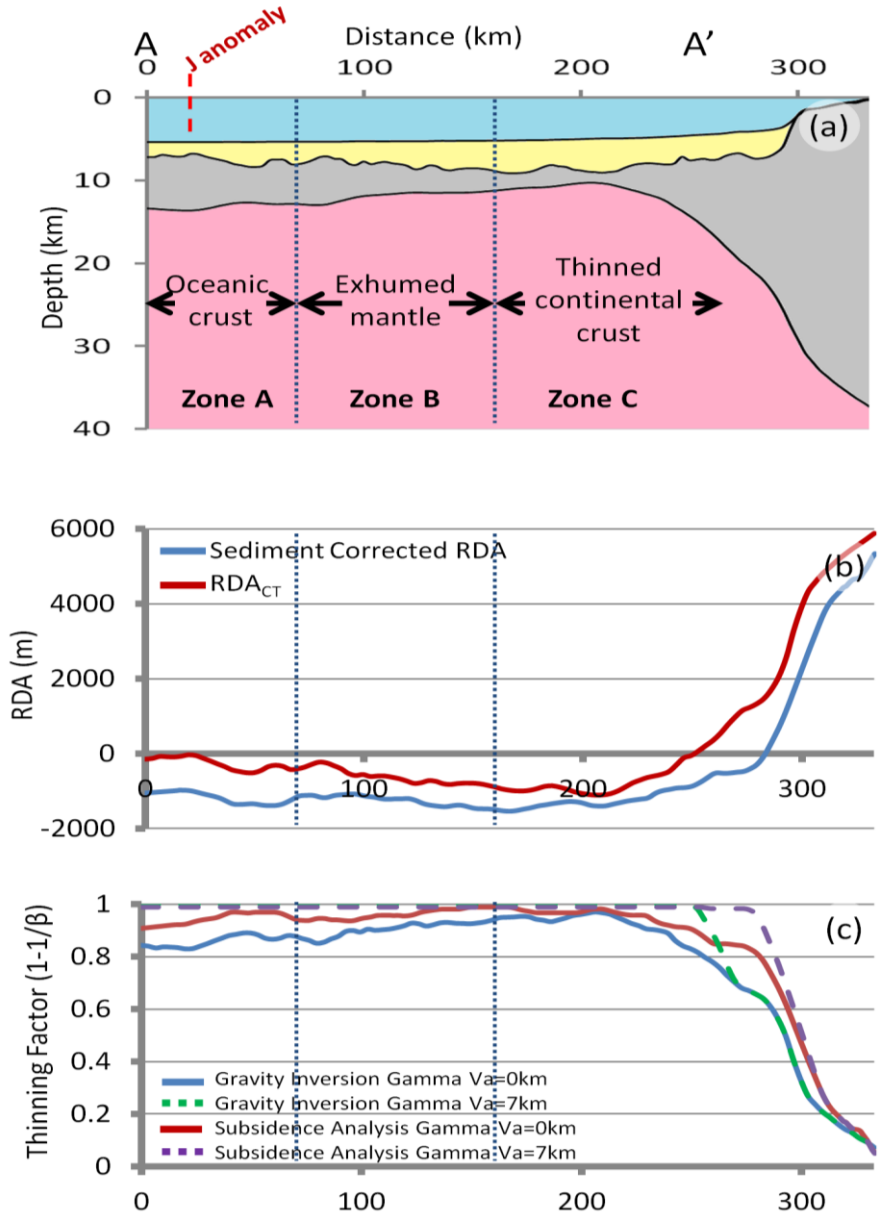

Figure 2.14 – Composite analysis plot along IAM9, showing interpretations of crustal zones made from the integrated quantitative analysis. (a) Crustal cross section along profile IAM9 (A-A') from gravity anomaly inversion (b) Sediment corrected RDA and the RDA component from crustal thickness variations (RDA_{CT}) along IAM9. (c) Continental lithosphere thinning factors from subsidence analysis and gravity anomaly inversion assuming a magma-poor solution. The inner dashed line indicates the distal extent of unequivocal continental crust (possible interpretation of the COB) and its boundary with exhumed mantle, whilst the outer dashed line indicates the boundary between exhumed mantle and oceanic crust. The location of the J anomaly is indicated in red.

Zone A – oceanic crust

In zone A, the crustal basement thicknesses from gravity anomaly inversion are between 6km and 7km. The sediment corrected RDA and RDA_{CT} are both negative in this region. The negative sediment corrected RDA is indicative of crust which is thinner than 7km or anomalous subsidence, whilst the negative RDA_{CT} corresponds to the presence of thin crust derived from gravity anomaly inversion. The continental lithosphere thinning factors in zone A derived from gravity anomaly inversion and subsidence analysis using 'normal' magmatic solution (Va=7km) are 1.0, implying the presence of oceanic crust. If a magma-poor solution (Va=0km) is assumed, the thinning factors range between 0.85 and 1.0, which implies very thin continental crust or serpentinised exhumed mantle. However, at the western end of zone A, a 'normal' magmatic solution is preferred.

The interface between zones A and B corresponds to the boundary between oceanic crust and serpentinised exhumed mantle and is located by the inflection points in Moho depth, RDA signal and continental lithosphere thinning factors determined assuming magma-poor solution.

Zone B – exhumed mantle

In zone B, the crustal basement thicknesses decrease from 7km in the west to approximately 3km at the eastern end of the zone. These very low values of crustal basement thicknesses are apparent crustal thicknesses derived from the mass deficiency of serpentinised exhumed mantle with respect to unserpentinized mantle below and are interpreted as being indicative of serpentinised exhumed mantle. The very low crustal thicknesses derived from gravity anomaly inversion are not interpreted as very thin continental or oceanic crust. Sediment corrected RDA and RDA_{CT} are both negative in zone B, corresponding to the presence of crust, which is thinner than 7km or anomalous subsidence. The continental lithosphere thinning

factors from gravity anomaly inversion and subsidence analysis range between 0.9 and 1.0 assuming a magma-poor solution, whereas similarly to zone A, a 'normal' magmatic solution predicts thinning factors of 1.0.

The interface between zones B and C corresponds to the boundary between thinned continental crust and exhumed mantle and is located by the inflection points in Moho depth, RDAs and continental lithosphere thinning factors determined assuming magma-poor solution. Gravity anomaly inversion, RDA and subsidence analysis results show that the OCT along IAM9 is relatively narrow, with the distance between the COB and the margin hinge (the point at which the continental crust starts to thin) measuring approximately 100km.

Zone C- thinned continental crust

In zone C, the crustal basement thicknesses increase gradually to approximately 35km at the eastern end of the profile, although the poor resolution of sediment thickness in this region may result in an overestimate of Moho depth. Both the sediment corrected RDA and RDA_{CT} increase eastwards. The continental lithosphere thinning factors from gravity anomaly inversion and subsidence analysis show a corresponding eastwards decrease. Continental lithosphere thinning factors predicted from gravity anomaly inversion are generally in good agreement with the continental lithosphere thinning factors predicted from subsidence analysis. At the eastern end of the profile, zone C, a magma-poor solution is preferred.

2.7.2. Lusigal 12

The composite analysis plot for the Lusigal 12 profile in the Iberian Abyssal Plain (Figure 2.15) is interpreted as showing two distinct crustal zones: zone B - serpentinised exhumed mantle; and zone C - thinned continental crust. No unequivocal oceanic crust of normal thickness (corresponding to zone A on the IAM9 profile) is evident on Lusigal 12. The interpretation of

the zones of serpentinised exhumed mantle and thinned continental crust, and their boundary, along Lusigal 12 can be validated against ODP well data.

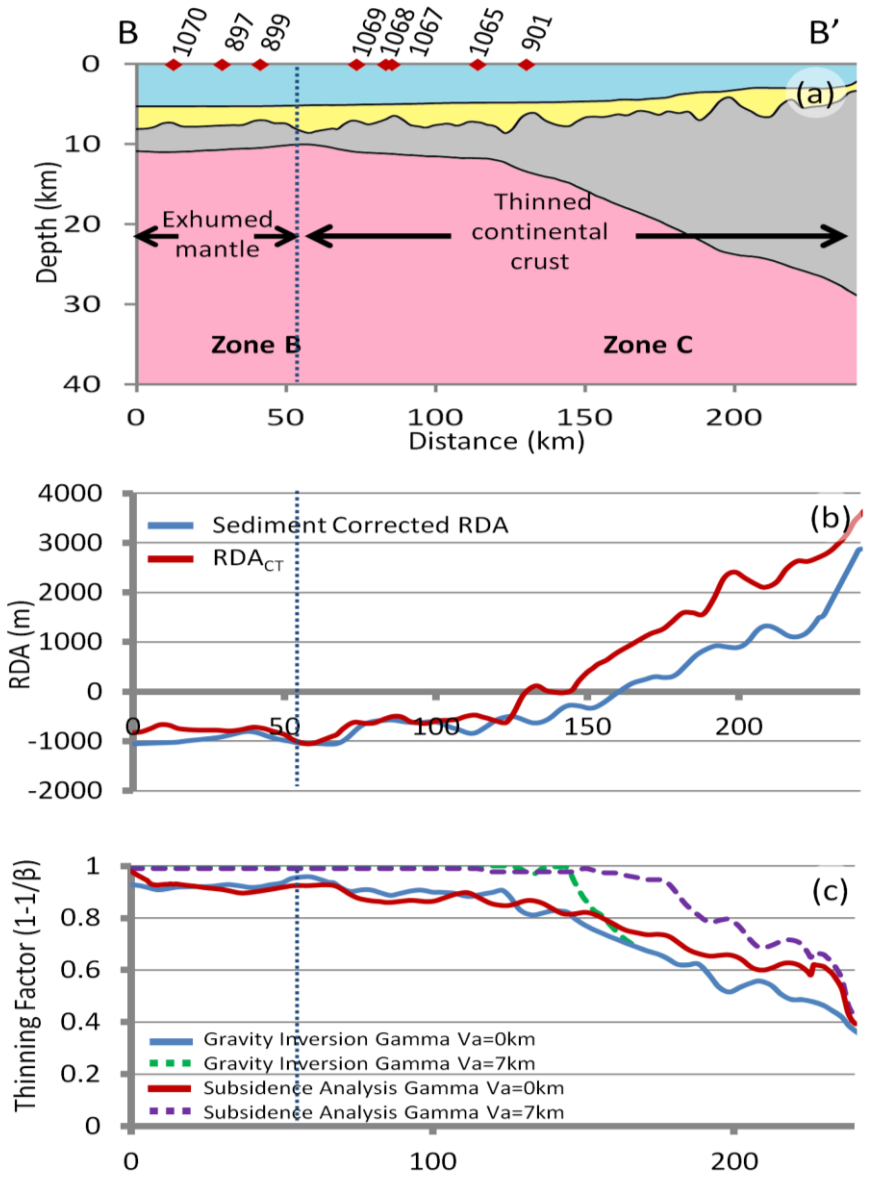

Figure 2.15 - Composite analysis plot along Lusigal 12 (with TGS-extension) showing interpretations of crustal zones made from the integrated quantitative analysis, which have been compared to observations from ODP well data. (a) Crustal cross section along profile Lusigal 12 (B-B') from gravity anomaly inversion. Locations of the ODP wells are indicated. (b) Sediment corrected RDA and the RDA component from crustal thickness variations (RDA_{CT}) along Lusigal 12. (c) Continental lithosphere thinning factors from subsidence analysis and gravity anomaly inversion assuming a magma-poor solution. The dashed line indicates the distal extent of unequivocal continental crust and its boundary with exhumed mantle, which could be interpreted as the COB.

Zone B – exhumed mantle

In zone B, the crustal basement thicknesses predicted, from gravity anomaly inversion, range between 2km and 4km (Figure 2.15(a)). These very low values of crustal thickness are interpreted as being indicative of serpentinised exhumed mantle (see earlier discussion for IAM9). Both the sediment corrected RDA and RDA_{CT} are negative in this region, ranging between -500m and -1500m (Figure 2.15(b)). The sediment corrected RDA is negative between -500m and -1500m, implying that the crust in this region is less than 7km or that there is anomalous subsidence. The RDA_{CT} ranges between -800m and -1000m, corresponding to the presence of thin crust or serpentinised exhumed mantle. The continental lithosphere thinning factors are high in zone B (Figure 2.15(c)); if a 'normal' magmatic solution (Va=7km) is assumed, the continental lithosphere thinning factors from gravity anomaly inversion and subsidence analysis are 1.0, implying the presence of oceanic crust. If a magma-poor solution is assumed, continental lithosphere thinning factors from subsidence analysis and gravity anomaly inversion range between 0.8 and 1.0 with an average of approximately 0.9, implying either very thin continental crust or serpentinised exhumed mantle. Continental lithosphere thinning factors predicted from gravity anomaly inversion and subsidence analysis are generally in good agreement. For zone B, a magma-poor solution is preferred, as it predicts high thinning factors without the requirement of magmatic addition (and the formation of oceanic crust).

The COB, corresponding to the interface between zones B and C, is located by the inflection points in Moho depth, RDAs and continental lithosphere thinning factors determined assuming magma-poor magmatic solution. Gravity anomaly inversion, RDA analysis and subsidence analysis results show that the OCT along Lusigal 12 is wider than that for IAM9, with the distance between the COB and the margin hinge measuring more than 150km.

Zone C - thinned continental crust

In zone C, crustal thicknesses predicted from gravity anomaly inversion increase eastwards towards the continent, as do the sediment corrected RDAs and RDA_{CT}, whilst the continental lithosphere thinning factors from gravity anomaly inversion and subsidence analysis decrease (Figure 2.15). This is indicative of zone C corresponding to thinned continental crust. A magma-poor solution for the prediction of RDA and continental lithosphere thinning factors is preferred for this zone.

Comparison with ODP well observations

Observations from the ODP drill logs (897, 899, 901, 1065, 1067, 1068, 1069 and 1070) along Lusigal 12 are shown in Table 2.1; these observations have been compared to our interpretations made from integrated quantitative analysis are shown on the composite analysis plot for Lusigal 12 (Figure 2.15). The ODP well logs (1070, 899 and 897), in zone B, show the presence of serpentinized peridotite, serpentinite, serpentinized plagioclase, breccia and mantle, which are in agreement with our interpretation of the composite analysis plots which indicate the presence of exhumed mantle in this zone. The ODP wells (1069, 1068, 1067, 1065 and 901), in zone C, indicate the presence of pre-tectonic outer-shelf carbonates, which suggest the occurrence of upper crust, which is in agreement with our interpretations of the composite analysis plot.

ODP Well	Depth (m)	Description
1070	719	Serpentinized peridotite
897	837	Serpentinized mantle
899	562	Serpentinized breccias
1069	959	Carbonates, upper crust
1068	956	Serpentinised peridotite (overlain by polymict breccias)
1067	856	Amphibolite, Minor tonalite, Meta-gabbros
1065	631	Pre-tectonic sediments (carbonates) over upper crust
901	248	Pre-tectonic sediments (carbonates) over upper crust

Table 2.1 – ODP well observations along Lusigal 12 (Boillot et al., 1987; Sawyer et al., 1994; Tucholke et al., 2007; Whitmarsh et al., 1998; Whitmarsh and Sawyer, 1996).

2.7.3. ISE-01

Interpretation of the composite analysis plots of profile ISE-01 on Galicia Bank (Figure 2.16) suggests that there are two crustal zones along the profile; these are zones B and C. Zone B is interpreted as thin oceanic crust (which may correspond to proto-oceanic crust) or exhumed mantle and zone C is interpreted as thinned continental crust. These interpretations, based on gravity anomaly inversion, RDA and subsidence analysis, are consistent with ODP well data on profile ISE-01. As with Lusigal 12, no unequivocal oceanic crust of normal thickness (corresponding to zone A on the IAM9 profile) is evident on ISE-01.

Zone B – exhumed mantle

In zone B at the western end of the profile, crustal basement thicknesses, from gravity anomaly inversion, range between 4km and 5km and RDA analysis shows negative sediment corrected RDAs and RDA_{CT} in this region. The low values of crustal thickness from gravity anomaly inversion in this region (and the resulting RDA_{CT} ranging between zero and -1000m)

are interpreted as being indicative of serpentinised exhumed mantle (see earlier discussion for IAM9). The sediment corrected RDA (Figure 2.16(b)) ranges between zero and -800m, which implies either the presence of crust, which is thinner than 7km, or anomalous subsidence. In zone B, if a 'normal' magmatic solution (Va=7km) is assumed, the continental lithosphere thinning factors from gravity anomaly inversion and subsidence analysis are 1.0, implying the total absence of continental crust. If a magma-poor solution is assumed (Va=0km), the continental lithosphere thinning factors are high, approximately 0.9, indicating the near absence of continental crust even without magmatic addition and consistent with the presence of serpentinised exhumed mantle.

The COB for profile ISE-01 is interpreted as being at the interface between zones B and C and corresponds to inflection points in Moho depth, RDA and continental lithosphere thinning factors determined assuming magma-poor solution. In contrast to profiles IAM9 and Lusigal 12, ISE01 shows a very broad region between margin hinge and COB; the distance separating these is of the order 250 km.

Zone C - thinned continental crust

In zone C, the crustal basement thickens and the RDA values increase eastwards towards the continent. These and the corresponding decrease in continental lithosphere thinning factors imply the presence of thinned continental crust in this zone. Continental lithosphere thinning factors predicted from gravity anomaly inversion are in good agreement with those predicted from subsidence analysis as shown in Figure 2.16(c).

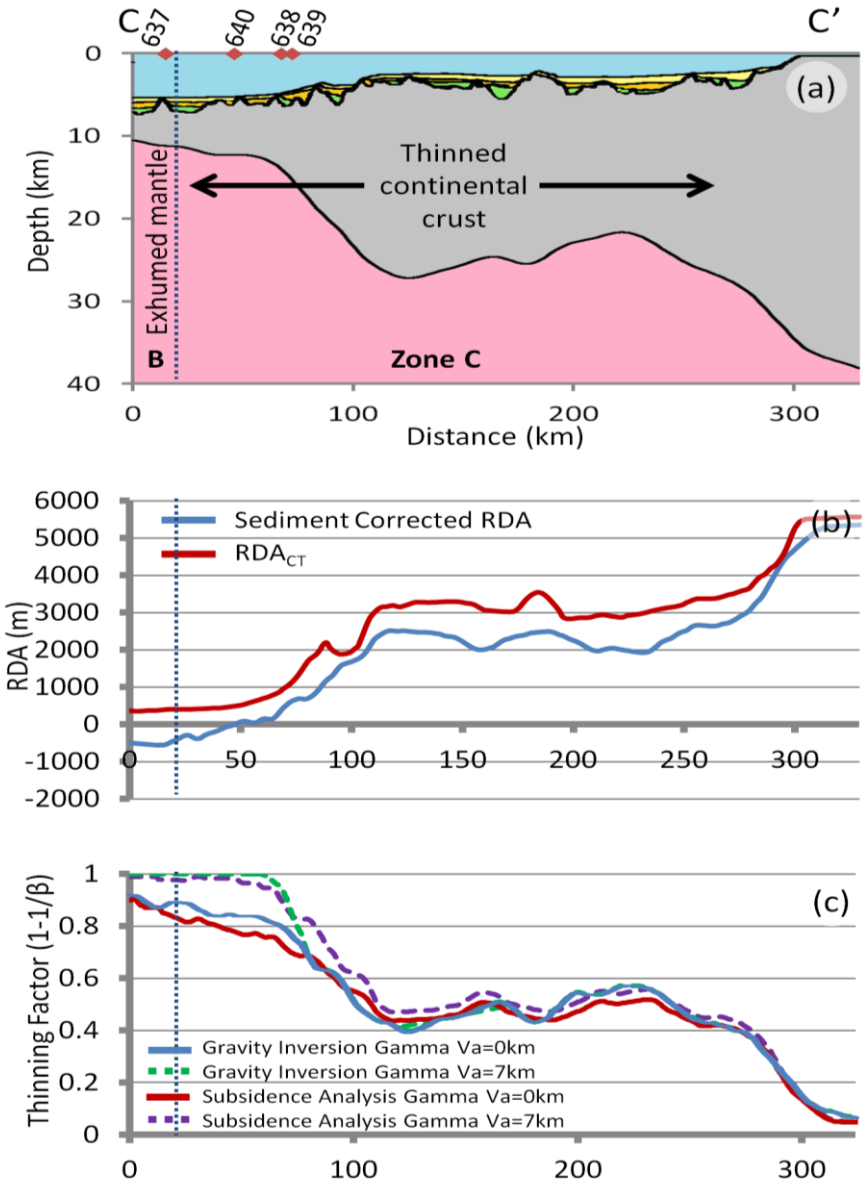

Figure 2.16 – Composite analysis plot along ISE-01 showing interpretations of crustal zones made from the integrated quantitative analysis, which have been compared to observations from ODP well data. (a) Crustal cross section along profile ISE-01 (C-C') from gravity anomaly inversion. Locations of the ODP wells are indicated. (b) Sediment corrected RDA and the RDA component from crustal thickness variations (RDA_{CT}) along ISE-01. (c) Continental lithosphere thinning factors from subsidence analysis and gravity anomaly inversion assuming a magma-poor solution. The dashed line indicates the distal extent of unequivocal continental crust (possible interpretation of the COB) and its boundary with exhumed mantle.

Comparison with ODP well observations

Observations from the ODP drill logs (637, 638, 639 and 640) along profile ISE-01 are shown in Table 2 and have been compared to our interpretations made from the integrated quantitative analysis shown on the composite analysis plot for profile ISE-01. The ODP well 637, in zone B, shows the presence of serpentinized peridotite, whilst ODP well 639, in zone C, shows the presence of continental basement. The interpretation of the composite analysis plot for profile ISE-01 is consistent with the ODP observations at both of these wells. ODP well logs 638 and 640, in zone C, are much shallower only showing the presence of syn-rift sediments.

ODP Well	Depth (m)	Description
637	286	Serpentinized peridotite
640	232	Syn-rift sediments
638	547	Syn-rift sediments
639	251	Continental basement

Table 2.2 – ODP well observations along ISE-01 (Boillot et al., 1987; Sawyer et al., 1994; Tucholke et al., 2007; Whitmarsh et al., 1998; Whitmarsh and Sawyer, 1996).

2.8. Conclusion

The gravity anomaly inversion, RDA analysis and subsidence analysis techniques are of global applicability and may be used on many deep-water frontier rifted continental margins, in order to understand the large scale distribution of thinned continental crust and lithosphere, the start of unequivocal oceanic crust and hence determine the structure of the OCT, COB location and magmatic type. Validation of these techniques has been carried out on the Iberian rifted continental margin, as this is one of the best-studied margins worldwide, due

to the abundance of ODP well data. Integrated quantitative analysis of the Iberian seismic profiles (IAM9, Lusigal 12 and ISE-01) has enabled further geological interpretations to be made of the crustal structure and distribution, which are validated using ODP well data, and where ODP well data are ambiguous, robust predictions have been made.

Integrated quantitative analysis of the Iberian seismic profiles show the crustal structure and the distribution of thinned continental crust, exhumed mantle and the start of unequivocal oceanic crust (where present) along the margin. The integrated approach, which considers the gravity anomaly inversion, RDA analysis and subsidence analysis techniques together, has enabled a robust geological interpretation of the OCT structure along the seismic profiles and a more accurate prediction of the COB location to be made. Predicted distances between the COB and the margin hinge for the Iberian margin range between 100km and 250km, with the greatest distances predicted for Galicia Bank.

An accurate identification of the crustal structure and the distribution of continental and oceanic crust remains crucial in order to fully understand the evolution of the Iberian rifted continental margin, with fundamental implications for building a better geodynamic history, plate tectonic reconstruction model and the evolution of petroleum systems.

2.9. References

Alvey, A., Gaina, C., Kusznir, N. J., and Torsvik, T. H., 2008, Integrated crustal thickness mapping and plate reconstructions for the high Arctic: Earth and Planetary Science Letters, v. 274, no. 3-4, p. 310-321.

Amante, C., and Eakins, B. W., 2009, ETOPO1 1 Arc-Minute Global Relief Model: Procedures, Data Sources and Analysis: NOAA Technical Memorandum NESDIS NGDC-24, p. 19.

Autin, J., Leroy, S., Beslier, M.-O., d'Acremont, E., Razin, P., Ribodetti, A., Bellahsen, N., Robin, C., and Al Toubi, K., 2010, Continental break-up history of a deep magma-poor margin based on seismic reflection data (northeastern Gulf of Aden margin, offshore Oman): Geophysical Journal International, v. 180, no. 2, p. 501-519.

Boillot, G., Recq, M., Winterer, E. L., Meyer, A. W., Applegate, J., Baltuck, M., Bergen, J. A., Comas, M. C., Davies, T. A., Dunham, K., Evans, C. A., Girardeau, J., Goldberg, G., Haggerty, J., Jansa, L. F., Johnson, J. A., Kasahara, J., Loreau, J. P., Luna-Sierra, E., Moullade, M., Ogg, J., Sarti, M., Thurow, J., and Williamson, M., 1987, Tectonic denudation of the upper mantle along passive margins: a model based on drilling results (ODP leg 103, western Galicia margin, Spain): Tectonophysics, v. 132, no. 4, p. 335-342.

Bronner, A., Sauter, D., Manatschal, G., Peron-Pinvidic, G., and Munschy, M., 2011, Magmatic breakup as an explanation for magnetic anomalies at magma-poor rifted margins, Nature Geoscience, Volume 4, Nature Publishing Group, a division of Macmillan Publishers Limited. All Rights Reserved., p. 5.

Carlson, R. L., and Herrick, C. N., 1990, Densities and porosities in the oceanic crust and their variations with depth and age: Journal of Geophysical Research: Solid Earth, v. 95, no. B6, p. 9153-9170.

Chappell, A. R., and Kusznir, N. J., 2008, Three-dimensional gravity inversion for Moho depth at rifted continental margins incorporating a lithosphere thermal gravity anomaly correction: Geophysical Journal International, v. 174, no. 1, p. 1-13.

Chian, D., Louden, K. E., Minshull, T. A., and Whitmarsh, R. B., 1999, Deep structure of the ocean-continent transition in the southern Iberia Abyssal Plain from seismic refraction

profiles: Ocean Drilling Program (Legs 149 and 173) transect: Journal of Geophysical Research: Solid Earth, v. 104, no. B4, p. 7443-7462.

Christensen, N. I., and Mooney, W. D., 1995, Seismic velocity structure and composition of the continental crust: A global view: Journal of Geophysical Research: Solid Earth, v. 100, no. B6, p. 9761-9788.

Contrucci, I., Matias, L., Moulin, M., Géli, L., Klingelhofer, F., Nouzé, H., Aslanian, D., Olivet, J.-L., Réhault, J.-P., and Sibuet, J.-C., 2004, Deep structure of the West African continental margin (Congo, Zaïre, Angola), between 5°S and 8°S, from reflection/refraction seismics and gravity data: Geophysical Journal International, v. 158, no. 2, p. 529-553.

Cowie, L., and Kusznir, N., 2012, Mapping crustal thickness and oceanic lithosphere distribution in the Eastern Mediterranean using gravity inversion: Petroleum Geoscience, v. 18, no. 4, p. 373-380.

Crosby, A. G., and McKenzie, D., 2009, An analysis of young ocean depth, gravity and global residual topography: Geophysical Journal International, v. 178, no. 3, p. 1198-1219.

Crosby, A. G., McKenzie, D., and Sclater, J. G., 2006, The relationship between depth, age and gravity in the oceans: Geophysical Journal International, v. 166, no. 2, p. 553-573.

D'Acremont, E., Leroy, S., Beslier, M.-O., Bellahsen, N., Fournier, M., Robin, C., Maia, M., and Gente, P., 2005, Structure and evolution of the eastern Gulf of Aden conjugate margins from seismic reflection data: Geophysical Journal International, v. 160, no. 3, p. 869-890.

Dean, S. M., Minshull, T. A., Whitmarsh, R. B., and Louden, K. E., 2000, Deep structure of the ocean-continent transition in the southern Iberia Abyssal Plain from seismic refraction profiles: The IAM-9 transect at 40°20'N: Journal of Geophysical Research: Solid Earth, v. 105, no. B3, p. 5859-5885.

Discovery 215 Working, G., Minshull, T. A., Dean, S. M., Whitmarsh, R. B., Russell, S. M., Louden, K. E., and Chian, D., 1998, Deep structure in the vicinity of the ocean-continent transition zone under the southern Iberia Abyssal Plain: Geology, v. 26, no. 8, p. 743-746.

Greenhalgh, E. E., and Kusznir, N. J., 2007, Evidence for thin oceanic crust on the extinct Aegir Ridge, Norwegian Basin, NE Atlantic derived from satellite gravity inversion: Geophysical Research Letters, v. 34, no. 6, p. L06305.

Hopper, J. R., Funck, T., Tucholke, B. E., Larsen, H. C., Holbrook, W. S., Louden, K. E., Shillington, D., and Lau, H., 2004, Continental breakup and the onset of ultraslow seafloor spreading off Flemish Cap on the Newfoundland rifted margin: Geology, v. 32, no. 1, p. 93-96.

Kusznir, N., and Karner, G., 1985, Dependence of the flexural rigidity of the continental lithosphere on rheology and temperature: Nature, v. 316, no. 6024, p. 138-142.

Kusznir, N. J., Roberts, A. M., and Morley, C. K., 1995, Forward and reverse modelling of rift basin formation: Geological Society, London, Special Publications, v. 80, no. 1, p. 33-56.

Manatschal, G., 2004, New models for evolution of magma-poor rifted margins based on a review of data and concepts from West Iberia and the Alps: International Journal of Earth Sciences, v. 93, no. 3.

Manatschal, G., Froitzheim, N., Rubenach, M., and Turrin, B. D., 2001, The role of detachment faulting in the formation of an ocean-continent transition: insights from the Iberia Abyssal Plain: Geological Society, London, Special Publications, v. 187, no. 1, p. 405-428.

Manatschal, G., Sutra, E., and Péron-Pinvidic, G., The lesson from the Iberia-Newfoundland rifted margins: how applicable is it to other rifted margins?, *in* Proceedings 2nd Central & North Atlantic Conjugate Margins: Rediscovering the Atlantic, New Insights, New winds for an old sea2010, Volume 2, p. 27 - 37.

McKenzie, D., 1978, Some Remarks on the Development of Sedimentary Basins Earth and Planetary Science Letters, v. 40, p. 25-32.

Müller, R. D., Sdrolias, M., Gaina, C., Steinberger, B., and Heine, C., 2008, Long-Term Sea-Level Fluctuations Driven by Ocean Basin Dynamics: Science, v. 319, no. 5868, p. 1357-1362.

Parker, R. L., 1972, The Rapid Calculation of Potential Anomalies: Geophysical Journal of the Royal Astronomical Society, v. 31, no. 4, p. 447-455.

Parsons, B., and Sclater, J. G., 1977, An Analysis of the Variation of Ocean Floor Bathymetry and Heat Flow with Age: Journal of Geophysical Research, v. 82, no. 5, p. 803-827.

Péron-Pinvidic, G., Manatschal, G., Minshull, T. A., and Sawyer, D. S., 2007, Tectonosedimentary evolution of the deep Iberia-Newfoundland margins: Evidence for a complex breakup history: Tectonics, v. 26, no. 2, p. TC2011.

Pickup, S. L. B., Whitmarsh, R. B., Fowler, C. M. R., and Reston, T. J., 1996, Insight into the nature of the ocean-continent transition off West Iberia from a deep multichannel seismic reflection profile: Geology, v. 24, no. 12, p. 1079-1082.

Reston, T. J., 2009, The structure, evolution and symmetry of the magma-poor rifted margins of the North and Central Atlantic: A synthesis: Tectonophysics, v. 468, no. 1–4, p. 6-27.

Roberts, A. M., Kusznir, N. J., Yielding, G., and Styles, P., 1998, 2D flexural backstripping of extensional basins; the need for a sideways glance: Petroleum Geoscience, v. 4, no. 4, p. 327-338.

Russell, S. M., and Whitmarsh, R. B., 2003, Magmatism at the west Iberia non-volcanic rifted continental margin: evidence from analyses of magnetic anomalies: Geophysical Journal International, v. 154, no. 3, p. 706-730.

Sandwell, D. T., and Smith, W. H. F., 2009, Global marine gravity from retracked Geosat and ERS-1 altimetry: Ridge segmentation versus spreading rate: Journal of Geophysical Research, v. 114, no. B1, p. B01411.

Sawyer, D. S., Whitmarsh, R. B., Klaus, A., and et al., 1994, Proceedings of the ODP, Initial Reports, 149: College Station, TX (Ocean Drilling Program).

Shipley, T., Gahagan, L., Johnson, K., and Davis, M., 2005, University of Texas Institute for Geophysics., *in* Center, S. D., ed., Volume 2012.

Stein, C. A., and Stein, S., 1992, A model for the global variation in oceanic depth and heat flow with lithospheric age: Nature, v. 359, no. 6391, p. 123-129.

Sutra, E., and Manatschal, G., 2012, How does the continental crust thin in a hyperextended rifted margin? Insights from the Iberia margin: Geology, v. 40, no. 2, p. 139-142.

Tucholke, B. E., and Ludwig, W. J., 1982, Structure and origin of the J Anomaly Ridge, western North Atlantic Ocean: Journal of Geophysical Research: Solid Earth, v. 87, no. B11, p. 9389-9407.

Tucholke, B. E., Sawyer, D. S., and Sibuet, J. C., 2007, Breakup of the Newfoundland–Iberia rift: Geological Society, London, Special Publications, v. 282, no. 1, p. 9-46.

Unternehr, P., Péron-Pinvidic, G., Manatschal, G., and Sutra, E., 2010, Hyper-extended crust in the South Atlantic: in search of a model: Petroleum Geoscience, v. 16, no. 3, p. 207-215.

White, R. S., McKenzie, D., and O'Nions, R. K., 1992, Oceanic Crustal Thickness From Seismic Measurements and Rare Earth Element Inversions: Journal of Geophysical Research, v. 97, no. B13, p. 19683-19715.

White, R. S., Smith, L. K., Roberts, A. W., Christie, P. A. F., and Kusznir, N. J., 2008, Lower-crustal intrusion on the North Atlantic continental margin: Nature, v. 452, no. 7186, p. 460 - 464.

Whitmarsh, R. B., Beslier, M. O., P.J., W., and et al., 1998, Proceedings of the ODP, Initial Reports, 173, College Station, TX (Ocean Drilling Program).

Whitmarsh, R. B., and Miles, P. R., 1995, Models of the development of the West Iberia rifted continental margin at 40°30'N deduced from surface and deep-tow magnetic anomalies: Journal of Geophysical Research: Solid Earth, v. 100, no. B3, p. 3789-3806.

Whitmarsh, R. B., Minshull, T. A., Russell, S. M., Dean, S. M., Louden, K. E., and Chian, D., 2001, The role of syn-rift magmatism in the rift-to-drift evolution of the West Iberia continental margin: geophysical observations: Geological Society, London, Special Publications, v. 187, no. 1, p. 107-124.

Whitmarsh, R. B., and Sawyer, D. S., 1996, The ocean-continent transition beneath the Iberia Abyssal Plain and continental rifting to seafloor spreading processes, *in* Whitmarsh, R. B., Sawyer, D. S., Klaus, A., and Masson, D. G., eds., Proceedings of the Ocean Drilling Program, Scientific Results 149: College Station, TX, p. 713 - 733.

Wilson, J. T., 1966, Did the Atlantic Close and then Re-Open?: Nature, v. 211, no. 5050, p. 676 - 681.

Zalán, P. V., Severino, M. C. G., Rigoti, C., Magnavita, L. P., Oliveira, J. A. B., and Viana, A. R., 2011, An entirely new 3D-view of the crustal and mantle structure of a ruptured South Atlantic passive margin – Santos, Campos and Espírito Santo Basins, Brazil (Expanded Abstract): AAPG Annual Convention & Exhibition Abstracts Volume CDROM,Paper 986156.

Zelt, C. A., Sain, K., Naumenko, J. V., and Sawyer, D. S., 2003, Assessment of crustal velocity models using seismic refraction and reflection tomography: Geophysical Journal International, v. 153, no. 3, p. 609-626.

Chapter 3

3. OCT Structure, COB Location and Magmatic Type of the Northern Angolan and South-eastern Brazilian Rifted Continental Margins

Preface

This chapter has been written in the form of a paper. Co-authors are N.J Kusznir (University of Liverpool) and B. Horn (ION-GXT). Section headers, figures and page numbers have been renumbered to conform to the format of this thesis.

Abstract

Integrated quantitative analysis using deep seismic reflection data and gravity anomaly inversion has been used to determine ocean continent transition (OCT) structure, continent ocean boundary (COB) location and magmatic type of the northern Angolan and south-eastern Brazilian margins. Knowledge of these margin parameters are of critical importance for understanding rifted continental margin formation processes and in evaluating petroleum systems in deep-water frontier oil and gas exploration. The OCT structure, COB location and magmatic type of the northern Angolan and south-eastern Brazilian rifted continental margins are much debated; exhumed and serpentinised mantle have been reported (Unternehr et al., 2010; Zalán et al., 2011) at these margins.

Gravity anomaly inversion, incorporating a lithosphere thermal gravity anomaly correction, has been used to determine Moho depth, crustal basement thickness and continental lithosphere thinning. Residual depth anomaly (RDA) analysis has been used to investigate OCT bathymetric anomalies with respect to expected oceanic bathymetries and subsidence analysis has been used to determine the distribution of continental lithosphere thinning. These techniques have been applied to the ION-GXT BS1-575, south-eastern Brazilian, and ION-GXT CS1-2400, northern Angolan, deep seismic reflection profiles, and have been validated on the Iberian rifted continental margin for profiles Lusigal 12 and ISE-01. In addition, a joint inversion technique using deep long offset seismic reflection and gravity anomaly data has been applied to these seismic reflection profiles. The joint inversion method solves for coincident seismic and gravity Moho in the time domain and calculates the lateral variations in crustal basement densities and seismic velocities along the profiles.

3.1. Introduction

An understanding of the distribution of oceanic and continental crust and hence the location of the continent ocean boundary (COB) along the southern Atlantic rifted continental margins is of great importance for the evaluation of potential petroleum systems in deep-water frontier oil and gas exploration. Knowledge of the ocean continent transition (OCT) structure, COB location and magmatic type (i.e. the volume of magmatic addition, whether the margin is 'normal' magmatic, magma-poor or magma-rich) of these margins is also critical for understanding rifted continental margin formation processes, which enable us to understand the geodynamics and tectonics of continental breakup. The south Atlantic rifted continental margins have been the subject of extensive seismic surveys (e.g. Contrucci et al. (2004), Moulin et al.(2005); Unternehr (2010) Zalán (2011) and Mohriak et al. (2008)) due to their economic potential; however, the OCT structure and COB location are still not fully understood, and are much debated. Along the northern Angolan margin both Unternehr et al. (2010) and Contrucci et al. (2004) report an anomalous layer in the OCT, which they interpret to be a zone of exhumed continental mantle, and along the south-eastern Brazilian margin Zalán et al. (2011) report exhumed mantle, south east of the Florianopolis Ridge.

Integrated quantitative analysis using gravity anomaly inversion, residual depth anomaly (RDA) analysis, subsidence analysis and deep seismic reflection data, has been applied to profiles along the northern Angolan and south-eastern Brazilian rifted continental margins in order to determine OCT structure, COB location and magmatic type. Gravity anomaly inversion, incorporating a lithosphere thermal gravity anomaly correction, has been used to determine Moho depth, crustal basement thickness and continental lithosphere thinning along these profiles. RDA analysis has been used to calculate departures from standard oceanic water depths, and subsidence analysis has been used to give the distribution of

continental lithosphere thinning. The gravity anomaly inversion, RDA analysis and subsidence analysis techniques have been validated on the Iberian rifted continental margin, specifically along profiles Lusigal 12 and ISE-01. A joint inversion technique, using deep seismic reflection and gravity anomaly data, has also been applied to the profiles to solve for coincident seismic and gravity Moho in the time domain and calculate the lateral variations in crustal basement densities and seismic velocities along profile. Whilst individually each of these techniques can be used to constrain the OCT structure, COB location and magmatic type of a rifted continental margin, the integrated methodology enables us to make robust and further constrained geological interpretations of the OCT structure and a more accurate prediction of the COB location.

Analysis of the south Atlantic conjugate margins focuses on the ION-GXT deep long offset seismic reflection profiles: CS1-2400 along the northern Angolan rifted continental margin and BS1-575 along the south-eastern Brazilian rifted continental margin. These ION-GXT deep seismic profiles are not conjugate profiles; however, they are considered to be important examples that summarise the structure of the OCT along the south Atlantic rifted continental margins. Deep seismic reflection data is an important observational data source that together with gravity data enables the determination of the structure of the OCT and the identification of the COB along the northern Angolan and south-eastern Brazilian profiles.

The south Atlantic rifted continental margins are the result of continental rifting and breakup between South America and Africa (Unternehr et al., 2010). The opening of the South Atlantic began in 140Ma (Lower Cretaceous), during the breakup of western Gondwana (Moulin et al., 2005). The South Atlantic underwent several phases of rifting, which have been identified in the sedimentary architecture of the margins (Aslanian et al., 2009; Moulin et al., 2005). The exact timing of these rift episodes is debated; however, the main rift episode is thought to have lasted approximately 30Myr from Berriasian to early Albian

(140Ma to 110Ma) (Teisserenc and Villemin, 1989). It is thought that the transition to sea floor spreading occurred at about 112Ma to 110Ma (Moulin et al., 2005).

Within the literature there are a range of different definitions of the OCT and COB (e.g. Pèron-Pinvidic et al. (2007), Whitmarsh and Miles (1995), Manatschal et al. (2001), Dean et al. (2000), Manatschal et al. (2010) and Discovery 215 Working et al. (1998)). Within this thesis, however, we define the OCT as the region between unequivocal continental crust of 'normal' thickness and unequivocal oceanic crust; the continental lithosphere in this region is highly thinned, with complex tectonics, variable magmatism and possible mantle exhumation. We define the COB as the distal limit of unequivocal continental crust; however, determining the location of the COB is made difficult by the presence of exhumed mantle and complex tectonics.

3.2. OCT structure and COB location: along the CS1-2400 profile, northern Angolan margin

The CS1-2400 profile, along the northern Angolan rifted continental margin, is used as the example for the South Atlantic rifted continental margin case history to describe the integrated quantitative analysis techniques in detail.

3.2.1. Background:

The northern Angolan rifted continental margin has been the subject of extensive seismic surveys (e.g. Moulin et al.(2005), Unternehr (2010) and Contrucci et al. (2004)), because of its hydrocarbon resources; however, the crustal structure, tectonics and the syn-rift stratigraphy is largely unknown due to the presence of a massive middle to upper Aptian salt sequence, which in places is approximately 5km thick.

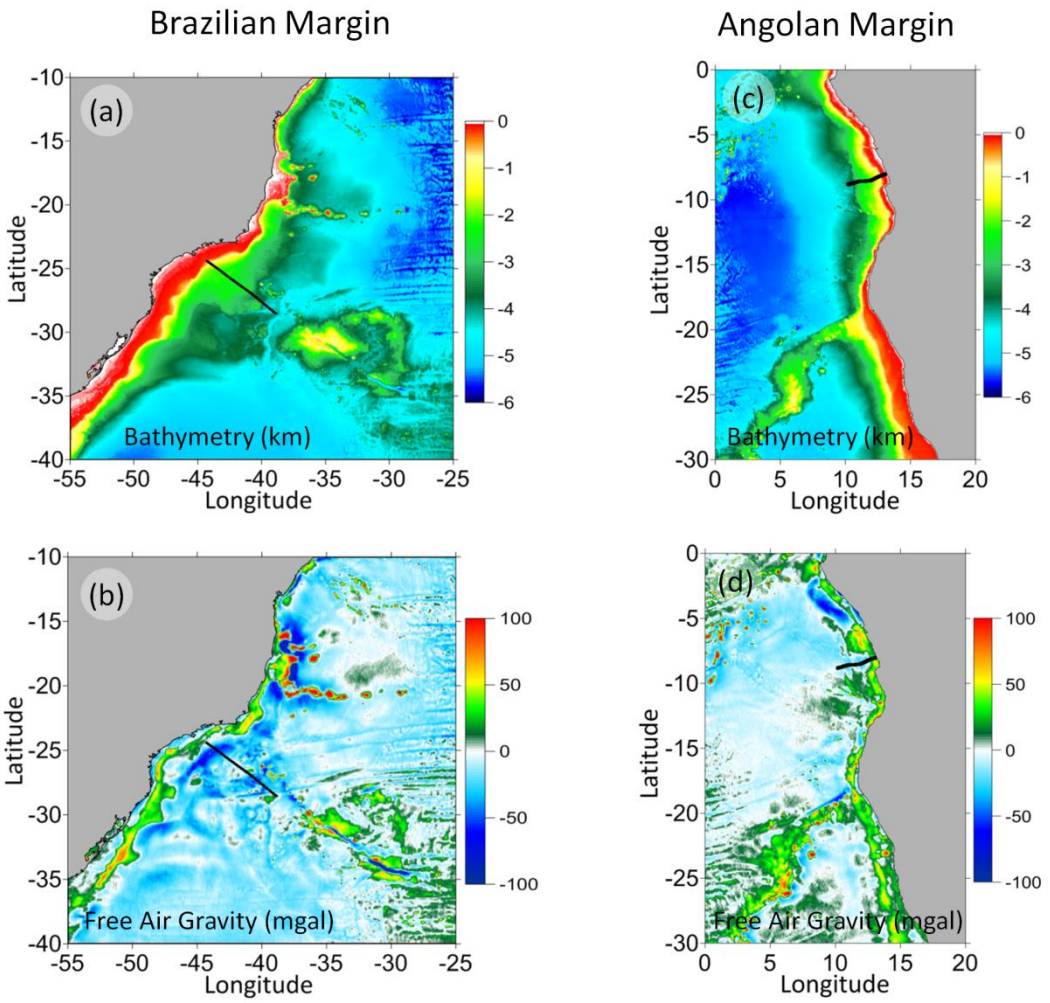

Figure 3.1 – Data used in the gravity anomaly inversion, RDA analysis and subsidence analysis for the south-eastern Brazilian and northern Angolan rifted continental margins. (a) Bathymetry (km) (Amante and Eakins 2009) along the south-eastern Brazilian margin, with the location of profile BS1-575 (B-B') indicated. (b) Free air gravity (mgal) (Sandwell and Smith 2009) along the south-eastern Brazilian margin. (c) Bathymetry (km) (Amante and Eakins 2009) along the northern Angolan margin, with the location of profile CS1-2400 (A-A') indicated. (d) Free air gravity (mgal) (Sandwell and Smith 2009) along the northern Angolan margin.

Analysis along the northern Angolan margin is focussed on the ION-GXT deep long offset seismic reflection profile, CS1-2400 (Figure 3.1(c)). The lack of observable oceanic or continental crust characteristics in the transitional domain has important implications for our understanding of the timing, evolution and processes involved in rifted continental margin formation. The interpretations from Contrucci et al. (2004) and Unternehr et al. (2010) of the deep seismic data, along the northern Angolan margin, suggest that there is a zone of

serpentinized continental mantle, identified by a high velocity (7.2kms^{-1} to 7.8kms^{-1}) layer, at the western end of their interpreted transitional domain.

3.2.2. Crustal basement thickness and continental lithosphere thinning from gravity anomaly inversion along the CS1-2400 profile

Gravity anomaly inversion has been used to determine Moho depth, crustal basement thickness and continental lithosphere thinning along the northern Angolan profile. The data used within the gravity anomaly inversion are bathymetry (Amante and Eakins, 2009) (Figure 3.1(c)), satellite derived free air gravity (Sandwell and Smith, 2009) (Figure 3.1(d)), 2D sediment thickness from PSDM (pre stacked depth migrated) seismic reflection data along ION-GXT profile CS1-2400 (Figure 3.2(b)) and ocean age isochrons from Müller et al.(2008). The methodology of the gravity anomaly inversion technique is described in Chappell and Kusznir (2008) and Greenhalgh and Kusznir (2007) and has been applied in Cowie and Kusznir (2012) and Alvey et al. (2008).

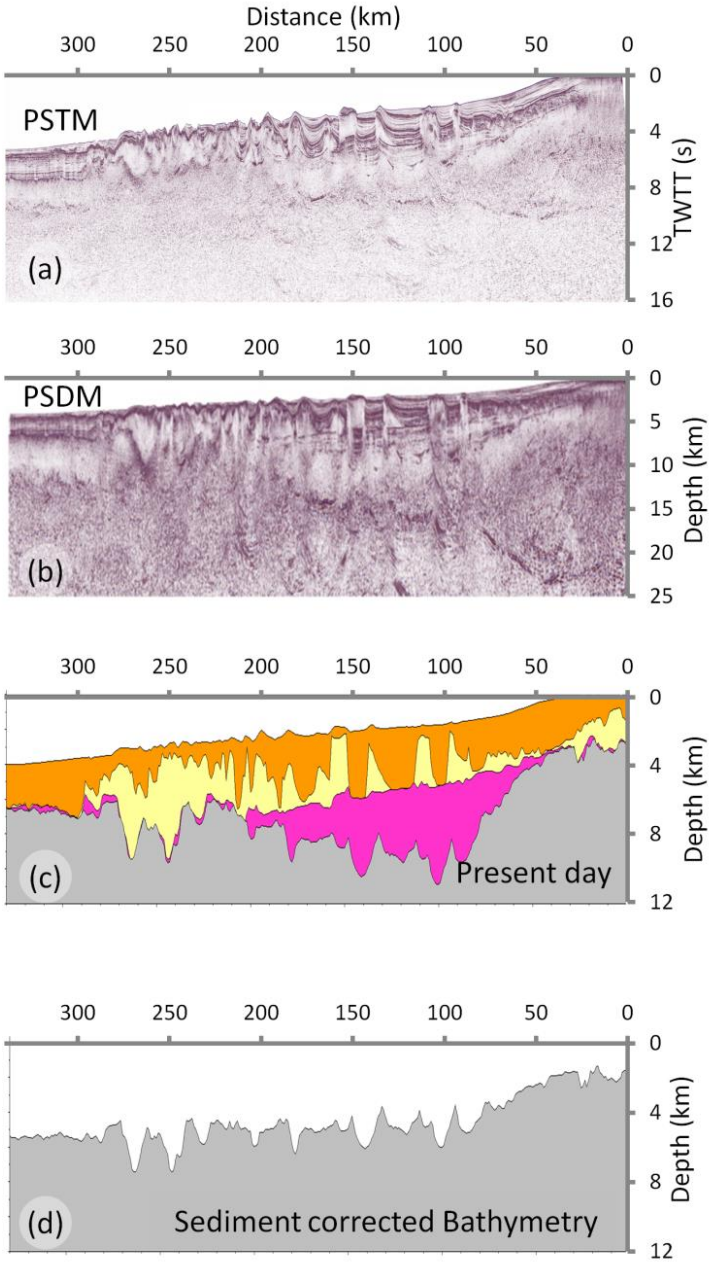

Figure 3.2 – (a) PSTM (pre stacked time migrated) seismic data for the ION-GXT CS1-2400 northern Angolan deep long offset seismic profile (b) PSDM (pre stacked depth migrated) seismic data for the ION-GXT CS1-2400 northern Angolan deep long offset seismic profile (c) Digitized present day cross section along the CS1-2400 profile; the pre-salt sedimentary layer is highlighted in pink; post-salt sedimentary layer in orange and the salt layer is highlighted in yellow (d) Sediment corrected bathymetry from flexural backstripping, assuming a Te=1.5km.

The gravity anomaly inversion method is carried out in the 3D spectral domain, using the scheme of Parker (1972) to predict Moho depth and hence determine crustal basement thickness. The gravity anomaly inversion incorporates a lithosphere thermal gravity anomaly

correction, to account for the elevated geothermal gradient within oceanic and rifted continental margin lithosphere. Failure to include the lithosphere thermal gravity anomaly correction can lead to predictions of Moho depth and crustal basement thickness, at rifted continental margins, which are substantially too great. The gravity anomaly inversion results are dependent on the age of continental breakup due to the lithosphere thermal gravity anomaly correction being dependent on the lithosphere thermal re-equilibration time. We have used 110Ma as the age of breakup, after Moulin (2005), but have also examined sensitivities to breakup ages, which span the period Berriasian (140Ma) to early Albian (110Ma); this range corresponds to the start and end of the main rifting episode in the South Atlantic (Teisserenc and Villemin, 1989). The gravity anomaly inversion predicted continental lithosphere thinning factor (γ) and the parameterization of the decompression melting model of White and McKenzie (1989) have been used to predict the thickness of the crustal magmatic addition. Sensitivities to magmatic addition, including solutions for magma-poor and 'normal' magmatic addition have been examined.

The reference Moho depth is an important parameter used within the gravity anomaly inversion that requires careful consideration and calibration (Cowie and Kusznir, 2012). The long wavelength components of the Earth's gravity anomaly field are controlled by deep mantle dynamic processes and are not related to lithosphere and crustal structure; as a consequence the reference Moho depth varies globally. Sensitivities to reference Moho depths of 32.5km, 35km, 37.5km and 40km have been examined. Moho depths predicted from gravity anomaly inversion for these sensitivities to reference Moho depth are shown in Figure 3.3(a). In order to constrain reference Moho depth, predicted Moho depths determined from gravity anomaly inversion have been calibrated against seismic Moho depths from the oceanic domain of the CS1-2400 profile using the clear Moho reflectors. Calibration shown in Figure 3.3(b), suggests that a reference Moho depth of 35.5km is

required in order to predict crustal basement thicknesses consistent with those seen in the oceanic domain of the CS1-2400 seismic reflection profile. The gravity anomaly inversion assumes a crustal basement density of 2850kgm^{-3} (Carlson and Herrick, 1990) and a mantle density of 3300kgm^{-3}; sensitivity tests to these values have been made. The sediment densities used within the gravity anomaly inversion, increase with depth assuming normal compaction corresponding to a shale-rich lithology .

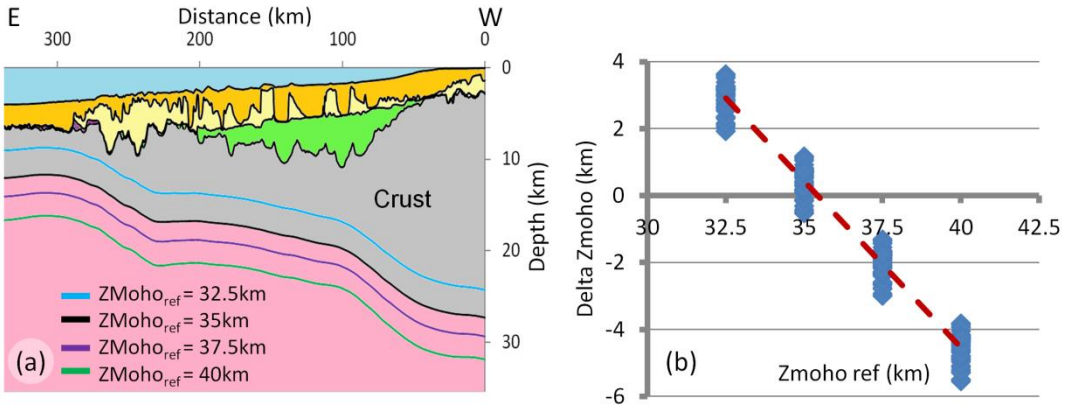

Figure 3.3 – Calibration of the reference Moho depth used in the gravity anomaly inversion along the CS1-2400 profile on the northern Angolan margin. (a) Gravity anomaly inversion predicted Moho depths have been calculated using sensitivities to reference Moho depths of 32.5km, 35km, 37.5km and 40km. The pre-salt sedimentary layer is shown in green, the salt layer in yellow and the post-salt sedimentary layer is orange. (b) Calibration of the reference Moho depth for the CS1-2400 profile shows that a reference Moho depth of 35.5km is required.

A crustal cross section along the CS1-2400 profile (Figure 3.4(a)) has been constructed using bathymetry and 2D sediment thickness with crustal basement thicknesses and Moho depths, predicted from gravity anomaly inversion, assuming the calibrated reference Moho depth of 35.5km. The crustal cross section highlights changes in crustal basement thicknesses along the CS1-2400 profile. At the western end of the profile the gravity anomaly inversion predicts crustal basement thicknesses between 5km and 7km; in the central region of the profile crustal basement thicknesses thicken to approximately 11km and at the eastern end of the profile the crustal basement thickens to approximately 25km. Moho depths determined from

the gravity anomaly inversion are in good agreement with those determined from the ION–GXT CS1-2400 deep long-offset seismic reflection profile.

Continental lithosphere thinning factor ($\gamma=1-1/\beta$) estimates for profile CS1-2400, derived from gravity anomaly inversion, using the calibrated reference Moho depth of 35.5km are shown in Figure 3.4(b). A 'normal' magmatic solution (Va=7km), a magma-poor solution (Va=0km) and a solution for serpentinised mantle have been examined. A 'normal' magmatic solution has a critical thinning factor for the initiation of decompression melting of 0.7 and a maximum magmatic addition of 7km (for β =1.0). This corresponds to 'normal' decompressional melting that predicts a 7km thick oceanic crust. Magma-poor solutions have less decompression melting, with a critical thinning factor of zero, where no magmatic addition by decompression melting is generated; whilst magma-rich margins have more decompression melting, with a critical thinning factor of 0.5 and a maximum magmatic addition of 10km. For a serpentinized mantle solution, serpentinization begins at approximately $\gamma=0.7$ and at $\gamma=1.0$ generates serpentinized exhumed mantle with a mass deficiency with respect to mantle, equivalent to crustal basement of thickness 3km.

Continental lithosphere thinning factors of zero indicate that there has been no stretching or thinning of the continental lithosphere, whereas a continental lithosphere thinning factor of one indicates that there has been infinite stretching and thinning of the original continental lithosphere and there is no continental lithosphere (or crust) remaining. Changes from high continental lithosphere thinning factors (between 0.8 and 1.0) to lower continental lithosphere thinning factors can be used constrain the COB location along the profile. At the western end of the profile the continental lithosphere thinning factors for a 'normal' magmatic solution are 1.0; for a magma-poor solution the continental lithosphere thinning factors are approximately 0.85, whereas for a solution for serpentinised mantle the continental lithosphere thinning factors are approximately 0.9. In the central section of the

profile, the continental lithosphere thinning factors, for all solutions examined, reduce to between 0.7 and 0.85.

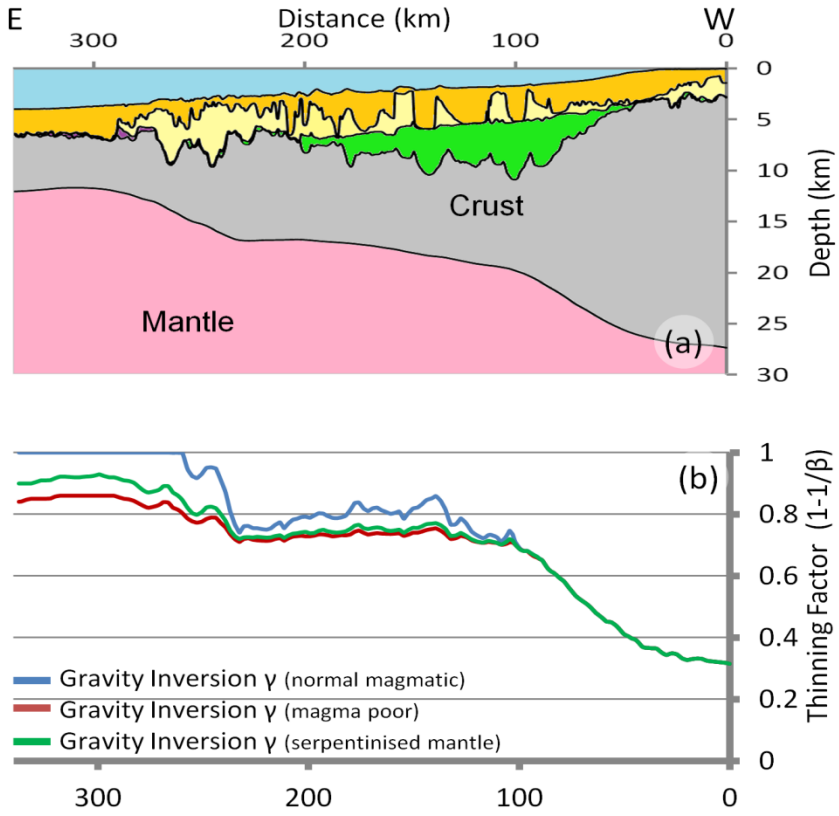

Figure 3.4 – (a) Crustal cross section across the northern Angolan margin. The pre-salt sedimentary layer is shown in green, the salt layer in yellow and the post-salt sedimentary layer is orange. (b) Gravity anomaly inversion predicted continental lithosphere thinning along the CS1-2400 profile. Sensitivities to a 'normal' magmatic margin (Va=7km), a magma-poor margin (Va=0km) and a solution for serpentinised mantle have been examined.

3.2.3. Residual depth anomaly (RDA) analysis along the CS1-2400 profile

In order to examine OCT bathymetric anomalies with respect to expected oceanic bathymetries along the northern Angolan profile, RDA analysis has been applied. An RDA, for oceanic crust, is the difference between observed (b_{obs}) and ocean age predicted bathymetry ($b_{predicted}$).

$$RDA = b_{obs} - b_{predicted} \quad (1)$$

Age predicted bathymetric anomalies have been calculated using the thermal plate model predictions from Crosby and McKenzie (2009). Sensitivities to the thermal plate model predictions from Parsons and Sclater (1977) and Stein and Stein (1992) have also been examined; RDA results computed using these different thermal plate model predictions do not vary significantly.

3.2.4. Sediment corrected RDA along the CS1-2400 profile

RDAs corrected for sediment loading, have been calculated along the northern Angolan profile, by comparing the observed bathymetries corrected for sediment loading and age predicted oceanic bathymetries. Present day bathymetry is corrected for sediment loading using flexural backstripping and decompaction (Kusznir et al., 1995) and comprises the removal of the sedimentary load, allowing for the flexural isostatic response and decompaction of the remaining sediments. Flexural backstripping and decompaction assumes a shale-rich lithology compaction and density parameters during the removal of the sedimentary layer, whilst the salt layer is given a simple salt lithology (Hudec and Jackson, 2007). Present day bathymetry and the depth to top basement, digitized from the CS1-2400 PSDM profile are shown in Figure 3.2(c) and bathymetry and depth to top basement corrected for sediment loading using flexural backstripping are shown in Figure 3.2(d). Removing the sedimentary and salt layers along the CS1-2400 profile results in excess of 1500m difference between the sediment corrected bathymetry and the observations of present day bathymetry.

The sediment corrected bathymetry shows the structural control from faulting and as a result has quite a noisy signal, which is carried through into the sediment corrected RDA calculations. Fault block spacing typically ranges between 15km and 20km. In order to remove the noise, we have ‘smoothed’ the sediment corrected RDA results by computing a

moving average, using a spatial gate of 30km. The RDA results shown in Figures 3.5, 3.6 and 3.9(b) have all been 'smoothed' by computing the moving average. The unsmoothed results are shown in Supplementary Figure S3.1.

Figure 3.5(b) shows a comparison of the uncorrected RDA and the sediment corrected RDA along the CS1-2400 profile Figure 3.5(a). At the western end of the profile there is approximately a 1500m difference between the uncorrected RDA and the sediment corrected RDA, the largest difference is seen in the central section of the profile. The sediment corrected RDA along the CS1-2400 profile, Figure 3.5(b), is positive with a magnitude between zero and +300m at the western end of the profile.

Age predicted oceanic bathymetries, used to calculate the sediment corrected RDA, are dependent on the oceanic lithospheric age. It is therefore necessary to consider sensitivities to oceanic lithospheric age as the Müller et al. (2008) global ocean age isochrons do not extend the entire length of profile CS1-2400. Two approaches have been examined: the first uses a constant value of 120Ma for the profile, whilst the second uses Müller et al. (2008) age isochrons with their age gradient extrapolated inboard. A comparison and sensitivity of the sediment corrected RDA results to ocean age isochrons is shown in Figure 3.5(c), both approaches produce similar results.

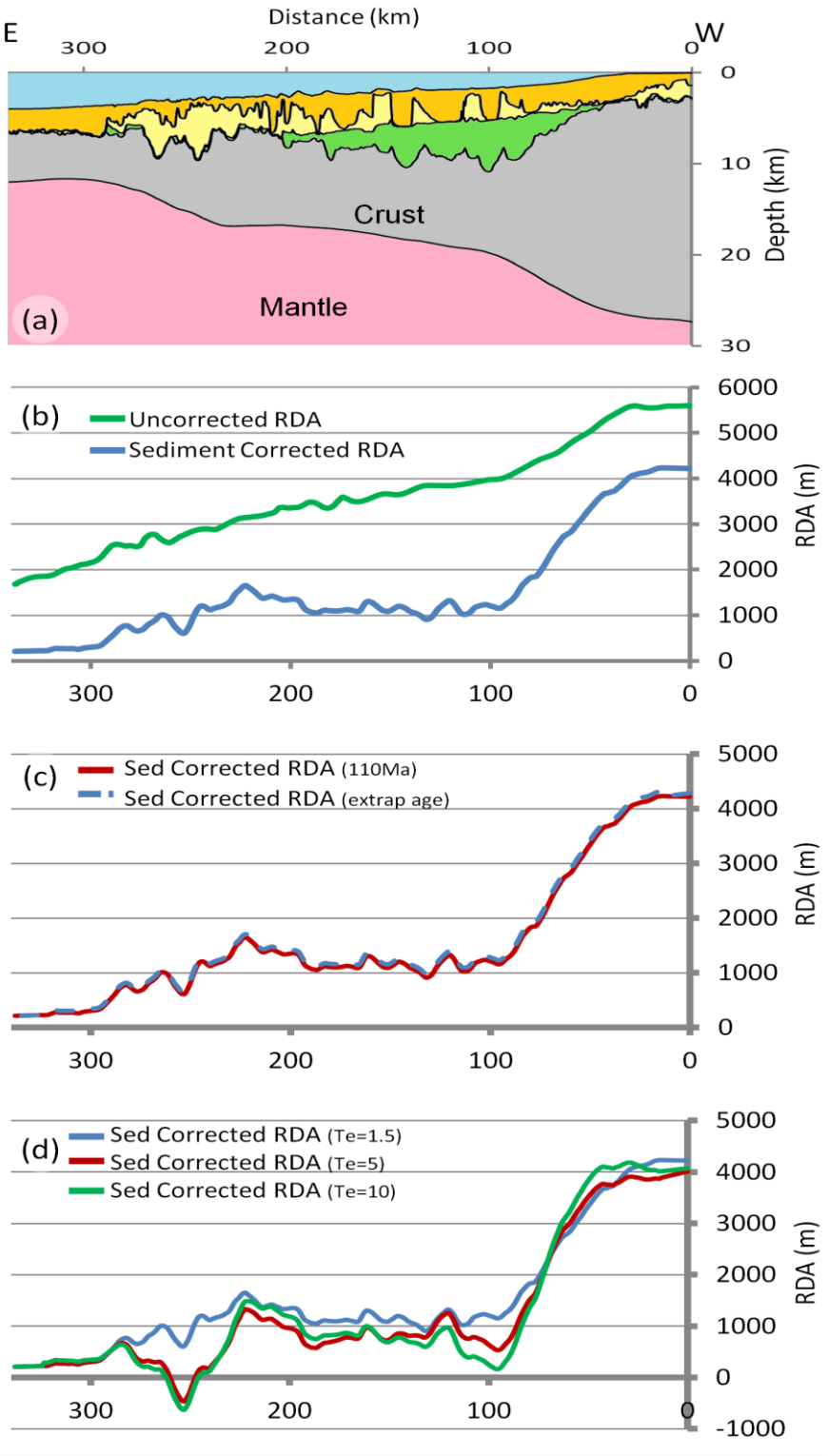

Figure 3.5 – (a) Crustal cross section along the CS1-2400 profile along the northern Angolan rifted continental margin. (b) Comparison of the uncorrected RDA results with the sediment corrected RDA results along the CS1-2400 profile. (c) The sensitivity to oceanic age for sediment corrected RDA results has been examined. Two approaches have been considered (i) a constant value of 120Ma for the profile and (ii) using Müller et al. (2008) age isochrons with their age gradient extrapolated inboard. (d) Sensitivity to the effective elastic thickness (Te's of 1.5km, 5km and 10km) for northern Angolan margin sediment corrected RDA results has been examined. All RDA results in this figure have been smoothed.

The flexural isostatic response of the removed layer of sediments is calculated using the flexural backstripping process, in which the effective elastic thickness (Te) controlling the flexural strength of the lithosphere is examined. For syn-rift extensional settings Te's between 1.5km and 5km have been determined (Roberts et al., 1998). The Te depends on the bending stresses applied to the plate, the rate of stress application, the lithosphere composition and the geothermal gradient (Kusznir and Karner, 1985). Sensitivities to Te's of 1.5km, 5km and 10km have been examined along the CS1-2400 profile (Figure 3.5(d)). At the western end of the profile, Te's of 1.5km, 5km and 10km produce sediment corrected RDAs of similar magnitude; however, beneath the thick salt in the central section of the profile, there is significant difference; the Te's of 5km and 10km produce negative sediment corrected RDAs (approximately -500m) whereas the Te of 1.5km produces a positive RDA (approximately 700m). A Te of 1.5km has been used as our preferred value within this paper, as a low Te is appropriate for the consideration of syn-rift sediments.

3.2.5. RDA component from crustal thickness variations (RDACT) along the CS1-2400 profile

The RDA component from variations in crustal basement thickness (RDA_{CT}) has been computed in addition to the sediment corrected RDA. The RDA_{CT} is computed using the difference between the crustal basement thickness (tc_{grav}) predicted from gravity anomaly inversion and the average global oceanic crustal thickness (tc_{ref}) of 7km (White et al., 1992), together with Airy isostasy. The local isostatic response to variations in gravity inverted non-continental crustal thickness, from the 7km global average oceanic crustal thickness (tc_{ref}) is given by:

$$RDA_{CT} = \frac{(tc_{ref} - tc_{grav})(\rho_m - \rho_c)}{(\rho_m - \rho_{infil})} \quad (2)$$

where ρ_m is the density of the mantle (3300kgm^{-3}) , ρ_c is the density of the crust (2850kgm^{-3}) (Carlson and Herrick, 1990) and ρ_{infill} is the density of the water infill (1000kgm^{-3}). A positive RDA_{CT} corresponds to crust that is thicker than 7km, whereas a negative RDA_{CT} reflects crust that is thinner than 7km or the presence of exhumed mantle and a RDA_{CT} of zero corresponds to crust that is approximately 7km thick. At the western end of the profile the RDA_{CT} (Figure 3.6(b)) along the CS1-2400 profile (Figure 3.6(a)) is negative, between -400m and -100m; in the central section of the profile the RDA_{CT} becomes positive ranging between zero and +550m, which further increases towards the eastern end of the profile.

3.2.6. RDAs corrected for sediment loading and crustal thickness variations along the CS1-2400 profile

RDAs corrected for sediment loading and crustal basement thickness variations along the CS1-2400 profile are shown in Figure 3.6(b). Changes in the RDA signature may be used to estimate the distal extent of continental crust and where unequivocal oceanic crust begins (i.e. potential COB location). For a region of unequivocal oceanic crust, the sediment corrected RDA and the RDA_{CT} results will be constant and near zero, however, for regions of thicker continental crust the RDA signal will show a positive trend. At the western end of the profile the sediment corrected RDA ranges between zero and +300m (Figure 3.6(b)), implying the presence of crust that is thicker than 7km or anomalous uplift. The RDA_{CT} ranges between -400m and -100m at the western end of the profile, corresponding to the presence of crust that is thinner than 7km or the presence of exhumed mantle. Both the sediment corrected RDA and the RDA_{CT} show the same general trend along the profile although they have different magnitudes.

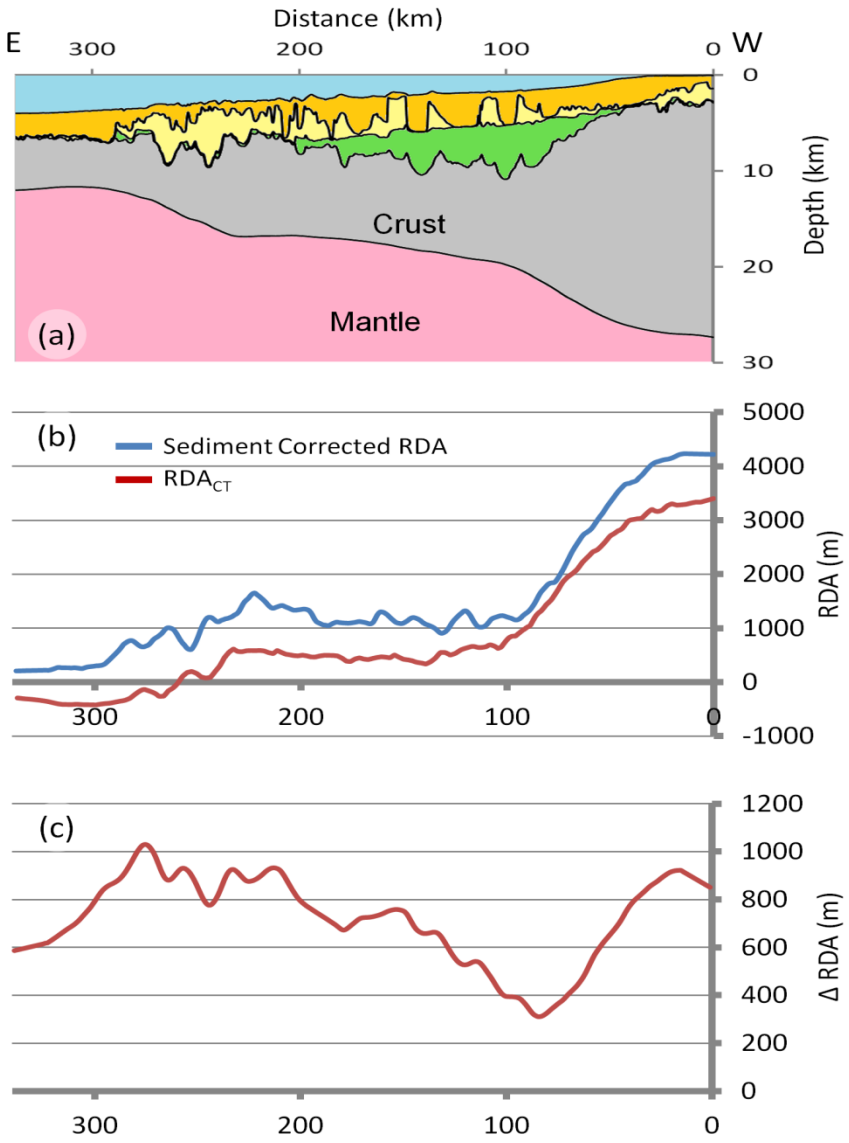

Figure 3.6 – (a) Crustal cross section A-A' across the northern Angolan Margin. The pre-salt sedimentary layer is shown in green, the salt layer in yellow and the post-salt sedimentary layer is orange. (b) Comparison of sediment corrected RDA with the RDA_{CT}. At the western end of the profile the sediment corrected RDA ranges between zero and +300m whilst the RDA_{CT} ranges between -400m and -100m. (c) The sediment corrected RDA, further corrected for variations in crustal thickness (ΔRDA), is positive ranging between approximately +500m and +900m at the western end of the profile. All RDA results in this figure have been smoothed.

In order to determine whether there is any anomalous uplift or subsidence along the CS12400 profile, the RDA corrected for sediment loading and crustal basement thickness variations has been calculated, by taking the difference (ΔRDA) between the sediment corrected RDA and the RDA_{CT}.

$$\Delta RDA = sediment\ corrected\ RDA\ -\ \mathrm{RDA_{CT}} \quad (3)$$

This ΔRDA corresponds to the sediment corrected RDA, which is further corrected for variations in crustal basement thickness. A positive ΔRDA implies anomalous uplift whereas a negative ΔRDA implies anomalous subsidence and a ΔRDA of zero implies that there is no anomalous uplift or subsidence at the margin. The ΔRDA along the CS1-2400 profile (Figure 3.6(c)) is between +500m and +900m at the western end of the profile, which we interpret as mantle dynamic uplift.

3.2.7. Continental lithosphere thinning from subsidence analysis along the CS1-2400 profile

The distribution of continental lithosphere thinning determined from subsidence analysis, involves the conversion of water loaded subsidence into continental lithosphere thinning factors, assuming the intra-continental rift model of McKenzie (1978) together with a correction for crustal magmatic addition from decompression melting. Sediment corrected bathymetry to top pre-rift and top oceanic crust is predicted from flexural backstripping. Sediment corrected bathymetry can be equated to water loaded subsidence, if it is assumed that the initial datum of original continental pre-rift surface that was at or near to sea-level. Water loaded subsidence is interpreted as the sum of initial (Si) and thermal (St) subsidence in the context of the McKenzie (1978) intra-continental rift model. A correction for magmatic addition due to adiabatic decompression (White and McKenzie, 1989) during continental rifting and seafloor spreading has been included. Magmatic addition from decompression melting results in an increase in the thickness of the already thinned continental crust, which causes a reduction in the initial subsidence as predicted by McKenzie (1978) during the formation of new oceanic crust. Initial subsidence corresponds to the isostatic response of the crustal thinning and thermal loads at the time of rifting, which is assumed to be

instantaneous; whilst total subsidence corresponds to the isostatic response of the crustal thinning and thermal loads after a defined time in the post-rift. As instantaneous rifting is assumed, the numerically calculated total subsidence from flexural backstripping is compared to that calculated analytically using McKenzie (1978) modified for magmatic addition. The predicted relationship between continental lithosphere thinning factor (γ) and water loaded subsidence is modified due to magmatic addition from decompression melting.

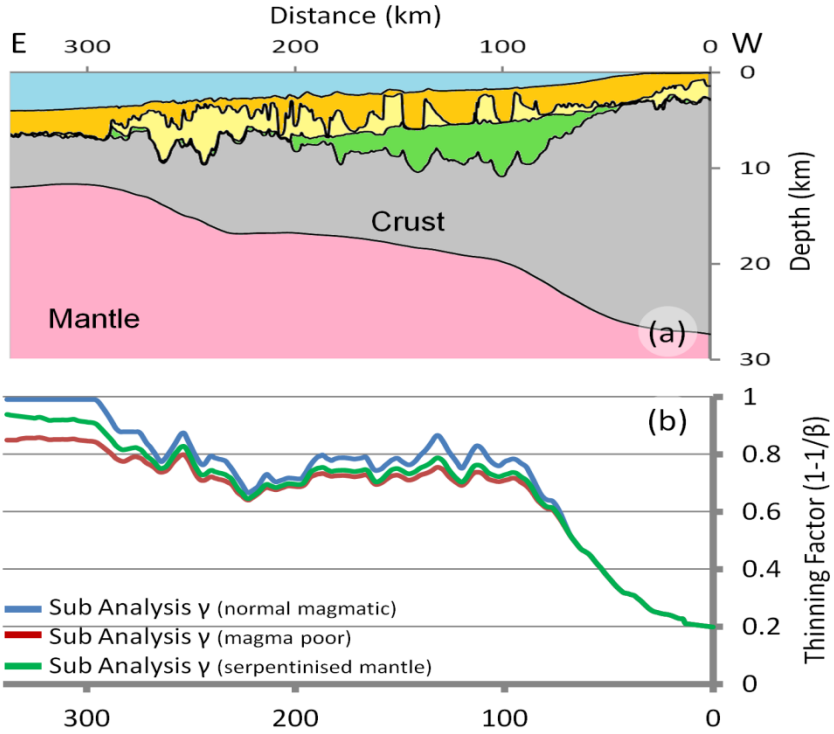

Figure 3.7 – (a) Crustal cross section A-A' across the northern Angolan Margin. The pre-salt sedimentary layer is shown in green, the salt layer in yellow and the post-salt sedimentary layer is orange. (b) Continental lithosphere thinning factors predicted from subsidence analysis, along the CS1-2400 profile. Sensitivities to a 'normal' magmatic margin (Va=7km), magma-poor solution (Va=0km) and a solution for serpentinised mantle have been examined. Subsidence analysis results in this figure have been smoothed.

Sensitivities to continental lithosphere thinning factors from subsidence analysis, as shown in Figure 3.7(b), with reference to the CS1-2400 profile (Figure 3.7(a)) have been examined. These sensitivities include: a 'normal' magmatic solution (Va=7km), a magma-poor solution (Va=0km), and a solution for serpentinized mantle. At the western end of the profile a 'normal' magmatic solution (Va=7km) predicts thinning factors of 1.0, a magma-poor solution

(Va=0km) predicts thinning factors of approximately 0.9, whilst the solution for serpentinized mantle predicts thinning factors of approximately 0.85 in this region.

As previously mentioned the sediment corrected bathymetry has a noisy signal due to fault controlled topography, we have therefore smoothed the subsidence analysis results using the same moving average as before. Unsmoothed subsidence analysis results are shown in Supplementary Figure S3.2.

3.2.8. Joint inversion of deep seismic and gravity anomaly data: application to the CS1-2400 profile

Joint inversion of deep seismic reflection and gravity anomaly data has been applied to the CS1-2400 profile, which solves for coincident seismic and gravity Moho in the time domain and calculates the lateral variations in crustal basement densities and seismic velocities along profile. The joint inversion is carried out in the time domain using the PSTM seismic data (Figure 3.2(a)), as this is the raw data and does not have the assumed basement seismic velocities of the pre stack depth migrated (PSDM) data.

The ION-GXT deep seismic profile CS1-2400 has been interpreted in both the time (PSTM) and depth (PSDM) (Figure 3.2(b)) domain. The sediment thicknesses from the depth section are used within the gravity anomaly inversion to predict Moho depth. The gravity anomaly inversion predicted Moho depths are then converted into the time domain; by calculating the crustal basement thickness in the depth domain:

$$CT_{depth} = Moho_{depth} - TB_{depth} \quad (4)$$

where CT_{depth} is the crustal basement thickness, $Moho_{depth}$ is the gravity anomaly inversion predicted Moho depth and TB_{depth} is the picked top basement. The crustal basement thickness is then converted into the time domain (two-way travel time (TWTT)):

$$CT_{time} = \left[\frac{CT_{depth}}{V_{p\ Basement}}\right] * 2 \quad (5)$$

where CT_{time} is the crustal basement thickness in the time domain and $V_{p\ Basement}$ is crustal basement velocity. In order to determine the gravity anomaly inversion predicted Moho TWTT, in the time domain ($Moho_{time}$), the crustal basement thickness is added to the top basement in the time domain (TB_{time});

$$Moho_{time} = TB_{time} + CT_{time} \quad (6)$$

Joint inversion determines the combination of basement seismic velocities and densities required, along profile, in order to match the Moho predicted from gravity anomaly inversion to the picked Moho, in the time domain. Figure 3.8(a) shows the Moho predicted from gravity anomaly inversion and our picked seismic Moho in the time domain. This comparison is an important validation for the pick of the Moho in the time domain. Beneath the thick salt package (between profile coordinates 210km and 265km), there are no clear Moho reflectors, consequently we have shaded out this area as the joint inversion results are not possible without a Moho pick.

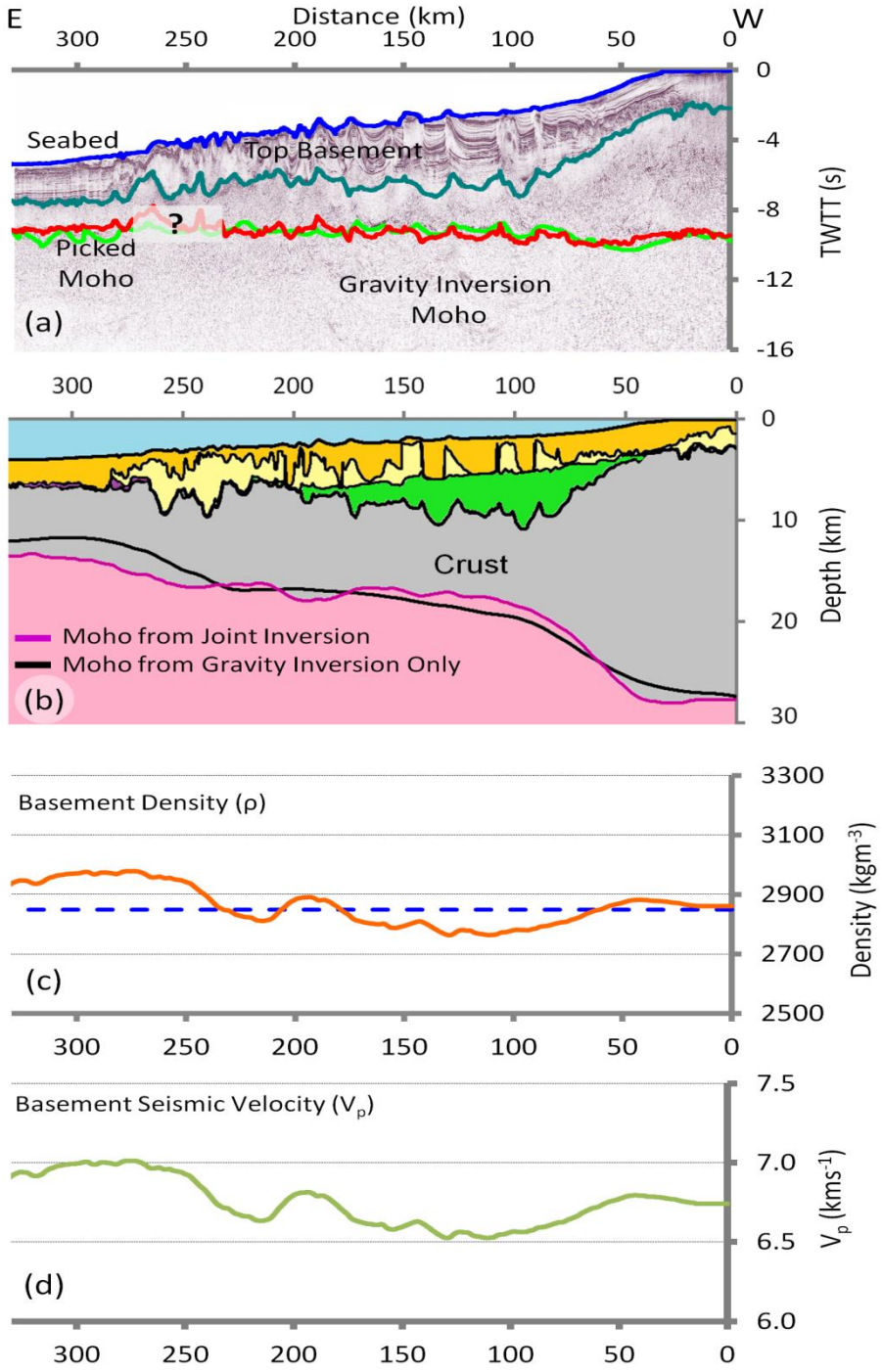

Figure 3.8 – (a) ION-GXT CS1-2400 PSTM deep long offset seismic profile along the northern Angolan rifted continental margin. The horizons for seabed, top basement, Moho predicted from gravity anomaly inversion and picked seismic Moho are indicted. (b) Crustal cross-section along the CS1-2400 northern Angolan profile showing the Moho depth determined from gravity anomaly inversion, and the Moho depth determined from joint inversion; both are in good agreement, with some variation in magnitude. The pre-salt sedimentary layer is shown in green, the salt layer in yellow and the post-salt sedimentary layer is orange. (c) Lateral variations in basement density along the CS1-2400 profile. The blue dashed line highlights the basement density of 2850kgm^{-3} which is the basement density used within the initial gravity anomaly inversion. Densities range between 2650kgm^{-3} and 3050kgm^{-3}. (d) The corresponding lateral variations in seismic velocity along the CS1-2400 profile. The joint inversion predicted Moho, basement density and velocity results) in this figure have been smoothed.

Basement seismic velocities along profile are computed using the empirical relationship between the P-wave velocity (V_p) and density (ρ) for crustal basement rocks (see Supplementary Figure S3.3), for this purpose we use the linear model from Birch (1964). The basement density along profile is computed by locally adjusting the reference basement density of 2850kgm^{-3} used within the gravity anomaly inversion. The changes in basement density and seismic velocity will move the Moho, predicted from gravity anomaly inversion, in the depth domain. Changing the corresponding seismic velocity will change the conversion of the new gravity Moho (depth domain) into the time domain. Solving for the coincident seismic and gravity anomaly inversion predicted Moho in the time domain gives an improved Moho, which satisfies both time and depth as shown in Figure 3.8(b). The lateral variations in basement density and velocity predicted from joint inversion are shown in Figure 3.8(c) and (d). All the joint inversion results in this chapter, including Moho depth, crustal basement densities and seismic velocities have been 'smoothed' by computing a moving average, using a spatial gate of 30km.

3.2.9. Interpretation of the integrated quantitative analysis results along CS1-2400

A composite analysis plot for profile CS1-2400 is shown in Figure 3.9, consisting (a) crustal cross section from gravity anomaly inversion, (b) sediment corrected RDA and RDA_{CT} along CS1-2400, (c) comparison of the continental lithosphere thinning factors predicted from gravity anomaly inversion and subsidence analysis and (d) lateral variations in basement density and (e) seismic velocity from joint inversion. The composite analysis plot is interpreted as showing two distinct crustal zones along the profile highlighted by the dashed line: zone A – oceanic crust and zone B – thinned continental crust. The location of the dashed line is an interpretation of the COB and is based on changes in crustal basement

thickness, sediment corrected RDA and RDA_{CT} signals and also changes in the continental lithosphere thinning from gravity anomaly inversion and subsidence analysis. Whilst the interface between zones A and B is shown as a sharp line, in reality it is likely to be a transitional boundary.

Zone A - Oceanic crust

In zone A, the crustal basement thicknesses range between 5km and 6km (Figure 3.9(a)). The sediment corrected RDA is positive, approximately +300m (Figure 3.9(b)), whilst the RDA_{CT} is negative ranging between approximately -300m and -400m (Figure 3.9(b)), in this region. The RDA analysis implies that there is thin crust in the oceanic domain with a component of mantle dynamic uplift. The continental lithosphere thinning factors predicted from gravity anomaly inversion and subsidence analysis are in good agreement (Figure 3.9(c)) and are high in zone A. Both gravity anomaly inversion and subsidence analysis predict continental lithosphere thinning factors of 1.0, for a 'normal' magmatic solution (Va=7km), implying the presence of oceanic crust. Joint inversion calculates crustal basement densities, which range between 2850kgm^{-3} and 3035kgm^{-3} (with an average basement density of approximately 2940kgm^{-3}) (Figure 3.9(d)) and seismic velocities, which range between 6.7kms^{-1} and 7.1kms^{-1} (Figure 3.9(e)). These basement densities (and corresponding seismic velocities) are larger than the crustal basement density (2850kgm^{-3}) used within the initial gravity anomaly inversion, which is to be expected as typical oceanic crustal densities range between 2860kgm^{-3} and 2900kgm^{-3} (Carlson and Herrick, 1990; Fowler, 2006).

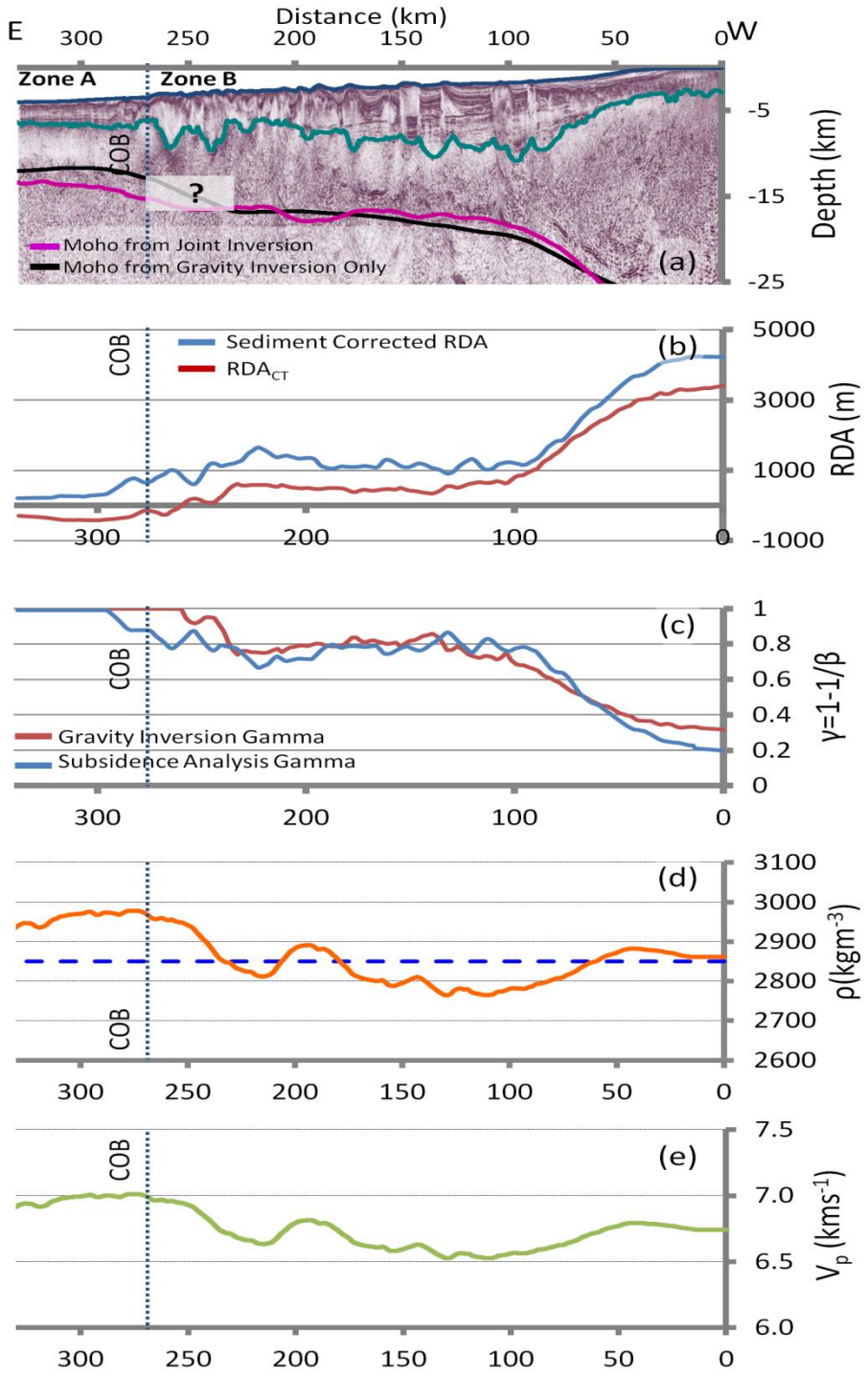

Figure 3.9 – Composite analysis plot for the northern Angolan rifted continental margin. (a) Crustal cross section along CS1-2400 profile from gravity anomaly inversion. (b) Sediment corrected RDA and RDA_{CT}; both have the same general trend along the profile although the magnitudes differ. (c) Comparison of continental lithosphere thinning factors determined using subsidence analysis and gravity anomaly inversion, assuming a 'normal' magmatic margin, shows that they are in good agreement with each other. (d) Basement densities predicted from the joint inversion. (e) Corresponding seismic velocities predicted from the joint inversion. The dashed lines indicate the distal extent of unequivocal continental crust and its boundary with exhumed mantle, which has been interpreted as a possible interpretation of the COB. This boundary is based on the results from gravity anomaly inversion, RDA and subsidence analysis. All results (RDA analysis, subsidence analysis and joint inversion predicted Moho, basement density and velocity results) in this figure have been smoothed.

Zone B - Thinned continental crust

The crustal basement thicknesses in zone B show an increase compared with those seen in zone A; they increase gradually from 8km in the west to 28km in the east (Figure 3.9(a)). At the western end of zone B, both the RDAs corrected for sediment loading and for variations in crustal basement thickness are positive (Figure 3.9(b)); the sediment corrected RDA ranges between +1000m and +1500m, whilst the RDA_{CT} is approximately +600m. The positive RDAs imply the presence of crust that is thicker than 7km. At the eastern end of zone B, both RDAs corrected for sediment loading and for variations in crustal basement thickness increase gradually across the margin, this may correspond to the necking zone. The continental lithosphere thinning factors from gravity anomaly inversion and subsidence analysis are in good agreement in zone B (Figure 3.9(c)). At the western end of zone B continental lithosphere thinning factors from subsidence analysis range between approximately 0.6 and 0.8, whilst the continental lithosphere thinning factors calculated from gravity anomaly inversion are approximately 0.8. Towards the eastern end of zone B the continental lithosphere thinning factors from gravity anomaly inversion and subsidence analysis continue to decrease and range between 0.2 and 0.3. Basement densities and seismic velocities, predicted from joint inversion, show a general decrease compared with those seen in zone A; in the central region of the CS1-2400 profile the basement densities range between approximately 2700kgm^{-3} and 3000kgm^{-3} (Figure 3.9(d)) and the corresponding seismic velocities range between 6.3kms^{-1} and 7.1kms^{-1} (Figure 3.9(e)). At the eastern end of the profile the predicted basement densities and velocities show a further decrease, with basement densities ranging between 2760kgm^{-3} and 2900kgm^{-3} and seismic velocities ranging between 6.5kms^{-1} and 6.8kms^{-1}. The average basement density for zone B is approximately 2825kgm^{-3}, which is within the range proposed for the density of continental

crust (Carlson and Herrick, 1990) and is similar to that used within the initial gravity anomaly inversion (2850kgm^{-3}).

3.3. OCT structure and COB location: along the BS1-575 profile, south-eastern Brazilian margin

3.3.1. Background:

The Santos, Campos and Espírito Santo rift basins of the south-eastern Brazilian margin formed as a result of Early Cretaceous rupturing and breakup of West Gondwana and subsequent seafloor spreading that led to the development and evolution of the South Atlantic Ocean (Mohriak et al., 2008; Scotchman et al., 2010). The south-eastern Brazilian rifted continental margin is sometimes considered to be a magmatic margin (Reston, 2009), whilst others regard it as a typical magma-poor margin (Zalán et al., 2011). The crustal structure of the south-eastern Brazilian rifted continental margin, in particular the OCT, is largely unknown due to the presence of a thick Aptian (middle to upper Aptian) salt sequence, including huge salt diapirs and salt walls in the deep-water region of the Espírito Santo, Campos and Santos basins (Mohriak et al., 2008). However, it has been proposed (Zalán et al., 2011) that there is a continuous belt of exhumed mantle in the OCT that can be mapped across all three basins. Analysis along the south-eastern Brazilian rifted continental margin is focussed on the ION-GXT deep long offset seismic reflection profile, BS1-575 (Figure 3.1(a)).

3.3.2. Crustal basement thickness and continental lithosphere thinning from gravity anomaly inversion along the BS1-575 profile

Gravity anomaly inversion has been applied to the ION-GXT deep seismic reflection profile BS1-575 in order to determine Moho depth, crustal basement thickness and continental lithosphere thinning along profile. The data used within the gravity anomaly inversion are bathymetry (Amante and Eakins, 2009) (Figure 3.1(a)), satellite derived free air gravity (Sandwell and Smith, 2009) (Figure 3.1(b)), and 2D sediment thickness from PSDM seismic reflection data along ION-GXT profile BS1-575 (Figure 3.10(b)). The Moho signature along the ION-GXT deep seismic profile, BS1-575, along the south-eastern Brazilian rifted continental margin, is not as clear as that seen for the northern Angolan profile (CS1-2400), however, it is still possible to calibrate the gravity anomaly inversion predicted Moho depths. Calibration suggests that a reference Moho depth of 37.5km is required, for the BS1-575 profile, in order to predict crustal basement thicknesses consistent with those seen in the seismic reflection data.

Along the BS1-575 seismic profile there is a significant salt layer, with salt diapirs in the west and a thick salt package in the central section of the profile. The salt layer has been given a simple salt lithology (Hudec and Jackson, 2007), using a density of 2200kgm^{-3} and a compaction coefficient of zero. Sediment densities used within the gravity anomaly inversion, increase with depth assuming normal compaction corresponding to a shaly-sand lithology .

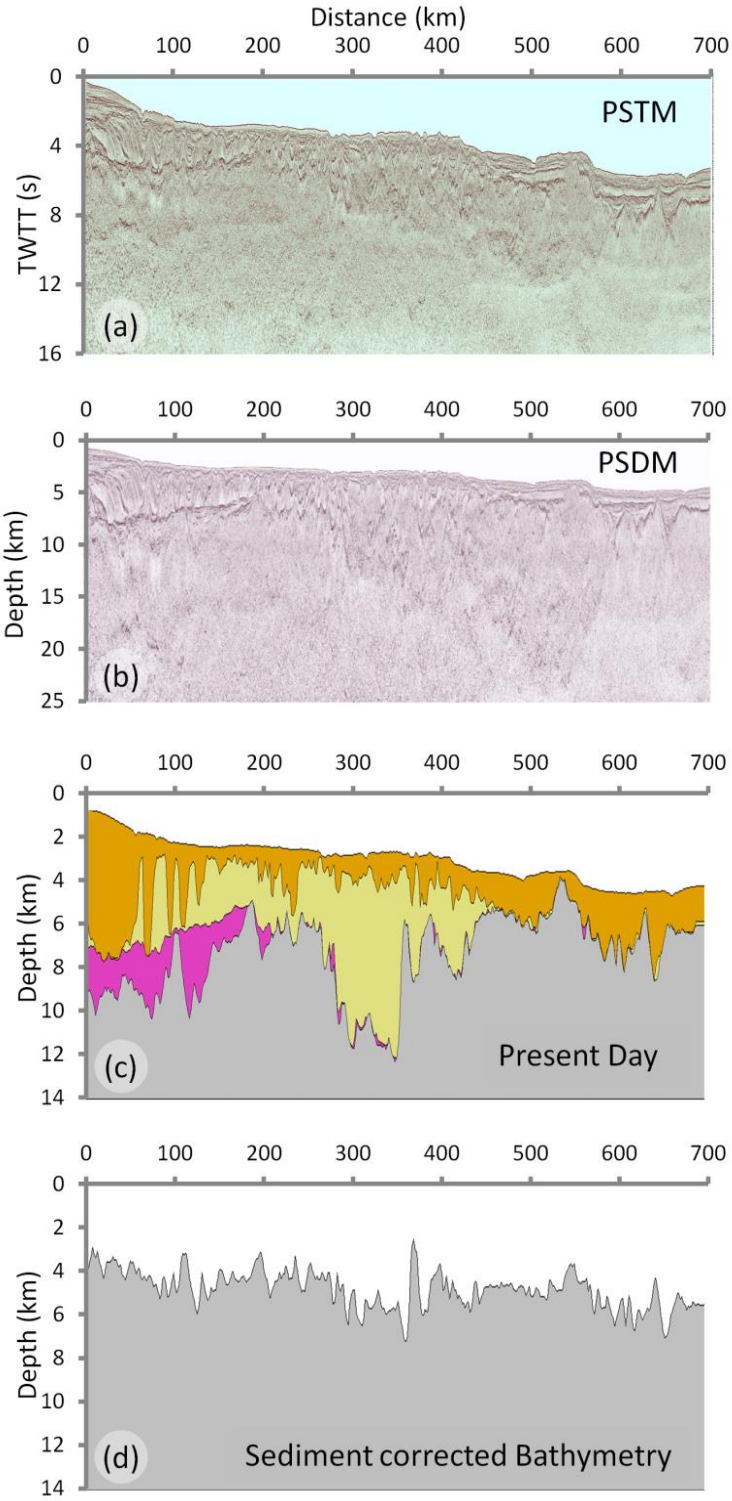

Figure 3.10 – (a) PSTM (pre stacked time migrated) seismic data for the ION-GXT BS1-575 south-eastern Brazilian deep long offset seismic profile (b) PSDM (pre stacked depth migrated) seismic data for the ION-GXT BS1-575 south-eastern Brazilian deep long offset seismic profile (c) Digitized present day cross section along the BS1-575 profile; the pre-salt sedimentary layer is highlighted in pink; post-salt sedimentary layer in orange and the salt layer is highlighted in yellow. (d) Sediment corrected bathymetry calculated using flexural backstripping, assuming a Te=1.5km.

A crustal cross section (Figure 3.11(a)) along BS1-575 profile is constructed using bathymetry (Amante and Eakins, 2009) and 2D sediment thickness from the PSDM seismic reflection data along the ION-GXT BS1-575 profile with Moho depth from gravity anomaly inversion. Using the calibrated reference Moho depth of 37.5km, crustal basement thicknesses of approximately 7km (or greater) are predicted, at the eastern end of the profile, adjacent to the Florianopolis Fracture Zone (FFZ). Crustal basement thicknesses predicted from gravity anomaly inversion under the Sao Paulo Plateau (SPP) and the Florianopolis Ridge (FR) are thicker than typical oceanic crust, but are substantially thinner than that expected for 'normal' thickness continental crust. Beneath the thick salt, the gravity anomaly inversion predicted Moho comes up into the sediment layer, which is an unphysical result. We believe this is because there are pre-salt sediments beneath this thick salt and the salt may not come all the way down to top basement as we have interpreted. We have considered a sensitivity test in which we omit the salt and treat the salt layer as a sedimentary layer (See Supplementary Figure S3.4); this produces a deeper Moho beneath the thick salt. The crust beneath this area is still very thin (approximately 5km thick). Although this sensitivity produces a physical result for the region of very thick salt, it is not valid for the rest of the profile. We have therefore used the solution, which included the salt layer, but have blanked out the unphysical solution beneath the thick salt for ease in interpretation.

The distribution of continental lithosphere thinning (γ) predicted from gravity anomaly inversion along the BS1-575 profile assuming three different magmatic addition solutions are shown in Figure 3.11(b). A 'normal' magmatic solution (Va=7km), a magma-poor solution (Va=0km), and a magma-rich solution (Va=10km) have all been examined. In addition a solution for serpentinised mantle has been examined (Figure 3.11(c)) due to the reported exhumed mantle, at the eastern end of the BS1-575 seismic profile (Zalán et al., 2011). Changes from high continental lithosphere thinning factors (between 0.8 and 1.0) to lower

continental lithosphere thinning factors have been used constrain the COB location along the BS1-575 profile.

Along the BS1-575 profile the continental lithosphere thinning (γ) predicted from gravity anomaly inversion vary considerably from east to west. At the eastern end of the profile the continental lithosphere thinning factors (Figure 3.11(b)) for a 'normal' magmatic solution are between 0.9 and 1.0. Continental lithosphere thinning factors are 1.0 for a magma-rich solution and for a magma-poor solution the continental lithosphere thinning factors are much less, approximately 0.8. In the central section of the profile, there is negligible difference between continental lithosphere thinning factors predicted from gravity anomaly inversion for a magma-poor solution and a 'normal' magmatic solution. The biggest difference in this central section is seen when comparing the magma-rich solution, which predicts much larger continental lithosphere thinning factors, between 0.8 and 1.0. Continental lithosphere thinning factors from gravity anomaly inversion, for a serpentinized mantle solution (Figure 3.11(c)), range between 0.8 and 0.9 at the eastern end of the profile. In the central section there is little difference between continental lithosphere thinning factors for the serpentinised mantle solution and the 'normal' magmatic solution.

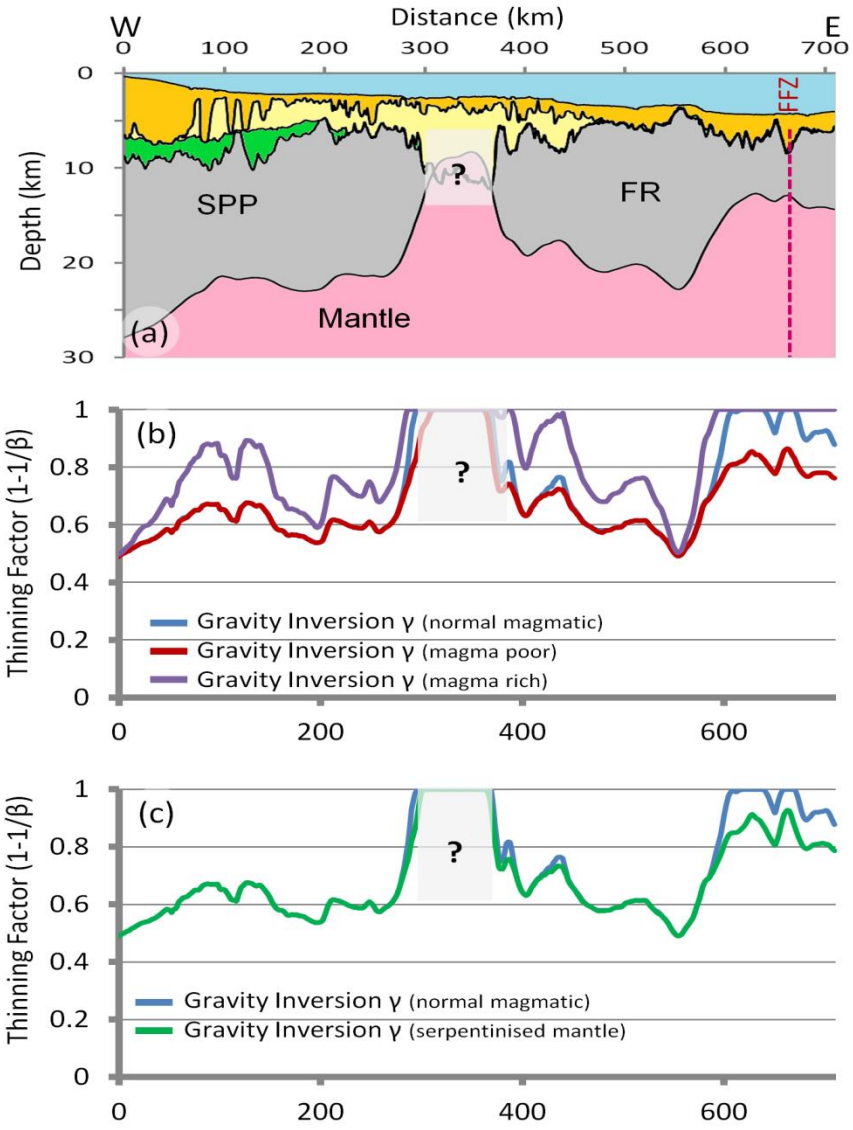

Figure 3.11 – (a) Crustal cross section along the BS1-575 profile along the south-eastern Brazilian rifted continental margin. Sao Paulo Plateau (SPP) and Florianopolis Ridge (FR) are highlighted. The pre-salt sedimentary layer is shown in green, the salt layer in yellow and the post-salt sedimentary layer is orange. (b) Continental lithosphere thinning predicted from gravity anomaly inversion. Sensitivities to a 'normal' magmatic solution (Va=7km), a magma-poor solution (Va=0km) and a magma-rich solution (Va=10km) have been examined. (c) Comparison of continental lithosphere thinning factors predicted from gravity anomaly inversion for a 'normal' magmatic margin and a solution for serpentinised mantle.

3.3.3. Sediment corrected RDA along the BS1-575 profile

Sediment corrected RDAs have been calculated along the south-eastern Brazilian margin, by comparing the observed bathymetries corrected for sediment loading and age predicted oceanic bathymetries. Present day bathymetry and depth to top basement digitized from the BS1-575 PSDM profile are shown in Figure 3.10(c). Sediment corrected bathymetry has been determined using flexural backstripping (Kusznir et al., 1995) and is shown in Figure 3.10(d).

Figure 3.12(b) shows a comparison of the uncorrected RDA and the sediment corrected RDA along the BS1-575 profile (Figure 3.12(a)); there is approximately a 1300m difference between the uncorrected RDA and the sediment corrected RDA at the eastern end of the profile, which increases to a maximum of +3000m at the western end of the profile. The sediment corrected RDA along the BS1-575 profile, Figure 3.12(b), is approximately zero at the eastern end of the profile.

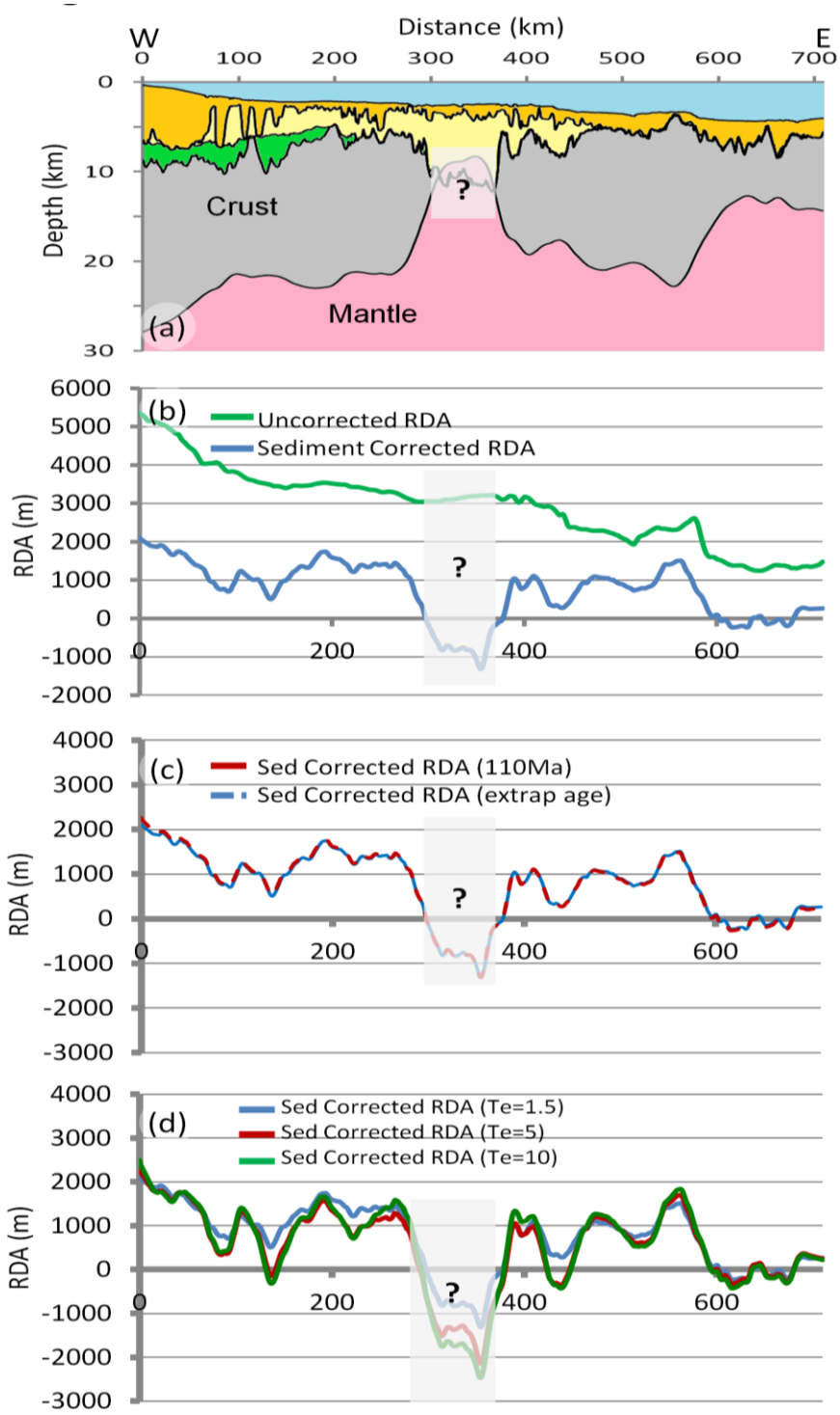

Figure 3.12 – (a) Crustal cross section along the BS1-575 profile along the south-eastern Brazilian rifted continental margin. The pre-salt sedimentary layer is shown in green, the salt layer in yellow and the post-salt sedimentary layer is orange. (b) Comparison of uncorrected RDA results with the sediment corrected RDA results. (c) The sensitivity to oceanic age for sediment corrected RDA results has been examined. Two approaches have been considered (i) a constant value of 120Ma for the profile and (ii) using Müller et al. (2008) age isochrons with their age gradient extrapolated inboard. (d) Sensitivity to the effective elastic thickness for northern Angolan margin sediment corrected RDA results has been examined. Te's of 1.5km, 5km and 10km produce sediment corrected RDAs of similar magnitude. The largest difference is seen beneath the thick salt. All RDA results in this figure have been smoothed.

As previously mentioned the sediment corrected RDA is calculated using age predicted oceanic bathymetries, which are dependent on oceanic lithospheric age. The Müller et al. (2008) global ocean age isochrons do not extend the entire length of profile BS1-575, it is therefore necessary to consider sensitivities to oceanic lithospheric age. As with the northern Angolan margin two approaches have been examined: the first uses a constant value of 120Ma for the profile, whilst the second uses Müller et al. (2008) age isochrons with their age gradient extrapolated inboard. A comparison and sensitivity of the sediment corrected RDA results to ocean lithospheric age isochrons is shown in Figure 3.12(c), both approaches produce similar results.

Sensitivities to effective elastic thicknesses of 1.5km, 5km and 10km have been examined along the south-eastern Brazilian profile and are shown in Figure 3.12(d). There is little effect on the sediment corrected RDA result when changing Te at the eastern end of the profile. A Te of 1.5km has been used as our preferred value for the BS1-575 profile.

As previously mentioned for the Angolan profile, the sediment corrected bathymetry shows structural control from faulting and as a result has a noisy signal. We have therefore applied a smoothing filter by computing a moving average for the sediment corrected RDA results. The unsmoothed sediment corrected RDA results along the BS1-575 profile are shown in Supplementary Figure S3.5.

3.3.4. RDA component from crustal thickness variations (RDACT) along the BS1-575 profile

The RDA component from crustal thickness variations (RDA_{CT}) has been computed in addition to the sediment corrected RDA along the BS1-575 profile. At the eastern end of the profile,

the RDA_{CT} (Figure 3.13(b)) is approximately zero (but ranges between ±100m); the RDA_{CT} increases westwards and ranges between +750m and +2300m.

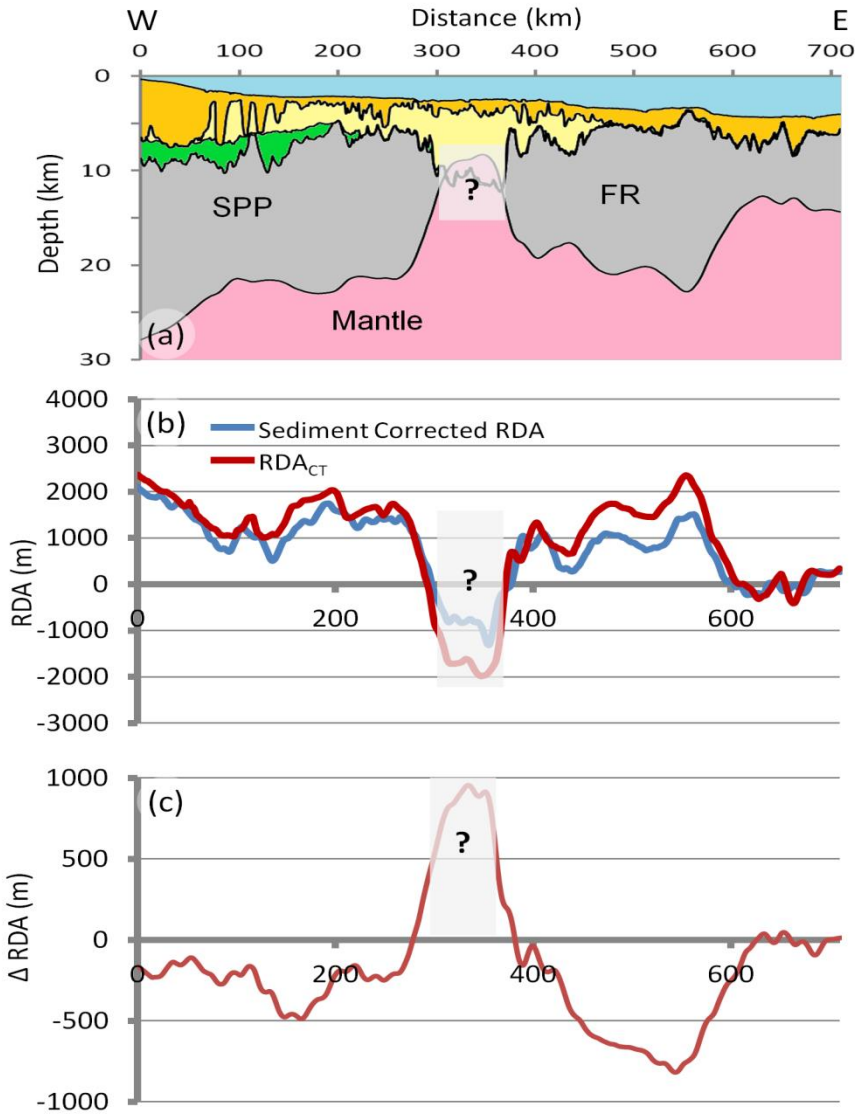

Figure 3.13 – (a) Crustal cross section across the south-eastern Brazilian margin. Sao Paulo Plateau (SPP) and Florianopolis Ridge (FR) are highlighted. The pre-salt sedimentary layer is shown in green, the salt layer in yellow and the post-salt sedimentary layer is orange. (b) Comparison of sediment corrected RDA with the RDA_{CT}; both RDA techniques are approximately zero at the eastern end of the profile. (c) The sediment corrected RDA further corrected for crustal thickness variations (ΔRDA) is approximately zero at the eastern end of the profile. All RDA results in this figure have been smoothed.

3.3.5. RDAs corrected for sediment loading and crustal thickness variations along the BS1-575 profile

Figure 3.13 (b) shows both the sediment corrected RDA and the RDA_{CT} along the BS1-575 seismic profile. The location of the COB can be further constrained using changes in crustal type, which are identified by changes in the RDA signal. At the eastern end of the profile both the sediment corrected RDA and the RDA_{CT} (Figure 3.13(b)) are approximately zero, corresponding to the presence of crust that is approximately 7km thick. Beneath the Sao Paulo Plateau and the Florianopolis Ridge the sediment corrected RDA and the RDA_{CT} are positive corresponding to thinned continental crust. Both the sediment corrected RDA and the RDA_{CT} show the same general trend along the profile although they have different magnitudes. The sediment corrected RDA further corrected for variations in crustal basement thickness (ΔRDA) (Figure 3.13(c)) has been computed and is approximately zero at the eastern end of the BS1-575 profile, which implies that there is negligible mantle dynamic topography in the oceanic domain.

3.3.6. Continental lithosphere thinning from subsidence analysis along the BS1-575 profile

Figure 3.14(b) shows the smoothed continental lithosphere thinning factors from subsidence analysis along the BS1-575 seismic profile (Figure 3.14(a)); unsmoothed subsidence analysis results are shown in Supplementary Figure S3.6. Sensitivities to magmatic addition are examined: a 'normal' magmatic solution (Va=7km), a magma-poor solution (Va=0km) and magma-rich solution (Va=10km). At the eastern end of the profile a 'normal' magmatic solution (Va=7km) and a magma-rich solution (Va=10km) both predict thinning factors of approximately 1.0 whilst the magma-poor solution (Va=0km) predicts thinning factors of approximately 0.8. Both the 'normal' magmatic solution and the magma-rich solution predict

oceanic crust at the eastern end of the BS1-575 seismic profile. In addition a solution for serpentinised mantle has been examined (Figure 3.14(c)), and predicts continental lithosphere thinning factors of 0.9 at the eastern end of the profile.

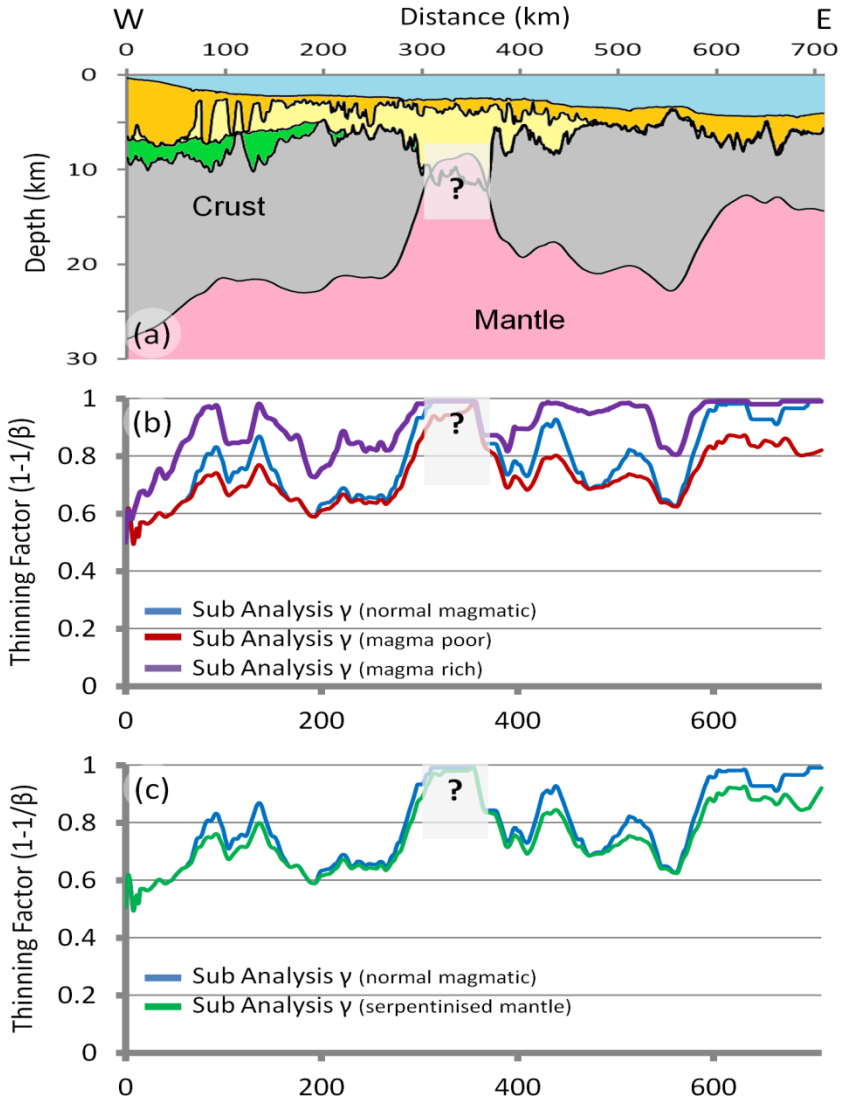

Figure 3.14 – (a) Crustal cross section across the south-eastern Brazilian Margin. The pre-salt sedimentary layer is shown in green, the salt layer in yellow and the post-salt sedimentary layer is orange. (b) Continental lithosphere thinning factors from subsidence analysis. Sensitivities to a 'normal' magmatic margin (Va=7km), a magma-poor margin (Va=0km) and a magma-rich margin (Va=10km) have been examined. (c) Comparison of the continental lithosphere thinning factors calculated from subsidence analysis for a 'normal' magmatic margin and a solution for serpentinised mantle. All subsidence analysis results in this figure have been smoothed.

3.3.7. Joint inversion of deep seismic and gravity anomaly data: application to the BS1-575 profile

Joint inversion technique of deep seismic reflection and gravity anomaly data has been applied to the BS1-575 profile, which solves for the coincident seismic and gravity Moho in the time domain and calculates the lateral variations in crustal basement densities and velocities along profile. The ION-GXT seismic profile BS1-575 has been interpreted in both the time (PSTM) (Figure 3.10(a)) and depth (PSDM) (Figure 3.10(b)) domain. The 2D sediment thicknesses from the depth section are used in the gravity anomaly inversion to predict Moho depth, which is then converted into the time domain; Figure 3.15(a) shows a comparison of both the Moho predicted from gravity anomaly inversion and the seismic pick of Moho in the time domain. Joint inversion determines the combination of basement seismic velocities and densities required, along profile, in order to match the Moho predicted from gravity anomaly inversion to the picked Moho in the time domain as shown in Figure 3.15(b). The lateral variations in basement density and velocity along the BS1-575 profile are shown in Figure 3.15(c) and (d) respectively. The joint inversion predicted Moho, crustal basement densities and seismic velocities have all been smoothed.

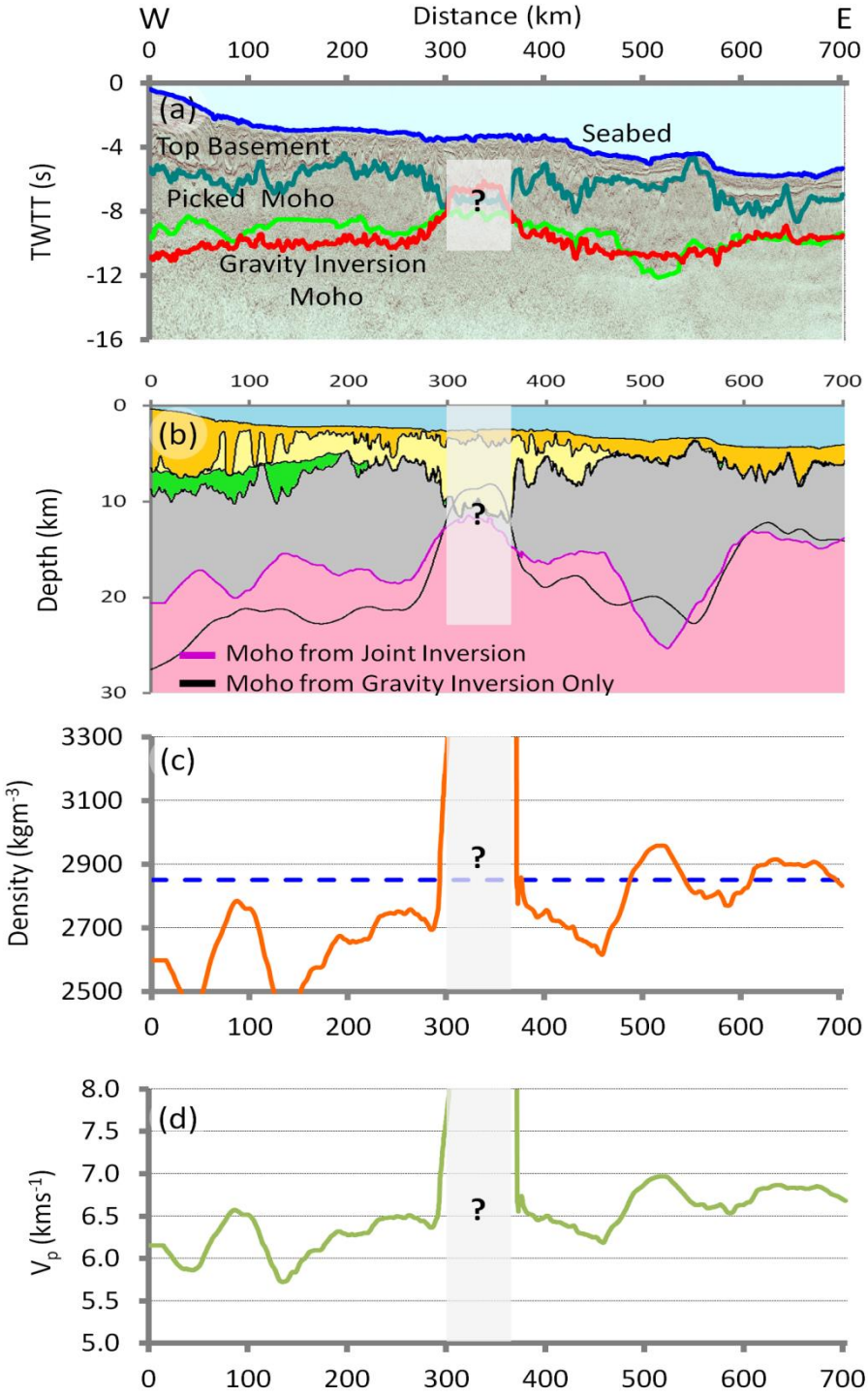

Figure 3.15 – (a) ION-GXT CS1-2400 PSTM deep long offset seismic profile along the south-eastern Brazilian rifted continental margin. The horizons for seabed, top basement, Moho predicted from gravity anomaly inversion and picked seismic Moho are indicted. (b) Crustal cross-section along the BS1-575 south-eastern Brazilian profile showing the Moho depth determined from gravity anomaly inversion, and the Moho depth determined from joint inversion. The pre-salt sedimentary layer is shown in green, the salt layer in yellow and the post-salt sedimentary layer is orange. (c) Lateral variations in basement density along the BS1-575 profile. The blue dashed line highlights the basement density of 2850kgm^{-3} which is the basement density used within the initial gravity anomaly inversion. (d) The corresponding lateral variations in seismic velocity along the BS1-575 profile. The joint inversion predicted Moho, basement density and velocity results in this figure have been smoothed.

3.3.8. Interpretation of the integrated quantitative analysis results along BS1-575

The composite analysis plot for profile BS1-575 Figure 3.16 consists of: (a) crustal cross section from gravity anomaly inversion, (b) sediment corrected RDA and RDA_{CT}, (c) comparison of the continental lithosphere thinning factors predicted from gravity anomaly inversion and subsidence analysis, (d) lateral variations in basement density and (e) seismic velocity from joint inversion. The composite analysis plot is interpreted as showing two primary zones: zone A – unequivocal oceanic crust and zone B' – thinned continental crust. Whilst the interface between zones A and B' is shown as a sharp line, in reality it is likely to be a transitional boundary.

Zone A - Oceanic crust

In zone A the crustal basement thicknesses from gravity anomaly inversion range between 7km and 8km (Figure 3.16(a)). The sediment corrected RDA and the RDA_{CT} are approximately zero in this region (Figure 3.16(b)), corresponding to the presence of 7km thick crust and no mantle dynamic topography. The continental lithosphere thinning factors in zone A derived from gravity anomaly inversion and subsidence analysis, using a 'normal' magmatic solution (Va=7km), are in good agreement ranging between 0.95 and 1.0 (Figure 3.16(c)), implying the presence of oceanic crust. Joint inversion predicts crustal basement densities, which range between approximately 2800$kgm^{-3}$and 2950kgm^{-3} (Figure 3.16(d)) and the corresponding seismic velocities, range between approximately 6.6kms^{-1} and 7.0kms^{-1} (Figure 3.16(e)). The average basement density in zone A is 2875kgm^{-3}, which is within the density range proposed for oceanic crust (Carlson and Herrick, 1990; Fowler, 2006).

Zone B' – Thinned continental crust with a high magmatic component

The crustal basement thicknesses, RDAs, and continental lithosphere thinning factors show considerable variation along BS1-575 in zone B' (Figure 3.16). The crustal basement thicknesses in zone B' (Figure 3.16(a)) show an increase compared with those seen in zone A; and range between 8km and 17km. Both the sediment corrected RDA and the RDA_{CT} are positive in zone B', and range between +500m and +2300m (Figure 3.16(b)). The continental lithosphere thinning factors from gravity anomaly inversion and subsidence analysis are in good agreement in zone B' (Figure 3.16(c)). The continental lithosphere thinning factors from subsidence analysis range between approximately 0.55 and 1.0, whilst the continental lithosphere thinning factors calculated from gravity anomaly inversion have a smaller range, between approximately 0.5 and 0.8.

The basement densities, from joint inversion, range between 2600kgm^{-3} and 2850kgm^{-3} and seismic velocities range between 6kms^{-1} and 6.7kms^{-1} under the Florianopolis Ridge. These basement densities are lower than typical continental crustal densities. However, beneath the Florianopolis Ridge (FR), west of the Florianopolis fracture zone we interpret a 'keel' structure, for which the joint inversion method predicts larger basement densities (approximately 2965kgm^{-3}) (Figure 3.16(d)) and seismic velocities (approximately 7kms^{-1}) (Figure 3.16(d)) than for the rest of the Florianopolis Ridge region. We believe that this structure is the result of a too deep interpretation of the Moho. The reflections used to pick the Moho are probably within the mantle. Therefore, there is a substantial difference between the picked Moho and the gravity anomaly inversion predicted Moho in this region, which results in the need for larger basement densities and seismic velocities for this 'keel' structure.

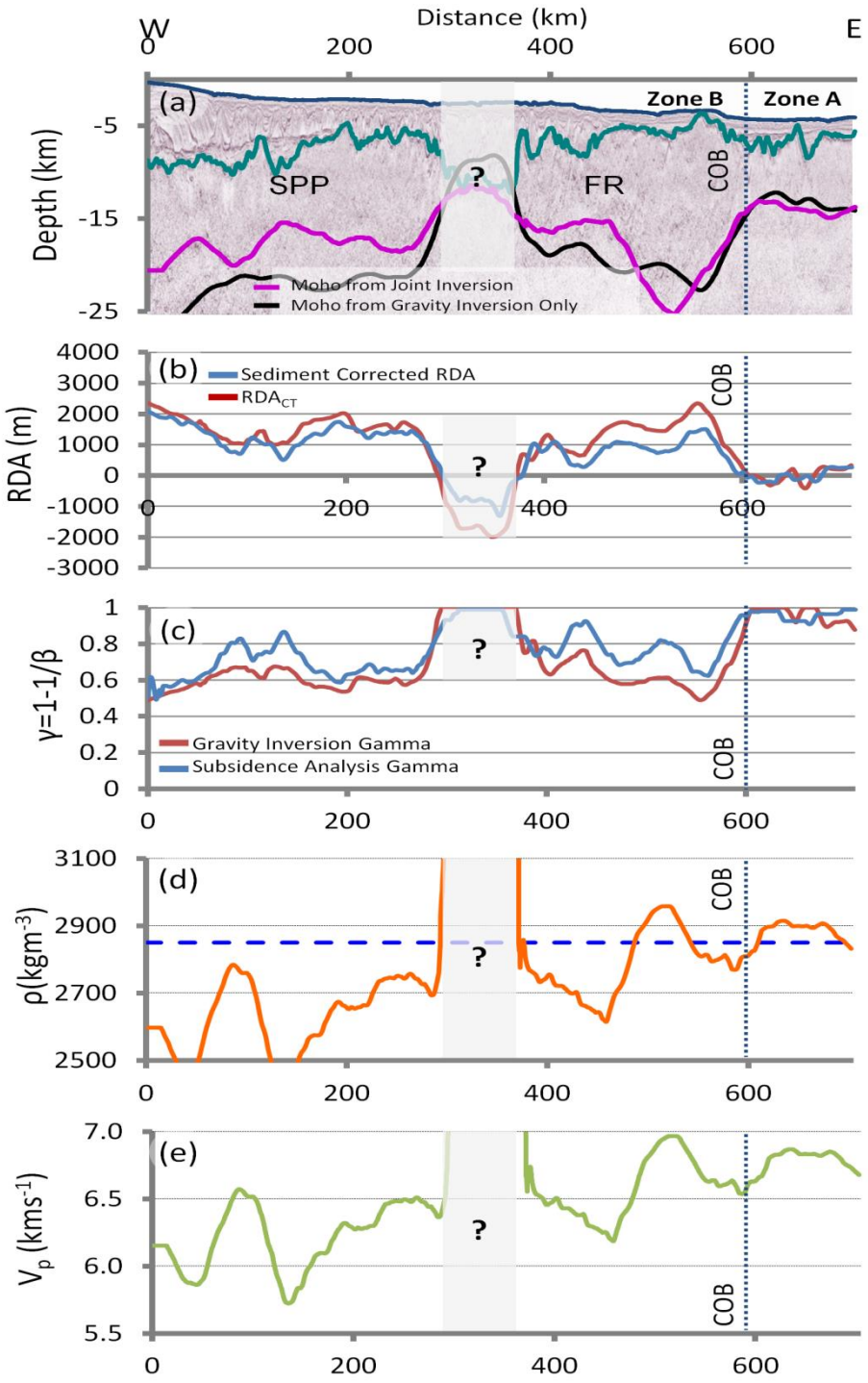

Figure 3.16 – Composite analysis plot for south-eastern Brazilian rifted continental margin. (a) Crustal cross section along BS1-575 profile from gravity anomaly inversion. Sao Paulo Plateau (SPP) and Florianopolis Ridge (FR) are highlighted. (b) Sediment corrected RDA and RDA_{CT}; both have the same general trend along the profile although the magnitudes differ. (c) Comparison of continental lithosphere thinning factors determined using subsidence analysis and gravity anomaly inversion, assuming a 'normal' magmatic margin, shows that they are in good agreement with each other. (d) Basement densities predicted from the joint inversion. (e) Corresponding seismic velocities predicted from the joint inversion. The dashed lines indicate the distal extent of unequivocal continental crust and its boundary with exhumed mantle, which has been interpreted as a possible interpretation of the COB. This boundary is based on the results from gravity anomaly inversion, RDA and subsidence analysis. All results (RDA analysis, subsidence analysis and joint inversion predicted Moho, basement density and velocity results) in this figure have been smoothed.

Under the Sao Paulo Plateau (SPP) joint inversion predicts basement densities, which range between 2450kgm^{-3} and 2850kgm^{-3} (with an average of approximately 2640kgm^{-3}) and corresponding seismic velocities, which range between 5.8kms^{-1} and 6.8kms^{-1}. These basement densities are considerably lower than expected for continental crust. There are two possible explanations for these low basement densities:

(i) Many authors believe that the continental crust beneath the Sao Paulo Plateau is intruded by volcanic rocks , so it is possible that our pick of the Moho is the top of the Paraná volcanics, which are laterally extensive in this region. It is proposed (e.g. Mohriak et al.(2008)) that the Paraná volcanics may be underlain by syn-rift sediments (possibly Neocomian in age). Both the Paraná volcanics and additional deeper sediments would act to lower the density beneath the Sao Paulo Plateau.

(ii) An alternative explanation is that there is a mass deficiency, e.g. presence of gabbroic material, which has been 'frozen' into the continental lithospheric mantle (Cannat et al., 2009) beneath the Sao Paulo Plateau. If this is the case, the gravity anomaly inversion will assume that this lighter material is crustal basement, and this will result in a deeper prediction of Moho depth.

3.4. Discussion and Summary

Integrated quantitative analysis using gravity anomaly inversion, RDA analysis, subsidence analysis and deep seismic reflection data has been used to determine the OCT structure, COB location and magmatic type along the northern Angolan profile CS1-2400 and south-eastern Brazilian profile BS1-575. Integrated quantitative analysis of these profiles shows the distribution of thinned continental crust and the start of unequivocal oceanic crust along the respective margins. Considering the gravity anomaly inversion, RDA and subsidence analysis techniques together has enabled a robust geological interpretation of the OCT along the

seismic profiles to be made and a more accurate interpretation of the COB location to be examined. Joint inversion of deep seismic and gravity anomaly data shows the contrast between density and seismic velocity between oceanic and continental crustal basement along both the Angolan and Brazilian profiles. This basement density and seismic velocity contrast between the oceanic and continental crustal basement is comparable to the location of the COB derived from integrated quantitative analysis.

Angolan Discussion:

Figure 3.17(a) shows our interpretation of the integrated quantitative analysis results along the CS1-2400 profile. Analysis of the northern Angolan rifted continental profile suggests that:

(i) serpentinised exhumed mantle is absent beneath the allochthonous salt, and the margin segment is not magma-poor.

(ii) Gravity and deep seismic reflection data predict that the earliest oceanic crust is approximately 5km to 7km thick.

(iii) Comparison of the sediment corrected RDA and the RDA_{CT} implies that this margin is experiencing between approximately +500m and +900m of mantle dynamic uplift.

(iv) Gravity anomaly inversion, RDA and subsidence analysis results show that the OCT along CS1-2400 is quite wide, with the distance between the COB and the margin hinge measuring approximately 180km.

(v) Joint inversion shows a contrast in basement density and seismic velocity between oceanic and continental crustal basement consistent with the location of the COB derived from integrated quantitative analysis.

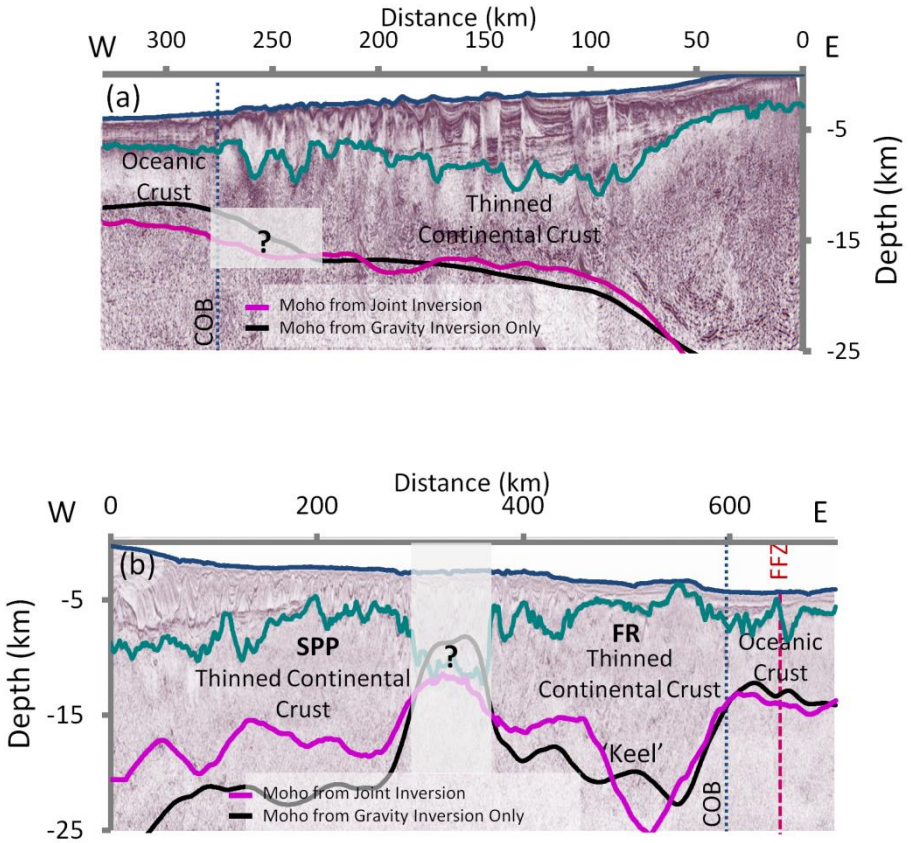

Figure 3.17 – (a) Interpretation of the integrated quantitative analysis results along the PSDM CS1-2400 profile. Seabed is shown in blue, top basement in green, Moho from gravity anomaly inversion in black and Moho from the joint inversion is shown in pink. Our interpretation of the COB from integrated quantitative analysis results is identified along the profile; to the west we interpret 'normal' thickness oceanic crust and to the east we interpret thinned continental crust. We have shaded out part of the Moho from joint inversion as there are no Moho reflectors in this region. (b) Interpretation of the integrated quantitative analysis results along the PSDM BS1-575 profile. Seabed is shown in blue, top basement in green, Moho from gravity anomaly inversion in black and Moho from the joint inversion is shown in pink. Our interpretation of the COB from integrated quantitative analysis results is identified along the profile; to the east we interpret approximately 'normal' thickness oceanic crust and to the west we interpret thinned continental crust beneath the Florianopolis Ridge and Sao Paulo Plateau. The location of the Florianopolis Fracture Zone (FFZ) is also identified. We have shaded out the region beneath the thick salt between the Florianopolis Ridge and Sao Paulo Plateau as the joint inversion predicts an unphysical result here. The Moho from joint inversion has been smoothed.

Brazil Discussion:

Figure 3.17(b) shows our interpretation of the integrated quantitative analysis results along the BS1-575 profile. Analysis of the south-eastern Brazilian rifted continental profile suggests that:

(i) there is no evidence for exhumed mantle along this margin profile.

(ii) Gravity and deep seismic reflection data predict that the earliest oceanic crust is between 7km and 8km thick.

(iii) Beneath the Sao Paulo Plateau and Florianopolis Ridge crustal basement thicknesses range between 10km and 15km.

(iv) RDA analysis implies negligible mantle dynamic topography.

(v) Gravity anomaly inversion, RDA and subsidence analysis results show that the OCT along BS1-575 is wide, with the distance between the COB and the margin hinge measuring approximately 540km.

(vi) The joint inversion of deep seismic and gravity anomaly data predict basement densities typical of 'normal' oceanic crust for the earliest oceanic crust.

(vii) For much of the north-western end of the Florianopolis Ridge, the joint inversion predicts basement densities that are less than expected for continental crust, similar to those seen for the Sao Paulo Plateau.

(viii) In contrast at the south-eastern end of the Florianopolis Ridge the joint inversion predicts basement densities and seismic velocities, which are much higher and are similar to those predicted for the oceanic crust. We interpret this region as a 'keel' structure, which is west of the COB.

(ix) Beneath the Sao Paulo Plateau joint inversion predicts basement densities substantially lower than expected for thinned continental crust, possibly due a

Neocomian rift basin under the Paraná volcanic or gabbroic material in the continental lithospheric mantle. Both of these would act to lower the density beneath the Sao Paulo Plateau.

(x) Joint inversion shows a contrast in basement density and seismic velocity between oceanic and continental crustal basement, which is comparable to the location of the COB derived from integrated quantitative analysis.

3.5. References

Alvey, A., Gaina, C., Kusznir, N. J., and Torsvik, T. H., 2008, Integrated crustal thickness mapping and plate reconstructions for the high Arctic: Earth and Planetary Science Letters, v. 274, no. 3-4, p. 310-321.

Amante, C., and Eakins, B. W., 2009, ETOPO1 1 Arc-Minute Global Relief Model: Procedures, Data Sources and Analysis: NOAA Technical Memorandum NESDIS NGDC-24, p. 19.

Aslanian, D., Moulin, M., Olivet, J.-L., Unternehr, P., Matias, L., Bache, F., Rabineau, M., Nouzé, H., Klingelheofer, F., Contrucci, I., and Labails, C., 2009, Brazilian and African passive margins of the Central Segment of the South Atlantic Ocean: Kinematic constraints: Tectonophysics, v. 468, no. 1–4, p. 98-112.

Birch, F., 1964, Density and composition of mantle and core: Journal of Geophysical Research, v. 69, no. 20, p. 4377-4388.

Cannat, M., Manatschal, G., Sauter, D., and Péron-Pinvidic, G., 2009, Assessing the conditions of continental breakup at magma-poor rifted margins: What can we learn from slow spreading mid-ocean ridges?: Comptes Rendus Geosciences, v. 341, no. 5, p. 406-427.

Carlson, R. L., and Herrick, C. N., 1990, Densities and porosities in the oceanic crust and their variations with depth and age: Journal of Geophysical Research: Solid Earth, v. 95, no. B6, p. 9153-9170.

Chappell, A. R., and Kusznir, N. J., 2008, Three-dimensional gravity inversion for Moho depth at rifted continental margins incorporating a lithosphere thermal gravity anomaly correction: Geophysical Journal International, v. 174, no. 1, p. 1-13.

Contrucci, I., Matias, L., Moulin, M., Géli, L., Klingelhofer, F., Nouzé, H., Aslanian, D., Olivet, J.-L., Réhault, J.-P., and Sibuet, J.-C., 2004, Deep structure of the West African continental margin (Congo, Zaïre, Angola), between 5°S and 8°S, from reflection/refraction seismics and gravity data: Geophysical Journal International, v. 158, no. 2, p. 529-553.

Cowie, L., and Kusznir, N., 2012, Mapping crustal thickness and oceanic lithosphere distribution in the Eastern Mediterranean using gravity inversion: Petroleum Geoscience, v. 18, no. 4, p. 373-380.

Crosby, A. G., and McKenzie, D., 2009, An analysis of young ocean depth, gravity and global residual topography: Geophysical Journal International, v. 178, no. 3, p. 1198-1219.

Dean, S. M., Minshull, T. A., Whitmarsh, R. B., and Louden, K. E., 2000, Deep structure of the ocean-continent transition in the southern Iberia Abyssal Plain from seismic refraction profiles: The IAM-9 transect at 40°20'N: Journal of Geophysical Research: Solid Earth, v. 105, no. B3, p. 5859-5885.

Discovery 215 Working, G., Minshull, T. A., Dean, S. M., Whitmarsh, R. B., Russell, S. M., Louden, K. E., and Chian, D., 1998, Deep structure in the vicinity of the ocean-continent transition zone under the southern Iberia Abyssal Plain: Geology, v. 26, no. 8, p. 743-746.

Fowler, C. M. R., 2006, The Solid Earth: An Introduction to Global Geophysics, Cambridge University Press, 685 p.:

Greenhalgh, E. E., and Kusznir, N. J., 2007, Evidence for thin oceanic crust on the extinct Aegir Ridge, Norwegian Basin, NE Atlantic derived from satellite gravity inversion: Geophysical Research Letters, v. 34, no. 6, p. L06305.

Hudec, M. R., and Jackson, M. P. A., 2007, Terra infirma: Understanding salt tectonics: Earth-Science Reviews, v. 82, no. 1–2, p. 1-28.

Kusznir, N., and Karner, G., 1985, Dependence of the flexural rigidity of the continental lithosphere on rheology and temperature: Nature, v. 316, no. 6024, p. 138-142.

Kusznir, N. J., Roberts, A. M., and Morley, C. K., 1995, Forward and reverse modelling of rift basin formation: Geological Society, London, Special Publications, v. 80, no. 1, p. 33-56.

Manatschal, G., Froitzheim, N., Rubenach, M., and Turrin, B. D., 2001, The role of detachment faulting in the formation of an ocean-continent transition: insights from the Iberia Abyssal Plain: Geological Society, London, Special Publications, v. 187, no. 1, p. 405-428.

Manatschal, G., Sutra, E., and Péron-Pinvidic, G., The lesson from the Iberia-Newfoundland rifted margins: how applicable is it to other rifted margins?, *in* Proceedings 2nd Central & North Atlantic Conjugate Margins: Rediscovering the Atlantic, New Insights, New winds for an old sea2010, Volume 2, p. 27 - 37.

McKenzie, D., 1978, Some Remarks on the Development of Sedimentary Basins Earth and Planetary Science Letters, v. 40, p. 25-32.

Mohriak, W., Nemčok, M., and Enciso, G., 2008, South Atlantic divergent margin evolution: rift-border uplift and salt tectonics in the basins of SE Brazil: Geological Society, London, Special Publications, v. 294, no. 1, p. 365-398.

Moulin, M., Aslanian, D., Olivet, J.-L., Contrucci, I., Matias, L., Géli, L., Klingelhoefer, F., Nouzé, H., Réhault, J.-P., and Unternehr, P., 2005, Geological constraints on the evolution of the Angolan margin based on reflection and refraction seismic data (ZaïAngo project): Geophysical Journal International, v. 162, no. 3, p. 793-810.

Müller, R. D., Sdrolias, M., Gaina, C., Steinberger, B., and Heine, C., 2008, Long-Term Sea-Level Fluctuations Driven by Ocean Basin Dynamics: Science, v. 319, no. 5868, p. 1357-1362.

Parker, R. L., 1972, The Rapid Calculation of Potential Anomalies: Geophysical Journal of the Royal Astronomical Society, v. 31, no. 4, p. 447-455.

Parsons, B., and Sclater, J. G., 1977, An Analysis of the Variation of Ocean Floor Bathymetry and Heat Flow with Age: Journal of Geophysical Research, v. 82, no. 5, p. 803-827.

Péron-Pinvidic, G., Manatschal, G., Minshull, T. A., and Sawyer, D. S., 2007, Tectonosedimentary evolution of the deep Iberia-Newfoundland margins: Evidence for a complex breakup history: Tectonics, v. 26, no. 2, p. TC2011.

Reston, T. J., 2009, The structure, evolution and symmetry of the magma-poor rifted margins of the North and Central Atlantic: A synthesis: Tectonophysics, v. 468, no. 1–4, p. 6-27.

Roberts, A. M., Kusznir, N. J., Yielding, G., and Styles, P., 1998, 2D flexural backstripping of extensional basins; the need for a sideways glance: Petroleum Geoscience, v. 4, no. 4, p. 327-338.

Sandwell, D. T., and Smith, W. H. F., 2009, Global marine gravity from retracked Geosat and ERS-1 altimetry: Ridge segmentation versus spreading rate: Journal of Geophysical Research, v. 114, no. B1, p. B01411.

Scotchman, I. C., Gilchrist, G., Kusznir, N. J., Roberts, A. M., and Fletcher, R., 2010, The breakup of the South Atlantic Ocean: formation of failed spreading axes and blocks of thinned continental crust in the Santos Basin, Brazil and its consequences for petroleum system development: Geological Society, London, Petroleum Geology Conference series, v. 7, p. 855-866.

Stein, C. A., and Stein, S., 1992, A model for the global variation in oceanic depth and heat flow with lithospheric age: Nature, v. 359, no. 6391, p. 123-129.

Teisserenc, P., and Villemin, J., 1989, Sedimentary basin of Gabon – geology and oil systems, *in* Edwards, J. D., and Santogrossi, P. A., eds., Divergent / Passive Margin Basins. Memoir of the American Association of Petroleum Geologists, Volume 48.

Unternehr, P., Péron-Pinvidic, G., Manatschal, G., and Sutra, E., 2010, Hyper-extended crust in the South Atlantic: in search of a model: Petroleum Geoscience, v. 16, no. 3, p. 207-215.

White, R., and McKenzie, D., 1989, Magmatism at Rift Zones: The Generation of Volcanic Continental Margins and Flood Basalts: Journal of Geophysical Research, v. 94, no. B6, p. 7685-7729.

White, R. S., McKenzie, D., and O'Nions, R. K., 1992, Oceanic Crustal Thickness From Seismic Measurements and Rare Earth Element Inversions: Journal of Geophysical Research, v. 97, no. B13, p. 19683-19715.

Whitmarsh, R. B., and Miles, P. R., 1995, Models of the development of the West Iberia rifted continental margin at 40°30'N deduced from surface and deep-tow magnetic anomalies: Journal of Geophysical Research: Solid Earth, v. 100, no. B3, p. 3789-3806.

Zalán, P. V., Severino, M. C. G., Rigoti, C., Magnavita, L. P., Oliveira, J. A. B., and Viana, A. R., 2011, An entirely new 3D-view of the crustal and mantle structure of a ruptured South Atlantic passive margin – Santos, Campos and Espírito Santo Basins, Brazil (Expanded Abstract): AAPG Annual Convention & Exhibition Abstracts Volume CDROM,Paper 986156.

3.6. Supplementary Figures

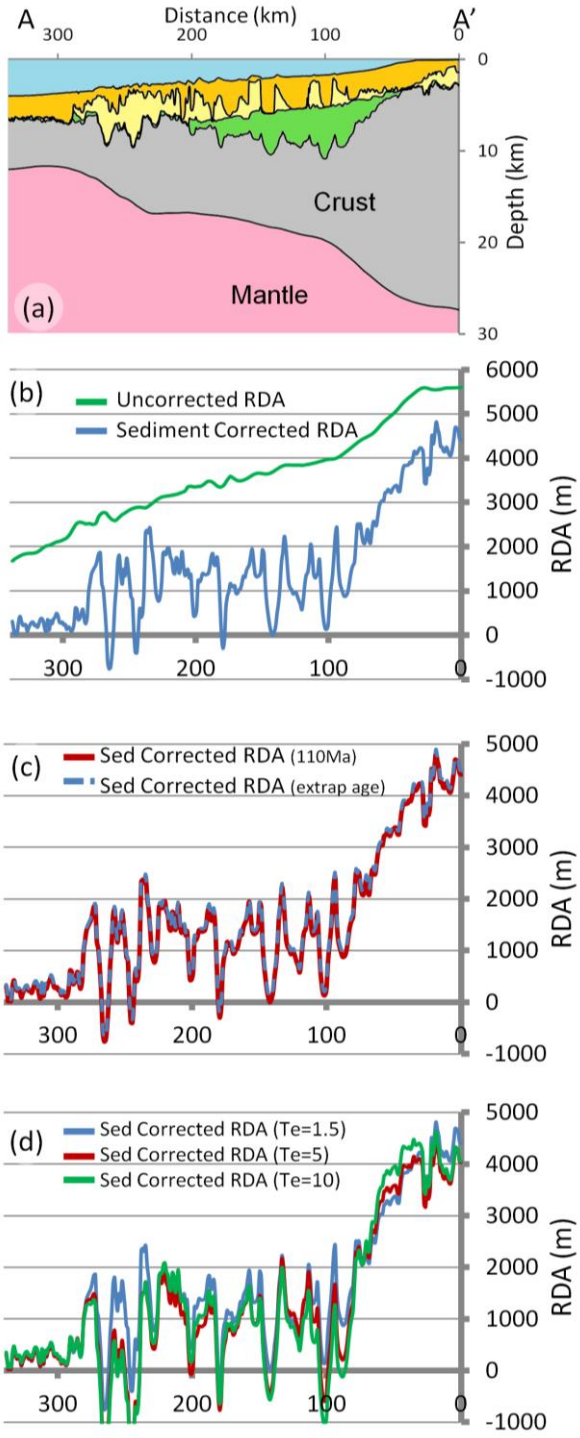

Supplementary Figure S3.1 –All RDA results in this figure are unsmoothed. (a) Crustal cross section along the CS1-2400 profile along the northern Angolan rifted continental margin. (b) Comparison of the uncorrected RDA results with the sediment corrected RDA results along the CS1-2400 profile. (c) The sensitivity to oceanic age for the sediment corrected RDA results has been examined. Two approaches have been considered (i) a constant value of 120Ma for the profile and (ii) using Müller et al. (2008) age isochrons with their age gradient extrapolated inboard. (d) Sensitivity to the effective elastic thickness (Te's of 1.5km, 5km and 10km) for northern Angolan margin sediment corrected RDA results has been examined.

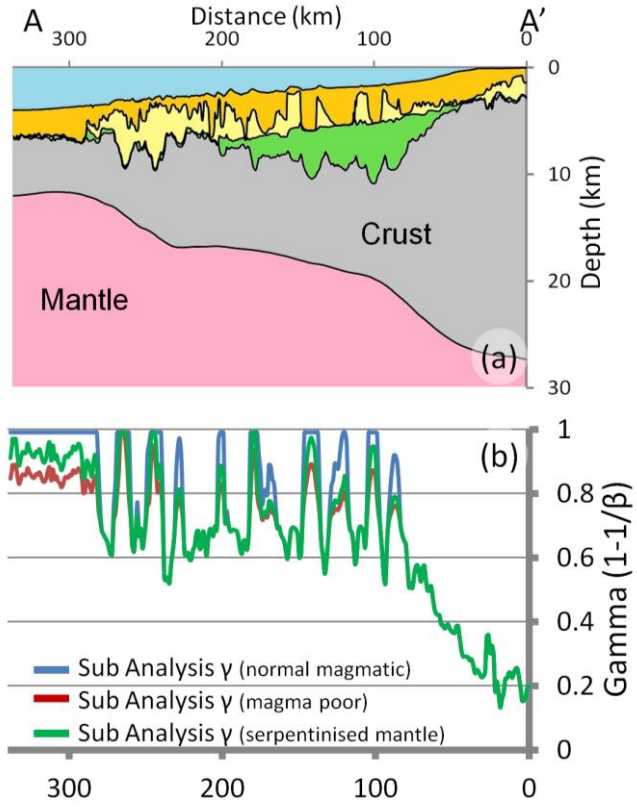

Supplementary Figure S3.2 – Subsidence analysis results in this figure are unsmoothed. (a) Crustal cross section A-A' across the northern Angolan Margin. The pre-salt sedimentary layer is shown in green, the salt layer in yellow and the post-salt sedimentary layer is orange. (b) Continental lithosphere thinning factors predicted from subsidence analysis, along the CS1-2400 profile. Sensitivities to a 'normal' magmatic margin (Va=7km), magma-poor margin (Va=0km) and a solution for serpentinised mantle have been examined.

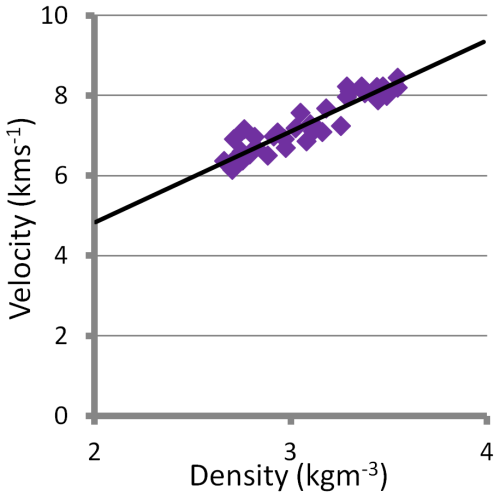

Supplementary Figure S3.3 – Linear relationship between seismic velocities and basement density, using Birch's Law (Birch, 1964).

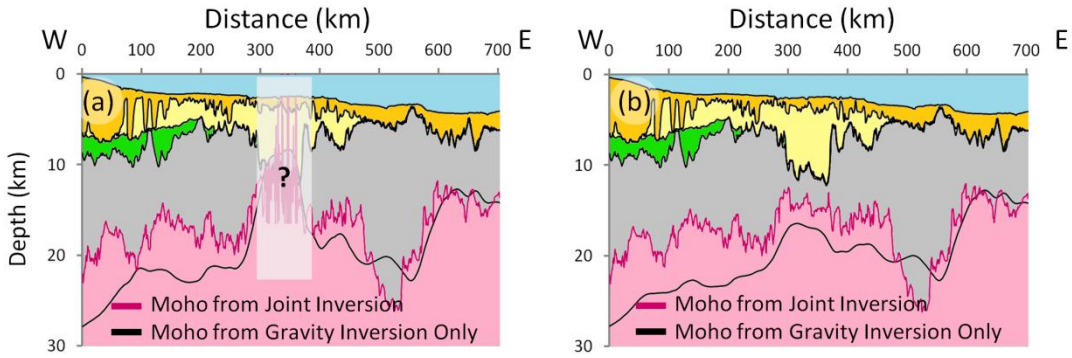

Supplementary Figure S3.4 – Comparison of the joint inversion and gravity anomaly inversion results examining the sensitivity to the salt layer along the BS1-575 profile. The pre-salt sedimentary layer is shown in green, the salt layer in yellow and the post-salt sedimentary layer is orange. (a) The salt layer (using salt density and compaction parameters) has been included. Beneath the thick salt both the gravity anomaly inversion and the joint inversion predict an unphysical result beneath the thick salt. We have blanked out the unphysical solution beneath the thick salt for ease in interpretation. (b) The salt has been omitted and the salt layer is treated as another sedimentary layer, assuming a shaly-sand lithology . This produces a deeper Moho beneath the thick salt, the crust beneath this area is still very thin (approximately 5km thick). Although this sensitivity produces a physical result for the region of very thick salt, it is not valid for the rest of the profile. We therefore prefer the solution, which includes the salt.

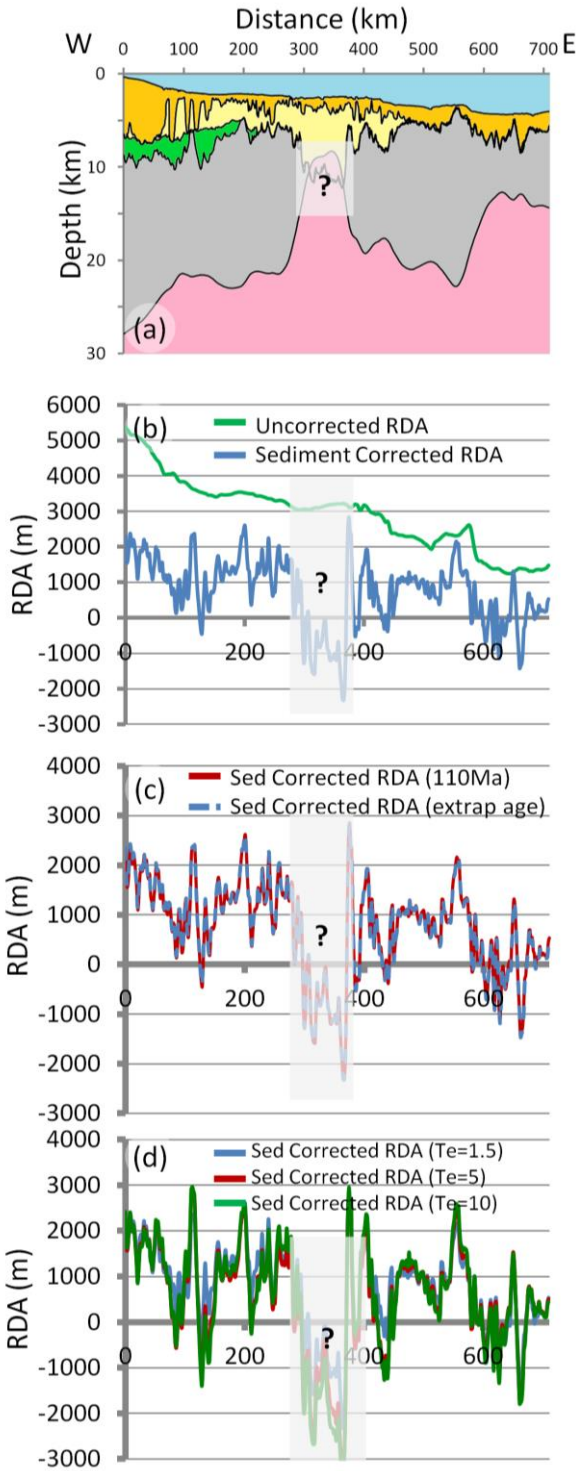

Supplementary Figure S3.5 – All RDA results in this figure are unsmoothed. (a) Crustal cross section along the BS1-575 profile along the south-eastern Brazilian rifted continental margin. The pre-salt sedimentary layer is shown in green, the salt layer in yellow and the post-salt sedimentary layer is orange. (b) Comparison of uncorrected RDA results with the sediment corrected RDA results. (c) The sensitivity to oceanic age for sediment corrected RDA results has been examined. Two approaches have been considered (i) a constant value of 120Ma for the profile and (ii) using Müller et al. (2008) age isochrons with their age gradient extrapolated inboard. (d) Sensitivity to the effective elastic thickness for northern Angolan margin sediment corrected RDA results has been examined. Te's of 1.5km, 5km and 10km produce sediment corrected RDAs of similar magnitude. The largest difference is seen beneath the thick salt.

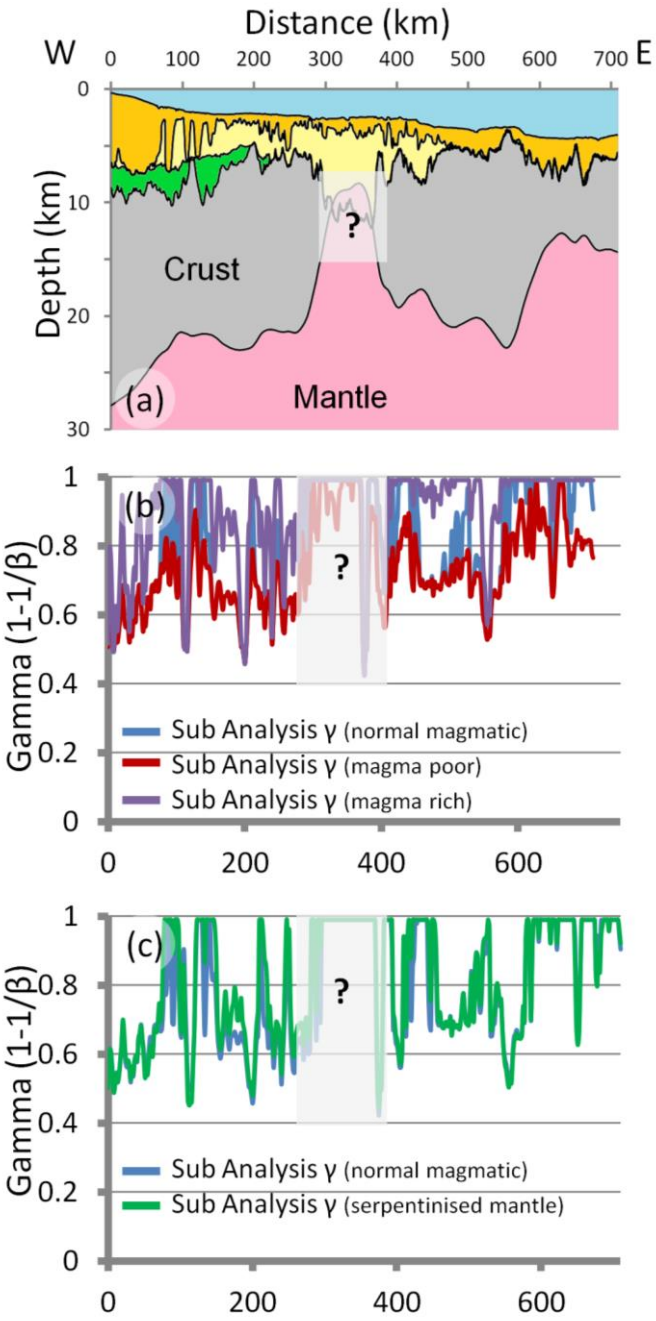

Supplementary Figure S3.6 – Subsidence analysis results in this figure are unsmoothed. (a) Crustal cross section across the south-eastern Brazilian Margin. The pre-salt sedimentary layer is shown in green, the salt layer in yellow and the post-salt sedimentary layer is orange. (b) Smoothed continental lithosphere thinning factors from subsidence analysis. Sensitivities to a 'normal' magmatic margin (Va=7km), a magma-poor margin (Va=0km) and a magma-rich margin (Va=10km) have been examined. (c) Comparison of the smoothed continental lithosphere thinning factors calculated from subsidence analysis for a 'normal' magmatic margin and a solution for serpentinised mantle. All subsidence analysis results in this figure have been smoothed.

Chapter 4

4. The Palaeo-Bathymetry of Base Aptian Salt Deposition on the Northern Angolan Rifted Margin: Constraints from Flexural Backstripping and Reverse Post-Breakup Thermal Subsidence Modelling

Preface

This chapter has been written in the form of a paper. Co-authors are R. M. Angelo (ConocoPhillips), N. J. Kusznir (University of Liverpool) and G. Manatschal (CNRS-EOST, Université de Strasbourg). Section headers, figures and page numbers have been renumbered to conform to the format of this thesis.

Abstract

The bathymetric datum with respect to global sea level for Aptian salt deposition in the South Atlantic is hotly debated. Some models propose that the salt was deposited in a deep isolated ocean basin in which local sea level was 2-3km below the global level. In this study, we determine the palaeo-bathymetry of base Aptian salt deposition on the Angolan rifted continental margin using reverse post-breakup subsidence modelling. The reverse post-breakup subsidence modelling consists of the sequential flexural isostatic backstripping of the post-breakup sedimentary sequences, decompaction of remaining sedimentary units and reverse modelling of post-breakup lithosphere thermal subsidence. The reverse modelling of post-breakup lithosphere thermal subsidence is carried out in 2D and requires 2D knowledge of the continental lithosphere stretching factor (β), which is determined from gravity anomaly inversion. The analysis has been applied to the ION-GXT CS1-2400 deep long-offset seismic reflection profile and the P3 and P7+11 seismic cross sections of Moulin (2005) and Contrucci et al. (2004) offshore northern Angola. Reverse post-breakup subsidence modelling restores the proximal autochthonous base salt to near sea level, at the time of breakup. In contrast, the most distal base salt does not restore to sea level and the predicted water loaded bathymetries are much greater ranging between 1km and 4km. The predicted bathymetries of the first unequivocal oceanic crust at breakup are approximately 2.5km, as expected for newly formed oceanic crust of 'normal' thickness. Several interpretations of these results are possible. One is that all Aptian salt on the northern Angola rifted continental margin was deposited at or near global sea level, but that the distal salt was formed during late syn-rift and the crust under it was being actively thinned during salt deposition resulting in additional tectonic subsidence from crustal thinning. Another interpretation is that the distal salt moved down-slope while breakup occurred to its present position in much deeper water. Although a structural barrier in the south is not dismissed,

we believe that there is no definite requirement to invoke a deep isolated ocean basin with local sea level 2-3km below the global level for the deposition of the Aptian salt on the northern Angolan rifted continental margin.

4.1. Introduction

The northern Angolan rifted continental margin has been the subject of extensive industry and academic seismic surveys (Contrucci et al., 2004; Moulin et al., 2005; Unternehr et al., 2010) due to its hydrocarbon resources. However, there are major scientific and technical challenges in imaging the structure of this rifted margin and understanding its evolution due to the thick sedimentary packages impacted by a massive middle to upper Aptian salt sequence. The presence of thick salt (up to 5km thickness in places) makes seismic imaging and interpretation of the sub-salt sedimentary packages, crustal structure and tectonic history difficult. The determination of whether the northern Angolan Aptian salt sequence is pre-breakup or post-breakup remains a topic of major debate, also the palaeo-water depths through the breakup period and the mechanisms responsible for generating accommodation space through time are uncertain (Jackson et al., 2000; Karner and Driscoll, 1999; Karner et al., 2003; Karner et al., 1997; Moulin, 2003; Moulin et al., 2005). There is also much debate about the fundamental questions concerning the crustal basement structure and the geometry and nature of the pre-salt basin. The analysis along the offshore northern Angolan margin is focussed along three profiles in the Kwanza region; locations are shown in Figure 4.1(a). The three profiles include the ION-GXT deep long offset seismic reflection profile CS1-2400 (Figure 4.1(c)) and the P3 (Figure 4.1(d)) and P7+11 profiles (Figure 4.1(e)) (Contrucci et al., 2004; Moulin et al., 2005).

There are many papers written on salt basins, specifically with reference to the formation and deposition of salt basins (e.g. Davidson (2007); Quirk et al.(2012); Torsvik et al. (2009):

and West (1989)), salt basin tectonics and geometry (e.g. Brun and Fort (2011); Davidson (2007) and Rowan (2014)), linkage and continuity between salt basins (i.e. whether the South Atlantic salt basins were formed as a single basin or whether they formed independently) (e.g. Davidson (2007)) and whether the salt basins were connected to the global sea during deposition (e.g. Burke et al. (2003); Burke and Sengör (1988); Davidson et al. (2012); Duval et al. (1992); Karner and Gambôa (2007); Pindell et al. (2014); Quirk et al. (2012); Schmalz (1969) and Torsvik et al.(2009))

Many of these papers do not go beyond speculation and qualification of these topics, which is why we have carried out a rigorous quantitative analysis of the northern Angolan salt basins, in order to try and further understand the complex nature, tectonics and palaeo-bathymetry of these salt basins. In particular we are using integrated quantitative analysis to try and address the base level of the salt deposition with respect to global sea level. Some authors (e.g. Burke and Sengör (1988), Burke et al. (2003) and Karner and Gambôa (2007)) advocate for the deposition of the salt in a deep isolated basin, whilst, in contrast others argue for a shallower basin (e.g. (Pindell et al., 2014) in which there is no need for such deep water depths to produce the vast volume of salt evident. The purpose of this chapter is to provide an understanding of the palaeo-bathymetries of the base Aptian salt (both proximal and distal) and to understand how the salt sits within the broad framework of the ocean continent transition (OCT) along the northern Angolan rifted continental margin.

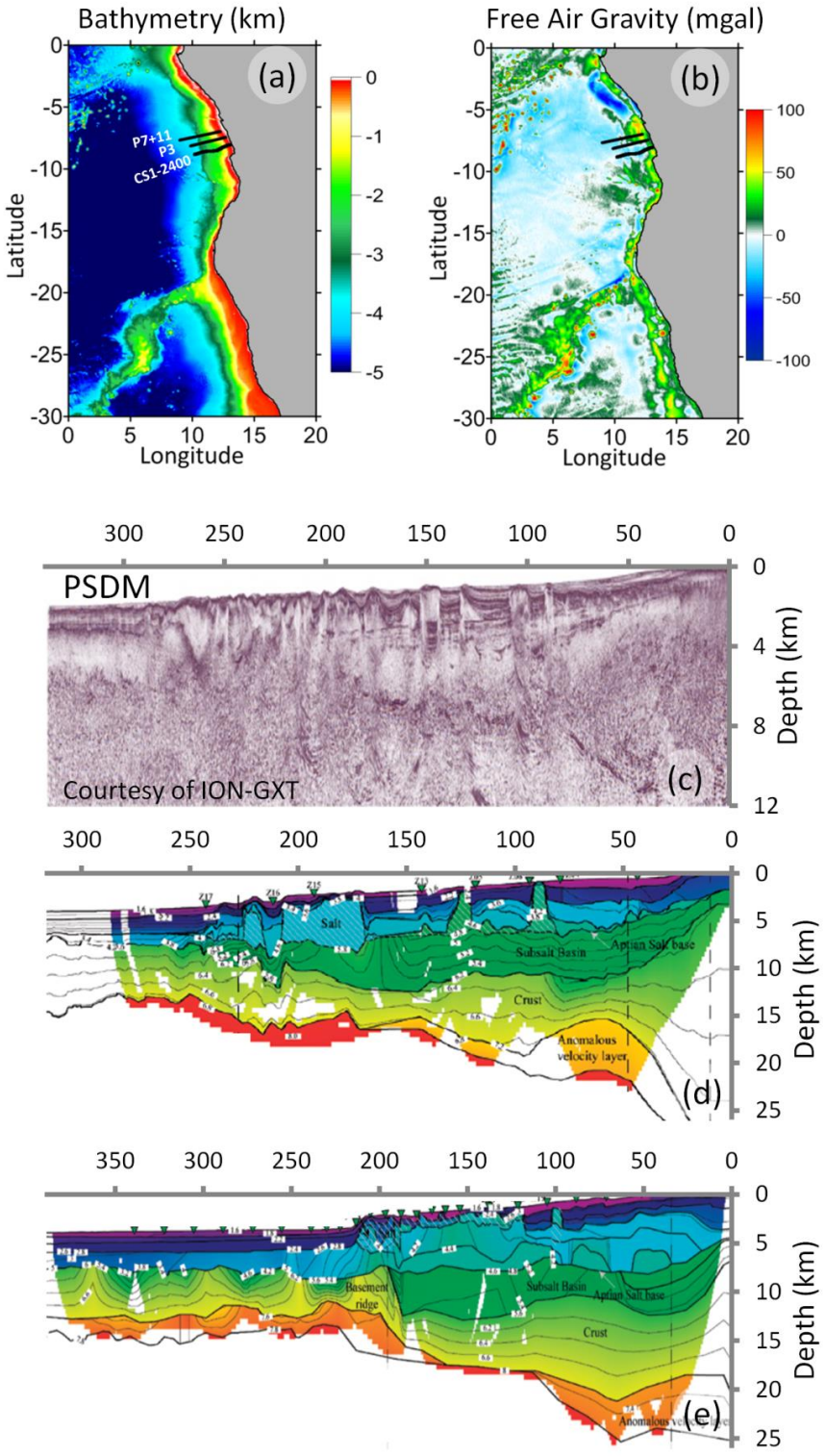

Figure 4.1 – Data used in the reverse post-breakup thermal subsidence modelling and gravity anomaly inversion for the northern Angolan rifted continental margin. (a) Bathymetry (km) (Amante and Eakins 2009), with the location of profiles CS1-2400, P3 and P7+11 indicated. (b) Satellite derived free air gravity (mgal) (Sandwell and Smith 2009). (c) Deep long offset seismic reflection depth section (PSDM – pre stacked depth migrated) for the ION-GXT CS1-2400 profile. (d) Seismic velocity model along the P3 profile (Contrucci et al., 2004; Moulin et al., 2005) from seismic refraction data. (e) Seismic velocity model along the P7+11 profile (Contrucci et al., 2004; Moulin et al., 2005) from seismic refraction data.

Within the literature there are a range of different definitions of the OCT and COB (e.g. Pèron-Pinvidic et al. (2007), Whitmarsh and Miles (1995), Manatschal et al. (2001), Dean et al. (2000), Manatschal et al. (2010) and Discovery 215 Working et al. (1998)). Within this paper, however, we define the OCT as the region between unequivocal continental crust of 'normal' thickness and unequivocal oceanic crust; the continental lithosphere in this region is highly thinned, with complex tectonics, variable magmatism and possible mantle exhumation. We define the COB as the distal limit of unequivocal continental crust. Determining the location of the COB is made difficult by the presence of exhumed mantle and complex tectonics.

4.2. Reverse post-breakup thermal subsidence modelling

Reconstructed palaeo-bathymetries of base Loeme salt (top Aptian) along the CS1-2400, P3 and P7+11 profiles has been determined using reverse post-breakup subsidence modelling (Kusznir et al., 1995; Roberts et al., 1998). Reverse post-breakup subsidence modelling (Figure 4.2) consists of the sequential flexural isostatic backstripping of the post-breakup sedimentary sequences, decompaction of the remaining sedimentary units and reverse modelling of post-breakup lithosphere thermal subsidence. The magnitude of β used in the reverse post-rift thermal subsidence modelling controls the restored model elevation relative to sea level and therefore the predicted palaeo-bathymetry (Roberts et al., 2009; Roberts et al., 1998). In the reverse post-breakup subsidence modelling, the magnitude of thermal subsidence is calculated from the continental lithosphere stretching factor (β) (McKenzie, 1978) determined from gravity anomaly inversion. The methodology of reverse post-breakup thermal subsidence modelling used in this chapter is described in detail for the CS1-2400 profile.

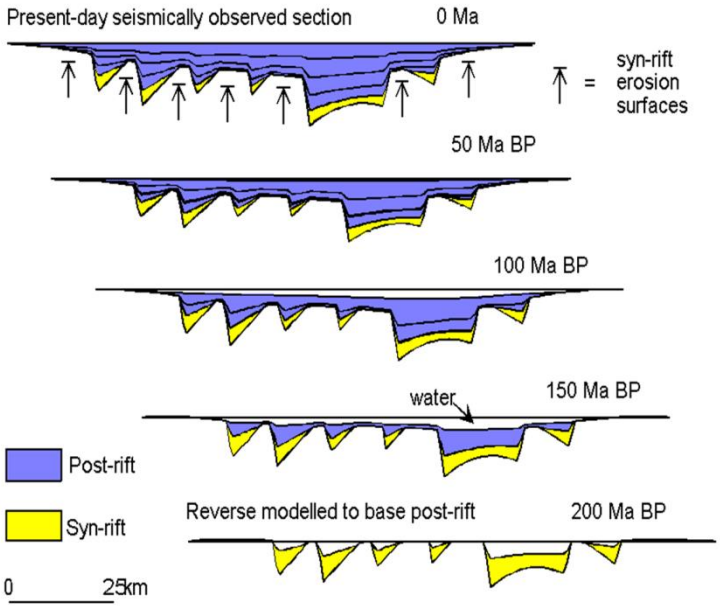

Figure 4.2 – Schematic series of sequential cross sections showing reverse post-breakup thermal subsidence modelling of rift basin development from Kusznir et al. (1995). Reverse post-rift subsidence modelling consists of the sequential flexural isostatic backstripping of the post-breakup sedimentary sequences, decompaction of remaining sedimentary units and reverse modelling of post-breakup lithosphere thermal subsidence.

4.2.1. Continental lithosphere thinning and crustal basement thickness from gravity anomaly inversion for CS1-2400

Continental lithosphere stretching factors (β) (McKenzie, 1978) which are used to drive the reverse post-rift thermal subsidence modelling are derived from gravity anomaly inversion. As β factors range between zero and infinity, we prefer to use the related parameter, continental lithosphere thinning factor ($\gamma=1-1/\beta$), which ranges between zero and one.

Gravity anomaly inversion, uses bathymetry (Amante and Eakins, 2009) (Figure 4.1(a)), satellite derived free air gravity (Sandwell and Smith, 2009) (Figure 4.1(b)), sediment thickness from the CS1-2400 profile (Figure 4.1(c)) and ocean age isochrons (Müller et al., 2008) to determine continental lithosphere thinning, crustal basement thickness and Moho depth along the northern Angolan rifted continental margin. The gravity anomaly inversion is carried out in the 3D spectral domain using the scheme of Parker (1972). The gravity

anomaly inversion also incorporates a lithosphere thermal gravity anomaly correction, to account for the lithosphere mass deficiency from the elevated geothermal gradient within oceanic and stretched and thinned rifted continental margin lithosphere. Failure to include the lithosphere thermal gravity anomaly correction can lead to predictions of Moho depth and crustal basement thickness, at rifted continental margins, which are substantially too great and continental lithosphere thinning factors, which are too low. The gravity anomaly inversion is dependent on the age of continental breakup due to the lithosphere thermal gravity anomaly correction being dependent on the lithosphere thermal re-equilibration time. We have used 110Ma as the age of breakup, after Moulin (2005), but have also examined sensitivities to breakup ages which span the period Berriasian (140Ma) to early Albian (110Ma); this range corresponds to the start and end of the main rifting episode in the South Atlantic (Teisserenc and Villemin, 1989). A more detailed methodology of the gravity anomaly inversion technique is described in Chappell and Kusznir (2008) and Greenhalgh and Kusznir (2007), whilst the application is described in Alvey et al. (2008) and Cowie and Kusznir (2012).

Moho depths determined from the gravity anomaly inversion are in good agreement with those determined from the CS1-2400 deep long-offset seismic reflection profile. The reference Moho depth used within the gravity anomaly inversion has been calibrated on the oceanic domain of the CS1-2400 profile using the clear Moho reflectors. Sensitivities to reference Moho depths of 32.5km, 35km, 37.5km and 40km have been examined for the CS1-2400 profile. Moho depths predicted from gravity anomaly inversion for these sensitivities to reference Moho depth are shown in Figure 4.3(a). Calibration shown in Figure 4.3(b), shows that a reference Moho depth of 35.5km is required in order to predict crustal basement thicknesses consistent with those seen in the oceanic domain of the CS1-2400 seismic reflection profile.

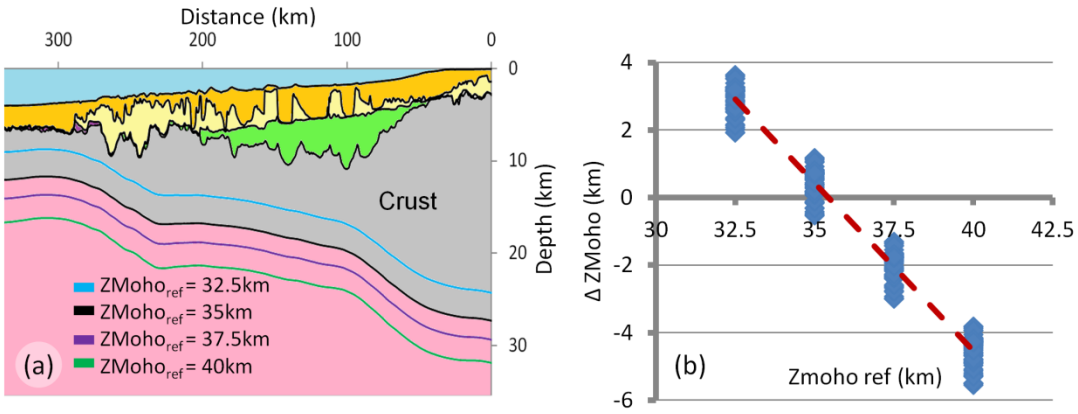

Figure 4.3 – Calibration of the reference Moho depth, in the oceanic domain, used in the gravity anomaly inversion along the CS1-2400 profile on the northern Angolan margin. (a) Gravity anomaly inversion predicted Moho depths have been calculated considering sensitivities to reference Moho depths of 32.5km, 35km, 37.5km and 40km. (b) Calibration of the reference Moho depth for the CS1-2400 profile shows that a reference Moho depth of 35.5km is required.

A crustal cross section along the CS1-2400 profile (Figure 4.4(a)) has been constructed using the bathymetry and 2D sediment thickness data with the crustal basement thicknesses and Moho depths predicted from gravity anomaly inversion, assuming the calibrated reference Moho depth of 35.5km. The corresponding continental lithosphere thinning factor (γ) profile predicted from gravity anomaly inversion, for CS1-2400, assuming depth uniform stretching and thinning is shown in Figure 4.4(b). Continental lithosphere thinning factors of zero indicate that there has been no stretching or thinning of the continental lithosphere, whereas a continental lithosphere thinning factor of one indicates that there has been infinite stretching and thinning of the original continental lithosphere and there is no continental lithosphere (or crust) remaining.

Stretching of continental lithosphere is commonly associated with a decrease in crustal basement thickness; however, decompression melting during rifting and seafloor spreading generates magmatic additions (e.g. SDRs (seaward dipping reflectors) and under-plated magmatic bodies), which act against thinning and can increase crustal basement thickness. A correction for magmatic addition has been included within the gravity anomaly inversion

method, which uses the parameterization of the decompression melting model of White and McKenzie (1989) to predict the thickness of the crustal magmatic addition. Sensitivities to magmatic addition including a 'normal' magmatic and a magma-poor solution have been examined along the CS1-2400 profile (Figure 4.4(b)). At the western end of the profile we prefer the 'normal' magmatic solution; however, in the central region of the profile we believe that the magma-poor solution is preferential due to the lack of clear evidence of important magmatic additions in the seismic section.

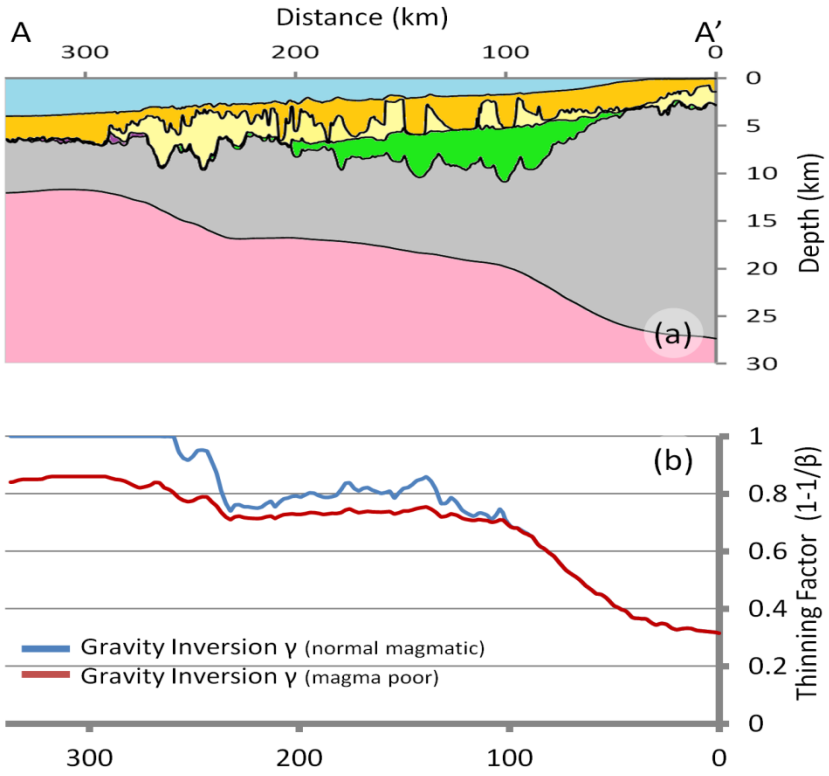

Figure 4.4 – (a) Crustal cross section along the CS1-2400 profile, showing Moho depth from gravity anomaly inversion, assuming the calibrated reference Moho depth of 35.5km. (b) Continental lithosphere thinning profile, predicted from gravity anomaly inversion, along the CS1-2400 profile. Sensitivities to a 'normal' magmatic solution (Va=7km) and a magma-poor solution (Va=0km) have been examined. A 'normal' magmatic solution predicts thinning factors of 1.0 at the western end of the profile and a magma-poor solution predicts continental lithosphere thinning factors of approximately 0.85 in this region.

4.2.2. Palaeo-bathymetry of the base Aptian salt deposition for the CS1-2400 profile

The present day CS1-2400 cross section is shown in Figure 4.5(a). Flexural backstripping and decompaction has been applied to the CS1-2400 profile (Figure 4.5(b)) to remove the salt and post-salt sedimentary layers in order to determine the bathymetry corrected for sedimentary loading to base salt. Flexural backstripping and decompaction assumes a shaly lithology compaction and density parameters during the removal of the sedimentary layer, whilst the salt layer is given a simple salt lithology (Hudec and Jackson, 2007). See Table 1 for the compaction and density parameters used within reverse post-breakup thermal subsidence modelling.

Layer	Lithology	Porosity (%)	Compaction coefficient (km^{-1})	Density (kgm^{-3})
Post-salt	Shaly – Sand (Shale rich)	63	0.51	2720
Salt	Salt	0	0	2200
Pre-salt	Shaly – Sand (Shale rich)	65	0.56	2720

Table 4.1 – Compaction and density parameters used within the reverse post-breakup thermal subsidence modelling.

The complex salt movement in this region may appear to be problematic for flexural backstripping. However, within the palaeo-bathymetric restoration we use the base salt as the target surface for backstripping, which allows us to ignore the salt movement, as we flexurally backstrip through the salt to the time of deposition. We are able to ignore the salt movement because as the salt moved the lithosphere would have responded isostatically to

compensate; hence the reverse post-rift modelling must be applied to the present day section and its isostatic balance.

The palaeo-bathymetry of the restored cross section (Figure 4.5(b)) is dependent on β, however, the resultant internal basin geometry is also controlled by the effective elastic thickness (Te) or lithosphere flexural strength (Bertotti et al., 1998; Galán and Casallas, 2010; Roberts et al., 1998). Roberts et al. (1998) have determined that for syn-rift extensional settings, effective elastic thicknesses between 1.5km and 5km are required. The Te depends on the bending stresses applied to the plate, the rate of stress application, the lithosphere composition and the geothermal gradient (Kusznir and Karner, 1985). Using a low value of Te (Te < 5km), the reverse post-breakup subsidence model will respond with a component of localized flexural response during restoration and will not show the unrealistic internal deformation of individual fault-blocks that occurs when applying Airy isostasy during backstripping (see Roberts et al. (1997) for full details). Sensitivities to Te's of 1.5km, 5km and 10km have been examined along the northern Angolan margin; in this study a Te of 1.5km has been used as the preferred value for all the models.

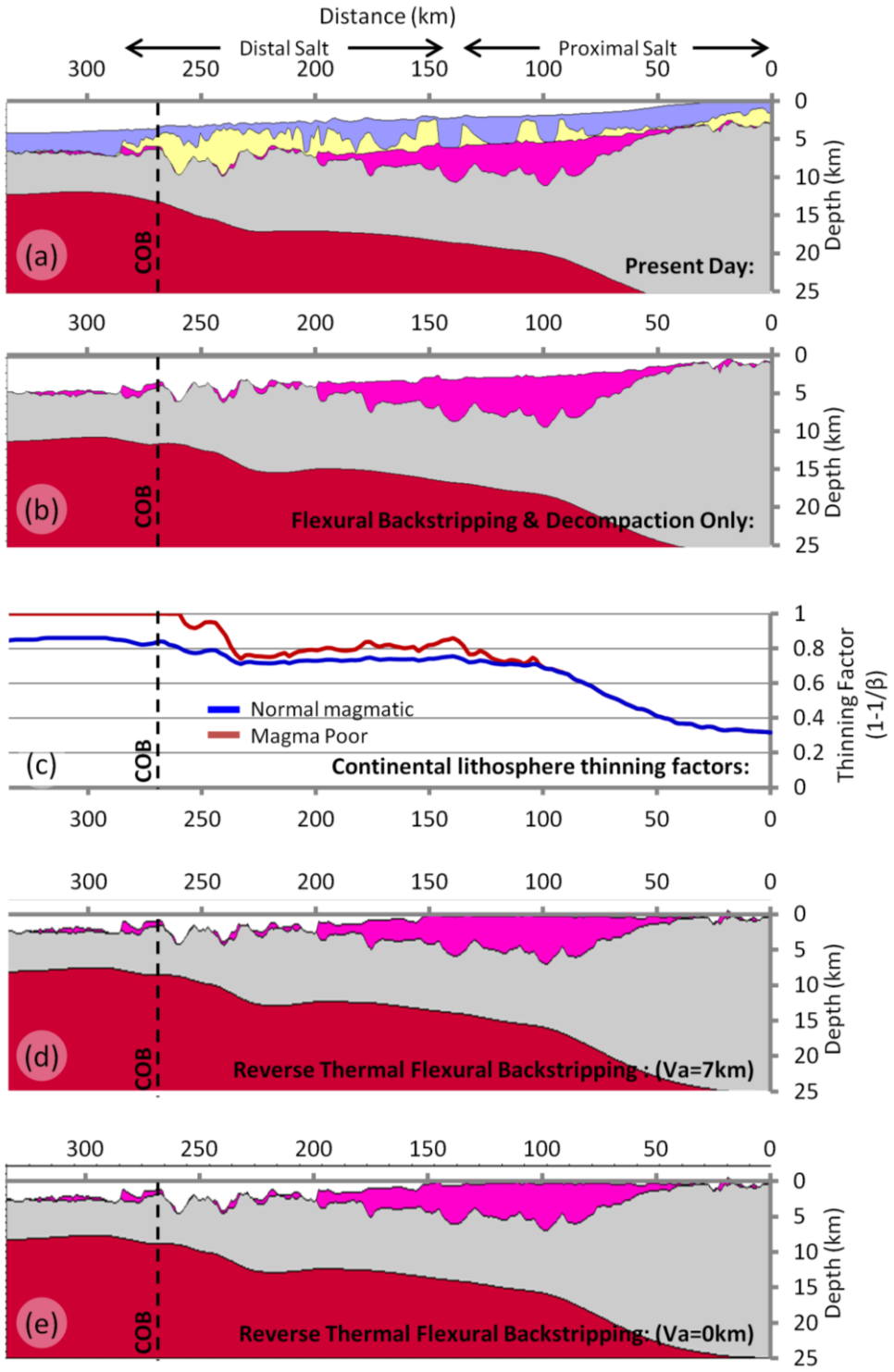

Figure 4.5 – Flexural backstripping and reverse post-breakup thermal subsidence modelling along the ION-GXT CS1-2400 profile. (a) Digitized present day cross section along the CS1-2400 profile; the post-salt sedimentary layer is highlighted in blue; pre-salt sedimentary layer in pink; the salt layer is highlighted in yellow; crust is grey and mantle is red. (b) Sediment corrected bathymetry to base salt calculated from flexural backstripping and decompaction, using a Te of 1.5km. (c) Continental lithosphere thinning profile, from gravity anomaly inversion, for 'normal' magmatic and magma-poor solutions. (d) Reverse post-breakup thermal subsidence modelling along the CS1-2400 profile, assuming a 'normal' magmatic solution (Va=7km). (e) Reverse post-breakup thermal subsidence modelling along the CS1-2400 profile, assuming a magma-poor solution (Va=0km).

4.2.3. Reverse post-breakup thermal subsidence for CS1-2400:

The application of flexural backstripping and decompaction gives an incomplete palaeo-bathymetric restoration of base salt because the full restoration of the base Loeme Aptian salt also requires the inclusion of reverse post-breakup thermal subsidence. The continental lithosphere thinning factors (γ), from gravity anomaly inversion, required to drive the reverse post-breakup thermal subsidence modelling are shown in Figure 4.5(c). Sensitivities to continental lithosphere thinning factors determined from gravity anomaly inversion for a 'normal' magmatic solution (Va=7km) and a magma-poor solution (Va=0km) are examined. At the western end of the CS1-2400 profile the continental lithosphere thinning factors for a 'normal' magmatic solution are 1.0; whereas for a magma-poor solution, the continental lithosphere thinning factors are approximately 0.85. In the central section of the profile, the continental lithosphere thinning factors, for both solutions examined, are between 0.7 and 0.85.

Predicted palaeo-bathymetry to base salt assuming a 'normal' magmatic solution

The restored palaeo-bathymetry to base salt is shown in Figure 4.5(d); a 'normal' magmatic solution (Va=7km) is assumed. The proximal base salt restores to near sea level with an average bathymetry of approximately 0.3km. In contrast the distal base salt does not restore to near sea level; palaeo-bathymetries for base salt between approximately 0.7km and 2.5km below sea level are predicted (smoothing through fault controlled topography). In the deep structural troughs, palaeo-bathymetries of approximately 4.0km below sea level are restored for the distal base salt.

Predicted palaeo-bathymetry to base salt assuming a magma poor solution

The restored palaeo-bathymetry to base salt, using a magma-poor solution, is shown in Figure 4.5(e). The proximal base salt restores to just below sea level. The distal base salt does not restore to sea level, with predicted base salt palaeo-bathymetries between approximately 0.9km and 3.0km below sea level (smoothing through fault controlled topography); in the deep structural troughs the palaeo-bathymetries are greater (approximately 4.5km below sea level).

An additional sensitivity to the continental lithosphere thinning factors, used to drive reverse thermal subsidence, has been examined along the CS1-2400 profile. A continental lithosphere thinning factor of 1.0, which should maximize the restored post-breakup thermal subsidence, has been applied to the entire profile. The proximal base salt restores to sea level with some subaerial exposure but it is still not possible to restore distal base salt to sea level.

In the oceanic domain, depths of approximately 2.5km (± 0.2km depending on magmatic solution), are predicted for both 'normal' magmatic and magma-poor solutions, consistent with the bathymetry expected for a newly formed oceanic ridge.

Due to the thick sedimentary cover and mobile salt (including salt diapirs and canopies) along the northern Angolan rifted continental margin, seismic imaging of the salt and pre-salt sedimentary units is difficult, which could lead to errors in our interpretation of the internal structure and thickness of the salt and the pre-salt sedimentary layers. We are, however, more confident in our pick of the base salt. In order to understand the implications of either over or under estimating the thickness of the salt layer we have examined the effect of

treating the salt layer as just another sedimentary layer (with a shale rich lithology) within the reverse post-breakup subsidence modelling (Supplementary Figure S4.1). If there was no salt along the margin, this would result in a deeper Moho, smaller continental lithosphere thinning factors, less reverse thermal subsidence and a deeper restoration of the base salt. The largest differences between the palaeo-bathymetric restorations of the base salt with the salt layer compared to that produced without the salt layer are seen in the large troughs at the western end of the profile (approximately 0.3km difference). An over-estimate of the thickness of the salt layer results in a shallower restoration of the base salt, but by no more than 0.3km.

4.2.4. Location of the distal salt with respect to COB location along the CS1-2400 profile

Knowledge of the horizontal position of the distal salt with respect to the continent ocean boundary (COB) and OCT structure is important for understanding the palaeo-bathymetries of the base Aptian salt and how the salt is located within the broad framework of the OCT. The structure of the OCT and COB location have been determined using a suite of integrated quantitative analysis techniques, which include gravity anomaly inversion, residual depth anomaly (RDA) analysis and subsidence analysis. A detailed methodology of the quantitative analysis techniques is beyond the scope of this chapter, but is described in earlier chapters.

The results from integrated quantitative analysis, along the CS1-2400 profile, are shown in the composite analysis plot in Figure 4.6. The composite analysis plot comprises of (a) the crustal cross section from gravity anomaly inversion, (b) RDAs corrected for sediment loading and crustal basement thickness variation, and (c) continental lithosphere thinning factors from gravity anomaly inversion and subsidence analysis. The composite analysis plot for the CS1-2400 profile is interpreted as showing two distinct crustal zones along the profile:

oceanic crust towards the western end of the profile and thinned continental crust in the central region. The composite analysis shows no evidence of exhumed mantle along the CS1-2400 profile. The dashed line indicates the COB and the start of 'normal' oceanic crust. Whilst this interface between oceanic crust and thinned continental crust is shown as a sharp line, in reality it is likely to be a transitional boundary. The location of the COB is based on changes in crustal basement thickness, inflections in the RDA signal and also changes in the continental lithosphere thinning, from subsidence analysis and gravity anomaly inversion.

We have identified the location of the COB on Figure 4.5, by the dashed line, in order to see where the salt sits within the OCT. The majority of the salt along the CS1-2400 profile is located to the east of the COB on thinned continental crust.

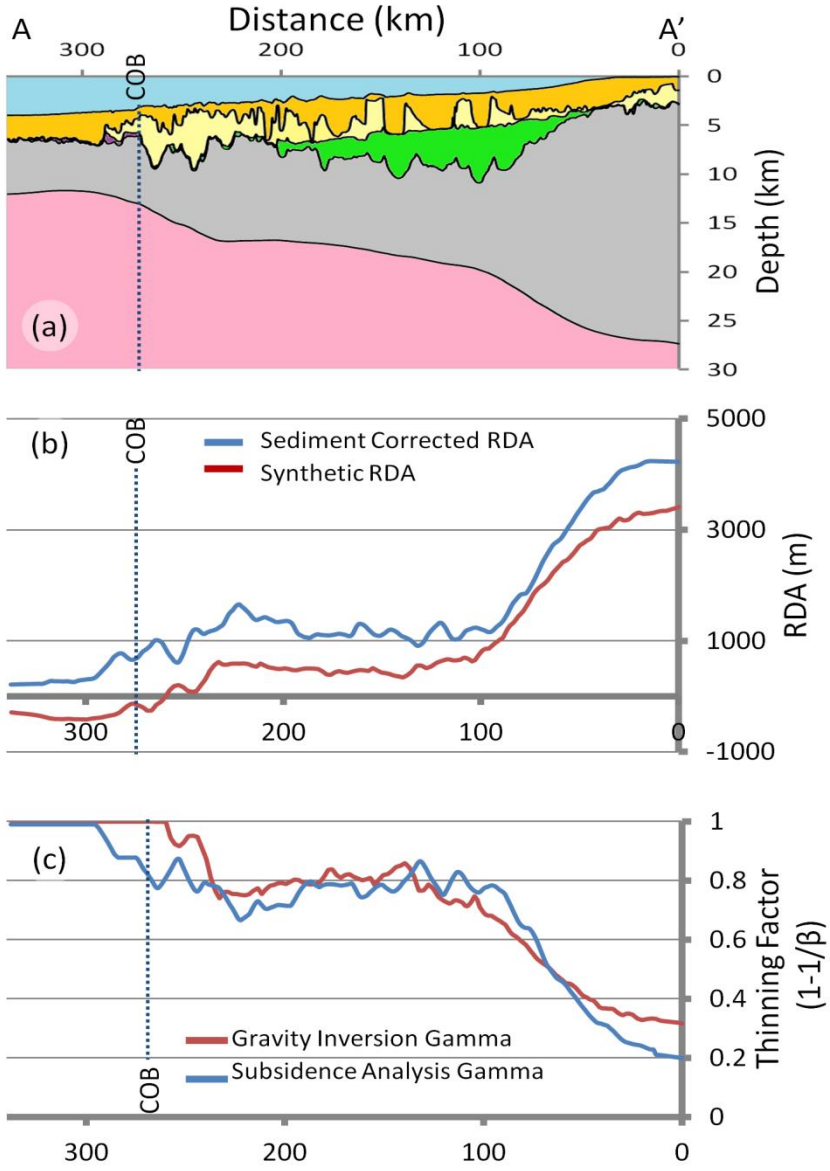

Figure 4.6 – Summary of the integrated quantitative analysis results for the CS1-2400 profile used to determine OCT structure and COB location. (a) Crustal cross section along CS1-2400 profile with Moho depth from gravity anomaly inversion. (b) The sediment corrected RDA and the RDA component from variations in crustal basement thickness both have the same general trend along the profile, although the magnitudes differ. This difference gives an indication of the magnitude of residual topography in this region, which we calculate to be approximately +700m of uplift. (c) Comparison of continental lithosphere thinning factors determined using subsidence analysis and gravity anomaly inversion, assuming a 'normal' magmatic solution (Va=7km) show the same general trend along profile. The dashed lines on the crustal cross section, RDA and continental lithosphere thinning plots indicate the distal extent of unequivocal continental crust and its boundary with oceanic crust, which is a possible interpretation of the COB.

4.3. Reverse post-breakup subsidence for the P3 and P7+11 profiles

4.3.1. Continental lithosphere thinning factors determined from gravity anomaly inversion for the P3 and P7+11 profiles

Continental lithosphere thinning factors determined from gravity anomaly inversion have also been calculated for the P3 and P7+11 profiles, located to the north of the CS1-2400 profile. Calibration of the reference Moho depth used within the gravity anomaly inversion predicts that a reference Moho depth of 37.5km is required. This is larger than that predicted for the CS1-2400 profile. We have therefore, considered the sensitivity to reference Moho depth within the reverse post-breakup thermal subsidence modelling (supplementary Figure S4.2), using CS1-2400 as the example. Increasing the reference Moho depth from 35.5km to 37.5km results in a deeper Moho and smaller continental lithosphere thinning factors, predicted from gravity anomaly inversion, and a deeper restoration of the base salt. The largest differences between the palaeo-bathymetric restorations of the base salt for a reference Moho depth of 35.5km compared to that produced with a reference Moho depth of 37.5km are seen in the large troughs at the western end of the profile, where the difference is approximately 0.35km.

4.3.2. Palaeo-bathymetry of the base Aptian salt deposition for the P3 profile

The present day P3 cross section is shown in Figure 4.7(a). Flexural backstripping and decompaction applied to the P3 profile (Figure 4.7 (b)) shows the sediment corrected bathymetry of the base salt, after the salt and post-salt sedimentary layers were removed. The full palaeo-bathymetric restoration of the base Loeme Aptian salt requires reverse post-breakup thermal subsidence.

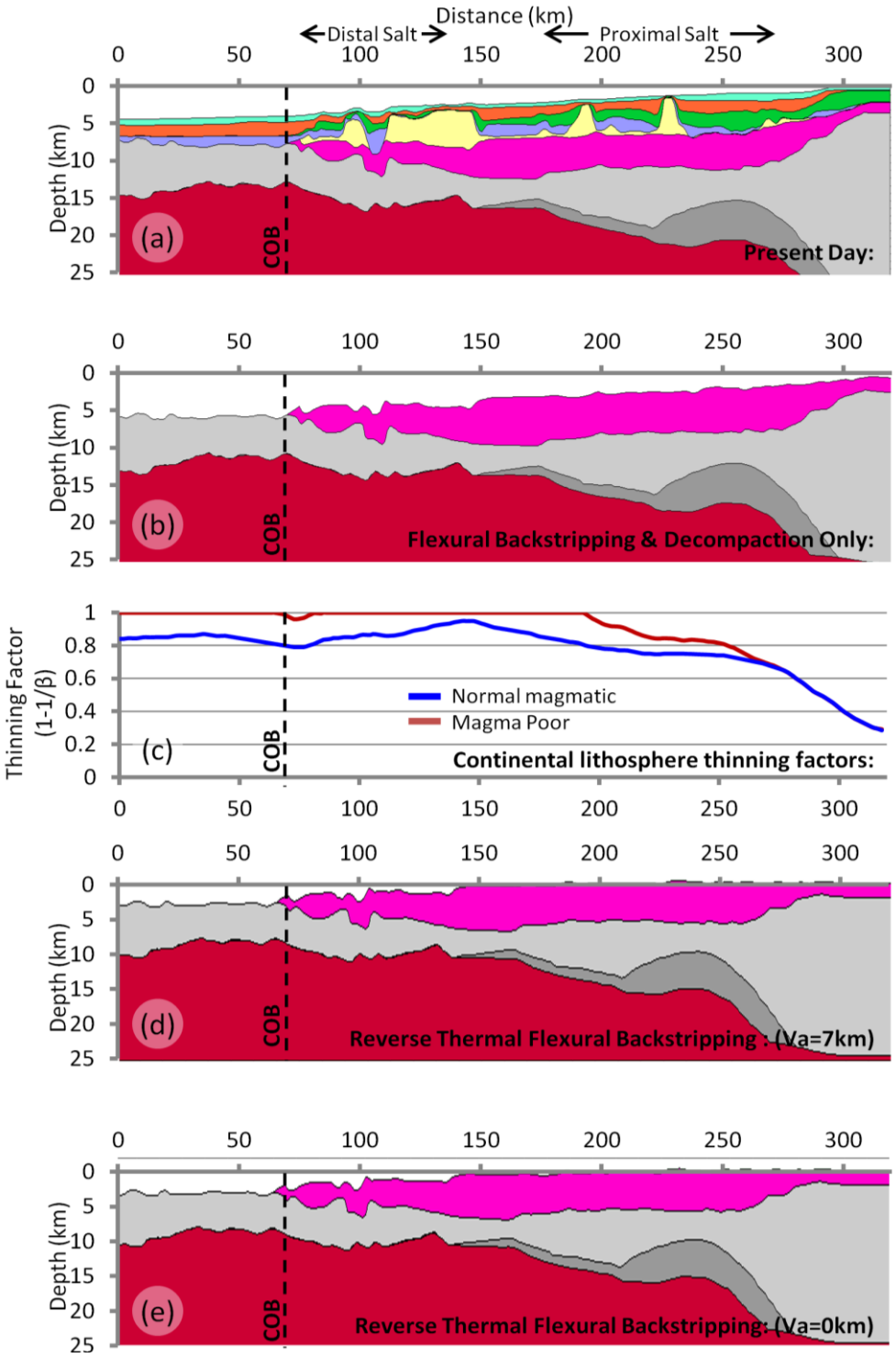

Figure 4.7 – Flexural backstripping and reverse post-breakup thermal subsidence modelling along the P3 profile (Contrucci et al., 2004; Moulin et al., 2005). (a) Digitized present day cross section along the P3 profile; the post-salt sedimentary layers are highlighted in turquoise, orange, green and blue; pre-salt sedimentary layer in pink; the salt layer is highlighted in yellow; upper crust is light grey, lower crust is dark grey and mantle is red. (b) Sediment corrected bathymetry to base salt calculated from flexural backstripping and decompaction, using a Te of 1.5km. (c) Continental lithosphere thinning factors from gravity anomaly inversion for a 'normal' magmatic and a magma-poor solution. (d) Reverse post-breakup thermal subsidence modelling along the P3 profile, assuming a 'normal' magmatic solution (Va=7km). (e) Reverse post-breakup thermal subsidence modelling along the P3 profile, assuming a magma-poor solution (Va=0km).

Continental lithosphere thinning factors used to drive reverse post-breakup thermal subsidence

Continental lithosphere thinning factors (γ) predicted from the gravity anomaly inversion, along the P3 profile are shown in Figure 4.7(c). A 'normal' magmatic solution (Va=7km) and a magma-poor solution (Va=0km) have been examined. At the western end and in the central section of the P3 profile, the continental lithosphere thinning factors for a 'normal' magmatic solution are 1.0, whereas for a magma-poor solution the continental lithosphere thinning factors are between approximately 0.85, which increase to 0.95 before reducing to 0.8 in the central region.

Predicted palaeo-bathymetry to base salt assuming a 'normal' magmatic solution

Results of reverse post-breakup subsidence modelling with continental lithosphere thinning factors for a 'normal' magmatic solution are shown in (Figure 4.7(d)). Reverse post-breakup thermal subsidence modelling predicts that the proximal base salt restores to sea level, or just above. Palaeo-bathymetries predicted for the distal base salt do not restore to sea level and are between approximately 0.5km and 2.0km below sea level.

Predicted palaeo-bathymetry to base salt assuming a magma poor solution

Reverse post-breakup thermal subsidence modelling, for a magma-poor solution (Va=0km) are shown in Figure 4.7(e). The proximal base salt restores to approximately sea level similar to that predicted when using continental lithosphere thinning factors assuming a 'normal' magmatic solution. Again, the reverse post-breakup thermal subsidence modelling does not

restore the distal base salt to sea level and palaeo-bathymetries between 1.2km and 2.5km below sea level are predicted.

Water depths of approximately 2.5km (±0.2km depending on magmatic solution) consistent with a newly formed oceanic ridge are predicted at breakup at the oceanic end of the P3 profile, for both a 'normal' magmatic and a magma-poor solution.

Integrated quantitative analysis has been applied to the P3 profile in order to determine the location of the COB. The dashed line, as shown in Figure 4.7, indicates a possible interpretation of the COB location; all the salt along the P3 profile is located east of the COB, on the thinned continental crust.

4.3.3. Palaeo-bathymetry of the base Aptian salt deposition for P7+11 profile

The present day P7+11 cross section is shown in Figure 4.8(a). Flexural backstripping and decompaction has been applied to the P7+11 profile to remove the salt and post-salt sedimentary layers in order to determine the bathymetry of the base salt corrected for sediment loading (Figure 4.8(b)). As previously mentioned reverse post-breakup thermal subsidence is needed in order to determine the full palaeo-bathymetric restoration of the base Loeme Aptian salt.

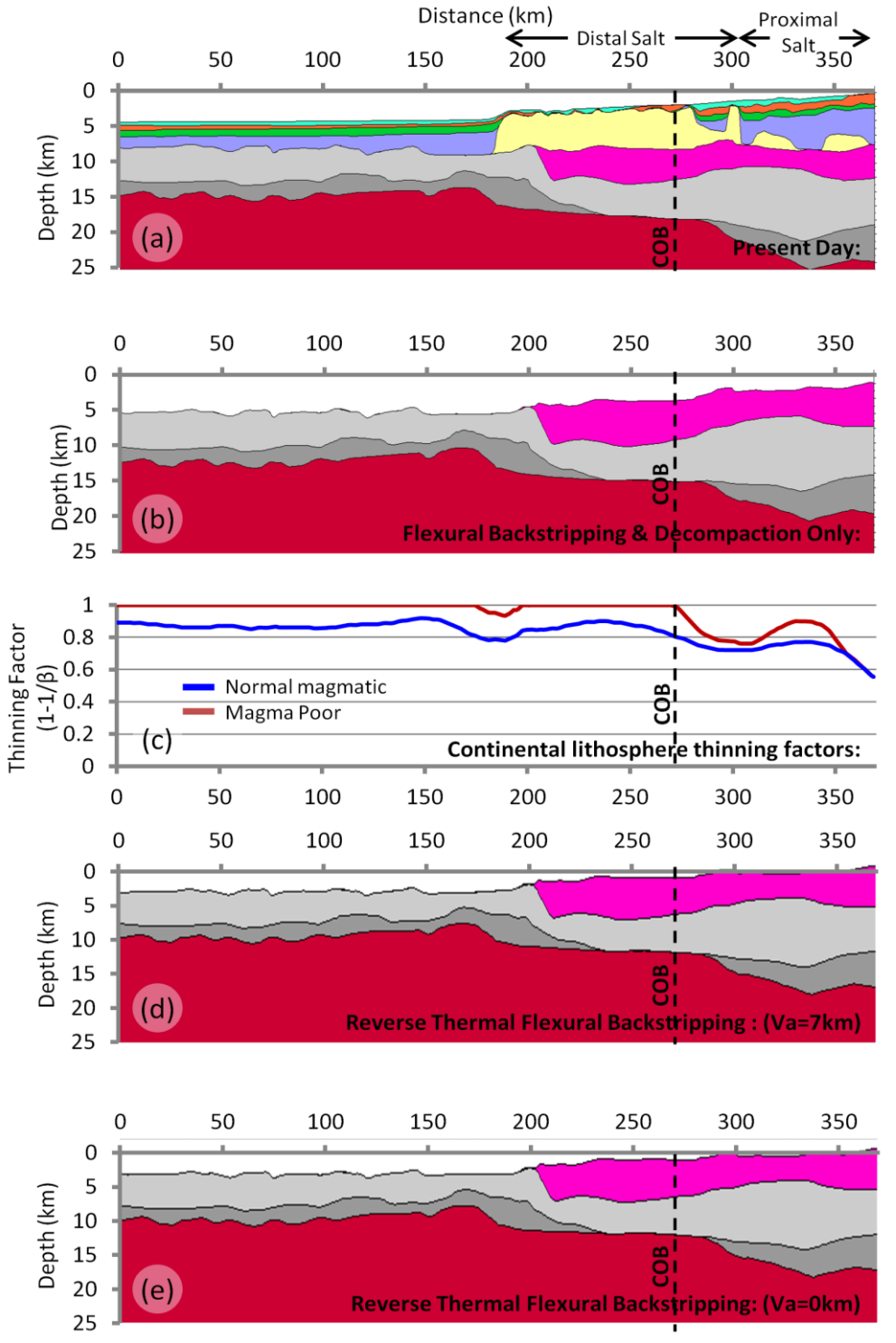

Figure 4.8 – Flexural backstripping and reverse post-breakup thermal subsidence modelling along the P7+11 profile (Contrucci et al., 2004; Moulin et al., 2005). (a) Digitized present day cross section along the P7+11 profile; the post-salt sedimentary layers are highlighted in turquoise, orange, green and blue; pre-salt sedimentary layer in pink; the salt layer is highlighted in yellow; upper crust is light grey, lower crust is dark grey and mantle is red. (b) Sediment corrected bathymetry to base salt calculated from flexural backstripping and decompaction using a Te of 1.5km. (c) Continental lithosphere thinning factors from gravity anomaly inversion for a 'normal' magmatic and a magma-poor solution. (d) Reverse post-breakup thermal subsidence modelling along the P7+11 profile, assuming a 'normal' magmatic solution (Va=7km). (e) Reverse post-breakup thermal subsidence modelling along the P7+11 profile, assuming a magma-poor solution (Va=0km).

Continental lithosphere thinning factors used to drive reverse post-breakup thermal subsidence modelling

Continental lithosphere thinning factors (γ) predicted from gravity anomaly inversion, along the P7+11 profile (Figure 4.8(c)) assuming a 'normal' magmatic solution (Va=7km) and a magma-poor solution (Va=0km), are used to drive the post-breakup thermal subsidence modelling. The P7+11 profile shows a similar distribution of continental lithosphere thinning to that of the P3 profile. At the western end and in the central section of the P7+11 profile the gravity anomaly inversion predicted continental lithosphere thinning factors are 1.0, for a 'normal' magmatic solution (Va=7km), whereas a magma-poor solution (Va=0km) predicts continental lithosphere thinning factors of approximately 0.9.

Predicted palaeo-bathymetry to base salt assuming a 'normal' magmatic solution

Reverse post-breakup thermal subsidence for a 'normal' magmatic solution (Figure 4.8(d), restores the proximal base salt to at, or just above, sea level. At the extreme eastern end of the profile, the predicted subaerial exposure of approximately 0.9km is probably an edge effect from the flexural backstripping. In comparison, the distal base salt restores to between approximately 0.9km and 2.0km below sea level.

Predicted palaeo-bathymetry to base salt assuming a magma poor solution

Reverse post-breakup thermal subsidence modelling, assuming a magma-poor solution (Va=0km) (Figure 4.8(e)), predicts palaeo-bathymetries for the proximal base salt between approximately sea level and 0.7km above sea level at the eastern end of the profile. The

reverse post-breakup thermal subsidence modelling restores the distal base salt to between 1.0km below sea level and 0.3km below sea level.

For both a 'normal' magmatic and a magma-poor solution, palaeo-bathymetries of approximately 2.5km (±0.2km depending on magmatic solution), consistent with that expected for a young ocean ridge, are predicted for the oceanic crust, at the western end of the P7+11 profile.

The location of the COB on the P7+11 profile, determined from integrated quantitative analysis, is shown on Figure 4.8. The dashed line, as shown on Figure 4.8, indicates a possible interpretation of the COB location; the majority of the salt along the P7+11 profile is located to the east of the COB on thinned continental crust.

4.4. Discussion

Predicted palaeo-bathymetries have been determined for the base Loeme salt using 2D-flexural backstripping and reverse post-breakup thermal subsidence modelling. Continental lithosphere thinning factors derived from gravity anomaly inversion have been used to determine the reverse post-breakup thermal subsidence. Sensitivities to 'normal' magmatic (Va=7km) and magma-poor (Va=0km) solutions have been examined for the reverse post-breakup subsidence modelling. Both the 'normal' magmatic and magma-poor solutions restore the proximal autochthonous base salt to near sea level, with some sub aerial exposure, at the time of breakup for all three profiles (CS1-2400, P3 and P7+11). The sub aerial exposure could be a result of present day mantle dynamic topography (White et al., 1992). In contrast, reverse post-breakup subsidence modelling does not restore the distal base salt to sea level; predicted water loaded bathymetries for the distal base salt range between 0.2km and 3km. Even if we apply a continental lithosphere thinning factor of 1.0

along the full length of the three profiles (which is unreasonable), the palaeo-bathymetries still do not restore to sea level, demonstrating that it is not possible to generate the subsidence of the base salt by post-breakup subsidence alone. The predicted bathymetries at breakup of the first unequivocal oceanic crust are approximately 2.5km as expected for newly formed oceanic crust of normal thickness. As previously mentioned, sensitivities to Te and breakup age have been examined. Changing the value of Te does not change the palaeo-bathymetry predictions in any significant way. Changing the breakup age has a small effect on the palaeo-bathymetry predictions, but does not change the overall conclusions.

There are several possible explanations of the palaeo-bathymetric restoration of the distal base salt to water depths substantially below sea level:

(i) our preferred interpretation is that all of the Aptian salt along the northern Angolan profiles was deposited at or just below global sea level, but that the distal salt was formed during the late syn-rift (syn-tectonic) when the crust under it was being actively thinned during salt deposition resulting in additional tectonic subsidence. This is consistent with seismic evidence, which shows that the distal base salt is extensionally faulted, while in contrast the proximal salt formed in a region where crustal thinning had already taken place, but had ceased. This interpretation suggests that the distal salt subsides by syn-rift crustal thinning and post-rift thermal subsidence, whilst the proximal salt subsides by post-rift thermal subsidence alone. This is consistent with breakup tectonic models proposed by Péron-Pinvidic and Manatschal (2008). This explanation would have significant implications for basin modelling workflows applied to exploration. If it is assumed that that the base Aptian salt is time-transgressive (younging ocean-ward), there are major implications for palaeo-bathymetry variation, hence potential reservoir distribution. As the stratigraphy becomes younger ocean-ward any age and thickness changes will have repercussions when

determining continental lithosphere thinning factors and related heat flow from sediment thickness information.

(ii) It is possible that during breakup the distal salt moved down-slope to its present position into much deeper water (and is para-autochthonous). If in the distal regions, the salt is para-autochthonous (or allochthonous) then the salt was not deposited in this deep-water locality and should not restore to sea level. This explanation is similar to that advocated in the Gulf of Mexico by Rowan et al. (2004) and could also explain the existence of salt in the outermost deep-water part of the Angolan margin.

(iii) An interpretation which is often invoked (e.g. Burke and Sengör (1988), Burke et al. (2003) and Karner and Gambôa (2007)) to explain the palaeo-bathymetry of the base Aptian salt along the northern Angolan margin is that the Aptian salt deposition occurred in confined environmental conditions (e.g. in a Messinian-type basin, isolated from global sea level). Although some isolation from global sea level is almost certainly required for the deposition of such large volumes of salt and a structural barrier in the south is not dismissed, we believe that there is no definite requirement to invoke an isolated deep ocean basin, with local sea-level 2-3km below global sea level for the deposition of the Aptian salt on the Angolan rifted margin. A strong argument against the deep isolated basin interpretation is presented by Pindell et al. (2014)(2014), with reference to the Gulf of Mexico, who argue that an isolated deep basin hypothesis is unlikely, as it requires a complicated scenario of inter-related events to occur. The salt deposition in a deep isolated basin hypothesis requires that first rifting must produce a large deep basin with a depositional surface remaining approximately 2.0km below sea level, and that there must also be a topographic barrier, which blocks out linkage to the global ocean. Then, at the time of salt deposition there needs to have been repeated spill/desiccation cycles [666] and a semi-permeable barrier which continuously allowed just the right amount of sea water into the basin so that shallow-water evaporative conditions were

maintained until the end of the salt deposition. Pindell et al. (2014) suggest that this fortuitous sequence of events is unlikely.

Our preferred interpretation of our palaeo-bathymetric restoration of the base Aptian salt along the northern Angolan profiles is a combination of the proposed first and second explanations. We believe that it is likely that all of the Aptian salt was deposited just below global sea level, but that the distal salt formed during late the syn-rift (syn-tectonic) while the crust under it was being actively thinned during salt deposition, which resulted in additional tectonic subsidence. We also believe that it is possible that some of the distal salt is para-autochthonous and moved down-slope to its present day position.

4.5. References:

Alvey, A., Gaina, C., Kusznir, N. J., and Torsvik, T. H., 2008, Integrated crustal thickness mapping and plate reconstructions for the high Arctic: Earth and Planetary Science Letters, v. 274, no. 3-4, p. 310-321.

Amante, C., and Eakins, B. W., 2009, ETOPO1 1 Arc-Minute Global Relief Model: Procedures, Data Sources and Analysis: NOAA Technical Memorandum NESDIS NGDC-24, p. 19.

Bertotti, G., Picotti, V., and Cloetingh, S., 1998, Lithospheric weakening during "retroforeland" basin formation: Tectonic evolution of the central South Alpine foredeep: Tectonics, v. 17, no. 1, p. 131-142.

Brun, J. P., and Fort, X., 2011, Salt Tectonics at Passive Margins: Geology versus Models: Marine and Petroleum Geology, v. 28.

Burke, K., MacGregor, D. S., and Cameron, N. R., 2003, Africa's petroleum systems: four tectonic 'Aces' in the past 600 million years: Geological Society, London, Special Publications, v. 207, no. 1, p. 21-60.

Burke, K., and Sengör, A. M. C., 1988, Ten metre global sea-level change associated with South Atlantic Aptian salt deposition: Marine Geology, v. 83, no. 1–4, p. 309-312.

Chappell, A. R., and Kusznir, N. J., 2008, Three-dimensional gravity inversion for Moho depth at rifted continental margins incorporating a lithosphere thermal gravity anomaly correction: Geophysical Journal International, v. 174, no. 1, p. 1-13.

Contrucci, I., Matias, L., Moulin, M., Géli, L., Klingelhofer, F., Nouzé, H., Aslanian, D., Olivet, J.-L., Réhault, J.-P., and Sibuet, J.-C., 2004, Deep structure of the West African continental margin (Congo, Zaïre, Angola), between 5°S and 8°S, from reflection/refraction seismics and gravity data: Geophysical Journal International, v. 158, no. 2, p. 529-553.

Cowie, L., and Kusznir, N., 2012, Mapping crustal thickness and oceanic lithosphere distribution in the Eastern Mediterranean using gravity inversion: Petroleum Geoscience, v. 18, no. 4, p. 373-380.

Davidson, I., 2007, Geology and Tectonics of the South Atlantic Brazilian Salt Basins, *in* Ries, A. C., Butler, R. W. H., and Graham, R. H., eds., Deformation of the Continental Crust: The Legacy of Mike Coward, Volume 272, Geological Society of London, p. 345-359.

Davidson, I., Anderson, L., and Nuttall, P., 2012, Salt Deposition, Loading and Gravity Drainage in the Campos and Santos Salt Basins, *in* Alsop, G. I., Archer, S. G., Hartley, A. J., Grant, N. T., and Hodgkinson, R., eds., Salt Tectonics, Sediments and Prospectivity, Volume 363, Geological Society of London, p. 159 -173.

Dean, S. M., Minshull, T. A., Whitmarsh, R. B., and Louden, K. E., 2000, Deep structure of the ocean-continent transition in the southern Iberia Abyssal Plain from seismic refraction profiles: The IAM-9 transect at 40°20'N: Journal of Geophysical Research: Solid Earth, v. 105, no. B3, p. 5859-5885.

Discovery 215 Working, G., Minshull, T. A., Dean, S. M., Whitmarsh, R. B., Russell, S. M., Louden, K. E., and Chian, D., 1998, Deep structure in the vicinity of the ocean-continent transition zone under the southern Iberia Abyssal Plain: Geology, v. 26, no. 8, p. 743-746.

Duval, B., Cramez, C., and Jackson, M. P. A., 1992, Raft Tectonics in the Kwanza Basin, Angola: Marine and Petroleum Geology, v. 9.

Galán, R. A., and Casallas, I. F., 2010, DETERMINATION OF EFFECTIVE ELASTIC THICKNESS OF THE COLOMBIAN ANDES USING SATELLITE-DERIVED GRAVITY DATA: Earth Sciences Research Journal, v. 14, p. 7-16.

Greenhalgh, E. E., and Kusznir, N. J., 2007, Evidence for thin oceanic crust on the extinct Aegir Ridge, Norwegian Basin, NE Atlantic derived from satellite gravity inversion: Geophysical Research Letters, v. 34, no. 6, p. L06305.

Hudec, M. R., and Jackson, M. P. A., 2007, Terra infirma: Understanding salt tectonics: Earth-Science Reviews, v. 82, no. 1–2, p. 1-28.

Jackson, M. P. A., Cramez, C., and Fonck, J.-M., 2000, Role of subaerial volcanic rocks and mantle plumes in creation of South Atlantic margins: implications for salt tectonics and source rocks: Marine and Petroleum Geology, v. 17, no. 4, p. 477-498.

Karner, G. D., and Driscoll, N. W., 1999, Tectonic and stratigraphic development of the West African and eastern Brazilian Margins: insights from quantitative basin modelling: Geological Society, London, Special Publications, v. 153, no. 1, p. 11-40.

Karner, G. D., Driscoll, N. W., and Barker, D. H. N., 2003, Syn-rift regional subsidence across the West African continental margin: the role of lower plate ductile extension: Geological Society, London, Special Publications, v. 207, no. 1, p. 105-129.

Karner, G. D., Driscoll, N. W., McGinnis, J. P., Brumbaugh, W. D., and Cameron, N. R., 1997, Tectonic significance of syn-rift sediment packages across the Gabon-Cabinda continental margin: Marine and Petroleum Geology, v. 14, no. (7-8), p. 973-1000.

Karner, G. D., and Gambôa, L. A. P., 2007, Timing and origin of the South Atlantic pre-salt sag basins and their capping evaporites: Geological Society, London, Special Publications, v. 285, no. 1, p. 15-35.

Kusznir, N., and Karner, G., 1985, Dependence of the flexural rigidity of the continental lithosphere on rheology and temperature: Nature, v. 316, no. 6024, p. 138-142.

Kusznir, N. J., Roberts, A. M., and Morley, C. K., 1995, Forward and reverse modelling of rift basin formation: Geological Society, London, Special Publications, v. 80, no. 1, p. 33-56.

Manatschal, G., Froitzheim, N., Rubenach, M., and Turrin, B. D., 2001, The role of detachment faulting in the formation of an ocean-continent transition: insights from the Iberia Abyssal Plain: Geological Society, London, Special Publications, v. 187, no. 1, p. 405-428.

Manatschal, G., Sutra, E., and Péron-Pinvidic, G., The lesson from the Iberia-Newfoundland rifted margins: how applicable is it to other rifted margins?, *in* Proceedings 2nd Central & North Atlantic Conjugate Margins: Rediscovering the Atlantic, New Insights, New winds for an old sea2010, Volume 2, p. 27 - 37.

McKenzie, D., 1978, Some Remarks on the Development of Sedimentary Basins Earth and Planetary Science Letters, v. 40, p. 25-32.

Moulin, M., 2003, Etude géologique et géophysique des marges continentales passives: exemple du Zaıre et de l'Angola [PhD: University de Bretagne Occidentale, 360 p.

Moulin, M., Aslanian, D., Olivet, J.-L., Contrucci, I., Matias, L., Géli, L., Klingelhoefer, F., Nouzé, H., Réhault, J.-P., and Unternehr, P., 2005, Geological constraints on the evolution of the Angolan margin based on reflection and refraction seismic data (ZaïAngo project): Geophysical Journal International, v. 162, no. 3, p. 793-810.

Müller, R. D., Sdrolias, M., Gaina, C., Steinberger, B., and Heine, C., 2008, Long-Term Sea-Level Fluctuations Driven by Ocean Basin Dynamics: Science, v. 319, no. 5868, p. 1357-1362.

Parker, R. L., 1972, The Rapid Calculation of Potential Anomalies: Geophysical Journal of the Royal Astronomical Society, v. 31, no. 4, p. 447-455.

Péron-Pinvidic, G., and Manatschal, G., 2008, The final rifting evolution at deep magma-poor passive margins from Iberia-Newfoundland: a new point of view: International Journal of Earth Sciences, v. 98, no. 7, p. 1581-1597.

Péron-Pinvidic, G., Manatschal, G., Minshull, T. A., and Sawyer, D. S., 2007, Tectonosedimentary evolution of the deep Iberia-Newfoundland margins: Evidence for a complex breakup history: Tectonics, v. 26, no. 2, p. TC2011.

Pindell, J., Graham, R., and Horn, B., 2014, Rapid outer marginal collapse at the rift to drift transition of passive margin evolution, with a Gulf of Mexico case study: Basin Research, p. n/a-n/a.

Quirk, D. G., Schødt, N., Lassen, B., Ings, S. J., Hsu, D., Hirsch, K. K., and Von Nicolai, C., 2012, Salt tectonics on passive margins: examples from Santos, Campos and Kwanza basins: Geological Society, London, Special Publications, v. 363, no. 1, p. 207-244.

Roberts, A. M., Corfield, R. I., Kusznir, N. J., Matthews, S. J., Hansen, E.-K., and Hooper, R. J., 2009, Mapping palaeostructure and palaeobathymetry along the Norwegian Atlantic continental margin: Møre and Vøring basins: Petroleum Geoscience, v. 15, no. 1, p. 27-43.

Roberts, A. M., Kusznir, N. J., Yielding, G., and Styles, P., 1998, 2D flexural backstripping of extensional basins; the need for a sideways glance: Petroleum Geoscience, v. 4, no. 4, p. 327-338.

Roberts, A. M., Lundin, E. R., and Kusznir, N. J., 1997, Subsidence of the Vøring Basin and the influence of the Atlantic continental margin: Journal of the Geological Society, v. 154, no. 3, p. 551-557.

Rowan, M. G., 2014, Passive-margin salt basins: hyperextension, evaporite deposition, and salt tectonics: Basin Research, v. 26, no. 1, p. 154-182.

Rowan, M. G., J, P. F., and C, V. B., 2004, Gravity-driven fold belts on passive margins, AAPG Memoir, Thrust tectonics and hydrocarbon systems.

Sandwell, D. T., and Smith, W. H. F., 2009, Global marine gravity from retracked Geosat and ERS-1 altimetry: Ridge segmentation versus spreading rate: J. Geophys. Res., v. B01411, no. 114(B1).

Schmalz, R. F., 1969, Deep-water Evaporite Deposition: A Genetic Model: The American Association of Petroleum Geologists Bulletin, v. 53, no. 4.

Teisserenc, P., and Villemin, J., 1989, Sedimentary basin of Gabon – geology and oil systems, *in* Edwards, J. D., and Santogrossi, P. A., eds., Divergent / Passive Margin Basins. Memoir of the American Association of Petroleum Geologists, Volume 48.

Torsvik, T. H., Rousse, S., Labails, C., and Smethurst, M. A., 2009, A new scheme for the opening of the South Atlantic Ocean and the dissection of an Aptian salt basin: Geophysical Journal International, v. 177, no. 3, p. 1315-1333.

Unternehr, P., Péron-Pinvidic, G., Manatschal, G., and Sutra, E., 2010, Hyper-extended crust in the South Atlantic: in search of a model: Petroleum Geoscience, v. 16, no. 3, p. 207-215.

West, D. B., 1989, Model for Salt Deformation on Deep Margin of Central Gulf of Mexico Basin: The American Association of Petroleum Geologists Bulletin, v. 73, no. 12.

White, R., and McKenzie, D., 1989, Magmatism at Rift Zones: The Generation of Volcanic Continental Margins and Flood Basalts: Journal of Geophysical Research, v. 94, no. B6, p. 7685-7729.

White, R. S., McKenzie, D., and O'Nions, R. K., 1992, Oceanic Crustal Thickness From Seismic Measurements and Rare Earth Element Inversions: Journal of Geophysical Research, v. 97, no. B13, p. 19683-19715.

Whitmarsh, R. B., and Miles, P. R., 1995, Models of the development of the West Iberia rifted continental margin at 40°30'N deduced from surface and deep-tow magnetic anomalies: Journal of Geophysical Research: Solid Earth, v. 100, no. B3, p. 3789-3806.

4.6. Supplementary Figures

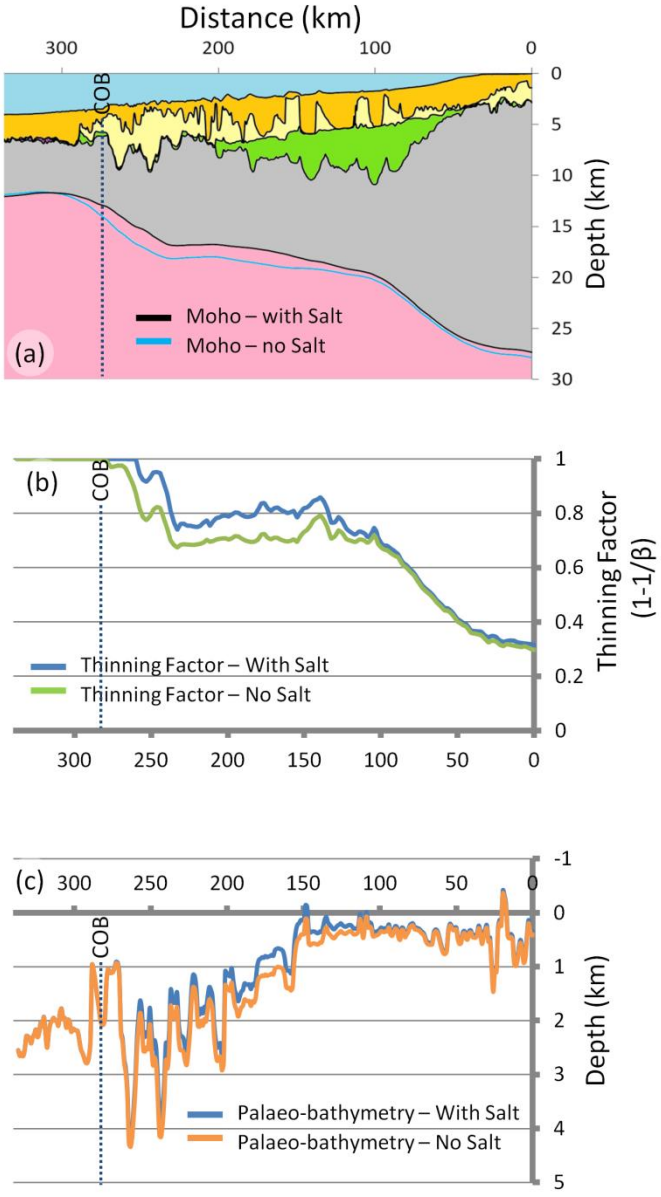

Supplementary Figure S4.1 – Sensitivity to the effect of over-estimating or under-estimating the thickness of the salt layer along CS1-2400. Two end member sensitivities have been considered: (i) having a salt layer (as used in the chapter) (labelled "With Salt") or (ii) treating the salt as just another sedimentary layer (labelled "No Salt"). (a) Crustal cross section from gravity anomaly inversion, showing two Moho depths (both using the calibrated reference Moho depth of 35.5km). The Moho in black is the result of having a salt layer in the gravity anomaly inversion, whereas the Moho in blue is the result of treating the salt layer as just another sedimentary layer. Removing the salt layer from the gravity anomaly inversion results in a deeper Moho depth prediction. (b) Comparison of the continental lithosphere thinning factors, predicted from gravity anomaly inversion for the two sensitivities: with salt (in blue) and no salt (in green). Removing the salt layer from the gravity anomaly inversion results in smaller continental lithosphere thinning factors. (c) The resulting palaeo-bathymetries from reverse post-breakup thermal subsidence modelling for the two sensitivities: with salt (in blue) and no salt (in orange). The "No Salt" sensitivity results in deeper palaeo-bathymetries, the biggest differences are observed in the central section of the profile.

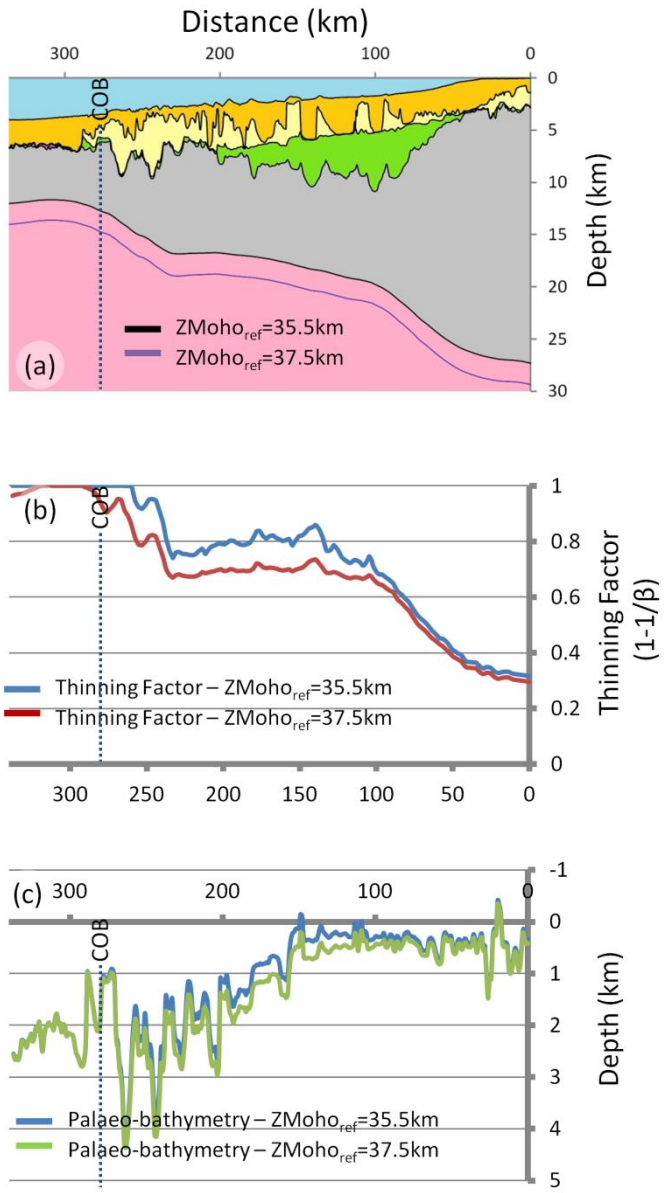

Supplementary Figure S4.2 – Sensitivity to changing the reference Moho depth between 35.5km (as calibrated for the CS1-2400 profile) to 37.5km (as calibrated for the P3 and P7+11 profiles). (a) Crustal cross section from gravity anomaly inversion, showing two Moho depths. The Moho in black is the result of using a reference Moho depth of 35.5km and the Moho in purple is the result of using a higher reference Moho depth of 37.5km. If we increase the reference Moho depth along the CS1-2400 profile, this results in a deeper Moho depth prediction. (b) Comparison of the continental lithosphere thinning factors, predicted from gravity anomaly inversion for the sensitivities to reference Moho depth. Using a reference Moho depth of 37.5km (in red) results in smaller continental lithosphere thinning factors along the CS1-2400 profile. (c) The resulting palaeo-bathymetries from reverse post-breakup thermal subsidence modelling for the two sensitivities to reference Moho depth: using a reference Moho depth of 35.5km (in blue) and using a reference Moho depth of 37.5km (in green). The larger reference Moho depth of 37.5km results in deeper palaeo-bathymetries; the biggest differences are observed in the central section of the profile.

5. Residual Topography Predictions from Residual Depth Anomaly Analysis: Applications to the Iberian, Gulf of Aden and Northern Angolan Rifted Continental Margins

Preface

This chapter has been written in the form of a paper. The co-author is N.J Kusznir (University of Liverpool). Section headers, figures and page numbers have been renumbered to conform to the format of this thesis.

Abstract

The best constraint on present day mantle dynamic topography is residual topography (Flament et al., 2013), which may be calculated by removing the isostatic effect of sediments, ice, crust and lithosphere (including oceanic lithosphere cooling) from the observed topography. Residual topography can be calculated most accurately for the oceans, in particular at rifted continental margins; where in recent years there has been an increase in our knowledge due to the increased availability of high quality data from hydrocarbon exploration and the increasing number of academic studies. Measurements of present day residual topography, which we attribute to mantle dynamic topography, have been made using residual depth anomaly (RDA) analysis for three rifted continental margins: offshore Iberia, the Gulf of Aden and northern Angola. RDAs have been calculated by comparing observed and age predicted oceanic bathymetries, using the thermal plate model predictions from Crosby and McKenzie (2009). RDAs have been computed along 2D profiles, which run from unequivocal oceanic crust across the continent ocean boundary (COB) onto thinned continental crust. Corrections for sediment loading have been made using flexural back-stripping and decompaction. In addition, crustal basement thicknesses predicted from gravity anomaly inversion together with Airy isostasy have been used to predict the RDA component due to departures from the standard oceanic crustal thickness of 7km.

In the oceanic domain of the Iberian Abyssal Plain, RDA analysis calculates approximately -650m of residual topography, indicating mantle dynamic subsidence. Whilst in the oceanic domains of the Gulf of Aden and the northern Angolan margin, mantle dynamic uplift is indicated by the positive measurements of residual topography, calculated from RDA analysis. In the Gulf of Aden we calculate +400m of residual topography and along the northern Angolan margin we calculate +700m of residual topography. We compare our calculated residual topography measurements from RDA analysis with published predictions

of residual topography extracted from global models, which show resemblance to our calculated residual topography measurements; however, they differ in amplitude, and in some places polarity.

5.1. Introduction

Large-scale variations in the Earth's observed surface topography originate from changes in crustal and lithospheric thickness, and/or the lateral variations in density (Lithgow-Bertelloni and Silver, 1998). Other large scale variations in topography are related to the interaction between mantle convection and the overriding plates; for example, uplift of the oceanic and continental lithosphere over hotspots, or subsidence of the oceanic and continental lithosphere in subduction retroarc regions. It is therefore possible to categorise the mechanisms for the support of the Earth's topography as isostatic or dynamic (Allen, 1997). The isostatic mechanisms are the result of variations in lithospheric density and thickness due to plate tectonics, whilst the dynamic mechanisms are the response of viscous mantle flow. Whole-mantle thermal convection results in the larger scale three-dimensional variations in mantle density, whereas smaller-scale heterogeneity is likely to be the result of mantle plume activity or from subduction zones.

The amplitude and wavelength of the Earth's surface topography due to deep mantle processes are not fully understood; however, there are many global models, which attempt to measure these parameters (e.g. Flament et al. (2013); Crosby and McKenzie (2009); Steinberger (2007) and Kaban et al. (2003)). These models measure residual topography, which may be defined as the topography remaining after the isostatic contributions from sediments, ice, crust and lithosphere (including oceanic lithosphere cooling) are removed. At long wavelengths these models give a broadly similar pattern; however, at shorter wavelengths they differ substantially in the predicted amplitude. These differences may be

the result of the methodologies used to measure residual topography and/or the different corrections applied; it is therefore clear that these global models of residual topography require further, more rigorous testing in order to constrain the measurement of residual topography at a global scale. Residual topography can be calculated most accurately for the oceans, in particular at rifted continental margins; where in recent years there has been an increase in the large availability of high quality data from hydrocarbon exploration. We have carried out detailed regional studies of residual topography, which we attribute to mantle dynamic topography, on three profiles at rifted continental margins, using residual depth anomaly (RDA) analysis. An RDA is the comparison of observed and age predicted oceanic bathymetries, and has been used to calculate departures from standard oceanic water depths, as predicted by Crosby et al. (2006) and Stein and Stein (1992). Corrections for sediment loading and variations in crustal basement thickness have been applied to the calculated RDAs. We carry out this analysis along profiles for the offshore Iberian (Figure 5.1 (a)), Gulf of Aden (Figure 5.1 (b)) and the northern Angolan rifted continental margins (Figure 5.1(c)).

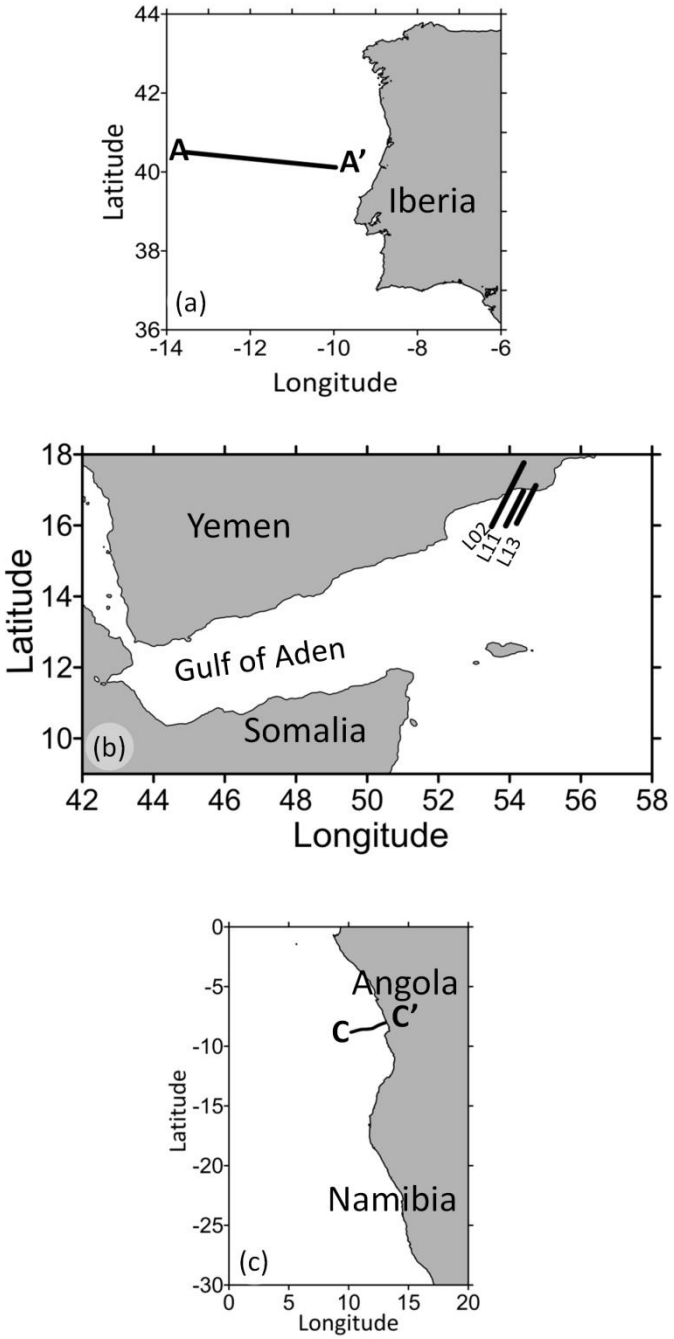

Figure 5.1 – Location map for (a) the Iberian Abyssal Plain, (b) the Gulf of Aden and (c) the northern Angolan rifted continental margins. Profile locations are indicated for each region.

The aim of this chapter is to compare our regional measurements of residual topography with the global model predictions of residual topography (e.g. Flament et al. (2013); Crosby and McKenzie (2009); Steinberger (2007) and Kaban et al. (2003)) in the oceanic domain. This will allow us to access the accuracy and precision of the residual topography predictions from

the global models and also to further understand the importance of the various corrections applied to the global model predictions.

5.1.1. Summary of the Global Residual Topography Models

Whilst most authors agree on the cause of the long wavelength residual topography, the methodologies used to calculate global models of residual topography and the corrections applied often differ significantly. The different global model residual topography measurements may give a broadly similar pattern at long wavelengths but they differ substantially in the predicted amplitude and polarity at shorter wavelengths. In this chapter, we have compared our sediment and crustal basement thickness corrected RDA analysis results with the residual topography measurements from the global models (Figure 5.2) of Flament et al. (2013), Crosby and McKenzie (2009), Steinberger (2007) and Kaban et al. (2003).

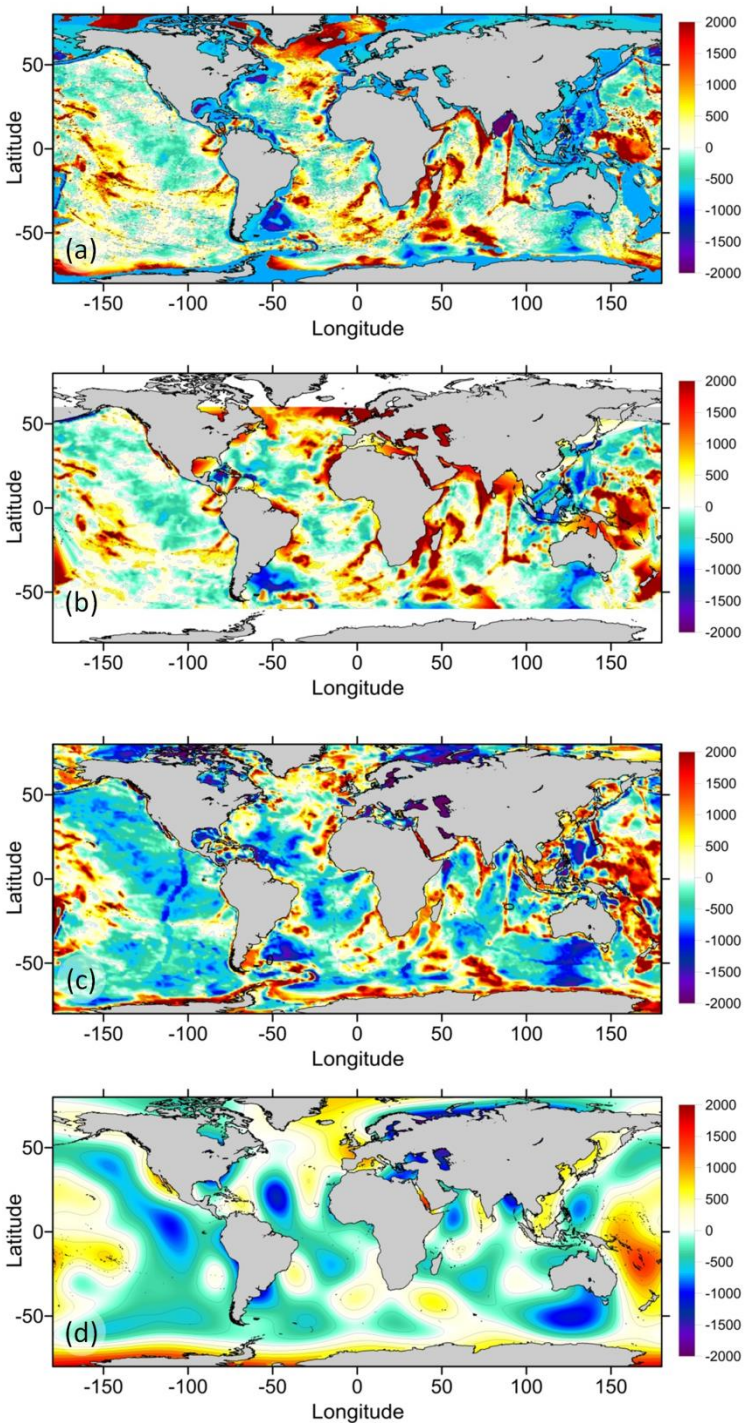

Figure 5.2 – Global residual topography models from (a) Flament et al. (2013), (b) Crosby and McKenzie (2009), (c) Steinberger (2007) and (d) Kaban et al. (2003). The methodology used to determine residual topography in each of these models varies. Flament et al. (2013) calculate residual topography in oceans by removing the cooling model (Crosby and McKenzie, 2009) from observed bathymetry after accounting for the isostatic loading due to sediments. Crosby and McKenzie (2009) determine residual ocean topography by removing age-predicated topography from sediment unloaded observations of present day topography. Steinberger (2007) computes residual topography by removing the topography due to ocean floor cooling and the topography isostatically compensated in the crust (assuming CRUST1.0 (Laske et al., 2013)) from actual topography. Kaban et al. (2003) calculate global residual topography by removing the isostatic effects of the crust and oceanic lithosphere thermal mass anomalies from the present day observed topography. The Kaban et al. (2003) residual topography model is filtered using a low pass filter and expanded in spherical harmonics to degree 12.

The global models suggest that residual topography is the result of two main sources: density variation in the upper mantle and normal stresses at the base of the lithosphere due to mantle flow. They also propose that residual topography is the surface expression of sub-lithospheric swells and downwellings. In general, similar methodologies are used by the different global models to measure residual topography; however, the corrections applied differ significantly. Flament et al. (2013) define residual topography as the topography remaining after the isostatic contribution from the sediments, ice, crust and lithosphere are removed. They calculate residual topography by removing the average continental elevation (529m calculated from ETOPO1 (Amante and Eakins, 2009)) from continents, and in the oceans the cooling model (Crosby and McKenzie, 2009) is removed from the observed bathymetry after accounting for the isostatic loading due to sediments (from Divins (2003)). Crosby and McKenzie (2009) determine residual ocean topography as the topography, which remains after removing age-predicated topography from sediment unloaded observations of present day topography. Their determined residual topography reflects changes in crustal basement thickness and mantle dynamic topography. The Crosby and McKenzie (2009) global model of residual topography excludes areas where the sediment thickness is more than 1.5km thick. It also excludes flexural moats, subduction zones and areas of thickened crust. Steinberger (2007) computes residual topography by removing the topography due to ocean floor cooling and the topography isostatically compensated in the crust (assuming CRUST1.0 (Laske et al., 2013)) from actual topography. Kaban et al. (2003) calculate global residual topography by removing the isostatic compensation masses produced by the crustal density structure, and the oceanic lithosphere thermal mass anomaly from present day observed topography.

A comparison of these four published residual topography models (Figure 5.2) shows that they are in broad agreement. The Flament et al. (2013), Crosby and McKenzie (2009) and Steinberger (2007) models all show unfiltered residual topography, whist the Kaban et al.

(2003) model shows residual topography, which has been filtered using a low-pass filter, tapered for wavelengths between 2000m and 5000m, and has been expanded in spherical harmonics to degree 12. At a global scale these models all show the same general areas of uplift and subsidence; however, the magnitude varies between the models and at a regional scale it is clear that there are differences in the amplitude and polarity of the residual topography predictions.

5.2. Residual Topography along the IAM9 Profile

In this section, we present our detailed RDA analysis methodology used to measure residual topography; we use the Iberian Abyssal Plain as the case example to describe the methodology in detail.

The Iberian rifted continental margin is the result of polyphase rifting of the North American and Iberian plates, during the Late Triassic to Early Cretaceous (Péron-Pinvidic et al., 2007). The Iberian Abyssal Plain Figure 5.1(a) is part of the north western non-volcanic Iberian rifted continental margin (Chian et al., 1999), located to the south-west of Galicia Bank, and is considered to be a 'type' example of a sediment-starved magma-poor rifted continental margin. RDA analysis and gravity anomaly inversion are focussed along the seismic profile IAM9 (A-A') (Dean et al., 2000).

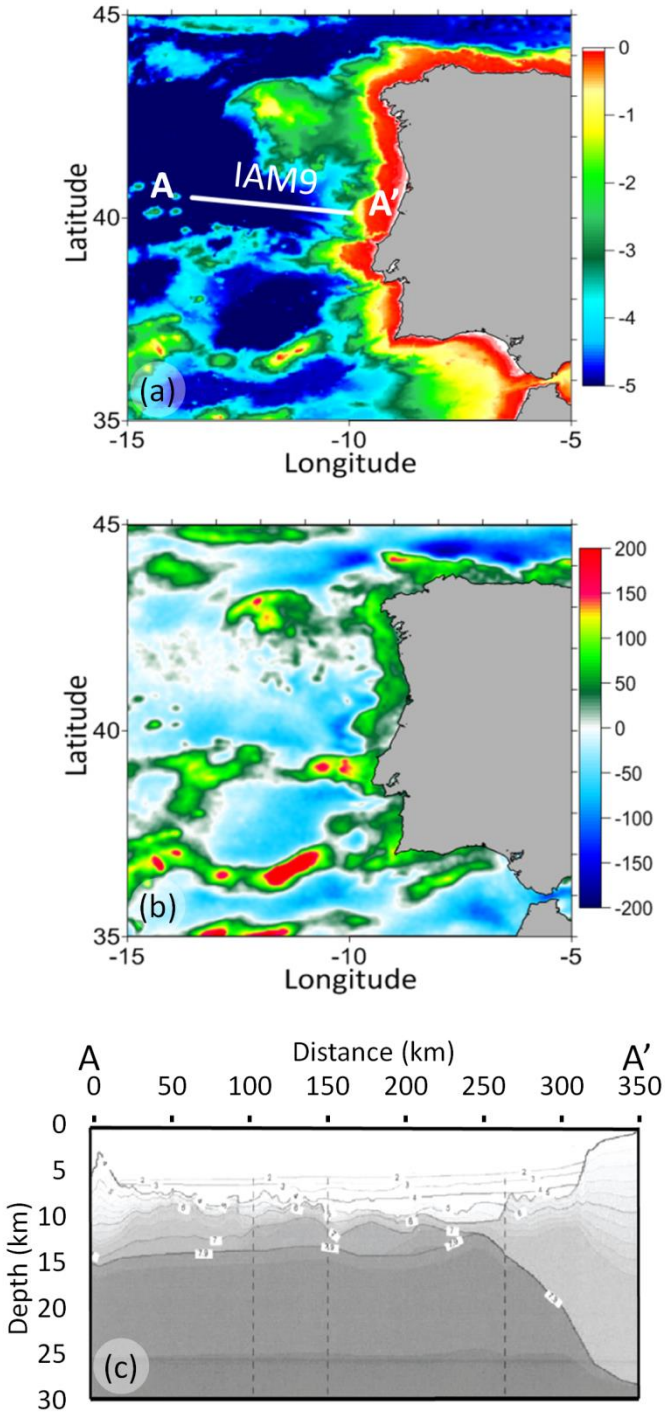

Figure 5.3 – Data used in the RDA analysis and the gravity anomaly inversion for the Iberian Abyssal Plain; (a) bathymetry (Amante and Eakins 2009); (b) free air gravity (Sandwell and Smith 2009); (c) wide angle seismic data adapted from Dean et al. (2000), from which we use 2D bathymetry and sediment thickness**.**

5.2.1. Residual Depth Anomaly along the IAM9 Profile

The RDA analysis technique is used to measure the magnitude of the residual topography in the ocean continent transition (OCT) of the rifted continental margin. The data used in the RDA analysis for the Iberian Abyssal Plain are bathymetry and 2D sediment thickness data (Figure 5.3(c)) from wide angle seismic data (Dean et al., 2000) and ocean age isochrons (Müller et al., 1997). A RDA for oceanic crust is calculated by comparing observed (b_{obs}) and age predicted ($b_{predicted}$) oceanic bathymetries in order to identify anomalous oceanic bathymetry.

$$RDA = b_{obs} - b_{predicted} \quad (1)$$

Age predicted bathymetric anomalies have been calculated using the thermal plate model predictions from Crosby and McKenzie (2009). Sensitivities to the thermal plate model predictions from Parsons and Sclater (1977) and Stein and Stein (1992) have also been examined (Supplementary Figure S5.1); RDA results computed using these different thermal plate model predictions do not vary significantly. Calculation of the age predicted bathymetry is dependent on the oceanic lithosphere age, as shown in equations 2 and 3, from Crosby and McKenzie (2009).

$$b_{predicted} = 2680 + 315t^{1/2} \qquad t < 75My \quad (2)$$

$$b_{predicted} = 5820 - 2500\exp(-0.025t) \qquad t > 75My \quad (3)$$

where t is oceanic lithosphere age. The age of breakup for the Iberian margin is often considered to be at the Aptian-Albian boundary, 112Ma (Péron-Pinvidic et al., 2007), whereas others consider an older breakup age of 126Ma, (Manatschal, 2004; Russell and Whitmarsh, 2003). Both these ages are greater than 75My, so age predicted bathymetry is calculated using equation 3.

5.2.2. Sediment Corrected Residual Depth Anomaly along the IAM9 Profile

RDAs have been calculated using sediment corrected bathymetry from flexural backstripping. Present day bathymetry is corrected for sediment loading using flexural backstripping and decompaction (Kusznir et al., 1995), which comprises the removal of the sedimentary load, allowing for the flexural isostatic response and decompaction of the remaining sediments. Flexural backstripping and decompaction assumes shaly-sand compaction and density parameters during the removal of the sedimentary layer. Figure 5.4(b) shows the comparison of the uncorrected and the sediment corrected RDAs along profile IAM9 (Figure 5.4(a)), correcting for the effect of sediment loading results in a larger negative RDA at the western end of the profile. The sediment corrected RDA along the western end of the IAM9 profile (Figure 5.4(b)) is negative with a magnitude between -1000m and -1500m implying either the presence of crust that is thinner than 7km, or anomalous subsidence at the margin.

The flexural backstripping process calculates the flexural isostatic response of the removed layer of sediments; within this calculation the effective elastic thickness (Te) is considered. For syn-rift extensional settings, Te's between 1.5km and 5km have been determined (Roberts et al., 1998). The Te depends on the bending stresses applied to the plate, the rate of stress application, the lithosphere composition and the geothermal gradient (Kusznir and Karner, 1985). The sensitivity to Te is shown for the sediment corrected RDA results along IAM9 (Figure 5.4(c)). Sensitivities to Te's of 1.5km, 5km and 10km have been examined, and Te of 1.5km has been used due to the negligible difference in the magnitude of the sediment corrected RDAs.

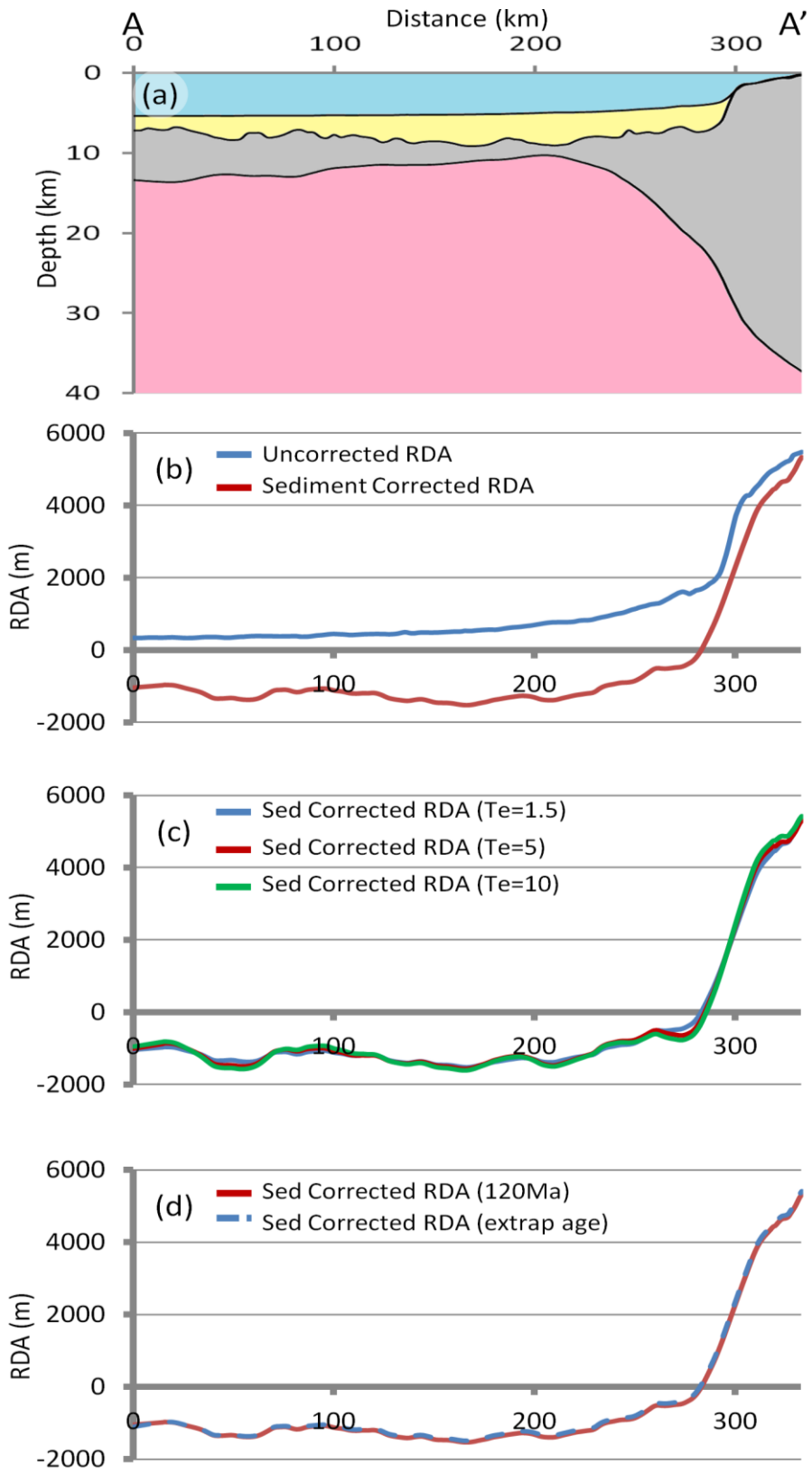

Figure 5.4 – (a) Crustal cross section along profile IAM9. (b) Comparison of uncorrected RDA results with the sediment corrected RDA results along IAM9. (c) Sensitivities to the effective elastic thickness (Te) for the sediment corrected RDA results have been examined. Te's of 1.5km, 5km and 10km produce sediment corrected RDAs of similar magnitude. (d) The sensitivity to oceanic lithospheric age for sediment corrected RDA results has been examined using two approaches: (i) a constant value of 120Ma for the profile and (ii) Müller et al. (2008) age isochrons with their age gradient extrapolated inboard.

As previously mentioned, age predicted oceanic bathymetries used to calculate the sediment corrected RDA are dependent on the oceanic lithospheric age. As the Müller (2008) global ocean age isochrons do not extend the entire length of profile IAM9, it is necessary to consider sensitivities to oceanic lithospheric age within the RDA calculations. Two approaches have been examined: the first uses a constant value of 120Ma for the profile, whilst the second uses Müller et al. (2008) age isochrons with their age gradient extrapolated inboard. The sensitivity of the sediment corrected RDA results to ocean age isochrons is shown in Figure 5.4(d), both approaches produce similar results.

5.2.3. Crustal Basement Thickness from Gravity Anomaly Inversion along the IAM9 Profile

Crustal basement thickness and Moho depth have been determined using gravity anomaly inversion, in order to correct the RDA for crustal thickness departures from the oceanic mean of 7km (White et al., 1992). The gravity anomaly inversion technique is described in Chappell and Kusznir (2008) and Greenhalgh and Kusznir (2007), and has been applied in Cowie and Kusznir (2012) and Alvey et al. (2008). The data used within the gravity anomaly inversion are bathymetry (Amante and Eakins, 2009) (Figure 5.3(a)), free air gravity (Sandwell and Smith, 2009) (Figure 5.3(b)), sediment thickness from the IAM9 wide angle seismic data of Dean et al. (2000) (Figure 5.3(c)) and ocean age isochrons (Müller et al., 2008).

The gravity anomaly inversion is carried out in the 3D spectral domain, using the scheme of Parker (1972). Gravity anomaly inversion results are dependent on the age of oceanic lithosphere and continental breakup due to the inclusion of the lithosphere thermal gravity anomaly correction. The lithosphere thermal gravity anomaly correction is required to compensate for the negative gravity anomaly component and the elevated geothermal gradient arising from oceanic and rifted continental margin lithosphere. Failure to include

this correction can lead to predictions of Moho depth and crustal basement thicknesses at rifted margins, which are substantially too great.

The thickness of the crustal magmatic addition is estimated using the parameterisation of the decompression melting model of White and McKenzie (1989), from the continental lithosphere thinning factor (*γ)* determined from gravity anomaly inversion, where

$$\gamma = 1 - \frac{1}{\beta} \quad (4)$$

This parameterisation of decompression melting is described in detail in Chappell & Kusznir (2008). For the Iberian Abyssal Plain we have examined sensitivities to both a 'normal' magmatic and a magma-poor solution; the effect of varying the magmatic addition will not change the gravity anomaly inversion predicted crustal basement thickness for this breakup age. For the Iberian Abyssal Plain we use a magma-poor solution, where no magmatic addition to the crust is generated.

The reference Moho depth is an important parameter used within the gravity anomaly inversion that requires careful consideration and calibration (Cowie and Kusznir, 2012). The long wavelength components of the free air gravity anomaly are not controlled by crustal or lithospheric structure, but by deep mantle processes, and as a consequence, the reference Moho depth varies globally. The gravity anomaly inversion calculates Moho topography, which needs to be referenced to a Moho depth datum. In order to constrain reference Moho depth, predicted Moho depths determined from gravity anomaly inversion need to be calibrated against seismic Moho depths. The gravity anomaly inversion assumes a crustal basement density of 2850kgm^{-3} (Carlson and Herrick, 1990; Christensen and Mooney, 1995) and a mantle density of 3300kgm^{-3} , sensitivities to these values have been examined. The sediment densities used within the gravity anomaly inversion increase with depth, assuming normal compaction corresponding to a shaly-sand lithology.

Moho depths predicted from gravity anomaly inversion along the IAM9 profile have been calibrated against seismic observations of Moho depth from the wide angle seismic data of Dean et al. (2000) (Figure 5.5(a)). Sensitivities to reference Moho depths of 35km, 37.5km, 40km and 42.5km have been examined and are shown on the crustal cross section along profile IAM9, Figure 5.5(b). Calibration shows a reference Moho depth of 41km Figure 5.5(c) is required in order to predict crustal basement thicknesses consistent with those seen in the wide angle seismic data.

The crustal cross section along profile IAM9 (Figure 5.6(a)), has been constructed using bathymetry and 2D sediment thickness data (Dean et al., 2000), with the gravity anomaly inversion predicted crustal basement thicknesses and Moho depths assuming the calibrated reference Moho depth of 41km. The cross section shows the distribution of oceanic and thinned continental crust, and highlights the OCT structure of the Iberian Abyssal Plain rifted continental margin. At the western end of the profile oceanic crust, between 5km and 7km in thickness, is predicted. This crust thins further to approximately 1km in the central section of the profile.

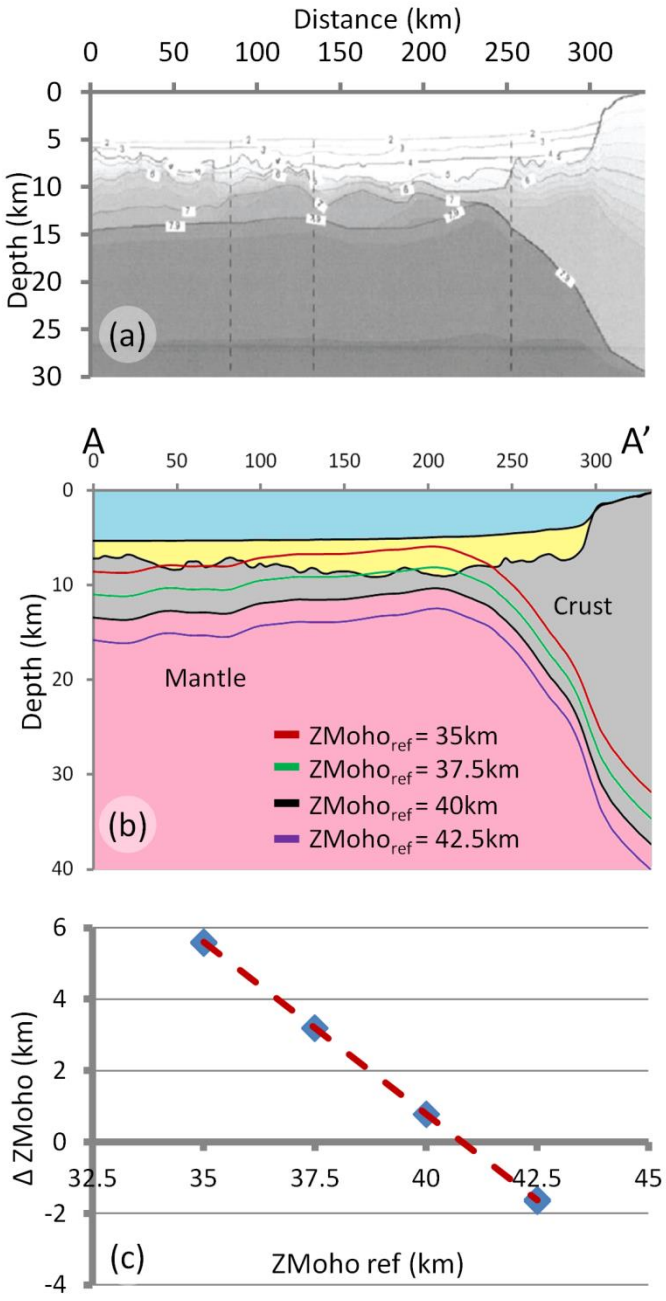

Figure 5.5 – Calibration of the reference Moho depth used in the gravity anomaly inversion along profile IAM9 in the Iberian Abyssal Plain. (a) Moho depths in the oceanic domain from wide angle seismic data adapted from Dean et al. (2000). (b) Moho depths predicted from gravity anomaly inversion have been calculated using reference Moho depths of 35km, 37.5km, 40km and 42.5km. (c) Calibration of the reference Moho depth for profile IAM9 shows that a reference Moho depth of 41km is required.

5.2.4. Predicted RDA from Crustal Thickness Variations (RDACT) along the IAM9 Profile

The RDA component from crustal basement thickness variations (RDA_{CT}) (Figure 5.6(b)) is determined using the difference between the gravity anomaly inversion predicted crustal basement thickness (tc_{grav}) and the average global oceanic crustal basement thickness (tc_{ref}), together with Airy isostasy. The local isostatic response to variations in gravity inverted non-continental crustal thickness, from the 7km global average oceanic crustal thickness (tc_{ref}) is given by:

$$RDA_{CT} = \frac{(tc_{ref} - tc_{grav})(\rho_m - \rho_c)}{(\rho_m - \rho_{infill})} \quad (5)$$

where ρ_m is the density of the mantle (3300kgm^{-3}), ρ_c is the density of the crust (2850kgm^{-3}) and ρ_{infill} is the density of the water infill (1000kgm^{-3}). 7km thick crust will have a corresponding RDA_{CT} of zero. A positive RDA_{CT} reflects crust that is thicker than 7km, whereas if the RDA_{CT} is negative, this corresponds to crust that is thinner than 7km or the presence of exhumed mantle. At the western end of the IAM9 profile the RDA_{CT} is negative and ranges between zero and -800m, consistent with the presence of thinned crust or exhumed mantle.

5.2.5. Residual Topography Measurements from RDA Analysis

In order to determine the magnitude of residual topography, and also determine whether the Iberian Abyssal Plain is experiencing uplift or subsidence, a ΔRDA corresponding to the sediment corrected RDA further corrected for variations in crustal basement thickness has been calculated (Figure 5.6(c)):

$$\Delta RDA = Sediment\ corrected\ RDA\ -\ RDA_{CT} \quad (6)$$

If both the sediment corrected RDA and the RDA_{CT} are the same magnitude (i.e. ΔRDA=0) this corresponds to no residual topography at the margin. If the ΔRDA is positive this indicates uplift, whereas a negative ΔRDA implies subsidence at the margin. At the western end of the IAM9 profile, the ΔRDA (Figure 5.6(c)) is negative, showing approximately -650m of residual topography, implying that there is anomalous present day subsidence affecting the Iberian Abyssal Plain.

5.2.6. Locating the Continent Ocean Boundary

As the RDA results are only valid for the oceanic domain, it is necessary to determine the COB location along the profile. We have used changes in the RDA signal and crustal basement thicknesses to identify the different crustal domains along profile, and hence locate the COB. In oceanic regions the sediment corrected RDA and the RDA_{CT} signal will be constant and near zero, however, for regions of thicker crust it is expected that the RDA signals will show a positive trend. The dashed line on Figure 5.6 indicates the COB and the start of 'normal' oceanic crust. Whilst this interface between oceanic crust and thinned continental crust is shown as a sharp line, in reality it is likely to be a transitional boundary. Consideration of the RDA results on the continental side of the COB is beyond the scope of this study.

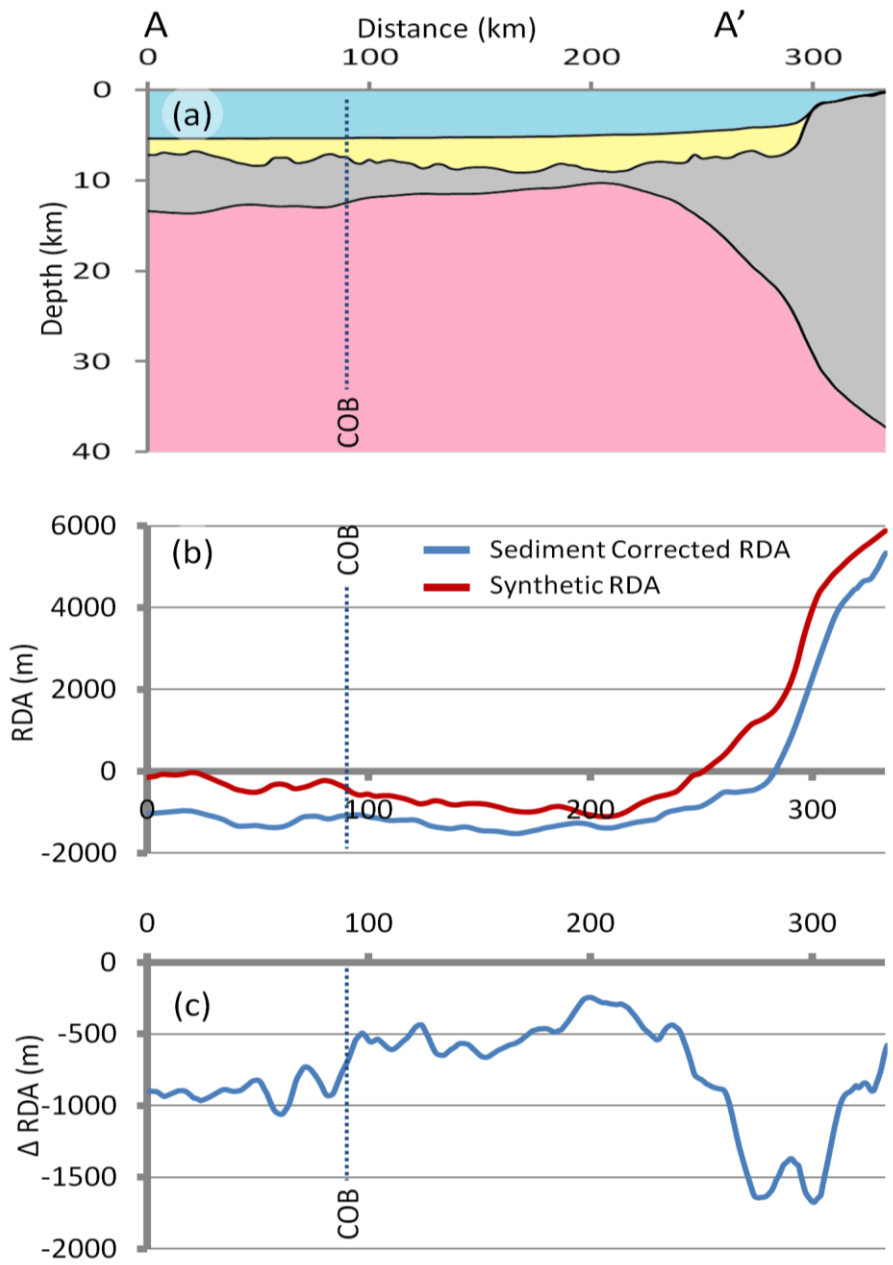

Figure 5.6 – (a) Crustal cross section along the IAM9 profile. (b) Sediment corrected RDA and the RDA component from crustal thickness variations (RDA_{CT}) along the IAM9 profile. The sediment corrected RDA and the RDA_{CT} are both negative; the sediment corrected RDA ranges between -1500m and -1000m, whereas the RDA_{CT} ranges between -500m and zero. (c) The negative sediment corrected RDA, further corrected for variations in crustal basement thickness (ΔRDA), implies mantle dynamic subsidence.

5.3. Residual Topography along the L11 Profile in the Gulf of Aden

The Gulf of Aden is an active young oblique rift system (D'Acremont et al., 2005; Leroy et al., 2010) at the southernmost tip of the Arabian plate, and separates Saudi Arabia to the north from Somalia in the south. Seafloor spreading in the Gulf of Aden began at 17.6Ma in the eastern part of the Gulf of Aden (D'Acremont et al., 2006; Fournier et al., 2004; Leroy et al., 2010; Lucazeau et al., 2008), whilst extension began much earlier at 35Ma (Watchorn et al., 1998).

RDA analysis is focussed along the seismic profile L11 (B-B') (Leroy et al., 2010) along the Omani margin of the eastern Gulf of Aden as shown in Figure 5.1(b). The data used in the RDA analysis are bathymetry and 2D sediment thickness data from seismic reflection data along profile L11 (Leroy et al., 2010) (Figure 5.7(c)). As the Gulf of Aden is a young rifted margin and breakup occurred at 17.6Ma, RDA calculations have been computed using equation 2. Ocean age isochrons from Leroy et al. (2010) for the Gulf of Aden extend along the full length of profile L11 and are well constrained. Sensitivities to Te including 1.5km, 5km and 10km, have been examined (Figure 5.8(b)), and as Te's of 1.5km, 5km and 10km all produce sediment corrected RDAs of a similar magnitude, we have used a Te of 1.5km. The sediment corrected RDA (Figure 5.8(b)) for the oceanic region of the L11 profile is positive, approximately +500m, which indicates either the presence of crust that is thicker than 7km or anomalous uplift.

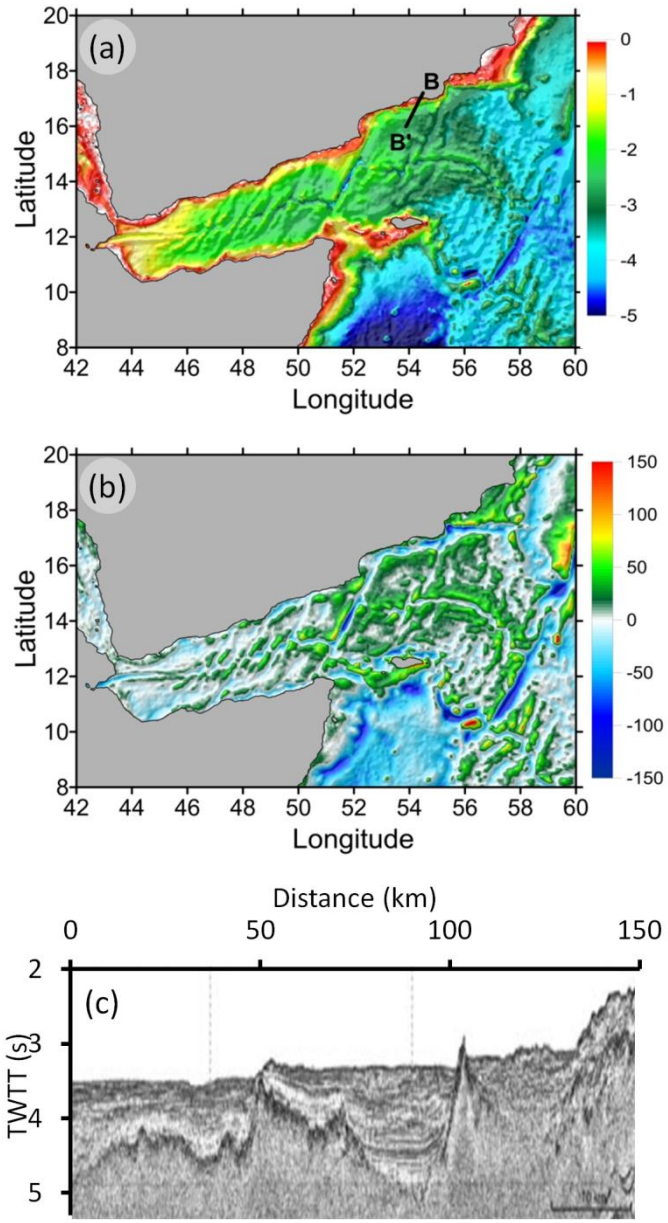

Figure 5.7 – Data used in the RDA analysis and the gravity anomaly inversion for the Gulf of Aden; (a) bathymetry (Amante and Eakins 2009); (b) free air gravity (Sandwell and Smith 2009); (c) seismic reflection data adapted from Leroy et al. (2010), from which we use 2D bathymetry and sediment thickness.

Crustal basement thicknesses and Moho depths along profile L11 (Figure 5.8(a)) have been determined from gravity anomaly inversion, and are used to correct the RDA for variations in crustal basement thickness from the oceanic mean. The data used within the gravity anomaly inversion are bathymetry (Amante and Eakins, 2009) (Figure 5.7(a)), free air gravity (Sandwell and Smith, 2009) (Figure 5.7(b)), 2D sediment thickness data from seismic reflection data (Leroy et al., 2010) (Figure 5.7(c)) and ocean age isochrons (Leroy et al., 2010). The Moho depths predicted from gravity anomaly inversion along the L11 profile have been calibrated against seismic refraction observations of Moho depth (Leroy et al., 2010) (Figure 5.9(a)). Sensitivities to reference Moho depths of 32.5km, 35km, 37.5km, 40km and 42.5km have been examined along profile L11 and are shown in Figure 5.9(b). The crustal cross section along the L11 profile (Figure 5.10(a)), has been constructed using the calibrated reference Moho depth of 38.5km (Figure 5.9(c)) and predicts crustal basement thicknesses of approximately 7km in the oceanic domain of the Gulf of Aden. Within the gravity anomaly inversion, sensitivities to magmatic addition, including 'normal' magmatic and magma-rich solutions, have been examined; a 'normal' magmatic solution is preferred.

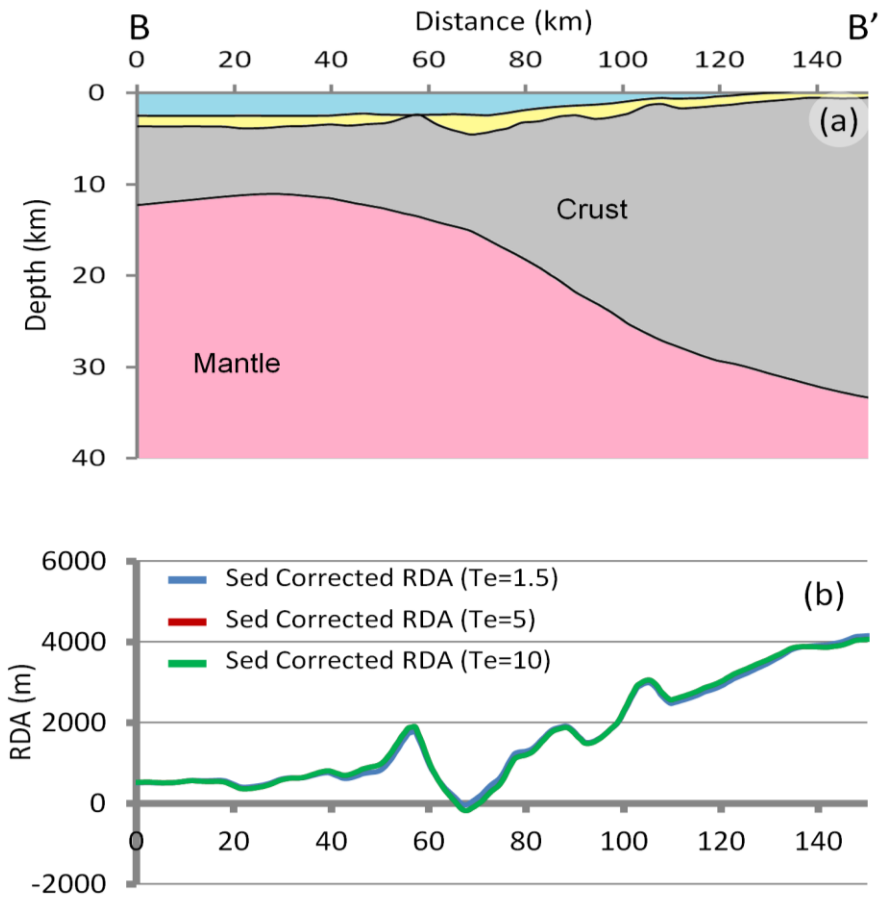

Figure 5.8 – (a) Crustal cross section along profile L11. (b) Sensitivity to the effective elastic thickness for the Gulf of Aden sediment corrected RDA results has been examined. Te's of 1.5km, 5km and 10km produce sediment corrected RDAs of similar magnitude.

The RDA_{CT} (Figure 5.10(b)) has also been computed along profile L11 in order to determine whether there is any anomalously thick or thin crust in the oceanic domain. The RDA_{CT} is approximately zero in the oceanic domain of the L11 profile, corresponding to crustal basement thicknesses of approximately 7km, as predicted from the gravity anomaly inversion.

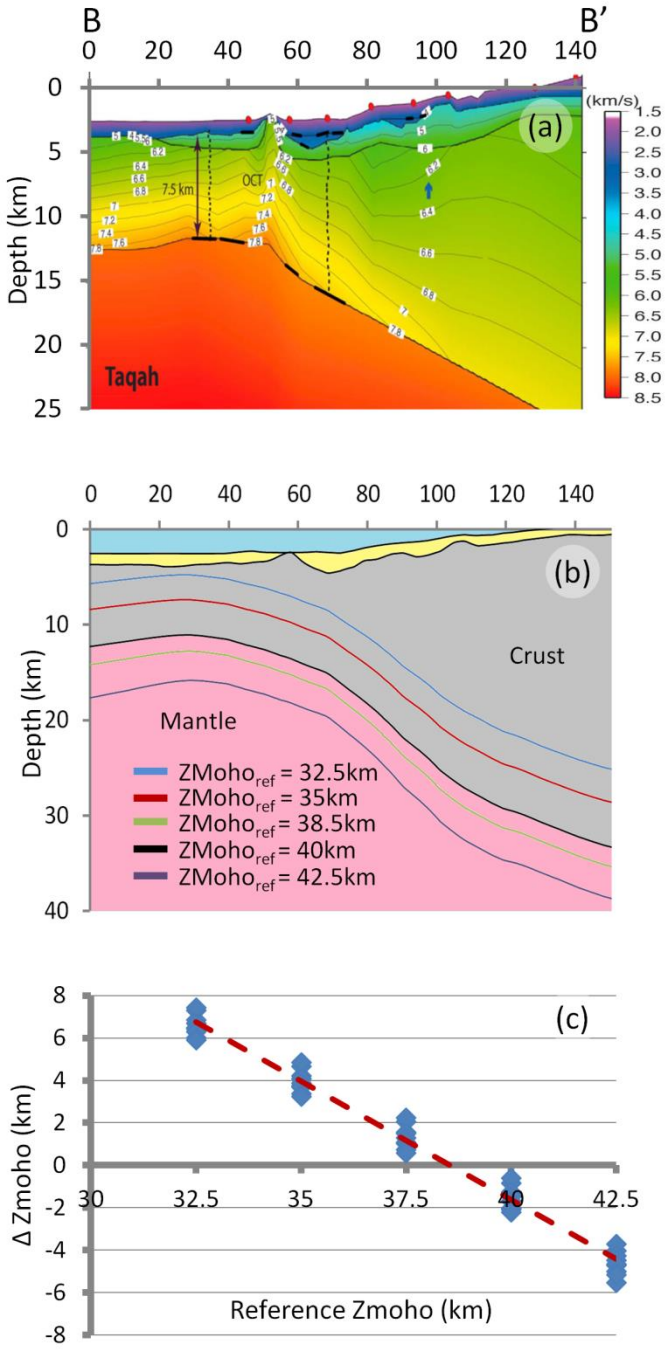

Figure 5.9 – Calibration of the reference Moho depth used in the gravity anomaly inversion along profile L11 in the Gulf of Aden. (a) Moho depths in the oceanic domain from the seismic refraction profile of Leroy et al. (2010). (b) Gravity anomaly inversion predicted Moho depths have been calculated using reference Moho depths of 32.5km, 35km, 37.5km, 40km and 42.5km. (c) Calibration of the reference Moho depth for profile L11 shows that a reference Moho depth of 38.5km is required.

The sediment corrected RDA further corrected for variations in crustal basement thickness (ΔRDA) is positive (Figure 5.10(c)). The ΔRDA shows approximately +400m of residual topography in the oceanic domain of the L11 profile, implying anomalous present day uplift.

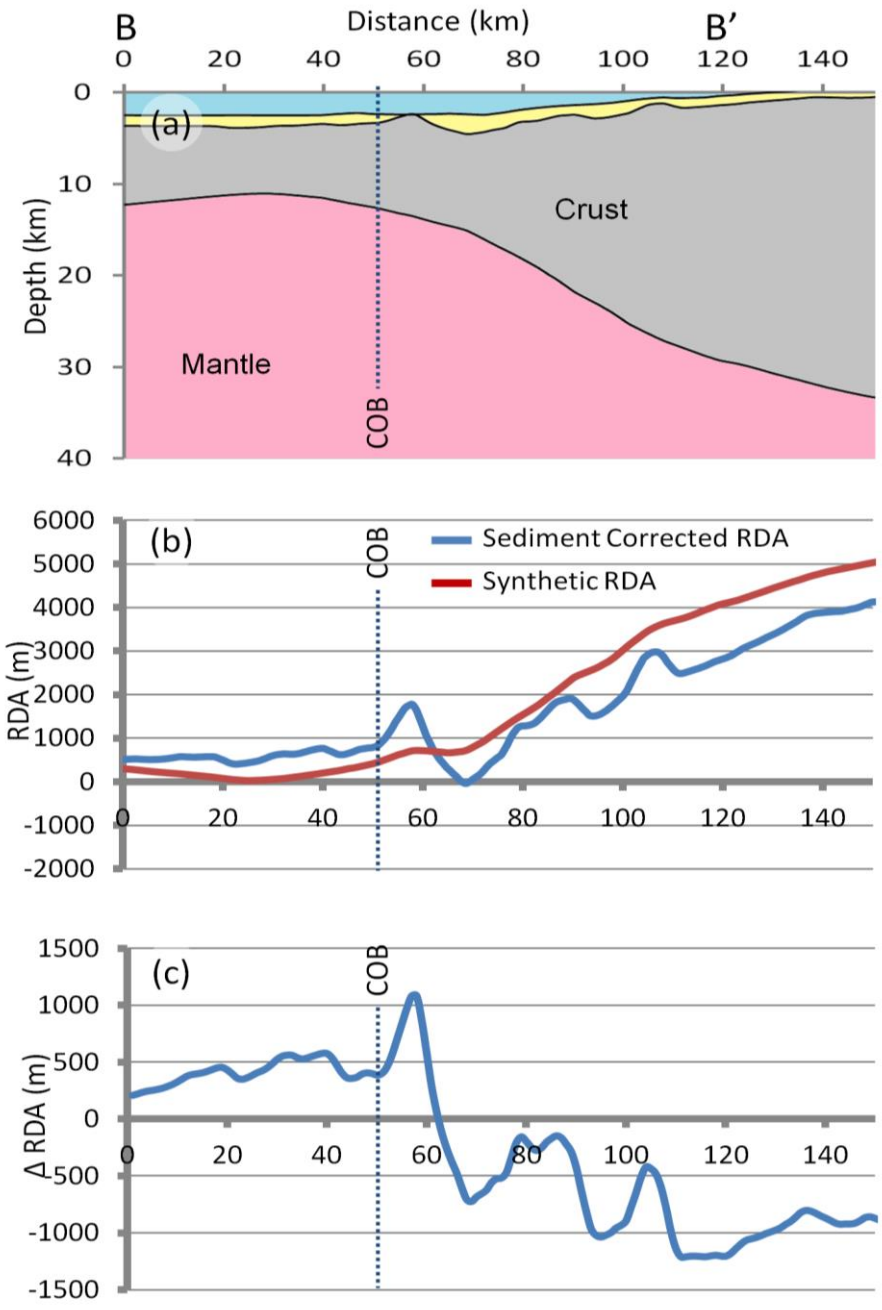

Figure 5.10 – (a) Crustal cross section along the L11 profile. (b) Sediment corrected RDA and the RDA component from crustal thickness variations (RDA_{CT}) along the L11 profile. In the oceanic domain the sediment corrected RDA is positive (+750m), whilst the RDA_{CT} is zero. (c) The sediment corrected RDA, further corrected for variations in crustal basement thickness (ΔRDA) is +400m, which implies mantle dynamic uplift.

In addition to the L11 profile, there are two further profiles (L02 and L13 locations indicated in Figure 5.1(b)), which have seismic refraction data showing Moho depths. We have applied the RDA analysis and gravity anomaly inversion methodologies to both these profiles in order to further constrain the residual topography measurements in the Gulf of Aden. However, the L02 profile spans over a volcano and therefore results from this profile are not reliable and are not discussed within this paper. Although the L11 profile is the focus profile for the Gulf of Aden section of this study, the L13 profile could have been used as an alternative. The L13 and L11 profiles are separated by approximately 40km. RDA analysis measures +450m of residual topography along the L13 profile (Supplementary Figure S5.2), which is of a similar magnitude to the residual topography measured along the L11 profile (+400m). The reference Moho depths also vary slightly between the two profiles; the calibrated reference Moho depth for the L11 profile (as discussed earlier) is 38.5km, whilst the calibrated reference Moho depth for the L13 profile is 39.5km.

5.4. Residual Topography along the Northern Angolan Margin

Our final case study is of the Kwanza region, offshore northern Angola (Figure 5.1(c)). The northern Angolan rifted continental margin is the result of continental rifting and breakup between South America and Africa (Contrucci et al., 2004; Unternehr et al., 2010), with the main rift episode and the transition to seafloor spreading occurring at approximately 110Ma (Moulin et al., 2005). The northern Angolan rifted continental margin has been extensively explored by the hydrocarbon industry; however, the geodynamics and evolution of this margin are still poorly understood due to the presence of thick sediments and mobile Aptian salt sequences, which have made deep seismic imaging in this region difficult.

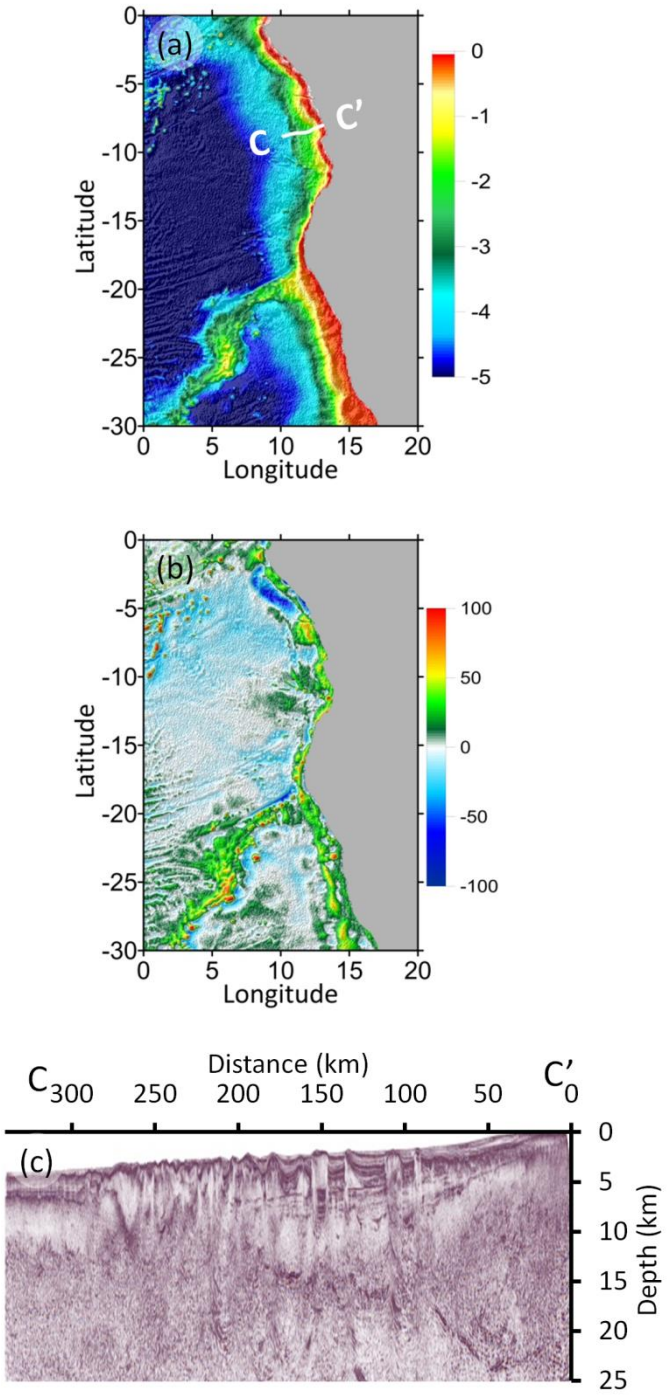

Figure 5.11 – Data used in the RDA analysis and the gravity anomaly inversion for the northern Angolan margin; (a) bathymetry (Amante and Eakins 2009); (b) free air gravity (Sandwell and Smith 2009); (c) ION-GXT CS1-2400 seismic profile, from which we use 2D bathymetry and sediment thickness.

RDA analysis is focussed along the CS1-2400 seismic profile, provided by ION-GXT. The data used in the RDA analysis are bathymetry and 2D sediment thickness data from the CS1-2400 profile as shown in Figure 5.11(c). The breakup ages proposed for the northern Angolan margin (i.e. from Berriasian to early Albian (140Ma to 110 Ma) (Teisserenc and Villemin, 1989)) are greater than 75My; therefore RDA calculations have been computed using equation 3. We have used 110Ma as the age of breakup, after Moulin (2005).

It has been necessary to consider sensitivities to oceanic lithospheric age along the CS1-2400 profile Figure 5.12(a), as the Müller (2008) global ocean age isochrons do not extend the entire length of the profile. As with the Iberian Abyssal Plain profile, two approaches have been examined: the first uses a constant value of 110Ma for the profile, whilst the second uses Müller et al. (2008) age isochrons with their age gradient extrapolated inboard. A comparison and sensitivity of the sediment corrected RDA results to ocean age isochrons is shown in Figure 5.12(b), and both approaches produce similar results.

Sensitivities to Te, for the sediment corrected RDA, have also been examined and are shown in Figure 5.12(c). Similarly to the Iberian Abyssal Plain and the Gulf of Aden, sediment corrected RDAs have been calculated using Te's of 1.5km, 5km and 10km. There is a noticeable variation between the sediment corrected RDA results when considering the different values of Te. Te's of 5km and 10km produce sediment corrected RDAs of similar magnitude, whereas a Te of 1.5km increases the sediment corrected RDA results beneath the thick salt in the central section of the profile. For consistency with the Iberian Abyssal Plain and the Gulf of Aden margins we have used a Te of 1.5km for the CS1-2400 profile. At the western end of the CS1-2400 profile the sediment corrected RDA ranges between zero and +300m (Figure 5.12(c)), implying either the presence of crust that is thicker than 7km or anomalous uplift.

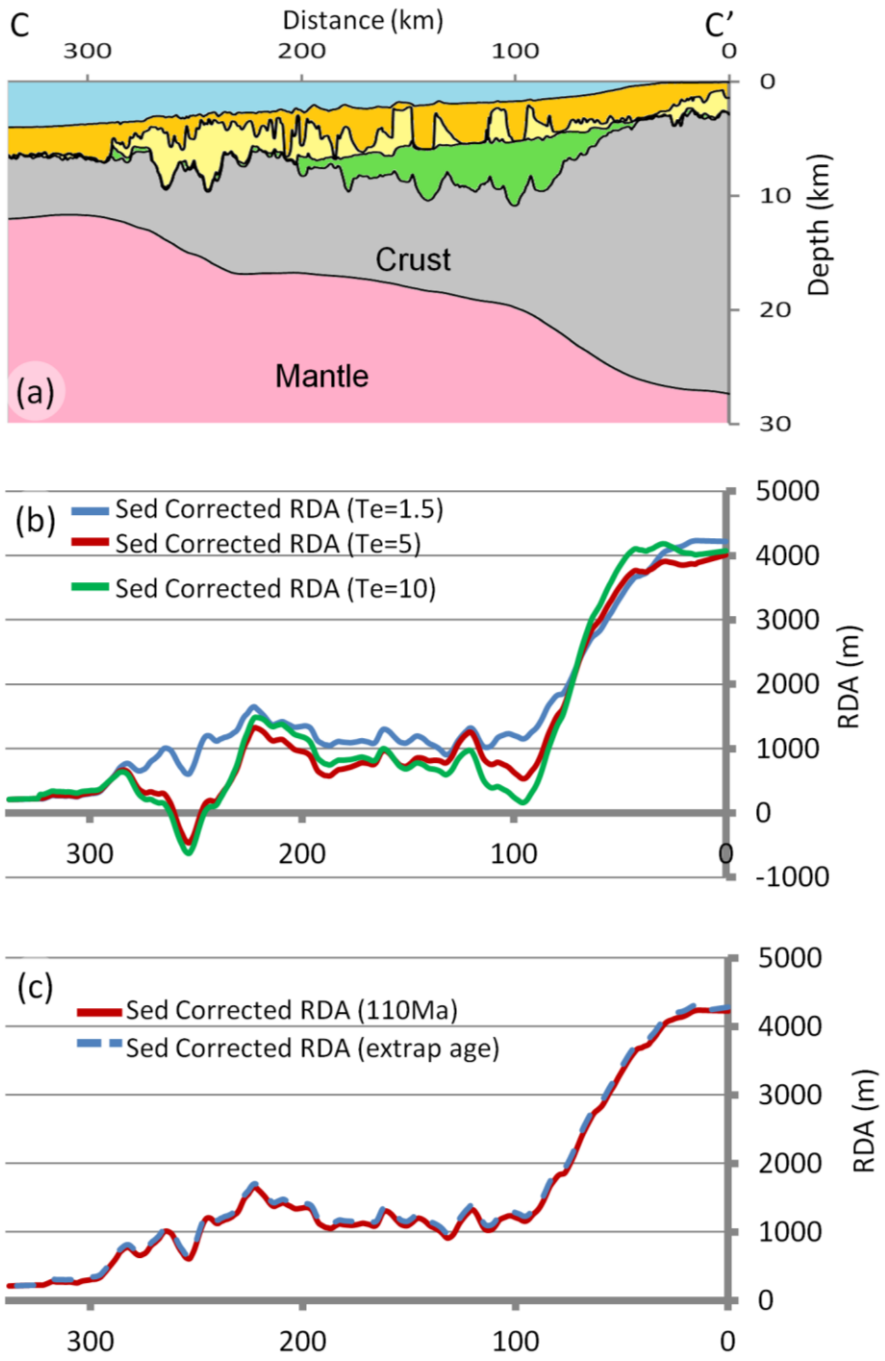

Figure 5.12 – (a) Crustal cross section along the CS1-2400 profile. (b) Sensitivities to the effective elastic thickness (Te) for the sediment corrected RDA results have been examined. Te of 5km and 10km produce sediment corrected RDAs of similar magnitude, whereas a Te of 1.5km produces smaller sediment corrected RDAs, particularly beneath the thick salt. (c) The sensitivity to oceanic lithospheric age for sediment corrected RDA results has been examined using two approaches: (i) a constant value of 110Ma for the profile and (ii) Müller et al. (2008) age isochrons with their age gradient extrapolated inboard.

Crustal basement thicknesses and Moho depths have been determined using gravity anomaly inversion along the CS1-2400 profile Figure 5.14(a). The crustal basement thicknesses are used to correct the RDA for crustal thickness departures from the oceanic mean. The data used within the gravity anomaly inversion are bathymetry (Amante and Eakins, 2009) (Figure 5.11(a)), free air gravity (Sandwell and Smith, 2009) (Figure 5.11(b)), 2D sediment thickness data from the CS1-2400 profile (Figure 5.11(c)) and ocean age isochrons (Müller et al., 2008). Sensitivities to reference Moho depths of 32.5km, 35km, 37.5km and 40km have been examined and are shown in Figure 5.13(b). The crustal cross section along the CS1-2400 profile has been constructed using the calibrated reference Moho depth of 35.5km (Figure 5.13(c)); crustal basement thicknesses of 6km are predicted at the western end of the CS1-2400 profile (Figure 5.14(a)). Within the gravity anomaly inversion sensitivities to magmatic addition including magma-poor and 'normal' magmatic solutions have been examined. For the northern Angolan rifted continental margin a 'normal' magmatic solution is preferred.

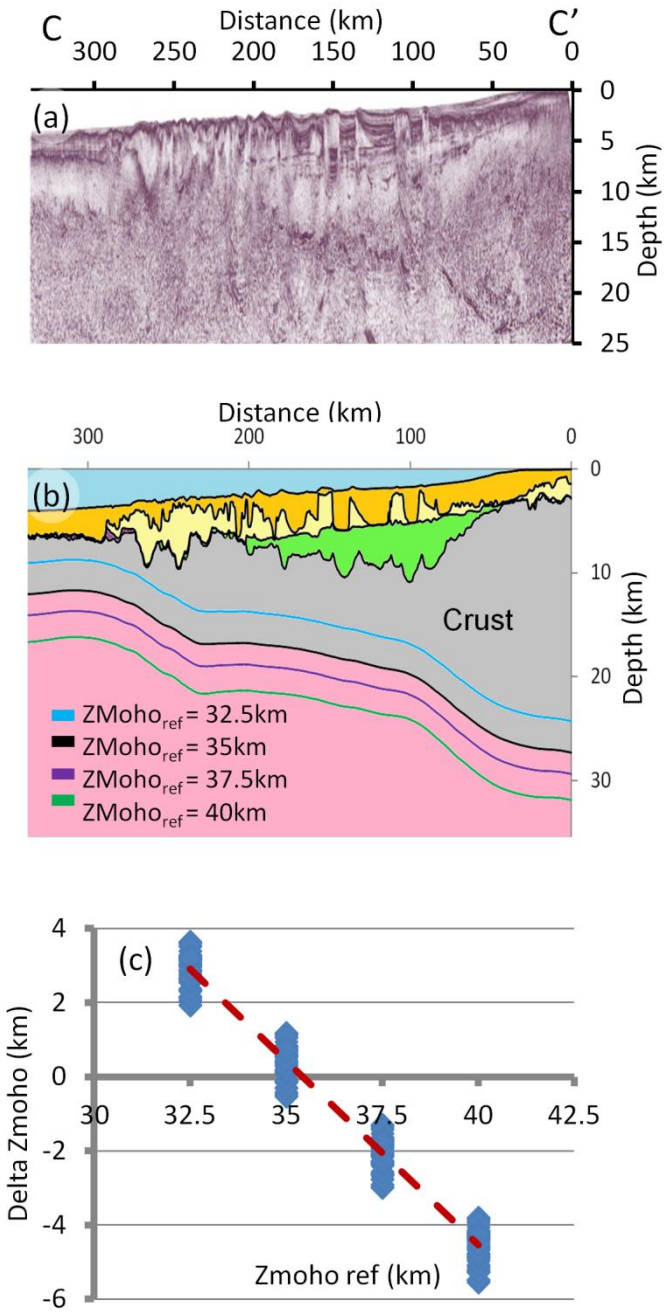

Figure 5.13 – Calibration of the reference Moho depth used in the gravity anomaly inversion along the CS1-2400 profile in northern Angola. (a) Moho depths in the oceanic domain from the ION-GXT deep long offset seismic reflection CS1-2400 profile. (b) Gravity anomaly inversion predicted Moho depths have been calculated using reference Moho depths of 32.5km, 35km, 37.5km and 40km. (c) Calibration of the reference Moho depth for northern Angola shows that a reference Moho depth of 35.5km is required.

The RDA_{CT} in the oceanic domain of the CS1-2400 profile is negative and ranges between -400m and -100m (Figure 5.14(b)), corresponding to crust that is thinner than 7km or the presence of exhumed mantle.

The sediment corrected RDA, further corrected for variations in crustal basement thickness (ΔRDA) (Figure 5.14(c)) is positive; approximately +700m in the oceanic domain. The positive ΔRDA implies that there is anomalous present day uplift.

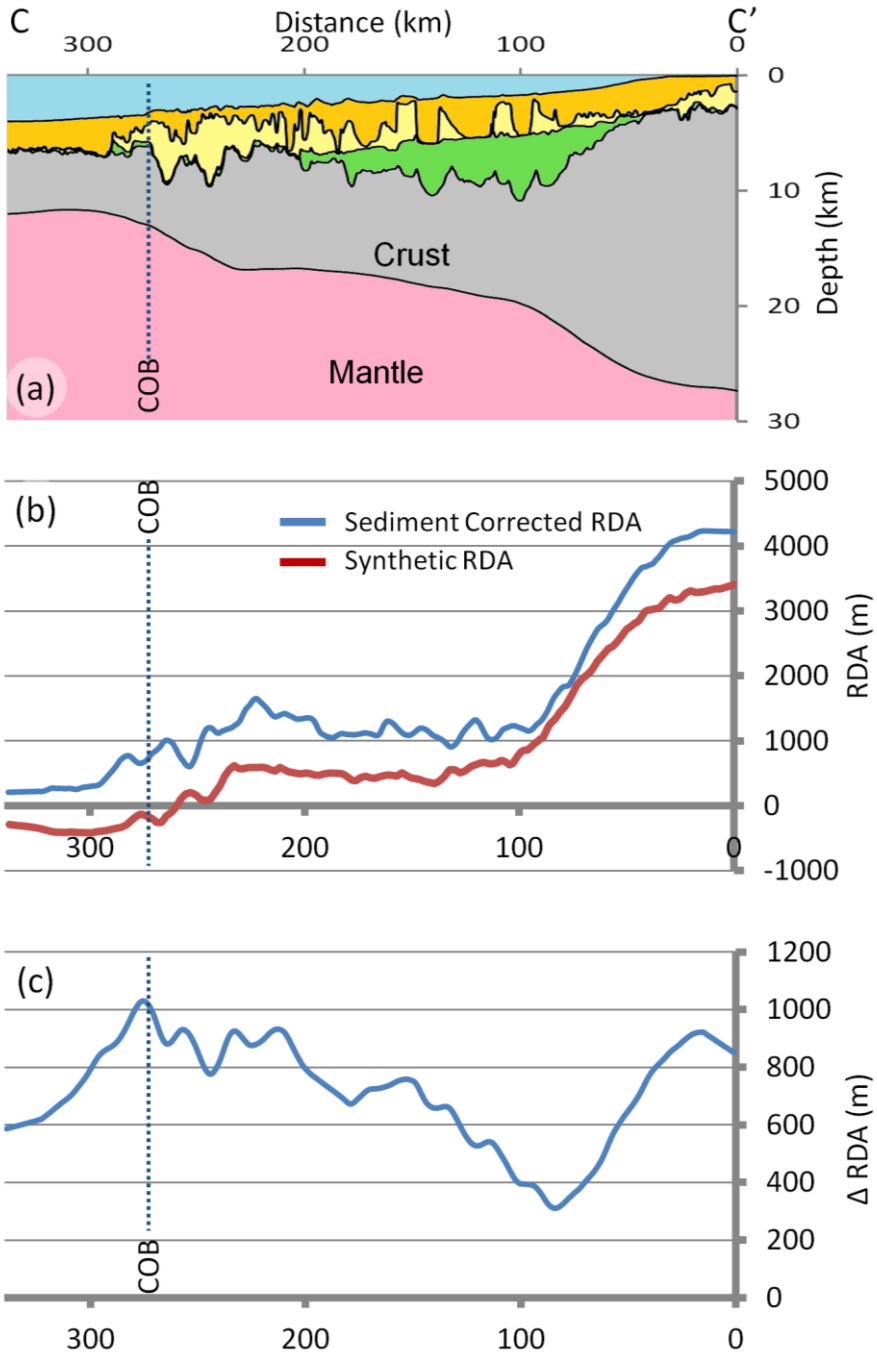

Figure 5.14 – (a) Crustal cross section along the CS1-2400 profile. (b) Sediment corrected RDA and the RDA component from crustal thickness variations (RDA_{CT}) along the CS1-2400 profile. In the oceanic domain the sediment corrected RDA is zero, whilst the RDA_{CT} is negative (-500m). (c) The sediment corrected RDA, further corrected for variations in crustal basement thickness (ΔRDA) averages +700m, which implies mantle dynamic uplift.

5.5. Comparison of Residual Topography Measurements from 2D RDA Analysis with Extracts from Global Models

The RDA analysis technique corrects for the effect of sediment loading and crustal basement thickness variations, and has been used to determine the magnitude of residual topography (either subsidence or uplift) along 2D profiles at the Iberian, Gulf of Aden and northern Angolan rifted continental margins.

A regional scale comparison of residual topography measurements from our 2D RDA analysis with extracts from global residual topography models (Crosby and McKenzie, 2009; Flament et al., 2013; Kaban et al., 2003; Steinberger, 2007) is discussed in this section. The regional residual topography from global models for the Iberian Abyssal Plain, the Gulf of Aden and the northern Angolan rifted continental margins are shown in Figure 5.15. We also compare residual topography extracts from these global models to our residual topography measurements from RDA analysis along 2D profiles (Figure 5.16). The range and average residual topography measurements in the oceanic domains of each profile are summarised in Table 5.1.

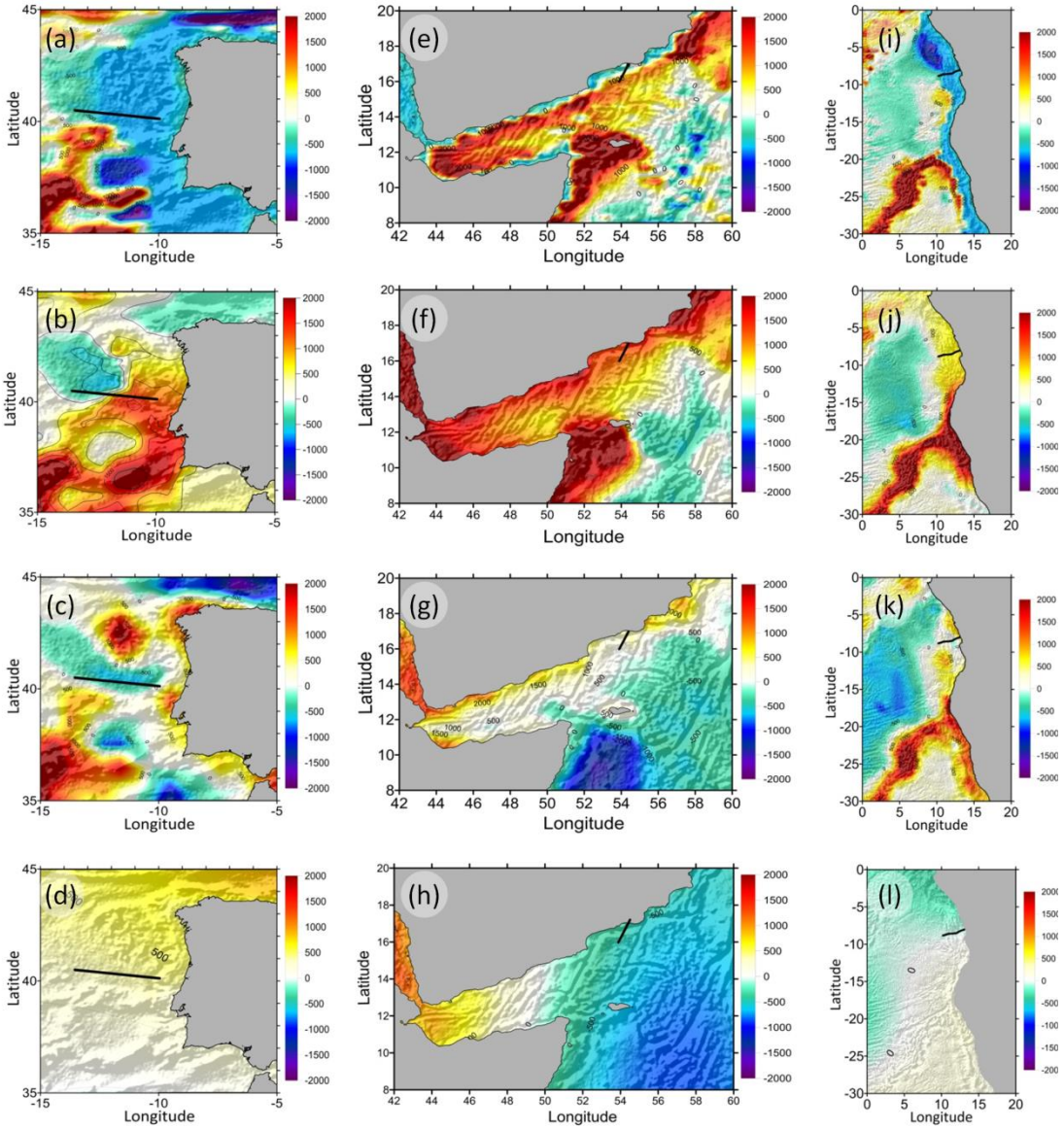

Figure 5.15 – Comparison of the global residual topography models focussing on the Iberian Abyssal Plain, the Gulf of Aden and the northern Angolan margins. (a), (e) and (i) use the Flament et al. (2013) global model; (b), (f) and (j) use the Crosby and McKenzie (2009) global model; (c), (g) and (k) use the Steinberger (2007) global model and (d), (h) and (l) use the Kaban et al. (2003) global model.

Location:		ΔRDA results	Residual Topography (Flament et al. 2013)	Residual Topography (Kaban et al. 2003)	Residual Topography (Steinberger 2007)	Residual Topography (Crosby and McKenzie 2009)
Iberian abyssal plain	Range:	-300m to -1000m	-395m to -695m	+350m to +370m	-120m to -545m	-325m to -470m
	Average:	-650m	-545m	+360m	-330m	-400m
Gulf of Aden	Range:	+220m to +580m	+1250m to +310m	-430m to -470m	+425m to +1030m	+1180m to +1290m
	Average:	+400m	+780m	-450m	+730m	+1235m
Northern Angola	Range:	+500m to +900m	-320m to -690m	-50m to -70m	+190m to +200m	+590m to +750m
	Average:	+700m	-505m	-60m	+195m	+670m

Table 5.1 – A comparison of the range and average residual topography measurements from RDA analysis and extracts from global residual topography models (Crosby and McKenzie, 2009; Flament et al., 2013; Kaban et al., 2003; Steinberger, 2007) for the three profiles considered; IAM9 for the Iberian Abyssal Plain, L11 in the Gulf of Aden and CS1-2400 for the northern Angolan rifted continental margin.

Iberian Abyssal Plain

Our residual topography measurements from RDA analysis predict approximately -650m of subsidence (Figure 5.16(a)) along the IAM9 profile at the Iberian Abyssal Plain. The global residual topography models of Flament et al. (2013), Crosby and McKenzie (2009) and Steinberger (2007) (Figures 5.15(a), (b) and (c) respectively) are in agreement with our residual topography measurements from RDA analysis and predict anomalous subsidence. However, the Kaban et al. (2003) model (Figure 5.15(d)) predicts anomalous uplift for this region. The extracted residual topography measurements from the global models are shown in Figure 5.16(a). In the oceanic domain of the IAM9 profile, all the extracted residual topography measurements from the global models plot above our residual topography measurements, suggesting that we measure more subsidence than the global models.

Gulf of Aden

In the Gulf of Aden, the global residual topography models of Flament et al. (2013), Crosby and McKenzie (2009), Steinberger (2007) and Kaban et al. (2003) show, to some degree, a transition from uplift in the west to subsidence in the east (Figure 5.15 (e), (f), (g) and (h)); this is most evident in the Kaban et al. (2003) global model (Figure 5.15(h)). The Flament et al. (2013) global residual topography model also shows a sharp north-south gradient along the Omani margin, with subsidence at the coast, changing to uplift further outboard. This change in polarity of the residual topography occurs over a distance less than 100km.

Our residual topography measurements from RDA analysis predict residual topography of approximately +400m (Figure 5.16(b)), corresponding to uplift along the L11 profile. Along the L11 profile, the global residual topography models of Flament et al. (2013), Crosby and McKenzie (2009) and Steinberger (2007) (Figure 5.15 (e), (f), (g) and (h)) predict anomalous uplift in agreement with our measurements, whilst the Kaban et al. (2003) model predicts

anomalous subsidence (Figure 5.15(h)). The extracted residual topography measurements from the global models are shown in Figure 5.16(b). In the oceanic domain of the L11 profile (and the L13 profile (Supplementary Figure S5.2)) our residual topography measurements plot below those from Flament et al. (2013), Crosby and McKenzie (2009) and Steinberger (2007) suggesting that in the case of the Gulf of Aden, we measure less uplift than these global models. However, the extracted residual topography measurements from the Kaban et al. (2003) model plots below our residual topography measurements, suggesting that in this case we are measuring a greater amount of uplift.

Northern Angola

Our residual topography measurements from RDA analysis predict approximately +700m of uplift along the CS1-2400 profile. Along the northern Angolan rifted continental margin the residual topography predicted from the global models of Flament et al. (2013) (Figure 5.15(i)) and Kaban et al. (2003) (Figure 5.15(l)) predict anomalous subsidence, whilst Crosby and McKenzie (2009) (Figure 5.15(j)) and Steinberger (2007) (Figure 5.15(k)) predict anomalous uplift in agreement with our measurements. The extracted residual topography measurements from the global models are shown in Figure 5.16(c). In the oceanic domain of the CS1-2400 profile, all the extracted residual topography measurements from the global models plot below our residual topography measurements, this suggests that we measure more uplift than the global models.

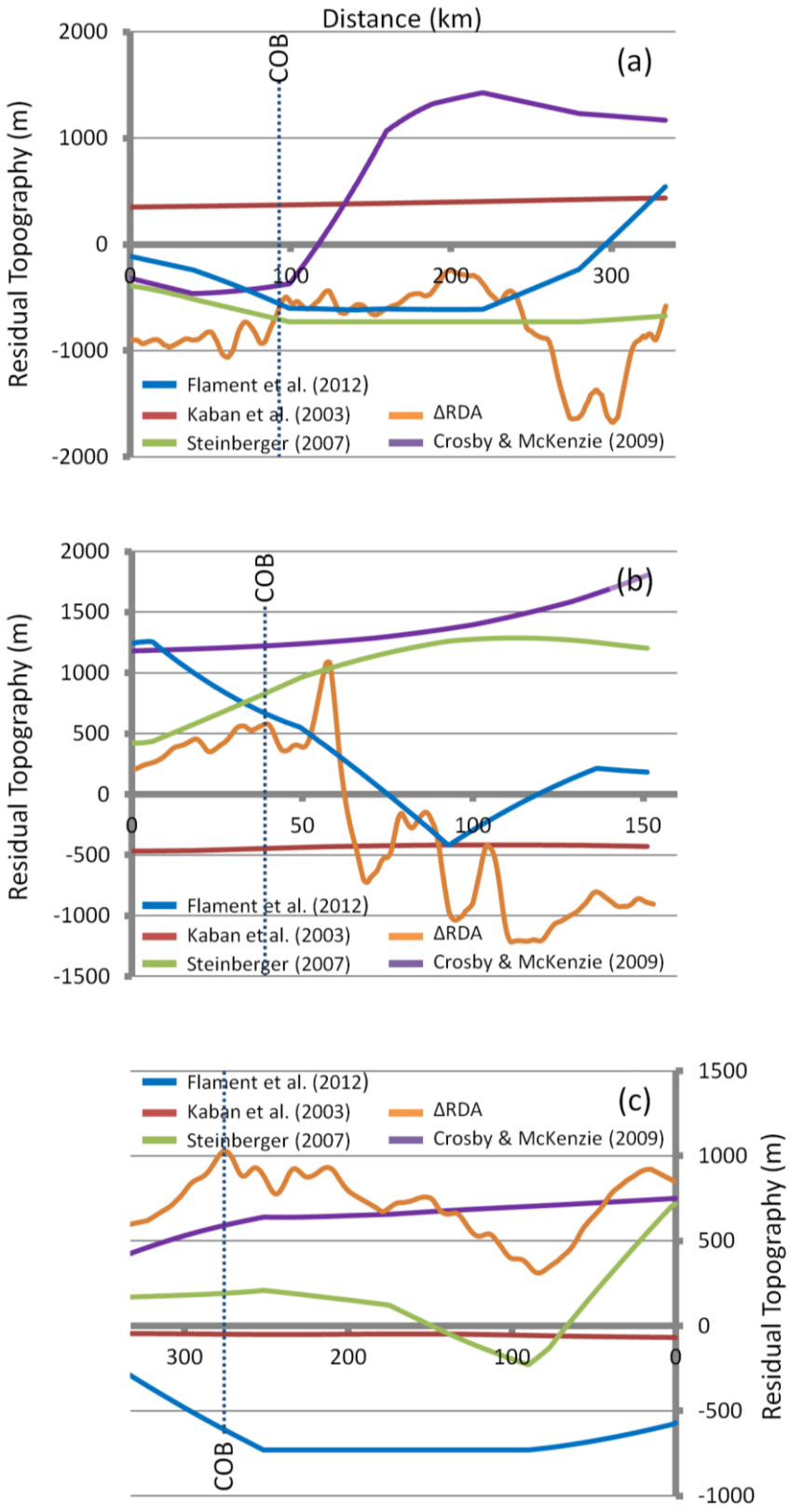

Figure 5.16 – Comparison of the residual topography measurements from the global models (Crosby and McKenzie, 2009; Flament et al., 2013; Kaban et al., 2003; Steinberger, 2007) with our calculated residual topography from ΔRDA for; (a) the Iberian Abyssal Plain along the IAM9 profile; (b) the Gulf of Aden along profile L11; (c) the northern Angolan margin along the ION-GXT CS1-2400 profile. The dashed line on each of these plots highlights the location of the COB.

5.6. Conclusion

The RDA analysis uses observational data including seismic reflection and refraction profiles to measure residual topography, and hence determine the magnitude of anomalous present day subsidence or uplift at rifted continental margins. Within the RDA analysis methodology, corrections to the observed topography for sediment loading, and crustal and thermal isostasy at a regional scale are made. The RDA analysis methodology is of global applicability and can be applied to any rifted continental margin, providing adequate observational data are available. The higher the quality of the observational data, the more precise the measurement of residual topography. Within this paper we have applied the RDA analysis to the Iberian Abyssal Plain, the Gulf of Aden and the northern Angolan rifted continental margins. Our measurements of residual topography in the oceanic domain, from RDA analysis, show that:

(i) at the Iberian Abyssal Plain we calculate between -300m and -1000m of anomalous present day subsidence, with an average of -650m;

(ii) in the Gulf of Aden we calculate between +220 and +580m of anomalous present day uplift, with an average of +400m,

(iii) and along the northern Angolan margin we calculate between +500 and +900m of anomalous present day uplift, with an average of +700m.

We have compared the global residual topography models from Flament et al. (2013), Crosby and McKenzie (2009), Steinberger (2007) and Kaban et al. (2003) to our measurements of residual topography from RDA analysis. At a regional scale these global models of residual topography show significant differences in the amplitude and polarity of the measured residual topography, however, these differences may be the result of the different methodologies used to determine the global models. At a regional scale, the Kaban et al.

(2003) model of residual topography shows little variation along profile and no real correlation with any of the other global residual topography models or with our measurements of residual topography from RDA analysis. These differences can probably be accounted for by the filtering that has been included within the Kaban et al. (2003) residual topography model.

The measurements of residual topography from RDA analysis corroborate the residual topography predictions from these models in some places, but appear to have a greater precision because they are applied to 2D regional profiles. In addition, this greater precision may be due to the corrections applied to account for sediment loading and variations in crustal basement thickness. The degree to which previously published models agree with our measurement of residual topography depends on which case study area we focus on.

(i) In the oceanic domain of the IAM9 profile, Iberian Abyssal Plain, the Crosby and McKenzie (2009) model shows the same general trend as that for the residual topography calculated from RDA analysis; however, the Crosby and McKenzie (2009) model calculates less subsidence than our RDA analysis.

(ii) In the oceanic domain of the L11 profile, Gulf of Aden, the Flament et al. (2013) model shows the same general trend and calculates a similar magnitude of uplift to that measured by RDA analysis.

(iii) In the oceanic domain of the CS1-2400 profile, northern Angolan margin, the Crosby and McKenzie (2009) model has the same general trend, but calculates less uplift that that calculated from RDA analysis.

5.7. References:

Allen, P. A., 1997, Earth Surface Processes, Hoboken, John Wiley & Sons, 404 p.:

Alvey, A., Gaina, C., Kusznir, N. J., and Torsvik, T. H., 2008, Integrated crustal thickness mapping and plate reconstructions for the high Arctic: Earth and Planetary Science Letters, v. 274, no. 3-4, p. 310-321.

Amante, C., and Eakins, B. W., 2009, ETOPO1 1 Arc-Minute Global Relief Model: Procedures, Data Sources and Analysis: NOAA Technical Memorandum NESDIS NGDC-24, p. 19.

Carlson, R. L., and Herrick, C. N., 1990, Densities and porosities in the oceanic crust and their variations with depth and age: Journal of Geophysical Research: Solid Earth, v. 95, no. B6, p. 9153-9170.

Chappell, A. R., and Kusznir, N. J., 2008, Three-dimensional gravity inversion for Moho depth at rifted continental margins incorporating a lithosphere thermal gravity anomaly correction: Geophysical Journal International, v. 174, no. 1, p. 1-13.

Chian, D., Louden, K. E., Minshull, T. A., and Whitmarsh, R. B., 1999, Deep structure of the ocean-continent transition in the southern Iberia Abyssal Plain from seismic refraction profiles: Ocean Drilling Program (Legs 149 and 173) transect: Journal of Geophysical Research: Solid Earth, v. 104, no. B4, p. 7443-7462.

Christensen, N. I., and Mooney, W. D., 1995, Seismic velocity structure and composition of the continental crust: A global view: Journal of Geophysical Research: Solid Earth, v. 100, no. B6, p. 9761-9788.

Contrucci, I., Matias, L., Moulin, M., Géli, L., Klingelhofer, F., Nouzé, H., Aslanian, D., Olivet, J.-L., Réhault, J.-P., and Sibuet, J.-C., 2004, Deep structure of the West African continental margin (Congo, Zaïre, Angola), between 5°S and 8°S, from reflection/refraction seismics and gravity data: Geophysical Journal International, v. 158, no. 2, p. 529-553.

Cowie, L., and Kusznir, N., 2012, Mapping crustal thickness and oceanic lithosphere distribution in the Eastern Mediterranean using gravity inversion: Petroleum Geoscience, v. 18, no. 4, p. 373-380.

Crosby, A. G., and McKenzie, D., 2009, An analysis of young ocean depth, gravity and global residual topography: Geophysical Journal International, v. 178, no. 3, p. 1198-1219.

Crosby, A. G., McKenzie, D., and Sclater, J. G., 2006, The relationship between depth, age and gravity in the oceans: Geophysical Journal International, v. 166, no. 2, p. 553-573.

D'Acremont, E., Leroy, S., Beslier, M.-O., Bellahsen, N., Fournier, M., Robin, C., Maia, M., and Gente, P., 2005, Structure and evolution of the eastern Gulf of Aden conjugate margins from seismic reflection data: Geophysical Journal International, v. 160, no. 3, p. 869-890.

D'Acremont, E., Leroy, S., Maia, M., Patriat, P., Beslier, M.-O., Bellahsen, N., Fournier, M., and Gente, P., 2006, Structure and evolution of the eastern Gulf of Aden: insights from magnetic and gravity data (Encens-Sheba MD117 cruise): Geophysical Journal International, v. 165, no. 3, p. 786-803.

Dean, S. M., Minshull, T. A., Whitmarsh, R. B., and Louden, K. E., 2000, Deep structure of the ocean-continent transition in the southern Iberia Abyssal Plain from seismic refraction profiles: The IAM-9 transect at 40°20'N: Journal of Geophysical Research: Solid Earth, v. 105, no. B3, p. 5859-5885.

Divins, D. L., 2003, Total Sediment Thickness of the World's Oceans & Marginal Seas, *in* Center, N. N. G. D., ed.: Boulder, CO.

Flament, N., Gurnis, M., and Müller, R. D., 2013, A review of observations and models of dynamic topography: Lithosphere, v. 5, no. 2, p. 189-210.

Fournier, M., Bellahsen, N., Fabbri, O., and Gunnell, Y., 2004, Oblique rifting and segmentation of the NE Gulf of Aden passive margin: Geochem. Geophys. Geosyst., v. 5, no. 11, p. Q11005.

Greenhalgh, E. E., and Kusznir, N. J., 2007, Evidence for thin oceanic crust on the extinct Aegir Ridge, Norwegian Basin, NE Atlantic derived from satellite gravity inversion: Geophysical Research Letters, v. 34, no. 6, p. L06305.

Kaban, M. K., Schwintzer, P., Artemieva, I. M., and Mooney, W. D., 2003, Density of the continental roots: compositional and thermal contributions: Earth and Planetary Science Letters, v. 209, no. 1–2, p. 53-69.

Kusznir, N., and Karner, G., 1985, Dependence of the flexural rigidity of the continental lithosphere on rheology and temperature: Nature, v. 316, no. 6024, p. 138-142.

Kusznir, N. J., Roberts, A. M., and Morley, C. K., 1995, Forward and reverse modelling of rift basin formation: Geological Society, London, Special Publications, v. 80, no. 1, p. 33-56.

Laske, G., Masters., G., Ma, Z., and Pasyanos, M., 2013, Update on CRUST1.0 - A 1-degree Global Model of Earth's Crust: Geophys. Res. Abstracts, v. 15.

Leroy, S., Lucazeau, F., d'Acremont, E., Watremez, L., Autin, J., Rouzo, S., Bellahsen, N., Tiberi, C., Ebinger, C., Beslier, M.-O., Perrot, J., Razin, P., Rolandone, F., Sloan, H., Stuart, G., Al Lazki, A., Al-Toubi, K., Bache, F., Bonneville, A., Goutorbe, B., Huchon, P., Unternehr, P., and Khanbari, K., 2010, Contrasted styles of rifting in the eastern Gulf of Aden: A combined wide-

angle, multichannel seismic, and heat flow survey: Geochem. Geophys. Geosyst., v. 11, no. 7, p. Q07004.

Lithgow-Bertelloni, C., and Silver, P. G., 1998, Dynamic topography, plate driving forces and the African superswell: Nature, v. 395, no. 6699, p. 269 - 272.

Lucazeau, F., Leroy, S., Bonneville, A., Goutorbe, B., Rolandone, F., d'Acremont, E., Watremez, L., Düsünur, D., Tuchais, P., Huchon, P., Bellahsen, N., and Al-Toubi, K., 2008, Persistent thermal activity at the Eastern Gulf of Aden after continental break-up: Nature Geoscience, v. 1, no. 12, p. 854-858.

Manatschal, G., 2004, New models for evolution of magma-poor rifted margins based on a review of data and concepts from West Iberia and the Alps: International Journal of Earth Sciences, v. 93, no. 3.

Moulin, M., Aslanian, D., Olivet, J.-L., Contrucci, I., Matias, L., Géli, L., Klingelhoefer, F., Nouzé, H., Réhault, J.-P., and Unternehr, P., 2005, Geological constraints on the evolution of the Angolan margin based on reflection and refraction seismic data (ZaïAngo project): Geophysical Journal International, v. 162, no. 3, p. 793-810.

Müller, R. D., Roest, W. R., Royer, J.-Y., Gahagan, L. M., and Sclater, J. G., 1997, Digital isochrons of the world's ocean floor: Journal of Geophysical Research, v. 102, no. B2, p. 3211-3214.

Müller, R. D., Sdrolias, M., Gaina, C., Steinberger, B., and Heine, C., 2008, Long-Term Sea-Level Fluctuations Driven by Ocean Basin Dynamics: Science, v. 319, no. 5868, p. 1357-1362.

Parker, R. L., 1972, The Rapid Calculation of Potential Anomalies: Geophysical Journal of the Royal Astronomical Society, v. 31, no. 4, p. 447-455.

Parsons, B., and Sclater, J. G., 1977, An Analysis of the Variation of Ocean Floor Bathymetry and Heat Flow with Age: Journal of Geophysical Research, v. 82, no. 5, p. 803-827.

Péron-Pinvidic, G., Manatschal, G., Minshull, T. A., and Sawyer, D. S., 2007, Tectonosedimentary evolution of the deep Iberia-Newfoundland margins: Evidence for a complex breakup history: Tectonics, v. 26, no. 2, p. TC2011.

Roberts, A. M., Kusznir, N. J., Yielding, G., and Styles, P., 1998, 2D flexural backstripping of extensional basins; the need for a sideways glance: Petroleum Geoscience, v. 4, no. 4, p. 327-338.

Russell, S. M., and Whitmarsh, R. B., 2003, Magmatism at the west Iberia non-volcanic rifted continental margin: evidence from analyses of magnetic anomalies: Geophysical Journal International, v. 154, no. 3, p. 706-730.

Sandwell, D. T., and Smith, W. H. F., 2009, Global marine gravity from retracked Geosat and ERS-1 altimetry: Ridge segmentation versus spreading rate: J. Geophys. Res., v. B01411, no. 114(B1).

Stein, C. A., and Stein, S., 1992, A model for the global variation in oceanic depth and heat flow with lithospheric age: Nature, v. 359, no. 6391, p. 123-129.

Steinberger, B., 2007, Effects of latent heat release at phase boundaries on flow in the Earth's mantle, phase boundary topography and dynamic topography at the Earth's surface: Physics of the Earth and Planetary Interiors, v. 164, no. 1–2, p. 2-20.

Teisserenc, P., and Villemin, J., 1989, Sedimentary basin of Gabon – geology and oil systems, *in* Edwards, J. D., and Santogrossi, P. A., eds., Divergent / Passive Margin Basins. Memoir of the American Association of Petroleum Geologists, Volume 48.

Unternehr, P., Péron-Pinvidic, G., Manatschal, G., and Sutra, E., 2010, Hyper-extended crust in the South Atlantic: in search of a model: Petroleum Geoscience, v. 16, no. 3, p. 207-215.

Watchorn, F., Nichols, G. J., and Bosence, D. W. J., 1998, Rift-related sedimentation and stratigraphy, southern Yemen (Gulf of Aden), *in* Purser, B., and Bosence, D. J., eds., Sedimentation and Tectonics in Rift Basins Red Sea:- Gulf of Aden, Springer Netherlands, p. 165-189.

White, R., and McKenzie, D., 1989, Magmatism at Rift Zones: The Generation of Volcanic Continental Margins and Flood Basalts: Journal of Geophysical Research, v. 94, no. B6, p. 7685-7729.

White, R. S., McKenzie, D., and O'Nions, R. K., 1992, Oceanic Crustal Thickness From Seismic Measurements and Rare Earth Element Inversions: Journal of Geophysical Research, v. 97, no. B13, p. 19683-19715.

5.8. Supplementary Figures

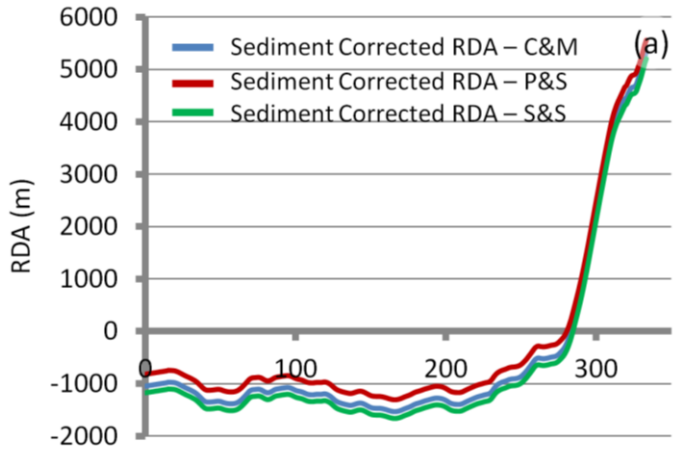

Supplementary Figure S5.1 – Sensitivities to the thermal plate model predictions from Crosby and McKenzie (2009) (C&M), Parsons and Sclater (1977) (P&S) and Stein and Stein (1992) (S&S) for the sediment corrected RDA results have been examined. There is little variation between the three models. The thermal plate model from Crosby and McKenzie (2009) is our preferred model within this paper. For the associated RDA equations see Supplementary Table S5.1.

Thermal Plate Model	RDA equations	Age
Crosby and McKenzie (2009)	$b_{predicted} = 2680 + 315t^{1/2}$	t < 75My
	$b_{predicted} = 5820 - 2500\exp(-0.025t)$	t ≥ 75My
Parsons and Sclater (1977)	$b_{predicted} = 2500 + 350t^{1/2}$	t < 70My
	$b_{predicted} = 6400 - 3200\exp(-0.0159t)$	t ≥ 70My
Stein and Stein (1992)	$b_{predicted} = 2600 + 365t^{1/2}$	t < 20My
	$b_{predicted} = 5651 - 2473\exp(-0.0278t)$	t ≥ 20My

Supplementary Table S5.1 – RDA equations from the thermal plate model solutions of Crosby and McKenzie (2009), Parsons and Sclater (1977) and Stein and Stein (1992).

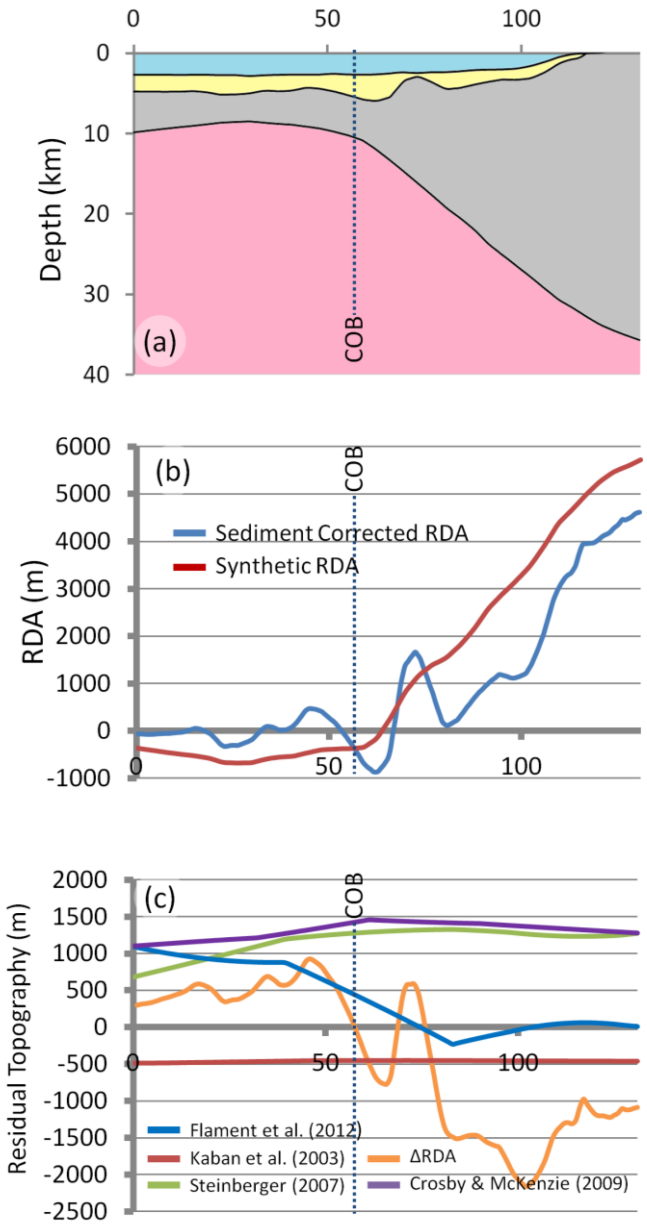

Supplementary Figure S5.2 – (a) Crustal cross section along the L13 profile. (b) Sediment corrected RDA and the RDA component from crustal thickness variations (RDA_{CT}) along the L11 profile. In the oceanic domain the sediment corrected RDA is approximately zero, whilst the RDA_{CT} is -500m. (c) Comparison of the residual topography measurements from the global models (Crosby and McKenzie, 2009; Flament et al., 2013; Kaban et al., 2003; Steinberger, 2007) with our calculated residual topography from ΔRDA for the L13 profile.

Chapter 6

6. Discussion and Summary

6.1. Introduction

The principle aim of this PhD thesis was the development of a suite of integrated quantitative analysis techniques to determine ocean continent transition (OCT) structure, continent ocean boundary (COB) location and magmatic type at rifted continental margins. The suite of integrated quantitative analysis techniques comprise:

(i) the determination of crustal basement thickness and Moho depth from gravity anomaly inversion,

(ii) the determination and analysis of residual depth anomalies (RDAs) corrected for sediment loading and crustal basement thickness variations,

(iii) the determination of continental lithosphere thinning from gravity anomaly inversion and subsidence analysis,

(iv) and the analysis of the lateral variations in basement density and seismic velocity along profiles, determined using the joint inversion of deep seismic reflection and gravity anomaly data.

These techniques have been used individually to investigate OCT structure, COB location and magmatic type. However, the integrated use of all the techniques together is a new approach, which provides a more robust geological interpretation of the OCT structure, COB location and magmatic type at rifted continental margins.

The second aim was the application of the integrated quantitative analysis methodologies to the offshore Iberia (Iberian Abyssal Plain and Galicia bank), northern Angolan, south-eastern Brazilian and the Gulf of Aden rifted continental margins. These case study areas have a large amount of observational data available, and hence provide ideal natural laboratories for studying the tectonic and magmatic processes involved in rifted continental margin formation and evolution. They also vary by magmatic type and OCT structure, which has enabled us to fully test and validate the integrated quantitative analysis methodologies. In addition, we have also examined the application of these methodologies to further understand the subsidence histories at these rifted continental margins.

This Chapter will discuss and summarize the observations, problems and solutions regarding OCT structure, COB location and magmatic type, whilst also considering the syn- and post-rift subsidence evolution and the resulting palaeo-bathymetries and depositional environments at the Iberian, northern Angolan, south-eastern Brazilian and the Gulf of Aden rifted continental margins.

6.2. Iberian Rifted Continental Margin

In Chapter 2, integrated quantitative analysis has been applied along profiles for Galicia Bank (ISE-01) and the Iberian Abyssal Plain (IAM9 and Lusigal 12 (with the TGS extension)) in order to determine OCT structure, COB location and magmatic type. Testing the integrated quantitative analysis methodologies on the Iberian rifted continental margin has allowed us to validate the methodologies and to fully understand our interpretations by comparing results to ODP well data (for profiles ISE-01 and Lusigal 12) and magnetic anomalies. It has also been possible to compare our predicted OCT structure and COB location with that inferred from direct well observations.

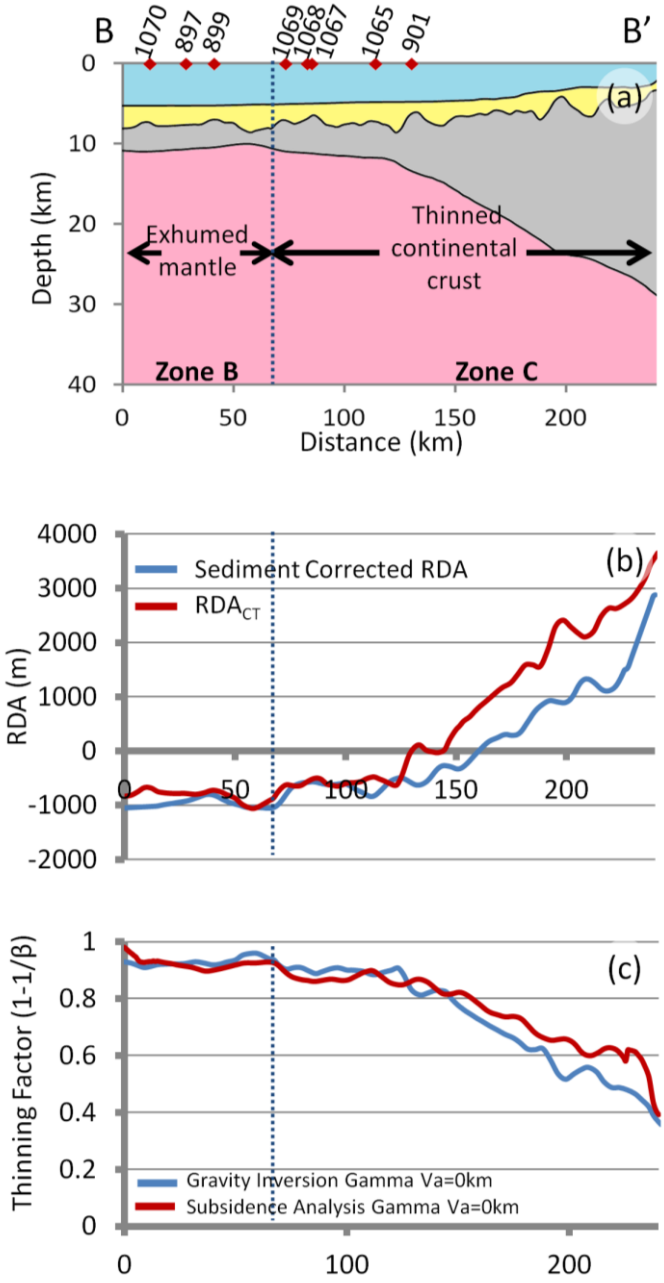

Figure 6.1 - Composite analysis plot along Lusigal 12 (with TGS extension) showing interpretations of crustal zones made from the integrated quantitative analysis, which have been validated using observations from ODP well data. ODP wells 897, 899 and 1070 show serpentinised mantle, whereas ODP wells 901, 1065, 1067, 1068 and 1069 drill into crustal rocks. (a) Crustal cross section along profile Lusigal 12 (B-B') from gravity anomaly inversion. Locations of the ODP wells are indicated. Sediments are in yellow, the crust is in grey and the mantle is pink. (b) Sediment corrected RDA and the RDA component from crustal thickness variations (RDA_{CT}) along Lusigal 12. (c) Continental lithosphere thinning factors from subsidence analysis and gravity anomaly inversion assuming a magma-poor solution. The dashed line indicates the distal extent of unequivocal continental crust and its boundary with exhumed mantle, which could be interpreted as the COB.

We see a clearly distinguished zone of exhumed mantle along the Iberian profiles, which has a corresponding signature within the integrated quantitative analysis results, and is also identified in the ODP well data. The composite analysis plot for the Lusigal 12 profile (Figure 6.1) is interpreted as showing two distinct crustal zones: zone B - serpentinised exhumed mantle; and zone C - thinned continental crust. No unequivocal oceanic crust of normal thickness is observed on the Lusigal 12 profile. Results from the integrated quantitative analysis and our consequent interpretation of the zones of serpentinised exhumed mantle and thinned continental crust, and their boundary, along the Lusigal 12 profile have been validated against ODP well data. We have interpreted a similar zone of exhumed mantle along the ISE01 profile, which has also been validated using the ODP well data.

There are no ODP wells along the IAM9 profile; however, we have compared the integrated quantitative analysis results to magnetic anomalies along the profile. The J anomaly, which is a structural ridge in the oceanic basement that lies beneath the J magnetic anomaly (Tucholke and Ludwig, 1982), crosses the oceanic end of the IAM9 profile. The J anomaly is identified at approximately 25km distance along the IAM9 profile (Bronner et al., 2011; Dean et al., 2000; Whitmarsh et al., 2001), and corresponds to inflection points in Moho depth, RDA and continental lithosphere thinning factors (Figure 6.2) within the oceanic domain.

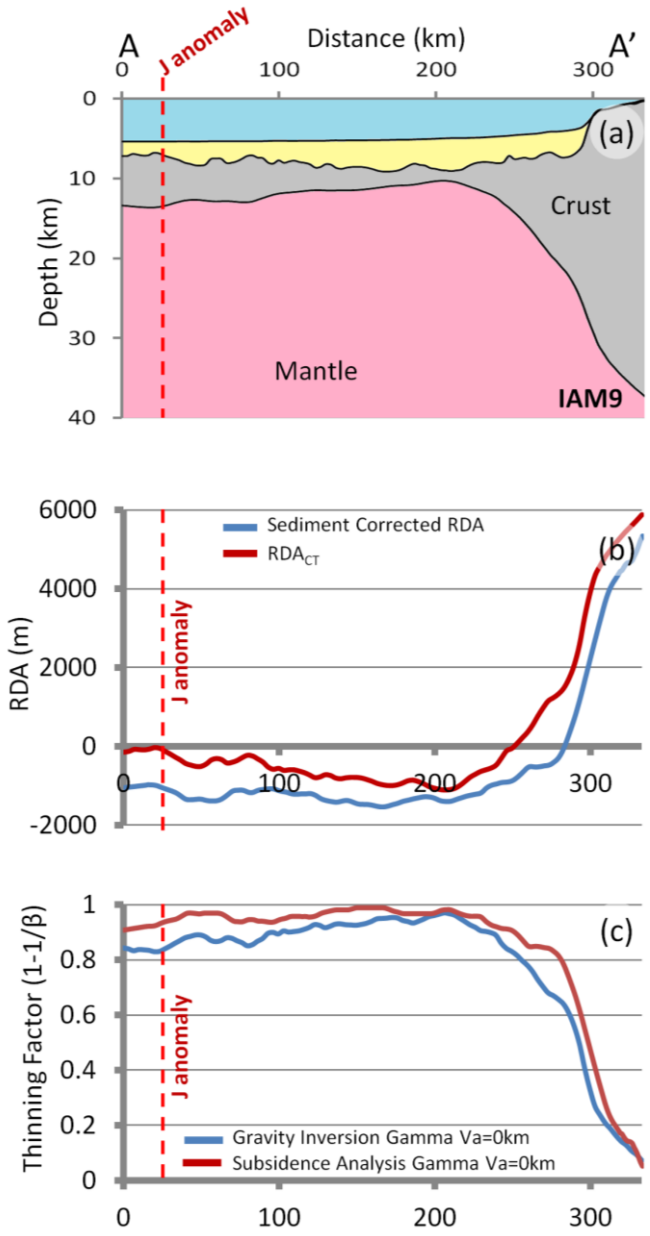

Figure 6.2 - Composite analysis plot along IAM9 with the location of the J anomaly indicated in red (approximately 25km distance along profile). Inflection points in the integrated quantitative analysis results correspond to the location of the J anomaly. (a) Crustal cross section along profile IAM9 (A-A') from gravity anomaly inversion. Sediments are in yellow, the crust is in grey and the mantle is pink. (b) Sediment corrected RDA and the RDA component from crustal thickness variations (RDA_{CT}) along IAM9. (c) Continental lithosphere thinning factors from subsidence analysis and gravity anomaly inversion assuming a magma-poor solution.

The main limitation in our results for the Iberian rifted continental margin is the calibration of reference Moho depth. Reference Moho depth varies globally due to the long wavelength components of the Earth's gravity anomaly field, which are controlled by deep mantle dynamic processes; it is therefore necessary to calibrate the reference Moho depth.

Calibration of Moho depths should only be done on unequivocal oceanic crust (or continental crust), and within this thesis we have calibrated the reference Moho depth with seismic Moho depths for unequivocal oceanic crust.

Along the Iberian rifted continental margin, we have used the IAM9 profile to calibrate reference Moho depth, as the wide angle seismic profile (Dean et al., 2000) shows a clear Moho in the oceanic domain. ODP wells along the Lusigal 12 and ISE-01 profiles do not observe oceanic crust, so calibration of the reference Moho depth on these profiles has not been possible. We have used the calibrated reference Moho depth of 41km from the IAM9 profile for both the Lusigal 12 and ISE-01 profiles. The reference Moho depth of 41km may be applicable to the Lusigal 12 profile due to the close proximity to IAM9. However, the ISE-01 profile is much further north so the 41km value may no longer be appropriate. We have attempted to further resolve the reference Moho depth along the ISE-01 profile using first arrival seismic tomography (FAST) data from Zelt et al. (2003). Zelt et al. (2003) identify the 7.0kms^{-1} and the 7.6kms^{-1} iso-velocity contours as possible indicators of the Moho along the ISE-01 FAST profile (Figure 6.3(a)). Both of these iso-velocity contours are less than the 8.0kms^{-1} iso-velocity contour that typically represents the Moho, and we have therefore used the 7.6kms^{-1} iso-velocity contour to try and further constrain the calibrated reference Moho depth. Calibration (Figure 6.3(b)) suggests that a reference Moho depth of 41km is required. Whilst this is the same as that calibrated for the IAM9 profile, it is important to note that the calibration along the ISE-01 profile was calculated on exhumed mantle, which questions the reliability of this result. In 2013, a 3D reflection and long offset seismic experiment was conducted at the Galicia rifted continental margin by investigators from the USA, UK, Germany and Spain. Part of this study included an extension to the ISE-01 profile to cover oceanic crust, but the results of this experiment have not yet been published. Once published, it would be interesting to use the oceanic Moho depths to accurately calibrate the reference Moho depth for the ISE-01 profile.

The 41km calibrated reference Moho depth for IAM9 is greater than the global average of 38km. This large reference Moho depth implies mantle dynamic subsidence in the range -600m, which is similar to that calculated using RDA analysis (-650m). The large reference Moho depth is comparable to the calibrated reference Moho depth of 41km further to the north east in the Bay of Biscay (Tugend 2013, pers. comms.).

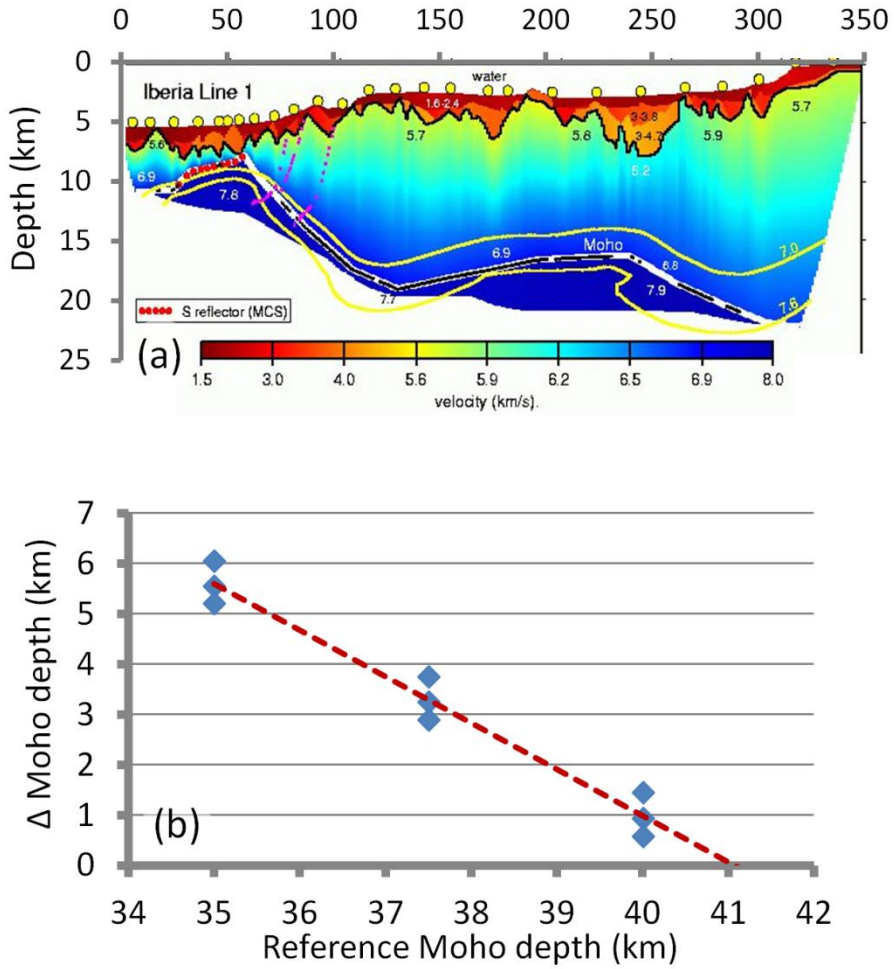

Figure 6.3 – Calibration of the reference Moho depth used in the gravity anomaly inversion along the ISE-01 profile for Galicia Bank. The profile does not extend onto unequivocal oceanic crust, therefore these calibration results are not reliable. (a) FAST data from Zelt et al. (2003); we have used the 7.6kms^{-1} iso-velocity contour to try and further constrain the calibrated reference Moho depth. (b) Calibration of the reference Moho depth for the ISE-01 profile shows that a reference Moho depth of 41km is required.

6.3. South Atlantic Rifted Continental Margins

In Chapter 3, we have applied the integrated quantitative analysis methodology, including the joint inversion of deep seismic and gravity anomaly data, to profiles along the northern Angolan and south-eastern Brazilian rifted continental margins.

6.3.1. Northern Angolan Rifted Continental Margin

Figure 6.4 shows our interpretation of the integrated quantitative analysis results along the CS1-2400 profile. Analysis of the northern Angolan rifted continental profile suggests that:

(i) gravity and deep seismic reflection data predict that the earliest oceanic crust is approximately 5km to 7km thick.

(ii) Serpentinised exhumed mantle is absent beneath the allochthonous salt, and the margin segment is not magma-poor.

(iii) Comparison of the sediment corrected RDA and the RDA component from crustal thickness variations (RDA_{CT}) implies that this margin is experiencing between approximately +500m and +900m of present day mantle dynamic uplift.

(iv) Gravity anomaly inversion, RDA and subsidence analysis results show that the OCT along CS1-2400 is quite wide, with the distance between the COB and the margin hinge measuring approximately 180km.

(v) Joint inversion shows a contrast in basement density and seismic velocity between oceanic and continental crustal basement consistent with the location of the COB derived from integrated quantitative analysis.

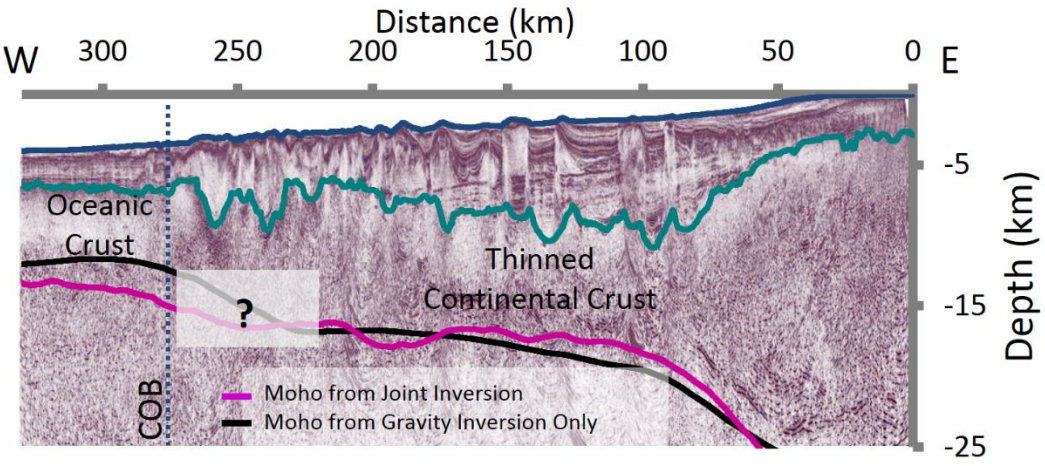

Figure 6.4 – Interpretation of the integrated quantitative analysis results along the PSDM CS1-2400 profile. Seabed is shown in blue, top basement in green, Moho from gravity anomaly inversion in black and Moho from the joint inversion is shown in pink. Our interpretation of the COB from integrated quantitative analysis results is identified along the profile; to the west we interpret 'normal' thickness oceanic crust and to the east we interpret thinned continental crust. We have shaded out part of the Moho from joint inversion as there are no Moho reflectors in this region. The Joint inversion predicted Moho is smoothed.

The sediment corrected bathymetry shows structural control from faulting, and as a result has quite a noisy signal, which has consequences for the sediment corrected RDA and subsidence analysis results. In order to remove this noise, it is necessary to smooth the data; we have 'smoothed' the sediment corrected RDA and subsidence analysis results by computing a moving average. Within this thesis a spatial gate of 30km has been used for the moving average, but sensitivities to spatial gates of 10km, 40km and 60km have also been examined (Figure 6.5). The larger the spatial gate, the greater the amount of 'smoothing'. A spatial gate of 10km is too small as the fault controlled topography is still evident. The larger spatial gates increase the amount of 'smoothing' and hence reduce the noise from fault controlled topography as seen with the spatial gates of 30km, 40km and 60km. We chose to use a spatial gate of 30km as we felt that this 'smoothed' the data and removed enough fault controlled topography noise without 'over-smoothing', and was greater than the fault block range (15km to 25km).

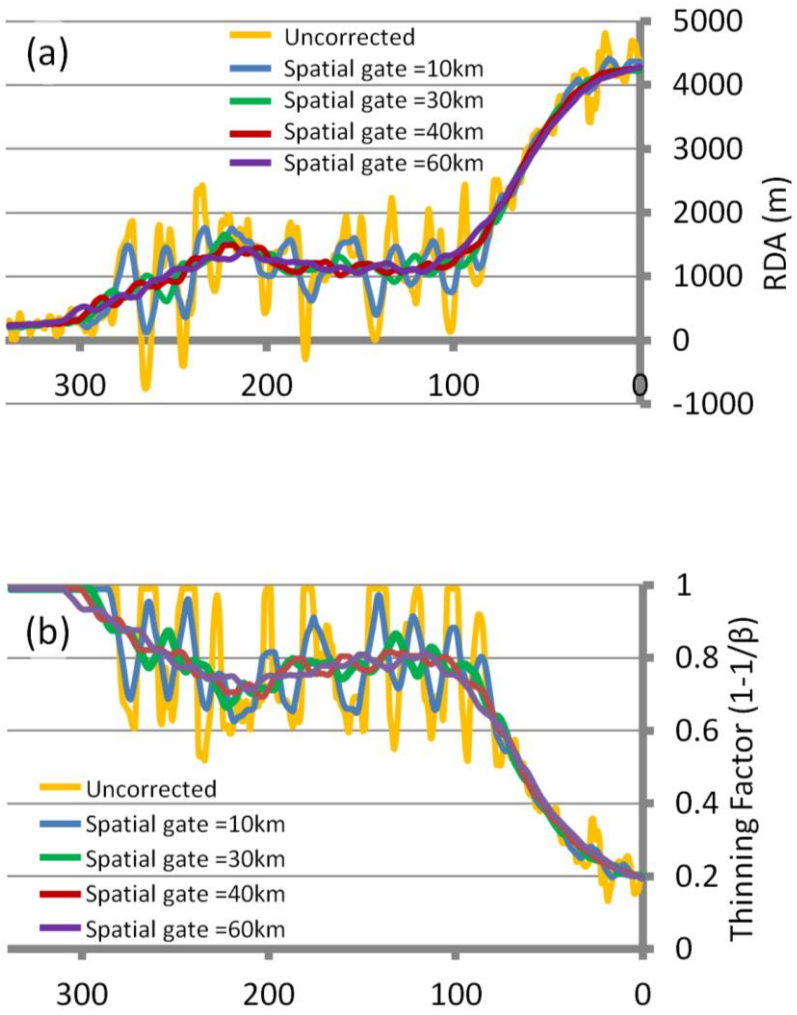

Figure 6.5 – The sediment corrected RDA and subsidence analysis results have been 'smoothed' using a moving average. Sensitivity to the spatial gates (10km, 30km, 40km and 60km) used in the moving average has been examined for (a) sediment corrected RDA results along the CS1-2400 profile and (b) subsidence analysis results along the CS1-2400 profile. The larger the spatial gate the greater the amount of 'smoothing'. A spatial gate of 30km is preferred.

Along the Angolan profiles an effective elastic thickness (Te) of 1.5km and a calibrated reference Moho depth of 35.5km have been used. Changing the value of Te or the reference Moho depth used, can change the overall conclusions significantly and a serpentinised mantle layer could be interpreted, as proposed by Unternehr et al. (2010). Changing the value of Te has consequences for the sediment corrected RDA (Figure 6.6(a)) and subsidence analysis (Figure 6.6(b)) results, therefore sensitivities to Te's of 1.5km, 5km and 10km have been examined. Fault block topography has been removed using a moving average, as

previously discussed. Low values of Te (1.5km to 3km) rather than high values of Te (10km to 20km) are appropriate to use for syn-rift flexural backstripping in order to preserve fault block topography (Kusznir et al., 1995; Roberts et al., 1998). During the post-rift the lithosphere cools and gets flexurally stronger, therefore, in the post-rift the Te's will be larger, which act to freeze in the structures and the isostatic response from the syn-rift. A high value of Te may be appropriate to use for the post-rift sediments. High values of Te (5km and 10km) produce a very negative sediment corrected RDA adjacent to the COB (Figure 6.6(a)). By comparison, the Iberian margin, where negative sediment corrected RDAs correspond to a validated zone of exhumed mantle, the negative sediment corrected RDAs along the Angolan margin could also correspond to exhumed mantle.

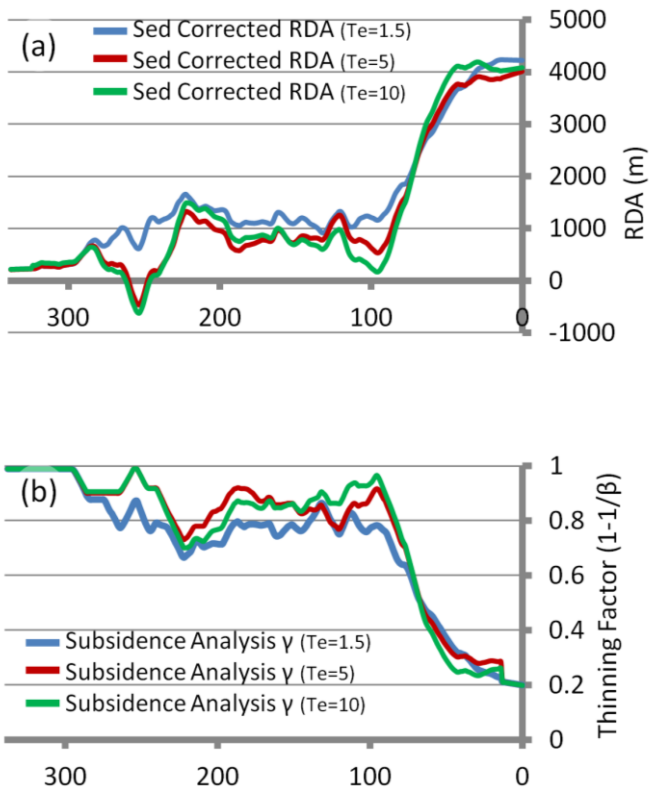

Figure 6.6 – Sensitivity to the effective elastic thickness (Te's of 1.5km, 5km and 10km) for northern Angolan CS1-2400 profile sediment corrected RDA results and subsidence analysis results have been examined. The results in these plots have been 'smoothed' using a spatial gate of 30km in the moving average. (a) Sensitivity to Te for the sediment corrected RDA results along the CS1-2400 profile. The main difference between the Te's is seen beneath the thick salt (approximately 250km along profile) where Te's of 5km and 10km are both very negative, whilst the Te of 1.5km is positive. (b) Sensitivity to Te for the subsidence analysis results along the CS1-2400 profile.

In Chapter 4, palaeo-bathymetric restorations to base Loeme salt (top Aptian) have been determined using reverse post-breakup subsidence modelling. The analysis has been applied to the ION-GXT CS1-2400 deep long-offset seismic reflection profile and the P3 and P7+11 seismic cross sections of Moulin (2005) and Contrucci et al. (2004) in the Kwanza region, offshore northern Angola. There are several possible explanations of the palaeo-bathymetric restoration of the distal base salt to water depths substantially below sea level:

(i) syn-rift crustal thinning during salt deposition resulting in additional tectonic subsidence,

(ii) the distal salt moved down-slope while breakup occurred, to its present position in much deeper water,

(iii) salt deposition occurred in confined environmental conditions, in a Messinian-type basin, isolated from global sea level.

If the distal salt was deposited onto the top-basement during the syn-rift, a low Te response is appropriate. However, if the salt moved after deposition that is during the post-rift a higher Te would be more appropriate. The sensitivity to Te's on the palaeo-bathymetric restoration of the Aptian salt is considered in Figure 6.7. Changing the value of Te does not make a substantial difference to the palaeo-bathymetric restoration of the base salt (Figure 6.7(c)), and does not change our overall conclusions. We believe that the salt was deposited during the syn-rift, but then moved during the post-rift, so using a low Te of 1.5km for the Angolan profiles will calculate accurate palaeo-bathymetric restorations. As a low syn-rift Te has been accepted for the northern Angolan profiles, this suggests that there is no evidence for exhumed mantle as proposed by Unternehr et al. (2010).

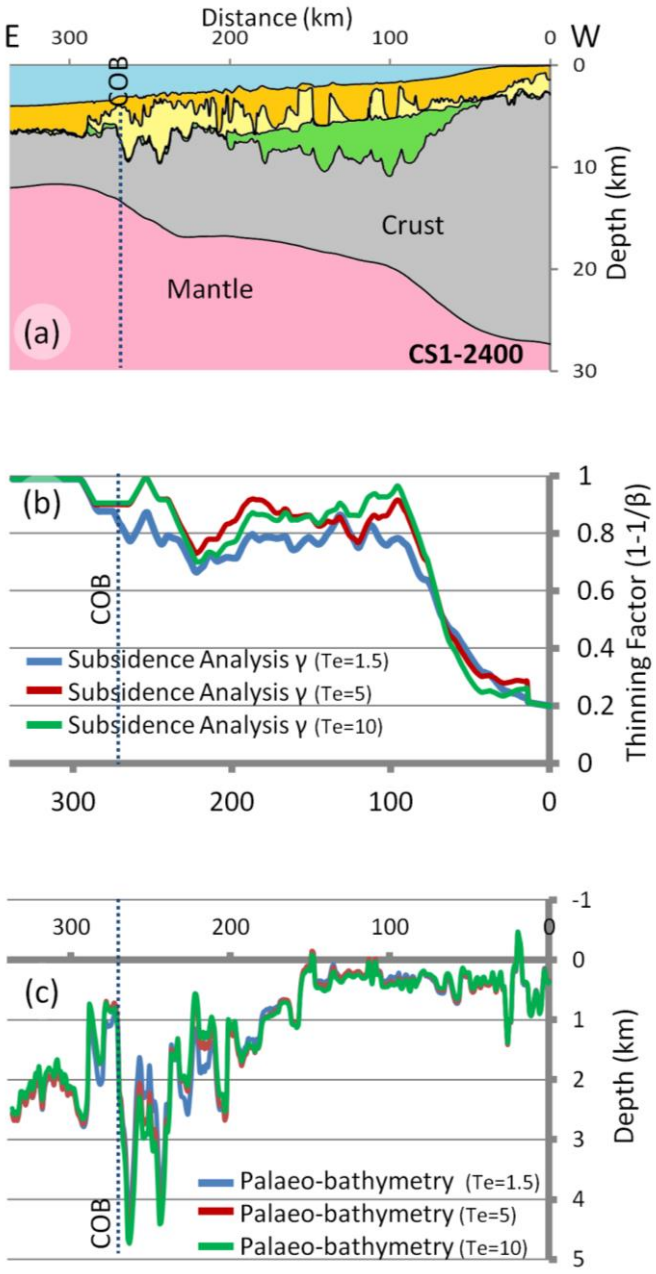

Figure 6.7 – Sensitivity to effective elastic thicknesses (Te) along the CS1-2400 profile. (a) Crustal cross section from gravity anomaly inversion. Post-salt sediments are in orange, the salt is in yellow, the pre-salt sediments are green, the crust is in grey and the mantle is pink. (b) Comparison of the continental lithosphere thinning factors, predicted from subsidence analysis for the sensitivities to Te's of 1.5km, 5km and 10km. (c) The resulting palaeo-bathymetries from reverse post-breakup thermal subsidence modelling for the sensitivities to Te: a Te of 1.5km (in blue), a Te of 5km (in red) and a Te of 10km (in green). The restored palaeo-bathymetries of the base salt do not differ significantly.

The calibrated reference Moho depth varies between the northern profiles (P3 and P7+11) and the profile to the south (CS1-2400); the calibrated reference Moho depth for profiles P3 and P7+11 is 37.5km, whilst the calibrated reference Moho depth for the CS1-2400 profile is

35.5km. Profiles P3 and P7+11 were calibrated using Moho depths from wide angle seismic refraction data from Contrucci et al. (2004), whilst the CS1-2400 profile is calibrated using Moho depths from the ION-GXT deep long offset seismic profile. The Moho reflectors and refractions along the P3 and P7+11 profiles are not as clear as those from the CS1-2400 profile, and as a result we are more confident in our calibration of the reference Moho depth along the CS1-2400 profile. We have considered the sensitivity to reference Moho depth within the reverse post-breakup thermal subsidence modelling (Figure 6.8). Increasing the reference Moho depth from 35.5km to 37.5km results in a deeper Moho (Figure 6.8(a)) and smaller continental lithosphere thinning factors (Figure 6.8(b)) predicted from gravity anomaly inversion, as well as a deeper restoration of the base salt (Figure 6.8(c)).

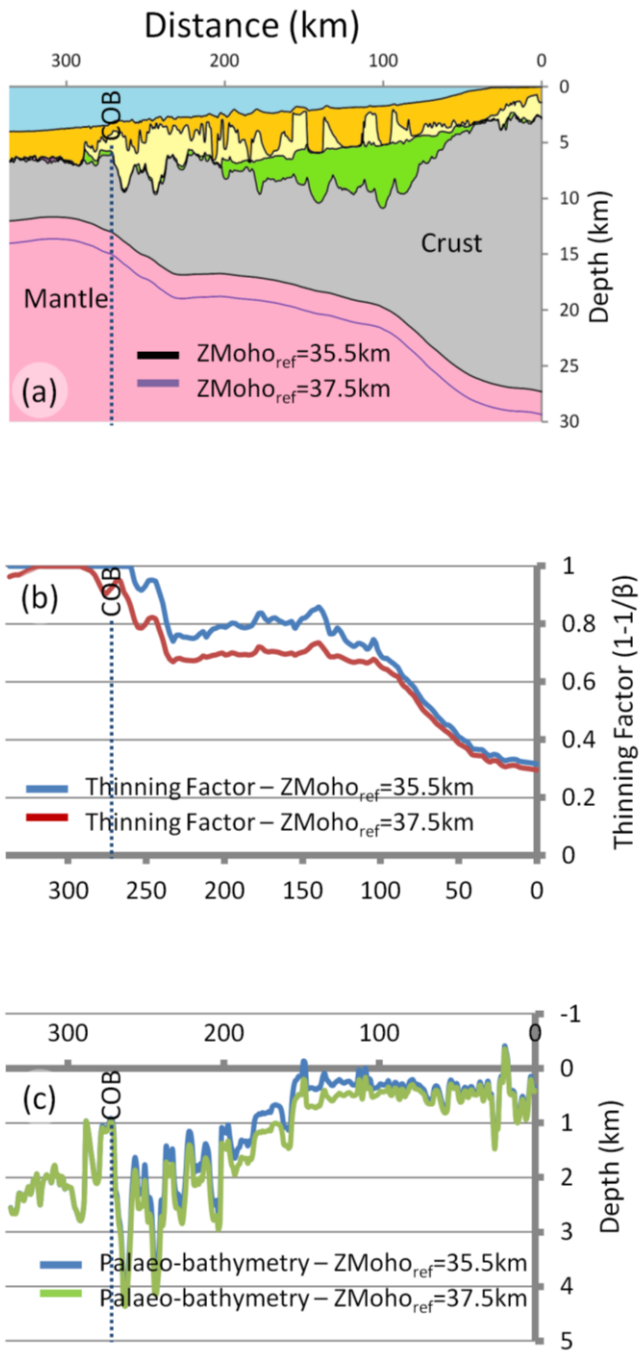

Figure 6.8 – Sensitivity to changing the reference Moho depth between 35.5km (as calibrated for the CS1-2400 profile) to 37.5km (as calibrated for the P3 and P7+11 profiles). (a) Crustal cross section from gravity anomaly inversion, showing two Moho depths. The Moho in black is the result of using a reference Moho depth of 35.5km and the Moho in purple is the result of using a higher reference Moho depth of 37.5km. If we increase the reference Moho depth along the CS1-2400 profile, this results in a deeper Moho depth prediction. Post-salt sediments are in orange, the salt is in yellow, the pre-salt sediments are green, the crust is in grey and the mantle is pink. (b) Comparison of the continental lithosphere thinning factors, predicted from gravity anomaly inversion for the sensitivities to reference Moho depth. Using a reference Moho depth of 37.5km (in red) results in smaller continental lithosphere thinning factors along the CS1-2400 profile. (c) The resulting palaeo-bathymetries from reverse post-breakup thermal subsidence modelling for the two sensitivities to reference Moho depth: using a reference Moho depth of 35.5km (in blue) and using a reference Moho depth of 37.5km (in green). The larger reference Moho depth of 37.5km results in deeper palaeo-bathymetries; the biggest differences are observed in the central section of the profile.

6.3.2. South-eastern Brazilian Rifted Continental Margin

Figure 6.9 shows our interpretation of the integrated quantitative analysis results along the BS1-575 profile. Analysis of the south-eastern Brazilian rifted continental profile suggests that:

(i) gravity and deep seismic reflection data predict that the earliest oceanic crust is between 7km and 8km thick.

(ii) Beneath the Sao Paulo Plateau and Florianopolis Ridge crustal basement thicknesses range between 10km and 15km.

(iii) There is no evidence for exhumed mantle along this margin profile.

(iv) RDA analysis implies negligible present day mantle dynamic topography.

(v) Gravity anomaly inversion, RDA and subsidence analysis results show that the OCT along BS1-575 is wide, with the distance between the COB and the margin hinge measuring approximately 540km.

(vi) The joint inversion of deep seismic and gravity anomaly data predict basement densities typical of 'normal' oceanic crust for the earliest oceanic crust.

(vii) For much of the north-western end of the Florianopolis ridge, the joint inversion predicts basement densities that are less than expected for continental crust, similar to those seen for the Sao Paulo Plateau.

(viii) In contrast at the south-eastern end of the Florianopolis Ridge, the joint inversion predicts basement densities and seismic velocities which are much higher and are similar to those predicted for the oceanic crust. We interpret this region as a 'keel' structure, which is west of the COB.

(ix) Beneath the Sao Paulo Plateau, joint inversion predicts basement densities substantially lower than expected for thinned continental crust, possibly due a Neocomian rift basin under the Paraná volcanic or gabbroic material in the

continental lithospheric mantle. Both of these would act to lower the density beneath the Sao Paulo Plateau.

(x) Joint inversion shows a contrast in basement density and seismic velocity between oceanic and continental crustal basement, which is comparable to the location of the COB derived from integrated quantitative analysis.

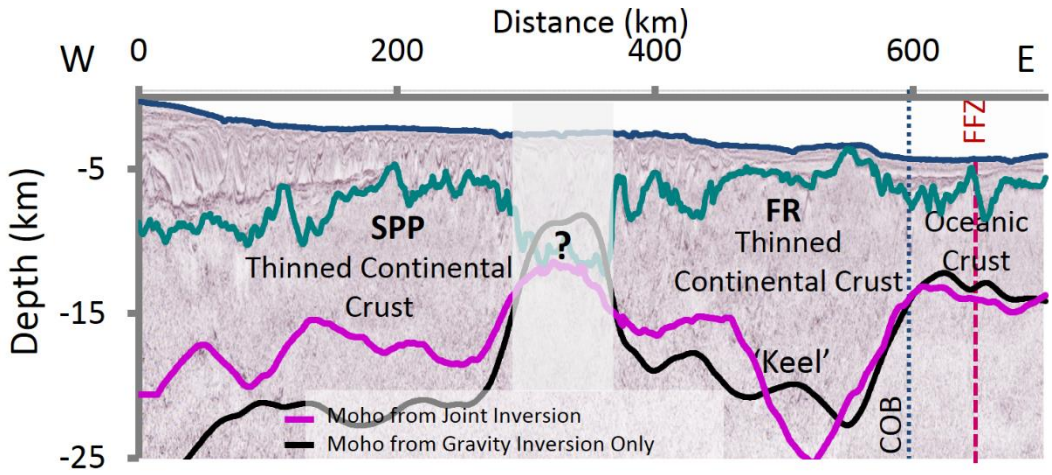

Figure 6.9 – Interpretation of the integrated quantitative analysis results along the PSDM BS1-575 profile. Seabed is shown in blue, top basement in green, Moho from gravity anomaly inversion in black and Moho from the joint inversion is shown in pink (this is smoothed). Our interpretation of the COB from integrated quantitative analysis results is identified along the profile; to the east we interpret approximately 'normal' thickness oceanic crust and to the west we interpret thinned continental crust beneath the Florianopolis Ridge and Sao Paulo Plateau. The location of the Florianopolis Fracture Zone (FFZ) is also identified. We have shaded out the region beneath the thick salt between the Florianopolis Ridge (FR) and Sao Paulo Plateau (SPP) as the joint inversion predicts an unphysical result here.

Similarly to the Iberian rifted continental margin, calibration of reference Moho depth is the biggest limitation to the integrated quantitative analysis results. We have calibrated the reference Moho depth along the BS1-575 using Moho reflectors from the oceanic domain of the ION-GXT deep long offset profile and found that a reference Moho depth of 37.5km is required. Calibration of the reference Moho depth for profiles further north (Mohriak et al., 2008) along the Brazilian rifted continental margin are lower, approximately 35km (Kusznir, 2014, pers. comms.). We have therefore considered sensitivities to reference Moho depth for the BS1-575 profile (Figure 6.10); reducing the reference Moho depth from 37.5km to

35km results in a shallower Moho. Zoomed in sections in time (Figure 6.11(a)) and depth (Figure 6.11(b)) of the oceanic domain of the BS1-575 show the Moho reflectors highlighted; there are no clear shallower reflectors that could be interpreted as the Moho, which validates our calibration of 37.5km.

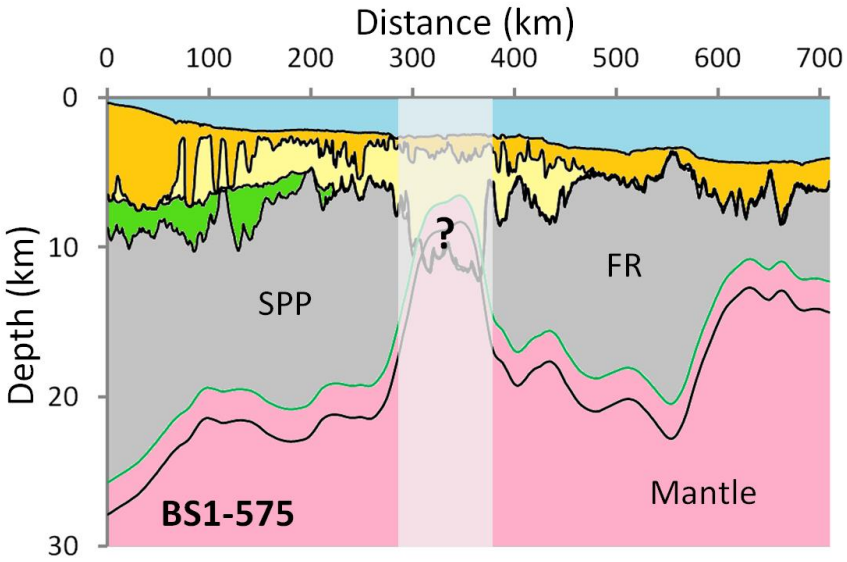

Figure 6.10 – Sensitivity to changing the reference Moho depth between 37.5km (as calibrated for the BS1-575 profile) to 35.5km (as calibrated for profiles further north along the Brazillian margin). Crustal cross section from gravity anomaly inversion, showing two Moho depths. The Moho in black is the result of using a reference Moho depth of 37.5km and the Moho in green is the result of using a lower reference Moho depth of 35.5km. If we decrease the reference Moho depth along the BS1-575 profile, this results in a shallower Moho depth prediction. Post-salt sediments are in orange, the salt is in yellow, the pre-salt sediments are green, the crust is in grey and the mantle is pink.

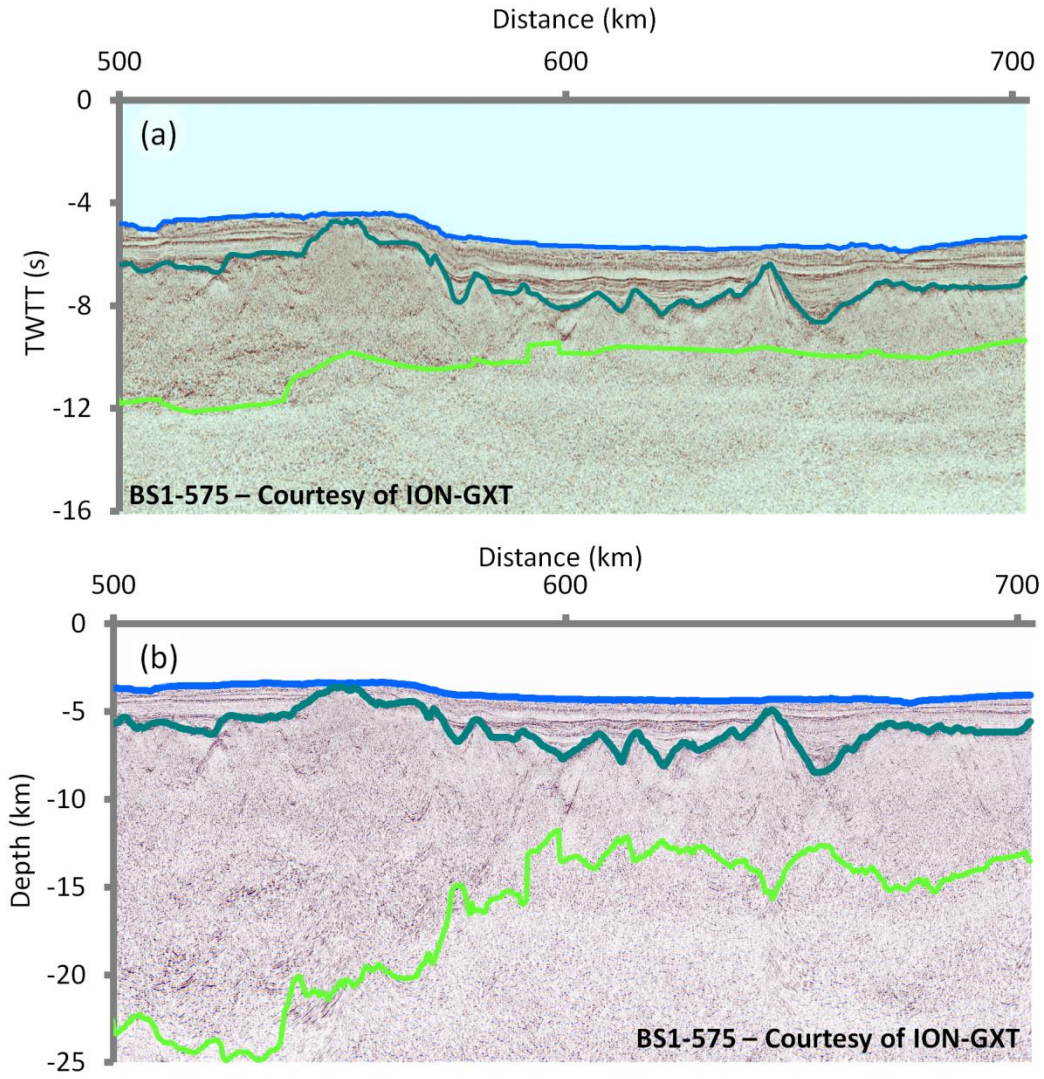

Figure 6.11 – Zoomed in sections of the oceanic end of the BS1-575 profile. (a) PSTM along the BS1-575 profile. (b) PSDM along the BS1-575 profile. The sea bed is highlighted in blue, the top basement is highlighted in teal and our picked Moho is in green. There are no clear reflectors above our interpretation of the Moho.

The thick sedimentary cover and mobile salt (including salt diapirs and canopies) makes seismic imaging of the salt and pre-salt sedimentary units difficult. Interpretation of the internal structure and thickness of the salt and the pre-salt sedimentary layers is therefore a generic problem. Along the south-eastern Brazilian margin there is a thick Aptian salt sequence, including huge salt diapirs and salt walls in the deep-water regions (Mohriak et al., 2008), evident along the BS1-575 profile. Beneath the thick salt, the gravity anomaly inversion predicted Moho comes up into the sediment layer, which is an unphysical result.

This has led us to question our interpretation of the salt layer, that is whether there are pre-salt sediments beneath this thick salt, or whether there are syn-rift sediments mixed in with the salt (i.e. mother salt with salt canopies above). We have considered a sensitivity test in which we treat the salt layer as just another sedimentary layer; integrated quantitative analysis results are shown in Figure 6.12. Treating the salt as a sedimentary layer produces a deeper Moho (Figure 6.12(b)), and although this sensitivity produces a physical result for the region of very thick salt, it is not valid for the rest of the profile.

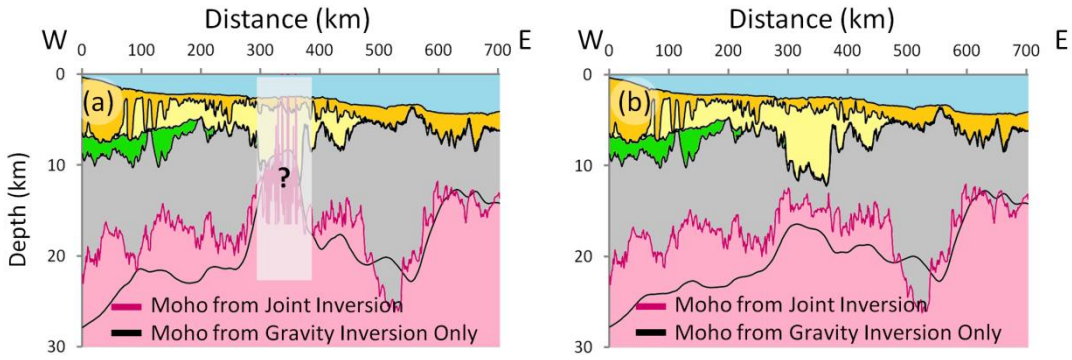

Figure 6.12 – Comparison of the joint inversion and gravity anomaly inversion results examining the sensitivity to the salt layer along the BS1-575 profile. Post-salt sediments are in orange, the salt is in yellow, the pre-salt sediments are green, the crust is in grey and the mantle is pink. (a) The salt layer (using salt density and compaction parameters) has been included. Beneath the thick salt both the gravity anomaly inversion and the joint inversion predict an unphysical result beneath the thick salt. We have blanked out the unphysical solution beneath the thick salt for ease in interpretation. (b) The salt has been omitted and the salt layer is treated as another sedimentary layer, assuming a shaly-sand lithology . This produces a deeper Moho beneath the thick salt, the crust beneath this area is still very thin (approximately 5km thick). Although this sensitivity produces a physical result for the region of very thick salt, it is not valid for the rest of the profile. We therefore prefer the solution, which includes the salt.

Under the Sao Paulo Plateau (SPP) joint inversion predicts average basement densities of approximately 2640kgm^{-3} (Figure 6.13). These basement densities are considerably lower than expected for continental crust. There are three possible explanations for these low basement densities:

(i) the lower densities beneath the Sao Paulo Plateau are the result of a significant difference between Moho predicted from gravity anomaly inversion and the picked

seismic Moho. If we used a lower reference Moho depth, this would predict a shallower Moho, hence reducing the difference between the picked seismic Moho and the Moho from gravity anomaly inversion. A smaller difference between the two Mohos would increase the basement densities calculated from the joint inversion, to values expected for continental crust. Whilst a lower reference Moho depth would result in sensible results at the western end of the profile, it would produce a Moho that is too shallow in the oceanic domain, which is unrealistic.

(ii) An alternative explanation is that there is a mass deficiency, e.g. presence of gabbroic material, which has been 'frozen' into the continental lithospheric mantle (Cannat et al., 2009) beneath the Sao Paulo Plateau. If this is the case, the gravity anomaly inversion will assume that this lighter material is crustal basement and this will result in a deeper prediction of Moho depth.

(iii) Many authors believe that the continental crust beneath the Sao Paulo Plateau is intruded by volcanic rocks (Hung Kiang et al., 1992), so it is possible that our pick of the Moho is the top of the Paraná volcanics which are laterally extensive in this region. It is proposed (e.g. Mohriak et al.) that the Paraná volcanics may be underlain by syn-rift sediments (possibly Neocomian in age). Both the Paraná volcanics and additional deeper sediments would act to lower the density beneath the Sao Paulo Plateau.

Beneath the Florianopolis Ridge (FR), west of the Florianopolis Fracture Zone we interpret a 'keel' structure (Figure 6.13(a)). The base of the 'keel' structure is at 12 seconds (or greater) two-way travel time (TWTT), which is deeper than the 8 to 11 seconds TWTT thought to correspond to the Moho , leading us to question our interpretation of the seismic Moho. We believe that the 'keel' structure is the result of an interpretation of the Moho that is too deep. The reflections, which we interpreted as Moho, may be within the mantle. As a result, there is a substantial difference between the picked Moho and the gravity anomaly inversion

predicted Moho in this region, which results in the need for larger 'basement' densities and seismic velocities for this 'keel' structure.

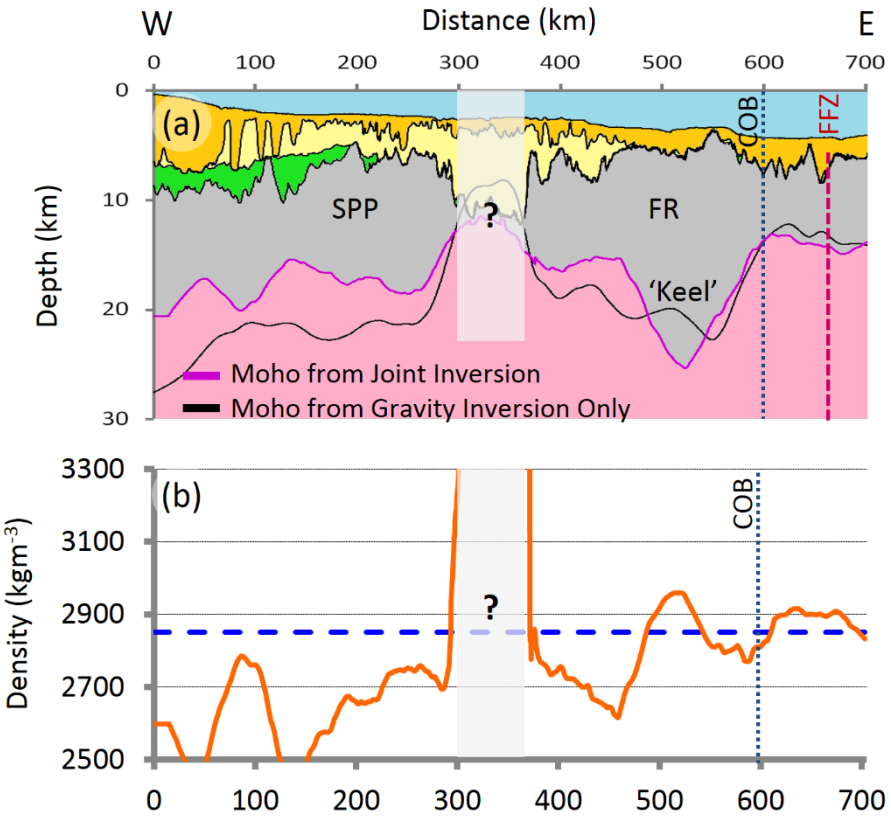

Figure 6.13 – (a) Crustal cross-section along the CS1-2400 northern Angolan profile showing the Moho depth determined from gravity anomaly inversion, and the Moho depth determined from joint inversion. Post-salt sediments are in orange, the salt is in yellow, the pre-salt sediments are green, the crust is in grey and the mantle is pink. (b) Lateral variations in basement density along the CS1-2400 profile. The blue dashed line highlights the basement density of 2850kgm^{-3} which is the basement density used within the initial gravity anomaly inversion. The average basement densities at the oceanic end the profile are within the range of typical oceanic basement densities; however, beneath the Sao Paulo Plateau and the Florianopolis Ridge the basement densities are lower than expected for thinned continental crust. Beneath the interpreted 'keel' structure the basement densities are similar to those at the oceanic end of the profile. The joint inversion predicted Moho and basement densities are smoothed.

Within this thesis, a large amount of the qualitative and quantitative analysis of geological data at rifted continental margins assumes a very simple crust-mantle interface; this clearly breaks down where we have serpentinised exhumed mantle (e.g. the Iberian rifted continental margin) and at the base of 'keel' structures (e.g. south-eastern Brazilian rifted continental margin). This leads us to question the need for a more sophisticated model for

the crust-mantle interface. However, with the availability of ODP well data, we are able to understand and predict the response from the integrated quantitative analysis results for these regions, hence enabling us to make accurate geological interpretations of crustal structure.

6.3.3. Petroleum Systems

As mentioned in the introductory chapter, rifted continental margins are key exploration frontiers, for the hydrocarbon industry, and knowledge of the OCT structure, COB location and magmatic type are important for deep-water frontier oil and gas exploration. OCT structure, COB location and magmatic type have significant consequences for petroleum systems in terms of source rocks, reservoirs and thermal maturation. The distribution of thinned continental crust and the start of unequivocal oceanic (i.e. the location of the COB) is particularly important for determining the thermal maturity of a petroleum system. Petroleum systems require heat during the maturation period; this heat, in part, comes from the radiogenic heat productivity within continental crust.

A key example of how the determination of OCT structure, COB location and magmatic type of rifted continental margins has improved our understanding of petroleum systems is the application of the integrated quantitative analysis to the south Atlantic margins. The south Atlantic rifted continental margins have been the subject of extensive seismic surveys (e.g. Moulin et al. (2005); Contrucci et al. (2004) and Mohriak et al. (2008)) due to their economic potential. However, along both the southern Brazilian and the northern Angolan rifted continental margins the structure of the OCT, the distribution of thinned continental crust and the start of unequivocal oceanic crust are unclear. At the distal end of the northern Angolan profile, both Unternehr et al. (2010) and Contrucci et al. (2004) report an anomalous layer in the OCT, which they interpret to be a zone of exhumed continental mantle. However,

in the same region, we interpret hyper-extended continental crust and we see no evidence of serpentinised exhumed mantle. Our interpretation of the crustal structure at the distal end of this profile would result in a higher prediction of radiogenic heat flow, than that of those authors interpreting exhumed mantle. Greater present day top basement heat flow under the distal salt will have important implications for hydrocarbon maturation. Along the south-eastern Brazilian margin, Zálan et al. (2011) report exhumed mantle, south east of the Florianopolis Ridge, which we have interpreted as oceanic crust, and again we see no evidence of exhumed mantle.

The presence of exhumed mantle or oceanic crust will not have an impact on top basement heat flow and hydrocarbon maturation; however, where the presence or absence of exhumed mantle is important is when the alternative is thinned continental crust, whose presence or absence will impact on hydrocarbon exploration.

6.4. Residual Topography

In Chapter 5 we used the integrated quantitative analysis results, primarily the RDA analysis results, to provide some constraints on margin subsidence. The RDA analysis uses observational data including seismic reflection and refraction profiles to measure residual topography, and hence determine the magnitude of anomalous present day subsidence or uplift at rifted continental margins. Reports of anomalous subsidence at rifted continental margins may partly (or wholly) be attributed to mantle dynamic topography. Within the RDA analysis methodology, corrections to the observed topography for sediment loading and crustal and thermal isostasy at a local scale are made. RDA analysis has been applied to the offshore Iberian, northern Angolan and the Gulf of Aden rifted continental margins. Our measurements of residual topography in the oceanic domain, from RDA analysis, show that:

(i) at the Iberian Abyssal Plain we calculate an average of -650m of anomalous present day subsidence,

(ii) in the Gulf of Aden we calculate an average of +400m of anomalous present day uplift,

(iii) and along the northern Angolan margin we calculate an average of +700m of anomalous present day uplift.

We have compared residual topography extracts from the global models (Crosby and McKenzie, 2009; Flament et al., 2013; Kaban et al., 2003; Steinberger, 2007) with our measurements of residual topography from RDA analysis. The global models of residual topography all make corrections for sediment loading and crustal basement thickness variations at a global scale using other global models (e.g. global models of sediment thickness (Divins, 2003; Laske and Masters, 1997) and crustal thickness models (Amante and Eakins, 2009; Laske et al., 2013)). The use of these global models reduces the accuracy within the corrections applied. At a global scale these models are in broad agreement, however, at a local scale these global models show significant differences in the amplitude and polarity of the predicted residual topography.

Mantle dynamic topography is a real phenomenon and should be factored into subsidence analysis and subsidence history calculations. There are multiple challenges which limit our understanding of global mantle dynamic topography, including different definitions of the term ‘mantle dynamic topography’, inaccurate estimates of present-day mantle dynamic topography in the absence of a detailed global model of the structure of the lithosphere, and contradicting model predictions of vertical motions (Flament et al., 2013; Müller et al., 2008). The best constraint on present day mantle dynamic topography is residual topography; measurements of residual topography are attributed to mantle dynamic topography. Precision is therefore important for residual topography measurements, particularly for

understanding the long and short wavelengths of mantle dynamic topography. Along the northern Angolan margin, there appears to be a short wavelength component of mantle dynamic topography; this is observed in the north-south variation in reference Moho depths between the northern (P3 and P7+11) profiles and the southern CS1-2400 profile, as discussed earlier.

Whilst we are able to measure present day residual topography to a high degree of precision in the oceanic domain of rifted continental margins, we need to consider how much of the residual topography in the OCT is directly related to mantle dynamic processes and how much is due to the compositional and density variations in the lithosphere and/or the upper asthenosphere. Within our residual topography measurements we account for temperature variations, using the thermal plate model predictions from Crosby and McKenzie (2009), however, variations in density and chemical composition are not considered.

6.5. Errors and Uncertainties in the Integrated Quantitative Analysis Results

Errors and uncertainties in the integrated quantitative analysis undoubtedly exist. The accuracy of the results from the integrated quantitative analysis techniques has, in general, been assessed using sensitivity tests of the input parameters, and where possible the results have been calibrated. The individual sensitivity tests and calibrations have been described in detail, in earlier chapters.

Errors within the gravity anomaly inversion results arise from uncertainties in: reference Moho depth, variations in basement density, breakup age, sediment thickness, bathymetry and free air gravity. Uncertainties in the parameters used within flexural backstripping, in particular: lithology and their compaction parameters, sediment thickness, breakup age, effective elastic thickness (Te) and magmatic addition, lead to errors in the RDA and

subsidence analysis results. Additional uncertainties in the initial crustal thickness and changes in mantle dynamic topography between present day and the syn-rift also lead to errors in the subsidence analysis results. The most significant uncertainties in the integrated quantitative analysis results are from sediment thickness and lithology.

Within this thesis we have focussed primarily on errors and uncertainties due to break-up age, effective elastic thickness, reference Moho depth and lithology. We have tried to understand and minimise these uncertainties through sensitivity tests and calibration. The integrated quantitative analysis results are shown as a range, which for this type of study is more valuable than looking at averages and using statistical error analysis.

6.6. Conclusions

The following summarises the main conclusions in this thesis:

(i) integrated quantitative analysis (the combined use of gravity anomaly inversion, RDA analysis, subsidence analysis and joint inversion of deep long offset seismic and gravity anomaly data) has been used to determine OCT structure, COB location and magmatic type at the Iberian, Gulf of Aden, northern Angolan and south-eastern Brazilian rifted continental margins.

(ii) The integrated quantitative analysis results have been validated using ODP well data and magnetic anomalies along the Iberian rifted continental margin.

(iii) A clearly defined zone of exhumed mantle is identified along the Iberian rifted continental margin from integrated quantitative analysis results and in the ODP well data.

(iv) Predicted OCT widths along the Iberian rifted continental margin range from approximately 100km in the south (Iberian Abyssal Plain) to 250km further north (Galicia Bank).

(v) Integrated quantitative analysis results along the northern Angolan rifted continental margin do not suggest that serpentinised exhumed mantle is present beneath the allochthonous salt or that the margin is magma-poor as proposed by authors (e.g. Unternehr et al. (2010)).

(vi) Integrated quantitative analysis predicts that the OCT along the Angolan margin is quite wide, approximately 180km.

(vii) Along the northern Angolan rifted continental margin, post-breakup subsidence modelling restores the proximal autochthonous base Loeme salt to near sea level, but not the distal allochthonous salt.

(viii) The distal Loeme salt formed during the late syn-rift while the crust under it was being actively thinned, resulting in additional tectonic subsidence. It is also thought that some of the distal salt moved down-slope during the post-rift.

(ix) Integrated quantitative analysis along the south-eastern Brazilian rifted continental margin predicts that the earliest oceanic crust is between 7km and 8km thick, and that there is no evidence of exhumed mantle as suggested by Zálan et al. (2011).

(x) The OCT is much wider along the south-eastern Brazilian margin, measuring approximately 540km.

(xi) RDAs corrected for sediment loading and crustal basement thicknesses have been used to determine residual topography, which we attribute to mantle dynamic topography at rifted continental margins:

a. -650m of present day anomalous subsidence is measured along the Iberian Abyssal Plain.

b. In the Gulf of Aden we calculate an average of +400m of anomalous present day uplift.

c. Anomalous present day uplift, in the order of +700m, is measured along the northern Angolan rifted continental margin.

6.7. References

Amante, C., and Eakins, B. W., 2009, ETOPO1 1 Arc-Minute Global Relief Model: Procedures, Data Sources and Analysis: NOAA Technical Memorandum NESDIS NGDC-24, p. 19.

Bronner, A., Sauter, D., Manatschal, G., Peron-Pinvidic, G., and Munschy, M., 2011, Magmatic breakup as an explanation for magnetic anomalies at magma-poor rifted margins, Nature Geoscience, Volume 4, Nature Publishing Group, a division of Macmillan Publishers Limited. All Rights Reserved., p. 5.

Cannat, M., Manatschal, G., Sauter, D., and Péron-Pinvidic, G., 2009, Assessing the conditions of continental breakup at magma-poor rifted margins: What can we learn from slow spreading mid-ocean ridges?: Comptes Rendus Geosciences, v. 341, no. 5, p. 406-427.

Contrucci, I., Matias, L., Moulin, M., Géli, L., Klingelhofer, F., Nouzé, H., Aslanian, D., Olivet, J.-L., Réhault, J.-P., and Sibuet, J.-C., 2004, Deep structure of the West African continental margin (Congo, Zaïre, Angola), between 5°S and 8°S, from reflection/refraction seismics and gravity data: Geophysical Journal International, v. 158, no. 2, p. 529-553.

Crosby, A. G., and McKenzie, D., 2009, An analysis of young ocean depth, gravity and global residual topography: Geophysical Journal International, v. 178, no. 3, p. 1198-1219.

Dean, S. M., Minshull, T. A., Whitmarsh, R. B., and Louden, K. E., 2000, Deep structure of the ocean-continent transition in the southern Iberia Abyssal Plain from seismic refraction profiles: The IAM-9 transect at 40°20'N: Journal of Geophysical Research: Solid Earth, v. 105, no. B3, p. 5859-5885.

Divins, D. L., 2003, Total Sediment Thickness of the World's Oceans & Marginal Seas, *in* Center, N. N. G. D., ed.: Boulder, CO.

Flament, N., Gurnis, M., and Müller, R. D., 2013, A review of observations and models of dynamic topography: Lithosphere, v. 5, no. 2, p. 189-210.

Hung Kiang, C., Kowsmann, R. O., Figueiredo, A. M. F., and Bender, A., 1992, Tectonics and stratigraphy of the East Brazil Rift system: an overview: Tectonophysics, v. 213, no. 1–2, p. 97-138.

Kaban, M. K., Schwintzer, P., Artemieva, I. M., and Mooney, W. D., 2003, Density of the continental roots: compositional and thermal contributions: Earth and Planetary Science Letters, v. 209, no. 1–2, p. 53-69.

Kusznir, N. J., Roberts, A. M., and Morley, C. K., 1995, Forward and reverse modelling of rift basin formation: Geological Society, London, Special Publications, v. 80, no. 1, p. 33-56.

Laske, G., and Masters, G., 1997, A Global Digital Map of Sediment Thickness, EOS Trans: AGU, v. 78, no. F483.

Laske, G., Masters., G., Ma, Z., and Pasyanos, M., 2013, Update on CRUST1.0 - A 1-degree Global Model of Earth's Crust: Geophys. Res. Abstracts, v. 15.

Mohriak, W., Nemčok, M., and Enciso, G., 2008, South Atlantic divergent margin evolution: rift-border uplift and salt tectonics in the basins of SE Brazil: Geological Society, London, Special Publications, v. 294, no. 1, p. 365-398.

Moulin, M., Aslanian, D., Olivet, J.-L., Contrucci, I., Matias, L., Géli, L., Klingelhoefer, F., Nouzé, H., Réhault, J.-P., and Unternehr, P., 2005, Geological constraints on the evolution of the Angolan margin based on reflection and refraction seismic data (ZaïAngo project): Geophysical Journal International, v. 162, no. 3, p. 793-810.

Müller, R. D., Sdrolias, M., Gaina, C., Steinberger, B., and Heine, C., 2008, Long-Term Sea-Level Fluctuations Driven by Ocean Basin Dynamics: Science, v. 319, no. 5868, p. 1357-1362.

Roberts, A. M., Kusznir, N. J., Yielding, G., and Styles, P., 1998, 2D flexural backstripping of extensional basins; the need for a sideways glance: Petroleum Geoscience, v. 4, no. 4, p. 327-338.

Steinberger, B., 2007, Effects of latent heat release at phase boundaries on flow in the Earth's mantle, phase boundary topography and dynamic topography at the Earth's surface: Physics of the Earth and Planetary Interiors, v. 164, no. 1–2, p. 2-20.

Tucholke, B. E., and Ludwig, W. J., 1982, Structure and origin of the J Anomaly Ridge, western North Atlantic Ocean: Journal of Geophysical Research: Solid Earth, v. 87, no. B11, p. 9389-9407.

Unternehr, P., Péron-Pinvidic, G., Manatschal, G., and Sutra, E., 2010, Hyper-extended crust in the South Atlantic: in search of a model: Petroleum Geoscience, v. 16, no. 3, p. 207-215.

Whitmarsh, R. B., Minshull, T. A., Russell, S. M., Dean, S. M., Louden, K. E., and Chian, D., 2001, The role of syn-rift magmatism in the rift-to-drift evolution of the West Iberia continental margin: geophysical observations: Geological Society, London, Special Publications, v. 187, no. 1, p. 107-124.

Zalán, P. V., Severino, M. C. G., Rigoti, C., Magnavita, L. P., Oliveira, J. A. B., and Viana, A. R., 2011, An entirely new 3D-view of the crustal and mantle structure of a ruptured South Atlantic passive margin – Santos, Campos and Espírito Santo Basins, Brazil (Expanded Abstract): AAPG Annual Convention & Exhibition Abstracts Volume CDROM,Paper 986156.

Zelt, C. A., Sain, K., Naumenko, J. V., and Sawyer, D. S., 2003, Assessment of crustal velocity models using seismic refraction and reflection tomography: Geophysical Journal International, v. 153, no. 3, p. 609-626.

Appendix A - Anomalous Subsidence at the Ocean Continent Transition of the Eastern Gulf of Aden Rifted Continental Margin

Introduction

It has been proposed that some rifted continental margins have anomalous subsidence, and that at breakup they were elevated at shallower bathymetries than the isostatic response predicted by classical rift models (e.g. McKenzie (1978)). The existence of anomalous syn- or early post-breakup subsidence of this form would have important implications for our understanding of the geodynamics of continental breakup and sea-floor spreading initiation. We have investigated the reports of anomalous subsidence along the young (breakup age 17.6Ma) rifted continental margin of the eastern Gulf of Aden, focussing on the ocean continent transition (OCT) of the western Omani margin and northern Socotra margin. Lucazeau et al. (2008) observed significant changes in heat flow at the proximal margin in the eastern Gulf of Aden. Modelling this change in heat flow, it was found that the predicted bathymetry was, in places, about 1km deeper than the observed bathymetry. Lucazeau et al. (2008) suggest that the bathymetric anomalies are the result of an additional thermal anomaly, due to small scale convection processes in the upper mantle. Knowledge and understanding of the OCT structure and continent ocean boundary (COB) location is essential in order to examine the proposition of an anomalous early post breakup subsidence history of the eastern Gulf of Aden. Gravity anomaly inversion has been used to determine Moho depth, crustal basement thickness and continental lithosphere thinning; RDAs have been used to investigate the OCT bathymetric anomalies with respect to expected oceanic

bathymetries at rifted margins, and subsidence analysis has been used to determine the distribution of continental lithosphere thinning.

Geological Setting

The Gulf of Aden is an active young oblique rift system (D'Acremont et al. 2005; Leroy et al. 2010) at the southernmost tip of the Arabian plate, which separates Saudi Arabia to the north from Somalia to the south (Figure A.1(a)). Extension in the eastern Gulf of Aden began at 35Ma (Watchorn et al. 1998), however, sea floor spreading in this region did not begin until much later at 17.6Ma (Leroy et al. 2010; D'Acremont et al. 2006; Fournier et al. 2004; Lucazeau et al. 2008).

We have focussed along eight profiles; the L02, L11, L13 and ENC21 profiles along the Omani margin and the ES30, ES28, ES26 and ES20 profiles along the northern Socotra margin, the location of which are shown in Figure A.1(a).

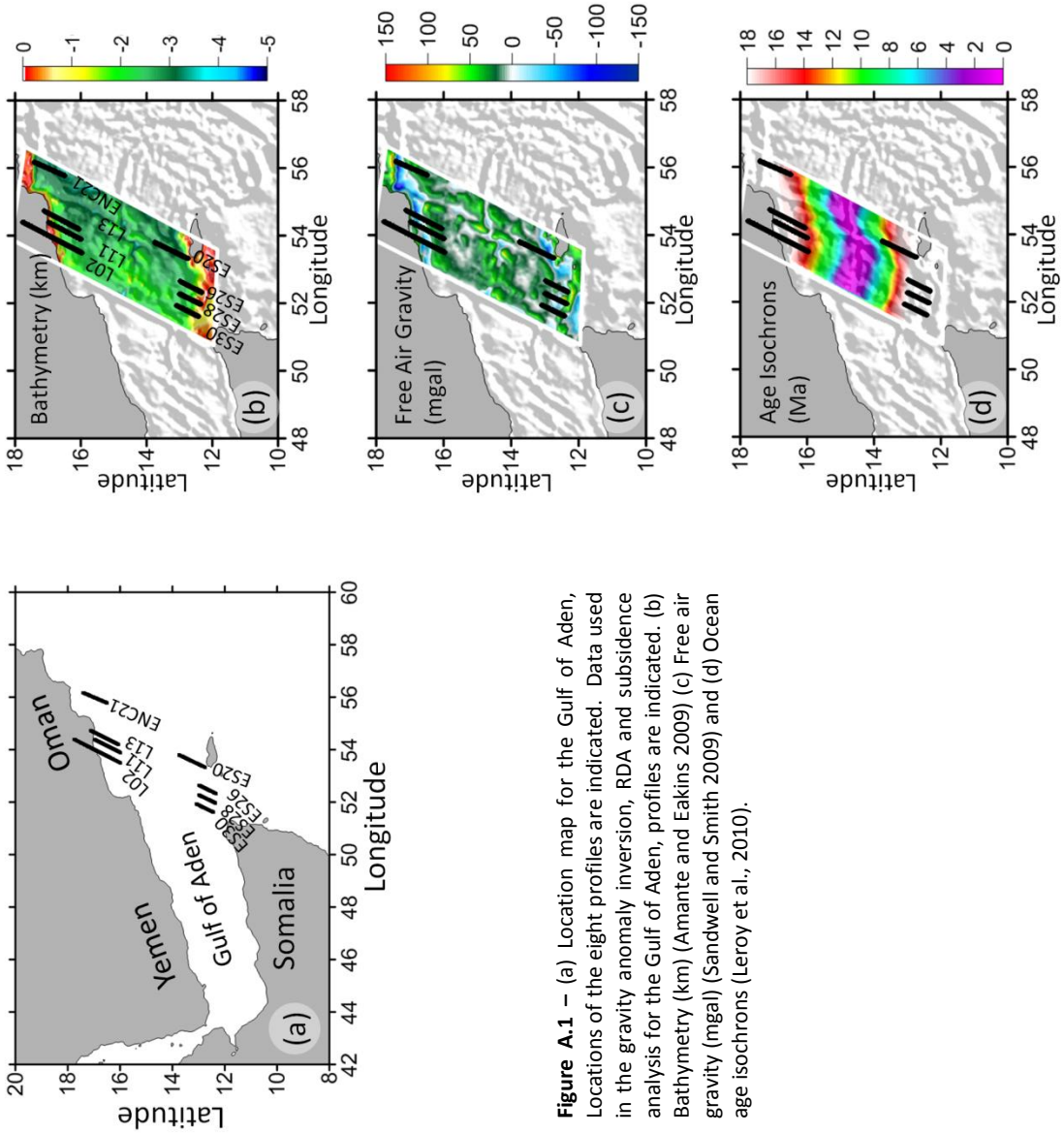

Figure A.1 – (a) Location map for the Gulf of Aden, Locations of the eight profiles are indicated. Data used in the gravity anomaly inversion, RDA and subsidence analysis for the Gulf of Aden, profiles are indicated. (b) Bathymetry (km) (Amante and Eakins 2009) (c) Free air gravity (mgal) (Sandwell and Smith 2009) and (d) Ocean age isochrons (Leroy et al., 2010).

Integrated Quantitative Analysis Methodology

The data used in the gravity anomaly inversion are free air gravity (Sandwell and Smith 2009) (Figure A.1(b)), bathymetry (Amante and Eakins 2009) (Figure A.1(c)), 3D sediment thickness data (Laske and Masters 1997) and ocean age isochrons (Leroy et al. 2004) (Figure A.1(d)). 2D sediment thickness data (D'Acremont et al. 2006; Leroy et al. 2010; Lucazeau et al. 2008; Autin et al. 2010; Watremez et al. 2011) from seismic profiles have been used to calculate 2D

regional gravity anomaly inversion and residual depth anomalies (RDAs), and in subsidence analysis along these Gulf of Aden profiles.

OCT structure, COB location and a measurement of the magnitude of anomalous subsidence have been determined using integrated quantitative analysis techniques, which include gravity anomaly inversion, bathymetric anomalies with respect to expected oceanic bathymetries from RDA analysis and continental lithosphere thinning from subsidence analysis and gravity anomaly inversion. A detailed methodology of the integrated quantitative analysis techniques is described in earlier chapters.

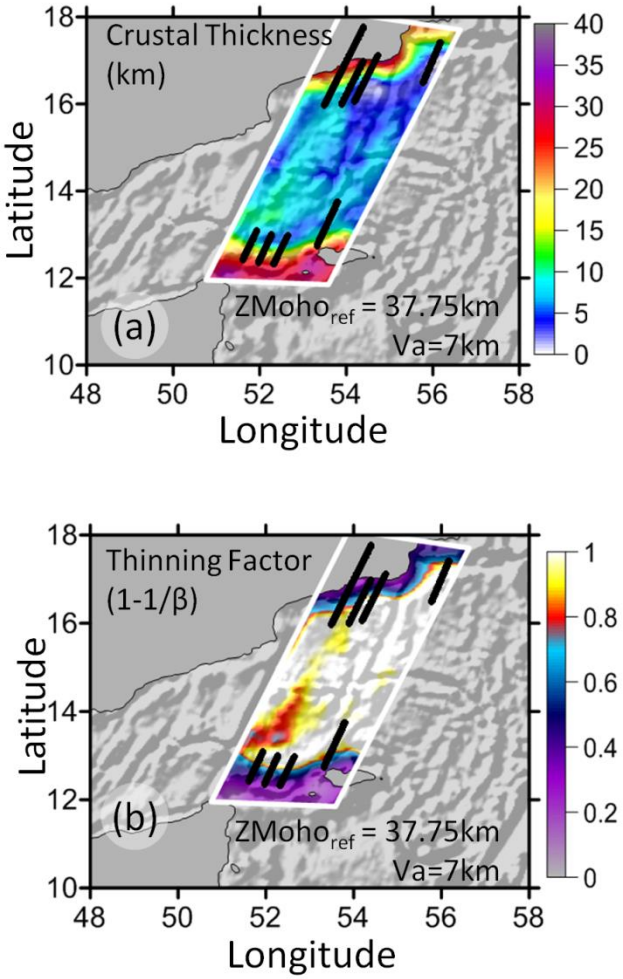

Figure 2 – Gravity anomaly inversion was applied to the Gulf of Aden, using a reference Moho depth ($ZMoho_{ref}$) of 37.5km and assuming a 'normal' magmatic margin (Va=7km). (a) Crustal basement thickness. (b) Continental lithosphere thinning factors (1-1/β). Both show shaded relief free air gravity in the background.

Gravity anomaly inversion is used to determine crustal basement thickness (Figure A.2(a)), Moho Depth and continental lithosphere thinning (Figure A.2(b)). The gravity anomaly inversion method, which is carried out in the 3D spectral domain, using the scheme of Parker (1972), incorporates a lithosphere thermal gravity anomaly correction and also includes a correction for magmatic addition due to decompression melting. Reference Moho depths used in the gravity anomaly inversion have been calibrated against seismic refraction Moho depths along the L02, L11 and L13 profiles (Leroy et al. 2010; Watremez et al. 2011; Autin et al. 2010). Sensitivities to reference Moho depths of 32.5km, 35km, 37.5km, 40km and 42.5km have been considered for these profiles. Calibration of all three profiles, shown in Figure A.3(a), suggests that a reference Moho depth of 38km is required in order to predict crustal basement thicknesses consistent with those seen in the seismic refraction data. However, when considering the profiles individually, we find that the reference Moho depth varies from west to east. Calibration along the westernmost profile (L02) suggests that a reference Moho depth of 34.5km is required (Figure A.3(b)). Moving further eastwards, to the central profile (L11), calibration shows that a larger reference Moho depth of 38.5km (Figure A.3(c)) is required, and calibration of the most eastern profile (L13) suggests that a reference Moho depth of 39.5km is required (Figure A.3(d)).

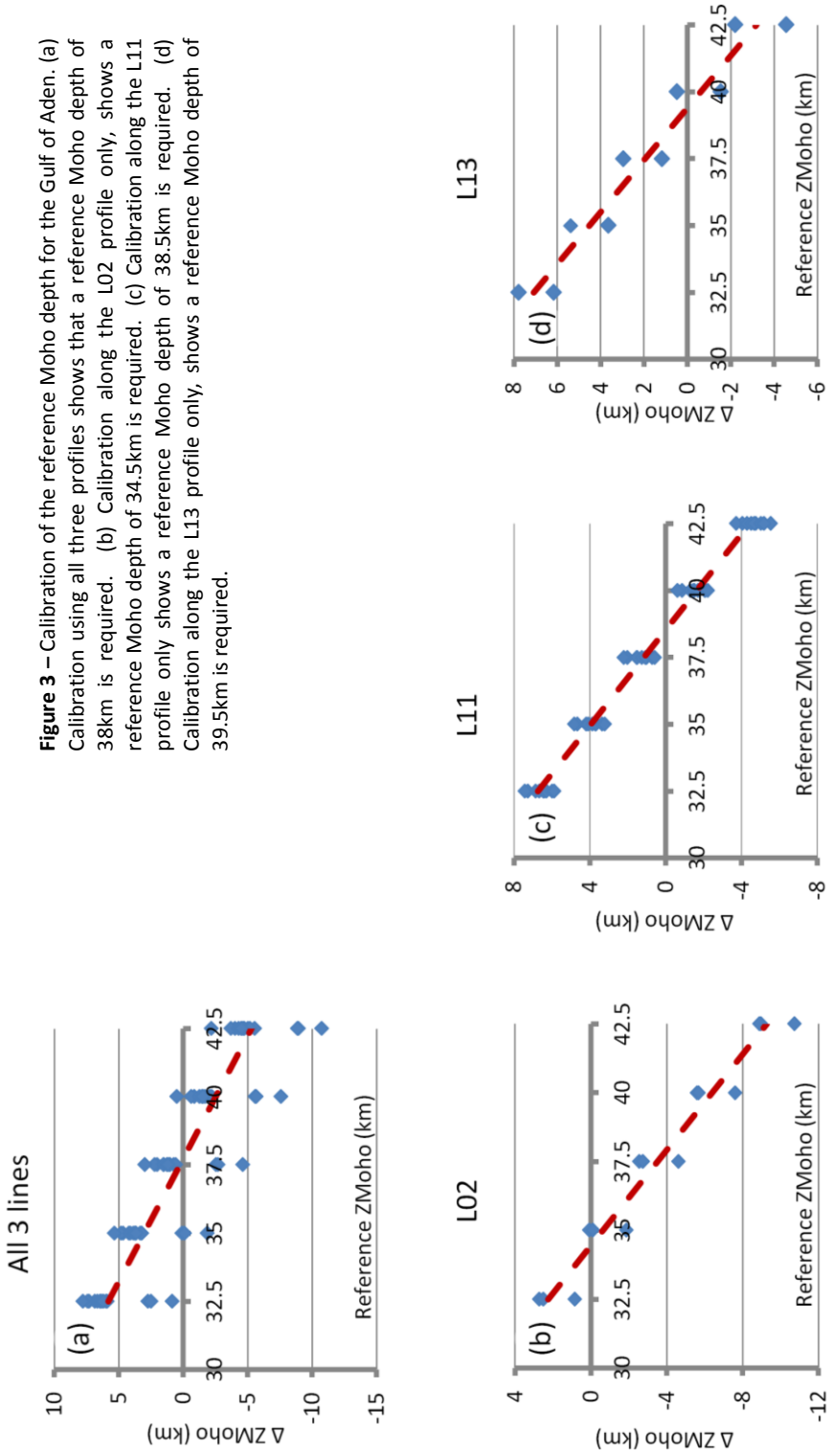

Figure 3 – Calibration of the reference Moho depth for the Gulf of Aden. (a) Calibration using all three profiles shows that a reference Moho depth of 38km is required. (b) Calibration along the L02 profile only, shows a reference Moho depth of 34.5km is required. (c) Calibration along the L11 profile only shows a reference Moho depth of 38.5km is required. (d) Calibration along the L13 profile only, shows a reference Moho depth of 39.5km is required.

RDAs corrected for sediment loading using flexural backstripping and decompaction have been calculated by comparing observed and age predicted oceanic bathymetries, in order to identify anomalous subsidence of the eastern Gulf of Aden rifted continental margin. Age predicted bathymetric anomalies have been calculated using the thermal plate model predictions of Crosby and McKenzie (2009). Oceanic crustal basement thicknesses from gravity anomaly inversion together with Airy isostasy have been used to predict the RDA component from crustal basement thicknesses (RDA_{CT}). The difference (ΔRDA) between the sediment corrected RDA and the RDA_{CT} has been computed in order to determine whether there is any anomalous subsidence or uplift at the Gulf of Aden. This difference (ΔRDA) corresponds to the sediment corrected RDA further corrected for variations in crustal thickness.

Continental lithosphere thinning has been determined from gravity anomaly inversion and subsidence analysis in order to determine the distal extent of continental crust in order to constrain the location of the inner and outer bounds of the OCT. Subsidence analysis involves the conversion of water loaded subsidence into continental lithosphere thinning factors, assuming McKenzie (1978), and includes a correction for decompression melting.

Integrated Quantitative Analysis Results

Composite analysis plots have been constructed for each of the Gulf of Aden profiles. The composite analysis plot consists of; (i) a crustal cross section from gravity anomaly inversion, (ii) sediment corrected RDA and RDA_{CT} along profile, and (iii) a comparison of the continental lithosphere thinning factors predicted from gravity anomaly inversion and subsidence analysis. Figure A.4 shows the composite analysis plots for the profiles along the western Omani margin, whilst Figure A.5 shows the composite analysis plots for the profiles along the northern Socotra margin.

Gravity anomaly inversion and the RDA_{CT} both show 'normal' thickness oceanic crust, with some localised thin oceanic crust along the western Omani margin and northern Socotra profiles. Continental lithosphere thinning factors determined from gravity anomaly inversion and subsidence analysis are in good agreement, and have been used to constrain the location of the COB along the profile lines. These techniques show that the OCT in the eastern Gulf of Aden is relatively narrow, with the distance between the COB and the margin hinge measuring less than 100km.

RDA analysis along the western Omani margin (L02, L11, L13 and ENC21) shows:

(i) Sediment corrected RDAs range between approximately -225m and +500m.

(ii) The RDA_{CT} is negative, ranging between approximately 0m and -700m, which corresponds to the presence of crust that is thinner than 7km.

(iii) Profile L02 and ENC21 have negative ΔRDAs (between approximately 0m and -1200m), which imply anomalous present day subsidence, whereas profiles L11 and L13 have positive ΔRDAs (between approximately 200m and 500m), implying anomalous present day uplift.

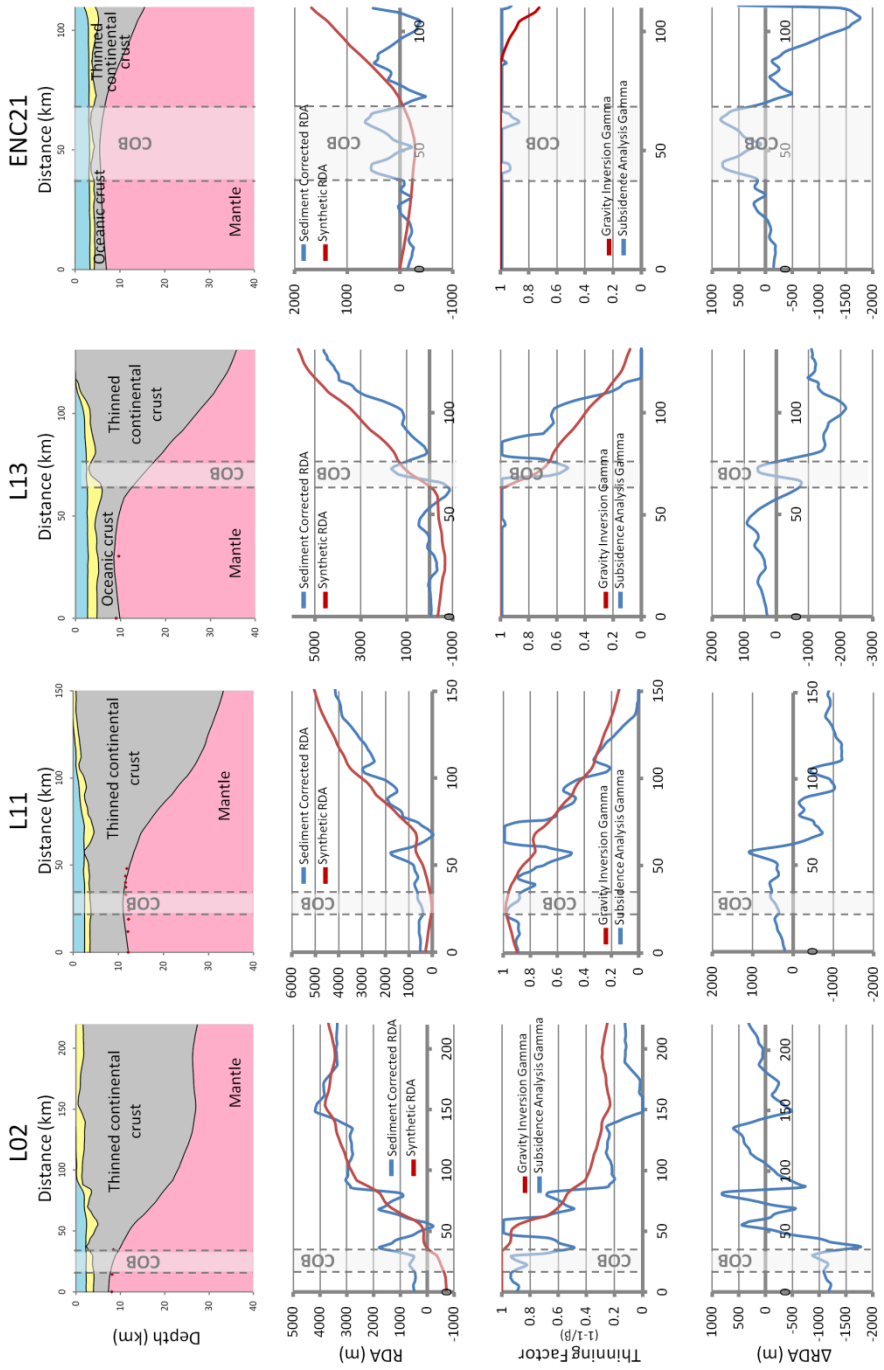

Figure A.4 – Composite analysis plot along the western Omani profiles, showing interpretations of crustal zones made from the integrated quantitative analysis. The composite plot consists of a crustal cross section, RDA analysis, continental lithosphere thinning factors from gravity anomaly inversion and subsidence analysis and a ΔRDA plot to measure the magnitude of anomalous uplift of subsidence in the oceanic domain. We have interpreted the inner and outer bounds of the COB. (a) Composite analysis plot for the L02 profile. (b) Composite analysis plot for the L11 profile. (c) Composite analysis plot for the L13 profile. (d) Composite analysis plot for the ENC21 profile.

Along the northern Socotra margin, RDA analysis shows:

(i) Positive sediment corrected RDAs, which range between approximately 0m and 1000m.

(ii) The RDA_{CT} is negative and range between approximately 0m and -400m, corresponding to the presence of crust that is thinner than 7km.

(iii) The ΔRDAs are positive, indicating anomalous present day uplift ranging between approximately 0m and 1500m, which is comparable to that reported (+1km) by Lucazeau et al. (2008).

The RDA analysis results show that there is heterogeneity not only between the profiles along the western Omani margin and those along the northern Socotra margin, but also between the eastern and western profiles along the western Omani margin of the Gulf of Aden rifted continental margin; this heterogeneity is surprising.

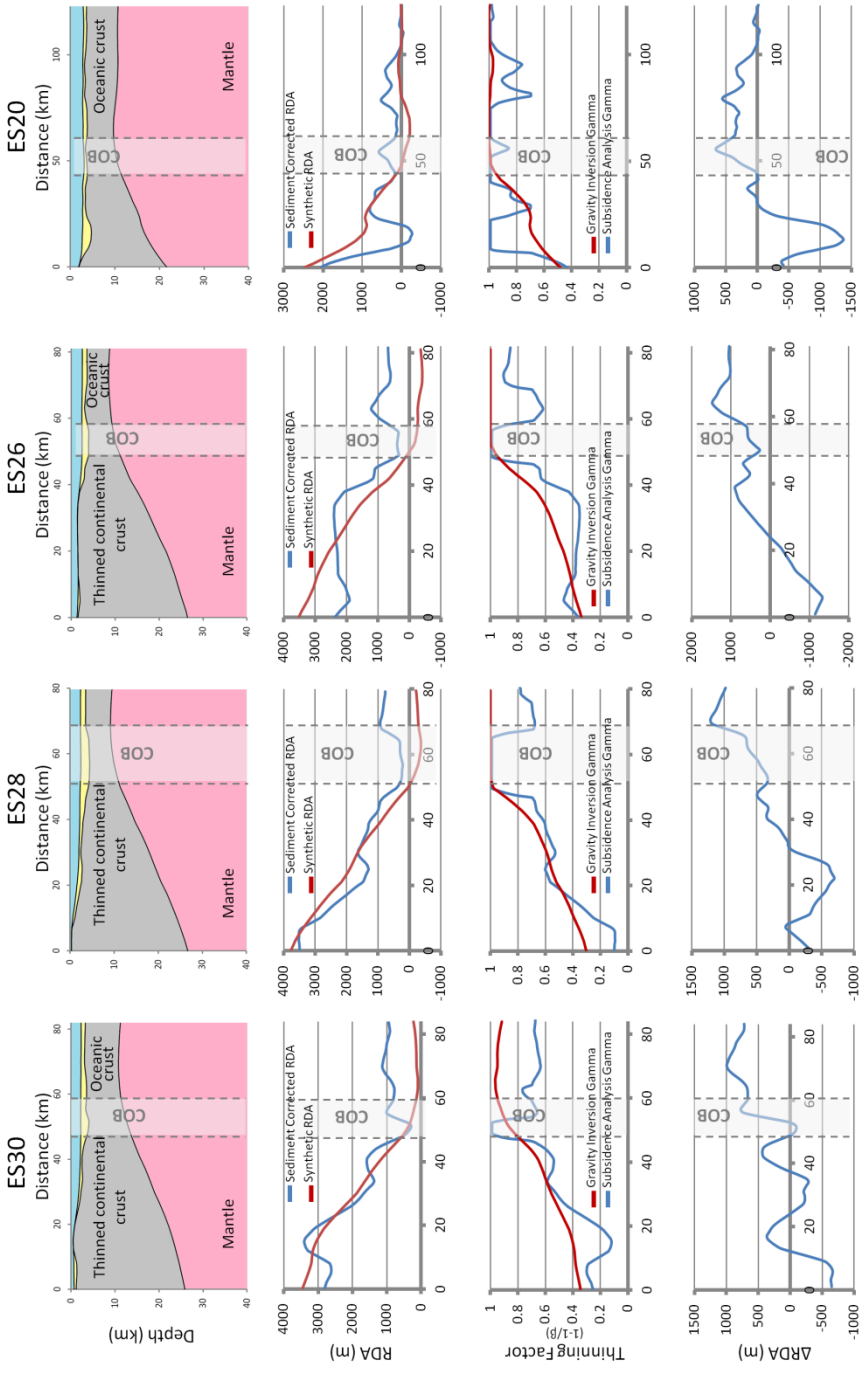

Figure 5 –Composite analysis plot along the northern Socotra profiles, showing interpretations of crustal zones made from the integrated quantitative analysis. The composite plot consists of a crustal cross section, RDA analysis, continental lithosphere thinning factors from gravity anomaly inversion and subsidence analysis and a ΔRDA plot to measure the magnitude of anomalous uplift of subsidence in the oceanic domain. We have interpreted the inner and outer bounds of the COB. (a) Composite analysis plot for the ES30 profile. (b) Composite analysis plot for the ES28 profile. (c) Composite analysis plot for the ES26 profile. (d) Composite analysis plot for the ES20 profile.

References

Amante C, Eakins BW (2009) ETOPO1 1 Arc-Minute Global Relief Model: Procedures, Data Sources and Analysis. NOAA Technical Memorandum NESDIS NGDC-24:19

Autin J, Leroy S, Beslier M-O, d'Acremont E, Razin P, Ribodetti A, Bellahsen N, Robin C, Al Toubi K (2010) Continental break-up history of a deep magma-poor margin based on seismic reflection data (northeastern Gulf of Aden margin, offshore Oman). Geophysical Journal International 180 (2):501-519. doi:10.1111/j.1365-246X.2009.04424.x

Crosby AG, McKenzie D (2009) An analysis of young ocean depth, gravity and global residual topography. Geophysical Journal International 178 (3):1198-1219. doi:10.1111/j.1365-246X.2009.04224.x

D'Acremont E, Leroy S, Beslier M-O, Bellahsen N, Fournier M, Robin C, Maia M, Gente P (2005) Structure and evolution of the eastern Gulf of Aden conjugate margins from seismic reflection data. Geophysical Journal International 160 (3):869-890. doi:10.1111/j.1365-246X.2005.02524.x

D'Acremont E, Leroy S, Maia M, Patriat P, Beslier M-O, Bellahsen N, Fournier M, Gente P (2006) Structure and evolution of the eastern Gulf of Aden: insights from magnetic and gravity data (Encens-Sheba MD117 cruise). Geophysical Journal International 165 (3):786-803. doi:10.1111/j.1365-246X.2006.02950.x

Fournier M, Bellahsen N, Fabbri O, Gunnell Y (2004) Oblique rifting and segmentation of the NE Gulf of Aden passive margin. Geochem Geophys Geosyst 5 (11):Q11005. doi:10.1029/2004gc000731

Laske G, Masters G (1997) A Global Digital Map of Sediment Thickness, EOS Trans. AGU 78 (F483)

Leroy S, Gente P, Fournier M, D'Acremont E, Patriat P, Beslier M-O, Bellahsen N, Maia M, Blais A, Perrot J, Al-Kathiri A, Merkouriev S, Fleury J-M, Ruellan P-Y, Lepvrier C, Huchon P (2004) From rifting to spreading in the eastern Gulf of Aden: a geophysical survey of a young oceanic basin from margin to margin. Terra Nova 16 (4):185-192. doi:10.1111/j.1365-3121.2004.00550.x

Leroy S, Lucazeau F, d'Acremont E, Watremez L, Autin J, Rouzo S, Bellahsen N, Tiberi C, Ebinger C, Beslier M-O, Perrot J, Razin P, Rolandone F, Sloan H, Stuart G, Al Lazki A, Al-Toubi K, Bache F, Bonneville A, Goutorbe B, Huchon P, Unternehr P, Khanbari K (2010) Contrasted styles of rifting in the eastern Gulf of Aden: A combined wide-angle, multichannel seismic, and heat flow survey. Geochem Geophys Geosyst 11 (7):Q07004. doi:10.1029/2009gc002963

Lucazeau F, Leroy S, Bonneville A, Goutorbe B, Rolandone F, d'Acremont E, Watremez L, Düsünur D, Tuchais P, Huchon P, Bellahsen N, Al-Toubi K (2008) Persistent thermal activity at the Eastern Gulf of Aden after continental break-up. Nature Geoscience 1 (12):854-858. doi:10.1038/ngeo359

McKenzie D (1978) Some Remarks on the Development of Sedimentary Basins Earth and Planetary Science Letters 40:25-32

Parker RL (1972) The Rapid Calculation of Potential Anomalies. Geophysical Journal of the Royal Astronomical Society 31 (4):447-455. doi:10.1111/j.1365-246X.1973.tb06513.x

Sandwell DT, Smith WHF (2009) Global marine gravity from retracked Geosat and ERS-1 altimetry: Ridge segmentation versus spreading rate. J Geophys Res B01411 (114(B1))

Watchorn F, Nichols GJ, Bosence DWJ (1998) Rift-related sedimentation and stratigraphy, southern Yemen (Gulf of Aden). In: Purser B, Bosence DJ (eds) Sedimentation and Tectonics in Rift Basins Red Sea:- Gulf of Aden. Springer Netherlands, pp 165-189. doi:10.1007/978-94-011-4930-3_11

Watremez L, Leroy S, Rouzo S, d'Acremont E, Unternehr P, Ebinger C, Lucazeau F, Al-Lazki A (2011) The crustal structure of the north-eastern Gulf of Aden continental margin: insights from wide-angle seismic data. Geophysical Journal International 184 (2):575-594. doi:10.1111/j.1365-246X.2010.04881.x

Appendix B - Crustal Thickness and the Distribution of Oceanic Lithosphere in the Western Mediterranean from Gravity Inversion

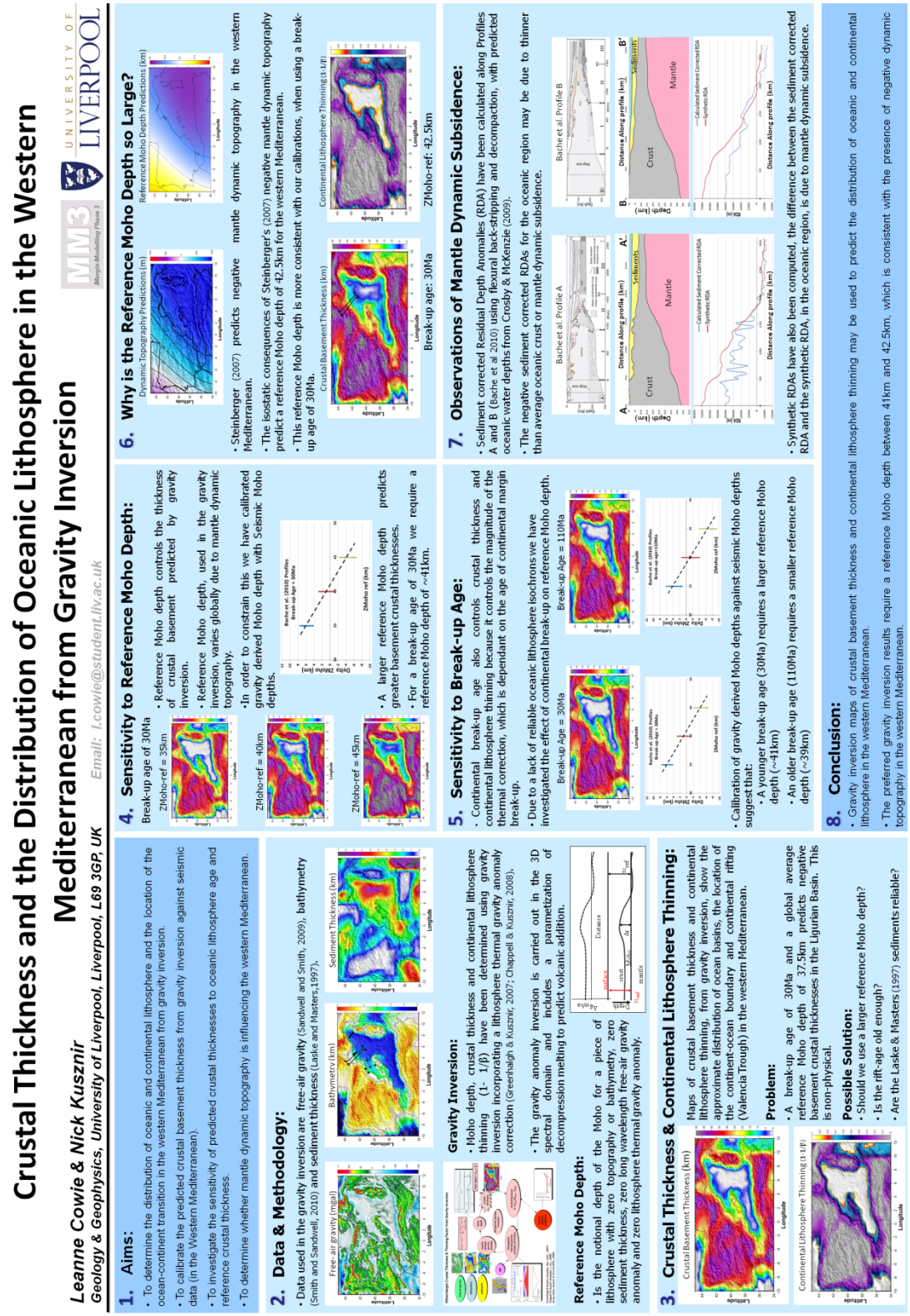

Appendix C - Crustal Thickness and the Distribution of Oceanic Lithosphere in the Eastern Mediterranean from Gravity Inversion

Preface

This appendix consists of a previously published paper, which can be found in *Petroleum Geoscience* 2012. v.18; p373-380

Mapping crustal thickness and oceanic lithosphere distribution in the Eastern Mediterranean using gravity inversion

Leanne Cowie* and Nick Kusznir

Geology & Geophysics, University of Liverpool, Liverpool L69 3BX, UK
**Corresponding author (e-mail: l.cowie@liverpool.ac.uk)*

ABSTRACT: Oceanic and continental lithosphere distribution within the eastern Mediterranean is not well understood. A gravity inversion, incorporating a lithosphere thermal gravity anomaly correction, has been used to map Moho depth, crustal thickness and lithosphere thinning for the eastern Mediterranean, from which the distribution of oceanic and continental lithosphere, the structure of the ocean–continent transition (OCT) and the location of the continent–ocean boundary (COB) can be determined. The gravity inversion results show thin crust and high continental lithosphere thinning under the Ionian Sea and the Herodotus Basin, consistent with these basins being underlain by oceanic crust. Moho depths from gravity inversion are in agreement with seismic refraction estimates in these basins. Highly thinned continental crust is predicted under the offshore Sirte and Levant basins. The sharp decrease in crustal thickness predicted by gravity inversion off the Libyan and Egyptian coast gives an indication of COB location. Crustal thickness and continental lithosphere thinning determined from gravity inversion have also been used to explore the relationship between the Cretaceous West and Central African Rift System (WCARS: Benue Trough, Chad, Central African Shear Zone (CASZ) and Sudan basins) and the eastern Mediterranean basins; continuity between the Cretaceous WCARS and the eastern Mediterranean basins is not apparent in the gravity inversion results.

INTRODUCTION

The distribution of oceanic and continental lithosphere in the eastern Mediterranean is not well understood; in particular the location of the continent–ocean boundary (COB) and the crustal structure of the basin regions and the ocean–continent transition (OCT) is a topic of much debate. Gravity inversion, incorporating a lithosphere thermal gravity anomaly correction, has been used to map Moho depth, crustal thickness and continental lithosphere thinning for the eastern Mediterranean, in order to determine the distribution of oceanic and continental lithosphere and the COB location.

The age of formation of the eastern Mediterranean basins, in particular the Ionian, the Herodotus and the Sirte basins, is uncertain. Dercourt *et al*. (1993) propose that the eastern Mediterranean is Cretaceous in age (Aptian to Campanian) and is linked to the closure of the Tethys Ocean, whereas Stampfli *et al*. (2008) and Hallett (2002) propose that the eastern Mediterranean is late Triassic in age and is linked to the break-up of Pangaea and the closure of the Neo-Tethys and Tethys oceans. The onshore and offshore Sirte Basins are known to be Cretaceous in age (Middle Aptian to Late Albian) (Gumati & Nairn 1991) and it is often assumed (e.g. Moulin *et al*. 2010) that the rifting that resulted in these basins is linked to that of the Cretaceous West and Central African Rift System (WCARS) which formed the Benue Trough, Chad, Central African Shear Zone (CASZ) and Sudan basins. The Early Cretaceous rifting episodes in West and Central Africa, located within Pan-African zones of lithospheric weakness (Daly *et al*. 1989), are related to the opening of the South and Equatorial Atlantic Ocean (Guiraud *et al*. 1992). The Cretaceous rift systems of West and Central Africa extend eastwards through southern Chad into South Sudan and Kenya (Binks & Fairhead 1992) and it has been proposed that this rifting extended northwards to form the Cretaceous Sirte Basin of the eastern Mediterranean. However, the question remains whether the eastern Mediterranean basins are Cretaceous in age and whether they and the Sirte Basin are related to the rifting that created the Cretaceous WCARS. Gravity inversion has been used to map crustal thickness and continental lithosphere thinning in order to delineate the geometry of the eastern Mediterranean basins and their possible connectivity to rifting within the Cretaceous WCARS. Gravity inversion sensitivities to break-up ages of 225 Ma (late Triassic) and 100 Ma (mid-Cretaceous) have been examined.

An understanding of crustal structure and the distribution of oceanic and continental lithosphere within the eastern Mediterranean region, and hence the location of the COB, is of great importance in order to build a better geodynamic history and plate tectonic reconstruction model for this area. The determination of the distribution of oceanic and continental lithosphere is also important for the evaluation of potential hydrocarbon prospects. Evidence and further understanding of the relationship that may exist between the Cretaceous WCARS and the eastern Mediterranean basins will provide further constraints

Petroleum Geoscience, Vol. **18**, 2012, pp. 373–380
DOI: 10.1144/petgeo2011-071.

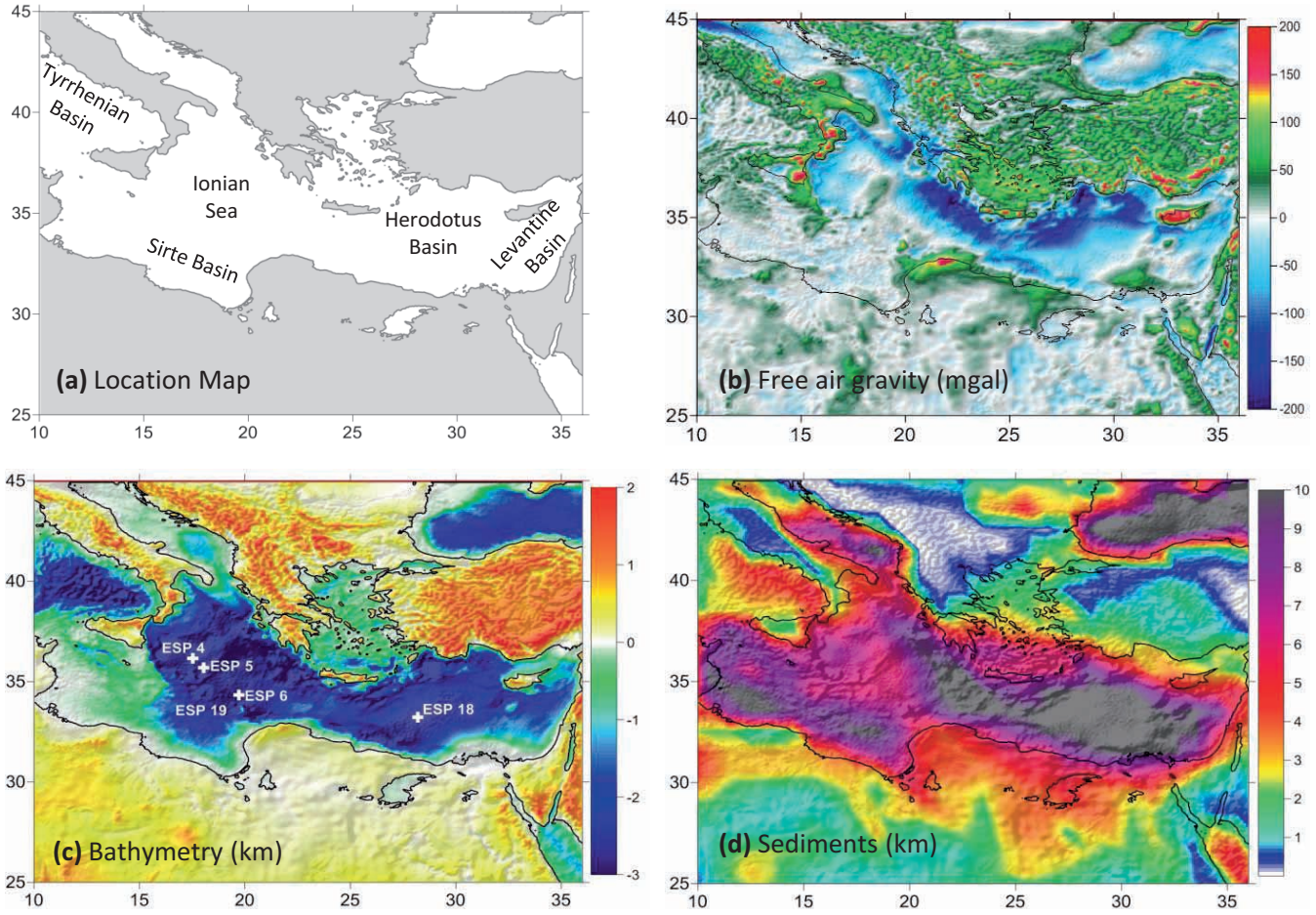

Fig. 1. Data used in the gravity inversion for the eastern Mediterranean: (**a**) location map identifying the key basins of the eastern Mediterranean; (**b**) free-air gravity anomaly (Sandwell & Smith 2009); (**c**) bathymetry (topography) (Sandwell & Smith 2009), with the locations of the ESP seismic data (de Voogd *et al*. 1992); (**d**) sediment thickness (Laske & Masters 1997).

for the formation processes of the eastern Mediterranean, whilst also providing further insight into the geodynamic history of this region. Gravity inversion, incorporating a lithosphere thermal gravity anomaly correction, has therefore been applied, in an attempt to better identify the distribution of oceanic and continental crust from the resulting crustal thickness and continental lithosphere thinning maps. The results from the inversion have been successfully tested against expanding spread profile (ESP) seismic estimates of Moho depth (de Voogd *et al*. 1992).

GRAVITY INVERSION DATA AND METHODOLOGY

The data used in the gravity inversion are free-air gravity and bathymetry (Sandwell & Smith 2009), and sediment thickness data (Laske & Masters 1997) as shown in Figure 1. Basin regions are identified in Figure 1a. The free-air gravity anomaly data (Fig. 1b) show a large negative anomaly corresponding to the subduction of the African plate beneath the Eurasian plate at the Hellenic Arc. Greatest bathymetric depths are observed in the basin regions of the Ionian, Tyrrhenian and the Herodotus seas (Fig. 1c). Thickest sediments are also observed in these basin regions (Fig. 1d). Moho depths from the gravity inversion are dependent on the age of oceanic lithosphere and continental break-up due to the lithosphere thermal gravity correction. As previously mentioned there are no ocean age isochrons available for the eastern Mediterranean and consequently continental break-up ages based on literature (Hallett 2002; Stampfli *et al*. 2008) have been assumed. A late Triassic age of 225 Ma and a mid-Cretaceous age of 100 Ma have both been examined within the gravity inversion. When considering the relationship between the Cretaceous WCARS and the eastern Mediterranean basins, a Cretaceous age of 100 Ma has been used.

In order to determine Moho topographic relief from gravity inversion, it is necessary to isolate the gravity anomaly due to changes in Moho depth. The principal contributions to the free-air gravity anomaly at rifted margins and in oceanic lithosphere are from the bathymetry (Δg_b), sediments (Δg_s), the Moho relief anomaly (Δg_{mra}) and the lithosphere thermal gravity anomaly (Δg_{tga}).

$$\Delta g_{fag} = \Delta g_b + \Delta g_s + \Delta g_{mra} + \Delta g_{tga}. \quad (1)$$

Moho relief (Δr) is calculated from the Moho relief anomaly, Δg_{mra}, where Δg_{mra} is given by,

$$\Delta g_{mra} = \Delta g_{fag} - \Delta g_b - \Delta g_s - \Delta g_{tga}. \quad (2)$$

The gravity inversion of Δg_{mra} to give Moho relief (Δr) is carried out in the 3D spectral domain using the scheme of

Parker (1972). Prior to the inversion of Δg_{mra} to give Moho depth, it was filtered to remove the high frequency components using a Butterworth low-pass filter with a cut-off wavelength of 100 km. This removes short-wavelength errors in Δg_b and Δg_s, and gravity anomalies due to crustal basement density variations. Basement crustal thickness (Ct) is calculated from the Moho relief (Δr) and reference Moho depth ($Zmoho_{ref}$)

$$Zmoho = Zmoho_{ref} + \Delta r, \tag{3}$$

$$Ct = Zmoho - b, \tag{4}$$

where $Zmoho$ is the Moho depth and b is the bathymetry. $Zmoho_{ref}$ is strongly influenced by mantle dynamic topography. In order to constrain $Zmoho_{ref}$, predicted Moho depths (or basement crustal thicknesses) determined from gravity inversion need to be calibrated against seismic Moho depths.

A crustal basement density of 2850 kgm^{-3} is assumed for both oceanic and continental crust (Chappell & Kusznir 2008). Sensitivity tests of this value have been carried out with the range 2800 kgm^{-3} to 2900 kg m^{-3} and do not change the interpretation of the results. Different values of oceanic and continental basement density are not used so as to avoid prejudicing the gravity inversion prediction of continent–ocean boundary with *a priori* information. Sediment densities used to determine Δg_s increase with depth, assuming normal compaction corresponding to a shaly-sand lithology. The gravity anomaly effect of the variation in lithosphere density due to elevated geothermal gradient (following continental lithosphere thinning and seafloor spreading) is taken into account by the lithosphere thermal gravity anomaly correction.

Lithosphere stretching and thinning of the rifted continental margin regions and oceanic seafloor spreading result in elevated lithosphere geotherms. The lithosphere thermal gravity anomaly, $\Delta g_{tga,}$ is caused by lateral variations in temperature and density between the hot oceanic and rifted continental margin lithosphere and the cooler unstretched continental lithosphere. The lithosphere thermal gravity correction, Δg_{tga}, is described in detail in Greenhalgh & Kusznir (2007), Alvey *et al*. (2008) and Chappell & Kusznir (2008).

The lithosphere thermal gravity anomaly correction using the lithosphere stretching and thinning model of McKenzie (1978) requires, at each aerial location, the lithosphere stretching factor, β, to define the lithosphere thermal perturbation, and the lithosphere thermal re-equilibration time, t. For oceanic lithosphere $\beta = \infty$, while for continental margin lithosphere β is calculated from the gravity inversion results using

$$\beta = \frac{Ct_{Init}}{Ct - Ct_{mag}}, \tag{5}$$

where Ct_{Init} is the initial continental crustal thickness, Ct is the present-day crustal thickness predicted from gravity inversion and Ct_{mag} is crustal volcanic addition from decompressional melting during continental break-up and rifting and seafloor spreading (White & McKenzie 1989), leading to the addition of volcanic material to the crust. It is assumed that lithosphere stretching and thinning is equal to crustal stretching and thinning; i.e. the lithosphere deforms by pure shear (Greenhalgh & Kusznir 2007; Alvey *et al*. 2008; Chappell & Kusznir 2008).

The thickness of the crustal volcanic addition is estimated using the parameterization of the decompressional melting model of White & McKenzie (1989), from the lithosphere thinning factor, γ, determined from gravity inversion, where

$$\gamma = 1 - \frac{1}{\beta} \tag{6}$$

(Greenhalgh & Kusznir 2007; Alvey *et al*. 2008). A critical thinning factor for the initiation of decompressional melting of 0.7 and a maximum volcanic addition of 7 km (for β=1) have been used for the eastern Mediterranean. This corresponds to 'normal' decompressional melt that predicts a 7 km thick oceanic crust.

The thermal equilibration time (cooling time) of continental margin lithosphere is equivalent to the continental break-up age. Continental break-up ages of 100 Ma and 225 Ma have been examined. In the absence of reliable oceanic isochrons for the eastern Mediterranean, continental break-up ages have been used to give the oceanic lithosphere thermal equilibration time.

CRUSTAL THICKNESS AND LITHOSPHERE THINNING FACTOR FOR THE EASTERN MEDITERRANEAN FROM GRAVITY INVERSION

Basement crustal thickness and continental lithosphere thinning factor maps produced by gravity inversion are shown in Figure 2, where the sensitivity of the gravity inversion to continental break-up age and reference Moho depth has been examined. Higher continental lithosphere thinning factors denote more stretching and thinning of continental lithosphere; thinning factors of 1 correspond to oceanic lithosphere. Both the crustal thickness and continental lithosphere thinning factor maps show thinner crust and higher lithosphere thinning for the Ionian, Herodotus and Tyrrhenian basins compared with the surrounding areas, consistent with these basins being underlain by oceanic crust or highly thinned continental crust. Thinned continental crust is also predicted under the offshore Sirte and the Levantine basins, and also under northern Egypt. Similar distributions of oceanic crust or thinned continental crust are seen in the crustal thickness and continental lithosphere thinning maps from gravity inversion using the two break-up ages and also the two reference Moho depths.

The reference Moho depths for the eastern Mediterranean have been determined by calibration using ESP seismic data (de Voogd *et al*. 1992). Reference Moho depth values of 35 km, 40 km, 45 km and 50 km have been considered for the eastern Mediterranean. Plots of the difference between seismic basement crustal thickness and gravity-derived crustal thickness (Δ crustal thickness) against reference Moho depths are shown in Figure 3. The sensitivity of the calibration to the continental break-up age used to give the thermal re-equilibration time (cooling time) for the lithosphere thermal re-equilibration after stretching and thinning has been examined. Figure 3a illustrates that for a mid-Cretaceous (100 Ma) break-up age, a reference Moho depth of approximately 47 km produces results most comparable to those seen in the ESP data, whereas for a late Triassic (225 Ma) break-up age (Fig. 3b), a reference Moho depth of 45 km produces the best comparison between the crustal thickness from gravity inversion, and that from the ESP data. Break-up ages of both 100 Ma and 225 Ma produce crustal thickness results comparable to those seen in the ESP data and it is concluded that, with the available data, it is not possible to further constrain break-up age.

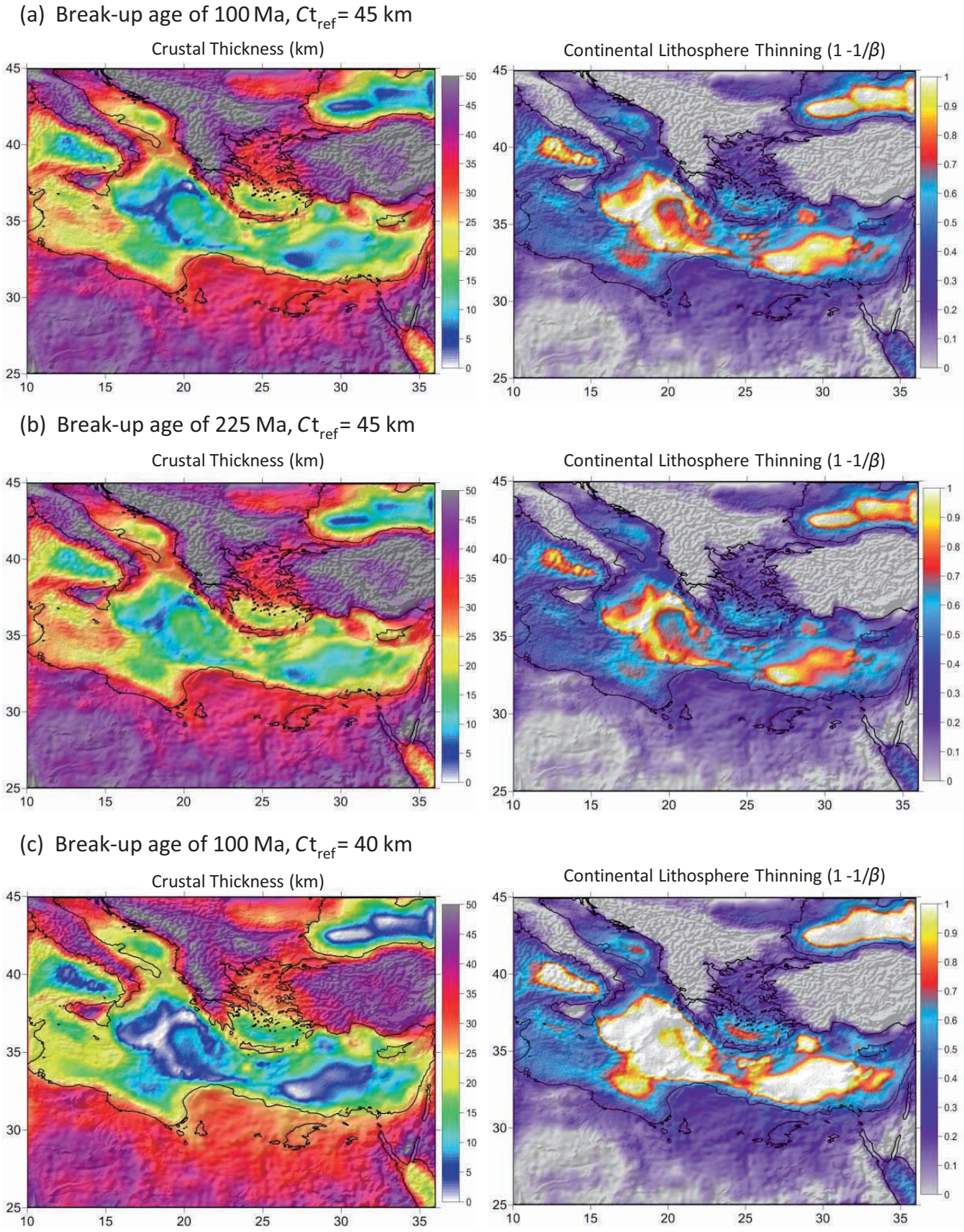

Fig. 2. Crustal thickness and continental lithosphere thinning factor maps, determined from gravity inversion, showing sensitivity to reference Moho depth and continental break-up age. (**a**) Break-up age of 100 Ma with a reference Moho depth of 45 km; (**b**) break-up age of 225 Ma with a reference Moho depth of 45 km; (**c**) break-up age of 100 Ma with a reference Moho depth of 40 km.

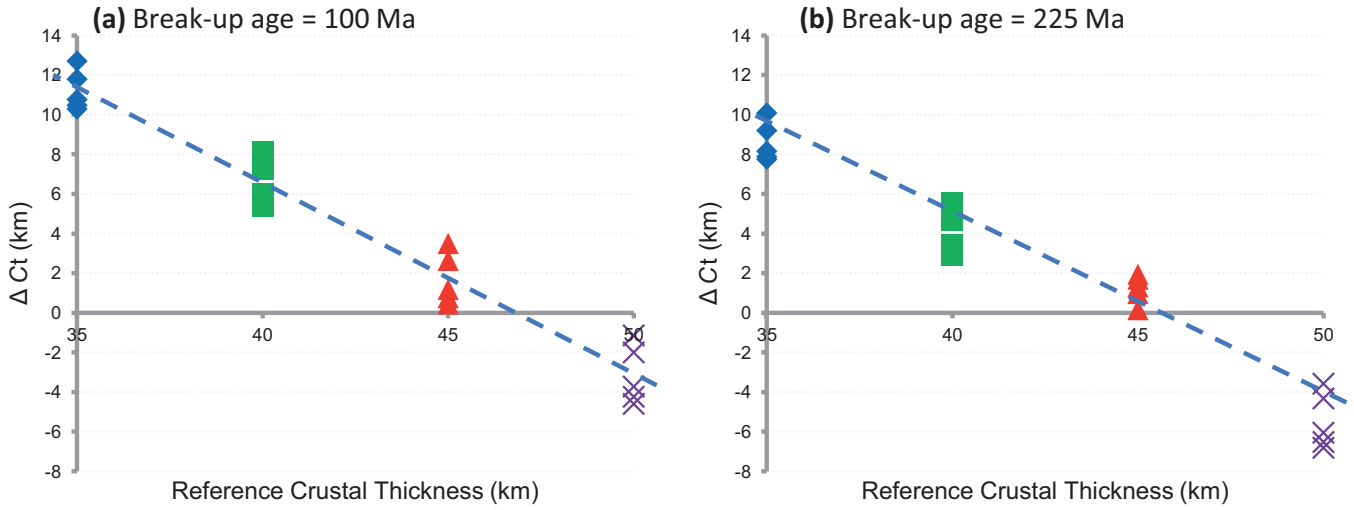

Fig. 3. Δ crustal thickness plots of the difference between seismic refraction (de Voogd *et al.* 1992) and gravity inversion estimates of basement thickness against reference Moho depths of 35, 40, 45 and 50 km used in the gravity inversion. (Δ crustal thickness = seismic basement crustal thickness – gravity-derived basement crustal thickness).

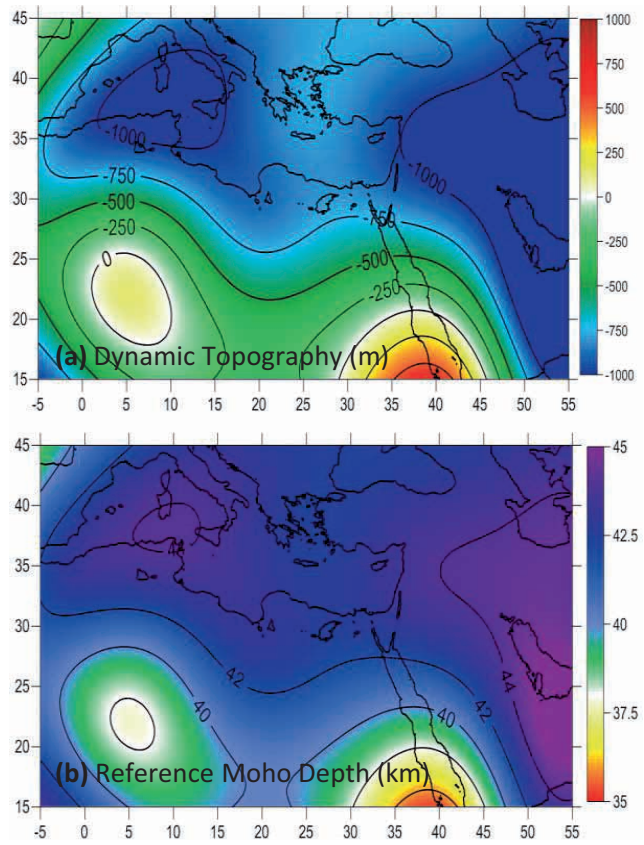

Fig. 4. (**a**) Mantle dynamic topography predicted by Steinberger (2007) showing mantle dynamic subsidence in the eastern Mediterranean. (**b**) Predicted reference Moho depth for the eastern Mediterranean calculated from dynamic topography. Values between 42 km and 44 km are predicted for the eastern Mediterranean.

Reference Moho depth is the notional depth of the Moho for a piece of lithosphere with zero topography or bathymetry, zero sediment thickness, zero long wavelength free-air gravity anomaly and zero lithosphere thermal gravity anomaly. Globally the reference Moho depth used in the gravity inversion technique described above, determined by calibration against seismic observation and assuming a crustal basement density of 2850 kg m^{-3}, is approximately 38 km; however, it varies regionally due to mantle dynamic topography. In regions of mantle dynamic uplift (e.g. above a mantle plume) it is decreased, while in regions of mantle dynamic subsidence (e.g. in a subduction retroarc region) it is increased. The values of reference Moho depth determined for the eastern Mediterranean, described above, are substantially greater than the global average of 38 km, but are consistent with this region experiencing mantle dynamic subsidence from subduction both past and present. Dynamic topography predictions (Fig. 4a) from Steinberger (2007) suggest that the eastern Mediterranean is experiencing negative dynamic topography in the range –800 m and –1000 m. The predicted reference Moho depth using the Steinberger (2007) dynamic subsidence, and simple isostasy, is shown in Figure 4b, for the eastern Mediterranean. The predicted values from dynamic topography are in the range 42 km to 44 km, which are near to the value of 45 km from the seismic calibration results (Fig. 3) when using a break-up age of 225 Ma. The remaining difference may be attributed to the long wavelength gravity anomaly signal of present-day Hellenic Arc subduction.

DISCUSSION

Sirte Basin and Ionian Sea

The very thin crust and high continental lithosphere thinning factors predicted from gravity inversion for the Sirte Basin and Ionian Sea (Fig. 5) are consistent with these basins being underlain by oceanic crust or highly thinned continental crust. This interpretation is not dependent on the age of formation of these basins used in the thermal gravity anomaly correction. Substantially thinned continental crust with thickness less than 25 km and thinning factors of 0.5 or greater are also predicted within the offshore Sirte Basin between onshore Libya and the Ionian Sea. Moho depths determined from gravity inversion have been used to construct crustal cross-sections (A–A′ and B–B′) across the Ionian and offshore Sirte Basins of the eastern Mediterranean, shown in Figure 5. These crustal cross-sections show the relationship between bathymetry, sediment cover and

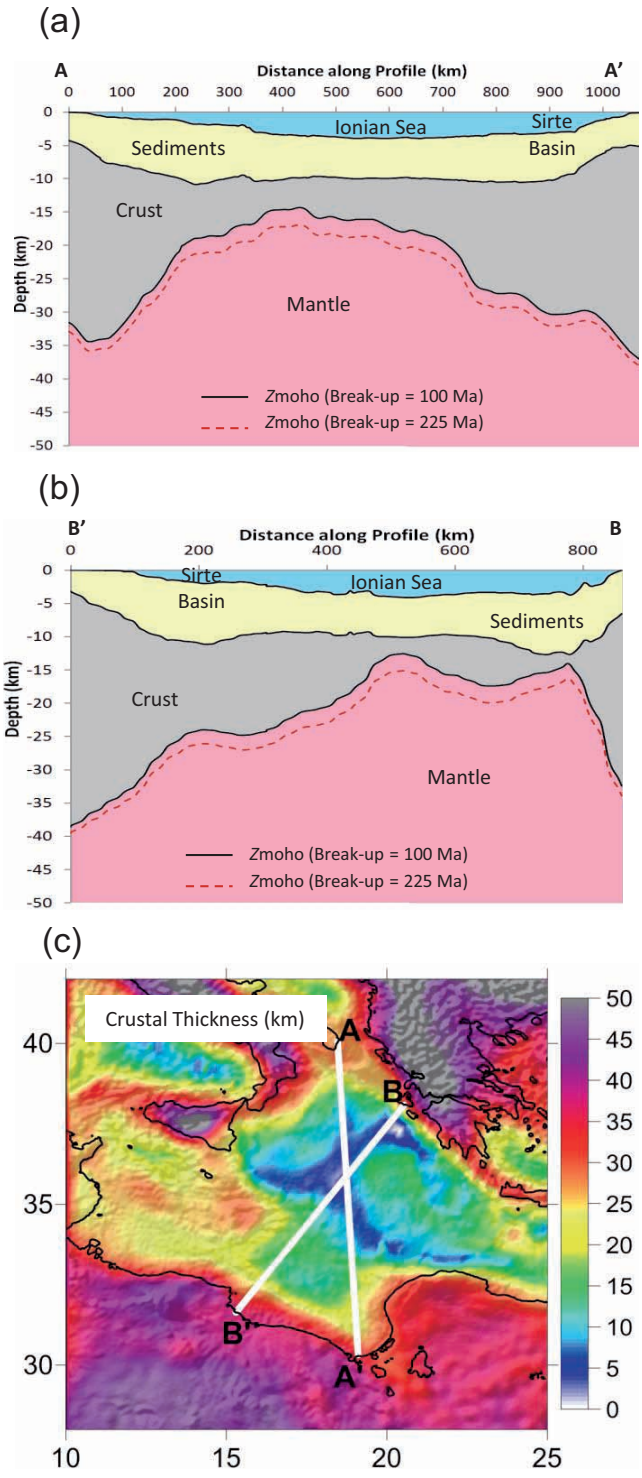

Fig. 5. (**a**) Map of the Sirte Basin and the Ionian Sea, showing predicted crustal thickness determined from gravity inversion using a late Triassic (225 Ma) break-up age. (**b**), (**c**) Crustal cross-section along profile A–A′ and B–B′ show bathymetry, sediment thickness and Moho depth determined from gravity inversion. Moho depth sensitivities to break-up age are indicated.

Moho depth calculated from the gravity inversion. Crustal thicknesses are greatest either side of the basin regions, for both break-up ages, with a maximum crustal thickness of 28 km for a break-up age of 225 Ma, and 32 km for a break-up age of 100 Ma. Minimum crustal thicknesses of 6 km for a break-up age of 225 Ma, and 10 km for a break-up age of 100 Ma, are predicted in the centre of the Ionian Basin.

A region of very thin continental crust, with thicknesses less than 15 km, is predicted within the eastern offshore Sirte Basin. Cross-sections A–A′ and B–B′, shown in Figure 5, cross this region and show that a broad region of highly thinned continental crust of 200 km width or greater lies between the continental margin hinge to the SW near the coast and the interpreted COB with the Ionian ocean basin to the NE. The broad region of highly thinned continental crust underlying the offshore Sirte Basin is similar to that observed on the northern Angolan margin (Contrucci *et al*. 2004) and on many other rifted continental margins.

Herodotus and Levantine Basins

In the Herodotus and Levantine basins (Fig. 6), crustal cross-sections (C–C′ and D–D′) have been used to examine the structure of the eastern margins of the eastern Mediterranean. The width of the transition region from thick crust inboard of the margin hinge to thin outboard oceanic crust may be used to help determine whether a margin is a transform or rifted continental margin. Gravity inversion predicts a broad transition from thick to thinned continental crust within the Levantine Basin (D–D′) located in the extreme east of the eastern Mediterranean (Fig. 6), which most probably indicates that this is a rifted continental margin. Rift basin axes in the Levantine Basin appear to be orientated NNE–SSW and are separated by intervening structural highs with a similar orientation.

To the south of the very thin crust predicted by gravity inversion, interpreted as oceanic crust, within the Herodotus Basin and the eastern Ionian Sea there is a sharp increase in crustal thickness on to continental crust. Interpretation of these results suggest that the COB to the south of the Herodotus Basin and the eastern Ionian Sea (to the north of Egypt and eastern Libya) corresponds to a transform margin (Fig. 6), although it is difficult to envisage how this relates to the proposed COB between the Sirte Basin and the SW Ionian Sea. A transform continental margin north of Egypt would, however, be consistent with the NNE–SSW rift basin axis and rifted COB within the Levantine Basin.

North Africa

Gravity inversion has also been applied to North Africa in order to examine the potential tectonic relationship between the Cretaceous WCARS and the Sirte and Ionian basins of the eastern Mediterranean. The continental lithosphere thinning factor map for North Africa from gravity inversion using a continental break-up age of 100 Ma is shown in Figure 7. From Figure 7, it is clear that there is no direct linkage between the extensional tectonics of the Cretaceous WCARS and that responsible for the formation of the Cretaceous Sirte Basin, as previously thought. There appears to be no continuity or connectivity between the Cretaceous WCARS (Benue Trough, Chad, CASZ and Sudan basins) and the Sirte and Ionian basins of the eastern Mediterranean. If that is true, then what are the origins and alternative regional tectonic linkages of Cretaceous Sirte Basin rifting? One possibility, consistent with the NW–SE strike orientation of the Sirte Basin, is that it may be a SE continuation of Early Cretaceous rifting to the NW which led to Albian–Cenomanian continental break-up and seafloor spreading within the Bay of Biscay. If the Ionian Sea is also underlain by Cretaceous oceanic crust, it may also form the SE extremity of this Late Cretaceous seafloor spreading system. As Cretaceous rifting in West and Central Africa does not link through to the eastern Mediterranean, the age of the eastern

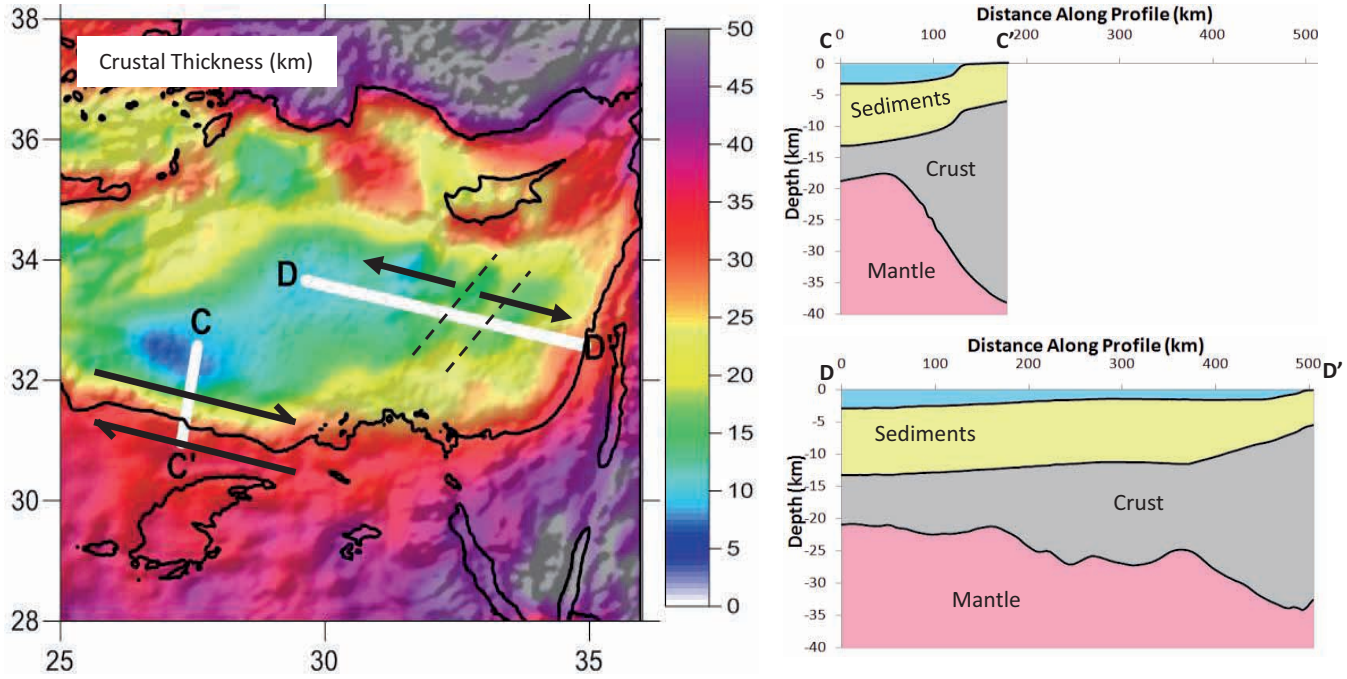

Fig. 6. Map of the Levantine Basin, showing predicted crustal thickness determined from gravity inversion using a late Triassic (225 Ma) break-up age. Arrows indicate rift and transform margin kinematics. Dashed lines indicate NE-SW strike of rifting on the Levant margin. Cross-sections C–C′ and D–D′ show crustal structure cross-section through the transform margin and the rift margin, respectively.

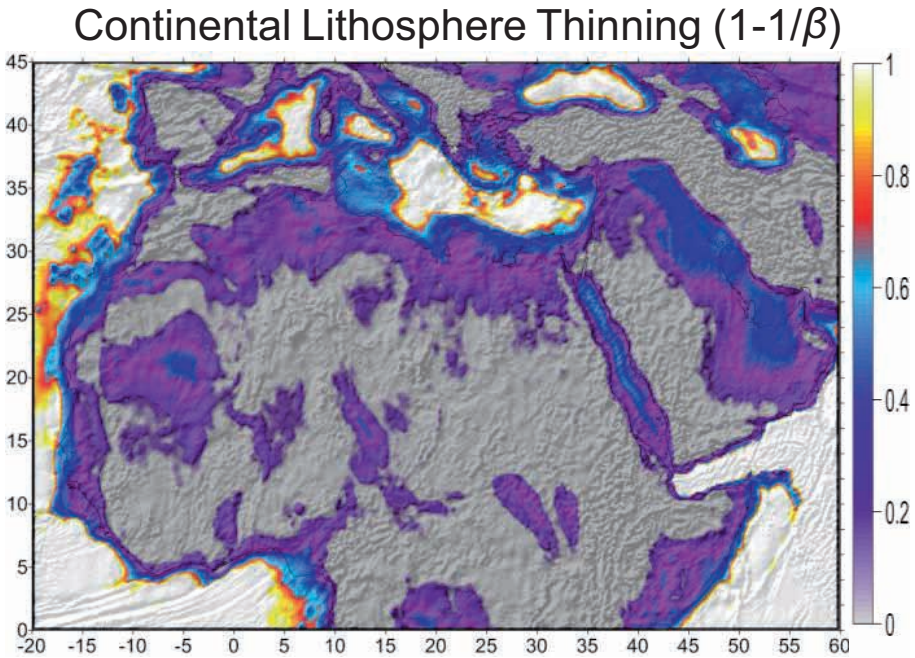

Fig. 7. Continental lithosphere thinning map for North Africa determined using gravity inversion with a Ct_{ref} of 37.5 km and a break-up age of 100 Ma corresponding to the age of the Cretaceous West and Central African Rift System (WCARS). The West and Central African rifting does not link northwards through to the Cretaceous rifts of the eastern Mediterranean.

Mediterranean rifting cannot be constrained by the Cretaceous rifting age of WCARS.

CONCLUSION

Gravity inversion using public domain data has been used to successfully map the distribution of oceanic and continental crust in the eastern Mediterranean. The gravity inversion technique is of global applicability and has been used on many deep-water frontier rifted continental margins, in order to understand the large-scale distribution of oceanic and continental lithosphere, the ocean–continent transition zone structure and the location of the continent–ocean boundary.

Crustal thickness and continental lithosphere thinning maps predicted by gravity inversion suggest that the Ionian Sea and Herodotus Basin of the eastern Mediterranean are underlain by oceanic crust or highly thinned continental crust. Highly thinned continental crust, with thicknesses less than 20 km and locally

15 km, is predicted to underlie the offshore Sirte and Levantine basins. Crustal thicknesses predicted by gravity inversion, for the Ionian Sea and the Herodotus Basin, are consistent with independent measurements from seismic refraction. While the predicted Moho depth and crustal basement thickness from gravity inversion are dependent on the continental break-up age used to calculate the lithosphere thermal gravity anomaly correction, it is not possible to distinguish between mid-Cretaceous (100 Ma) and late Triassic (225 Ma) formation ages for the Ionian Sea and the Herodotus Basin using the gravity inversion results.

Maps of continental lithosphere thinning for northern Africa, predicted by gravity inversion, show no linkage of the Cretaceous West and Central African Rift System through northern North Africa to the Sirte Basin and the basins of the eastern Mediterranean. The Cretaceous rifting of the Sirte Basin, and the Ionian Sea if it is Cretaceous, may be regionally related to Cretaceous rifting to the NW associated with rifting and seafloor spreading within the Bay of Biscay.

We thank two anonymous referees for their thoughtful and encouraging reviews and also Tim Bevan, Mark Longacre and Alan Roberts for very useful discussions. LC was funded by the MM3 Consortium.

REFERENCES

Alvey, A., Gaina, C., Kusznir, N.J. & Torsvik, T.H. 2008. Integrated crustal thickness mapping and plate reconstructions for the high Arctic. *Earth and Planetary Science Letters*, **274**(3–4), 310–321.

Binks, R.M. & Fairhead, J.D. 1992. A plate tectonic setting for Mesozoic rifts of West and Central Africa. *Tectonophysics*, **213**(1–2), 141–151. DOI: 10.1016/0040-1951(92)90255-5.

Chappell, A.R. & Kusznir, N.J. 2008. Three-dimensional gravity inversion for Moho depth at rifted continental margins incorporating a lithosphere thermal gravity anomaly correction. *Geophysical Journal International*, **174**(1), 1–13. DOI: 10.1111/j.1365-246X.2008.03803.x.

Contrucci, I., Matias, L., Moulin, M. *et al*. 2004. Deep structure of the West African continental margin (Congo, Zaïre, Angola), between 5°S and 8°S, from reflection/refraction seismics and gravity data. *Geophysical Journal International*, **158**(2), 529–553. DOI: 10.1111/j.1365-246X.2004.02303.x.

Dercourt J., Ricou L. E. & Vrielynck B. (eds) 1993. *Atlas Tethys Palaeoenvironmental Maps*. Gautier-VMars, Paris.

Daly, M.C., Chorowicz, J. & Fairhead, J.D. 1989. Rift basin evolution in Africa: the influence of reactivated steep basement shear zones. *In*: Cooper, M.A. & Williams, G.D. (eds) *Inversion Tectonics*. Geological Society, London, Special Publications, **44**, 309–334. DOI: 10.1144/gsl.sp.1989.044.01.17

de Voogd, B., Truffert, C., Chamot-Rooke, N., Huchon, P., Lallemant, S. & Le Pichon, X. 1992. Two-ship deep seismic soundings in the basins of the Eastern Mediterranean Sea (Pasiphae cruise). *Geophysical Journal International*, **109**(3), 536–552. DOI: 10.1111/j.1365-246X.1992.tb00116.x.

Greenhalgh, E.E. & Kusznir, N.J. 2007. Evidence for thin oceanic crust on the extinct Aegir Ridge, Norwegian Basin, NE Atlantic derived from satellite gravity inversion. *Geophysical Research Letters*, **34**(6), L06305. DOI: 10.1029/2007gl029440.

Guiraud, R., Binks, R.M., Fairhead, J.D. & Wilson, M. 1992. Chronology and geodynamic setting of Cretaceous–Cenozoic rifting in West and Central Africa. *Tectonophysics*, **213**(1–2), 227–234. DOI: 10.1016/0040-1951(92)90260-d.

Gumati, Y.D. & Nairn, A.E.M. 1991. Tectonic Subsidence of the Sirte Basin, Libya. *Journal of Petroleum Geology*, **14**(1), 93–102. DOI: 10.1111/j.1747-5457.1991.tb00301.x.

Hallett, D. 2002. *Petroleum Geology of Libya*. Elsevier, Amsterdam.

Laske, G. & Masters, G. 1997. A Global Digital Map of Sediment Thickness. *EOS Transactions of the AGU*, **78**(F483).

McKenzie, D. 1978. Some remarks on the development of sedimentary basins. *Earth and Planetary Science Letters*, **40**, 25–32.

Moulin, M., Aslanian, D. & Unternehr, P. 2010. A new starting point for the South and Equatorial Atlantic Ocean. *Earth-Science Reviews*, **98**(1–2), 1–37. DOI: 10.1016/j.earscirev.2009.08.001.

Parker, R.L. 1972. The rapid calculation of potential anomalies. *Geophysical Journal of the Royal Astronomical Society*, **31**(4), 447–455. DOI: 10.1111/j.1365-246X.1973.tb06513.x.

Sandwell, D.T. & Smith, W.H.F. 2009. Global marine gravity from retracked Geosat and ERS-1 altimetry: Ridge segmentation versus spreading rate. *Journal of Geophysical Research*, **114**(B1), B01411. DOI: 10.1029/2008jb006008.

Stampfli, G.M., Hochard, C., Wilhem, C. & Raumer, Jv. 2008. *Global Reconstruction and Database Project*. Search and Discovery Article #30055.

Steinberger, B. 2007. Effects of latent heat release at phase boundaries on flow in the Earth's mantle, phase boundary topography and dynamic topography at the Earth's surface. *Physics of the Earth and Planetary Interiors*, **164**(1–2), 2–20. DOI: 10.1016/j.pepi.2007.04.021.

White, R. & McKenzie, D. 1989. Magmatism at rift zones: The generation of volcanic continental margins and flood basalts. *Journal of Geophysical Research*, **94**(B6), 7685–7729. DOI: 10.1029/JB094iB06p07685.

Received 17 October 2011; revised typescript accepted 8 May 2012.

Appendix D - Gravity Inversion Mapping of Crustal Thickness and Lithosphere Thinning for the Eastern Mediterranean

Preface

This appendix consists of a previously published paper, which can be found in *The Leading Edge* July 2012; p936-940

Gravity inversion mapping of crustal thickness and lithosphere thinning for the eastern Mediterranean

LEANNE COWIE and NICK KUSZNIR, University of Liverpool

The distribution of oceanic and continental crust in the eastern Mediterranean region is not well understood but has major implications for tectonic evolution of this region and its petroleum systems. In particular the location of the continent-ocean boundary (COB), the ocean-continent transition (OCT) structure, and crustal thickness within the basin regions is a topic of much debate. While seismology, especially refraction seismology, is an ideal method for locally determining crustal thickness, it is limited to 2D as 3D mapping of crustal thickness is not practical or affordable over large areas. However, a recent development in 3D crustal thickness mapping uses gravity anomaly inversion. We illustrate the application of this technique using the example of the eastern Mediterranean (Figure 1). The new 3D gravity inversion technique, incorporating a lithosphere thermal gravity anomaly correction, is used to map Moho depth, crustal basement thickness, and continental lithosphere thinning. We then use this to determine the distribution of oceanic and continental crust, and ocean-continent transition structure, for the eastern Mediterranean.

Introduction

Knowledge and understanding of ocean-continent transition structure, the distribution and magnitude of thinned continental crust and lithosphere and the distal extent of continental crust are of critical importance in evaluating petroleum systems in deep-water frontier oil and gas exploration at continental margins. The mapping of crustal thickness, ocean-continent transition structure and continent-ocean boundary location at rifted continental margins is therefore a generic global problem. The new 3D gravity inversion technique, which maps Moho depth, crustal basement thickness and continental lithosphere thinning, has been developed in order to assist in determining this critical information.

We use the new 3D gravity inversion technique to explore crustal thickness, ocean-continent transition structure and continent-ocean boundary location for the Levantine, Herodotus, Ionian Sea, and offshore Sirte basins. The results have implications for the distribution of rift and transform continental margins within the eastern Mediterranean. Crustal thickness and continental lithosphere thinning determined from gravity inversion have also been used to explore the relationship between the Cretaceous West and Central African Rift System and the Sirte Basin.

Determining crustal thickness and continental lithosphere thinning from gravity inversion

Moho depth, crustal thickness, and continental lithosphere thinning factors (1- 1/β) have been determined for the eastern Mediterranean using a recently developed 3D gravity inversion technique which incorporates a lithosphere thermal gravity anomaly correction. The gravity anomaly inversion is carried out in the 3D spectral domain and includes a parametization of decompression melting to predict volcanic addition. The methodology is described in Greenhalgh and Kusznir (2007) and Chappell and Kusznir (2008). The lithosphere thermal gravity anomaly correction is required to compensate for the negative gravity anomaly component arising from oceanic and continental margin lithosphere which has an elevated geothermal gradient. Failure to include this correction can lead to predictions of Moho depth and crustal basement thickness at rifted margins which are too large by a substantial amount. This lithosphere thermal anomaly and gravity anomaly correction decays with time but is still significant for rifted continental margins as old as Cretaceous. The data used in the gravity inversion (Figure 2) are public domain free-air gravity (Sandwell and Smith, 2009), bathymetry (Amante and Eakins, 2009), and sediment thickness (Laske and Masters, 1997). The results from the inversion have been tested against Expanding Spread Profile (ESP) seismic estimates of Moho depth (de Voogd et al., 1992) for the Ionian Sea and Herodotus Basins.

The age of formation of the eastern Mediterranean basins, in particular that of the Ionian Sea and Herodotus Basins is uncertain. Some workers (e.g., Dercourt et al., 1993) have proposed that the

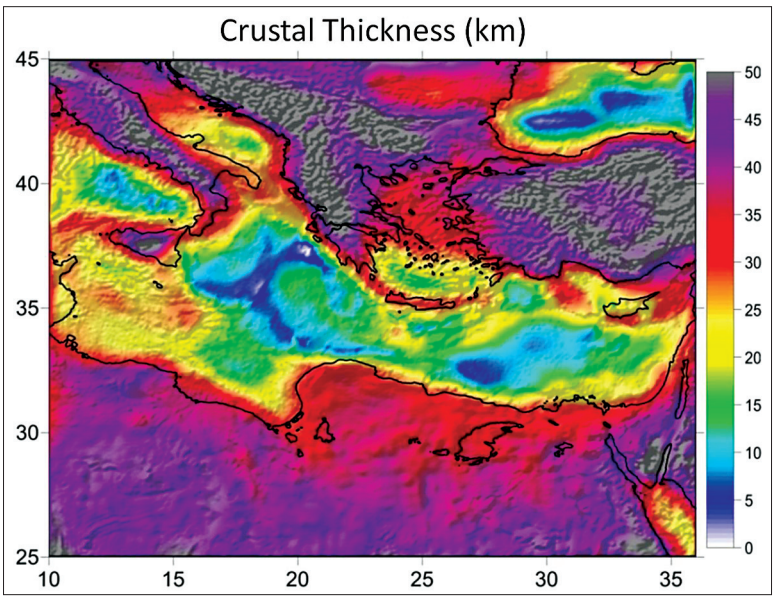

Figure 1. *Crustal basement thickness map of the eastern Mediterranean determined using gravity inversion assuming a mid-Cretaceous (100 Ma) breakup age to condition the lithosphere thermal gravity anomaly correction.*

eastern Mediterranean is Cretaceous in age (Aptian-to-Campanian) and is linked to the closure of the Tethys Ocean. In contrast, it has also been suggested (e.g., Stampfli et al., 2008) that the eastern Mediterranean is late Triassic in age and is linked to the breakup of Pangaea and the closure of the Neo-Tethys and Tethys oceans. We have considered both a late Triassic and an early Cretaceous breakup age within the gravity inversion. The gravity inversion technique requires a reference Moho depth (see detailed methodology papers) which has an average global value of around 37.5 km but varies regionally due to mantle dynamic topography. The reference crustal thickness used in the gravity inversion of the eastern Mediterranean has been calibrated with ESP seismic refraction data (de Voogd et al., 1992). Calibration results (Figure 3) show a trade-off between breakup age and reference crustal thickness (Ct_{ref}); a Cretaceous-age ocean requires a larger reference crustal thickness than a Triassic-age ocean. For a mid-Cretaceous (100 Ma) breakup age, a reference crustal thickness of 47 km produces results most comparable to those seen in the ESP data, whereas for a late Triassic (225 Ma) breakup age, a reference crustal thickness of 45 km is most appropriate. It is suggested that the large reference crustal thickness required for the Ionian Basin is caused by the Hellenic Arc subduction dynamic subsidence and long-wavelength gravity anomaly signal from the subduction process.

Crustal thickness and continental lithosphere thinning in the eastern Mediterranean

An important question is whether the eastern Mediterranean basins are underlain by oceanic or continental crust. Crustal basement thickness predicted by gravity inversion is shown in Figure 1, assuming a Cretaceous age for the Mediterranean basins; the corresponding continental lithosphere thinning factor is shown in Figure 3b. The low crustal thicknesses and high continental lithosphere thinning factors (1- 1/β) under the Ionian and Herodotus basins suggest that they are underlain by oceanic lithosphere or very thin continental crust. Predicted crustal thicknesses for the Ionian and Herodotus basins range from 5 to 8 km, and are consistent with independent measurements from ESP seismic measurements (de Voogd et al., 1992). Highly thinned continental crust, with thicknesses less than 20 km and locally 15 km, is predicted to underlie the offshore Sirte and Levantine basins. Continental lithosphere thinning factors predicted by the gravity inversion for the Ionian and Herodotus basins are in the region 0.8–1.0 (consistent with these basins being oceanic); a thinning factor of 1.0 indicates that no continental lithosphere remains.

The width of the transition region from thick continental crust inboard of the margin hinge to thin outboard oceanic crust may be used to help determinate whether a margin is a transform or rifted continental margin. The sharp increase in crustal thickness to the south of the very thin crust within the Herodotus Basin and eastern Ionian Sea (Figure 4) suggests that the continent-ocean boundary to the north of Egypt and eastern Libya is a transform margin. In contrast, the much broader transition from thick to thin crust in the Levantine

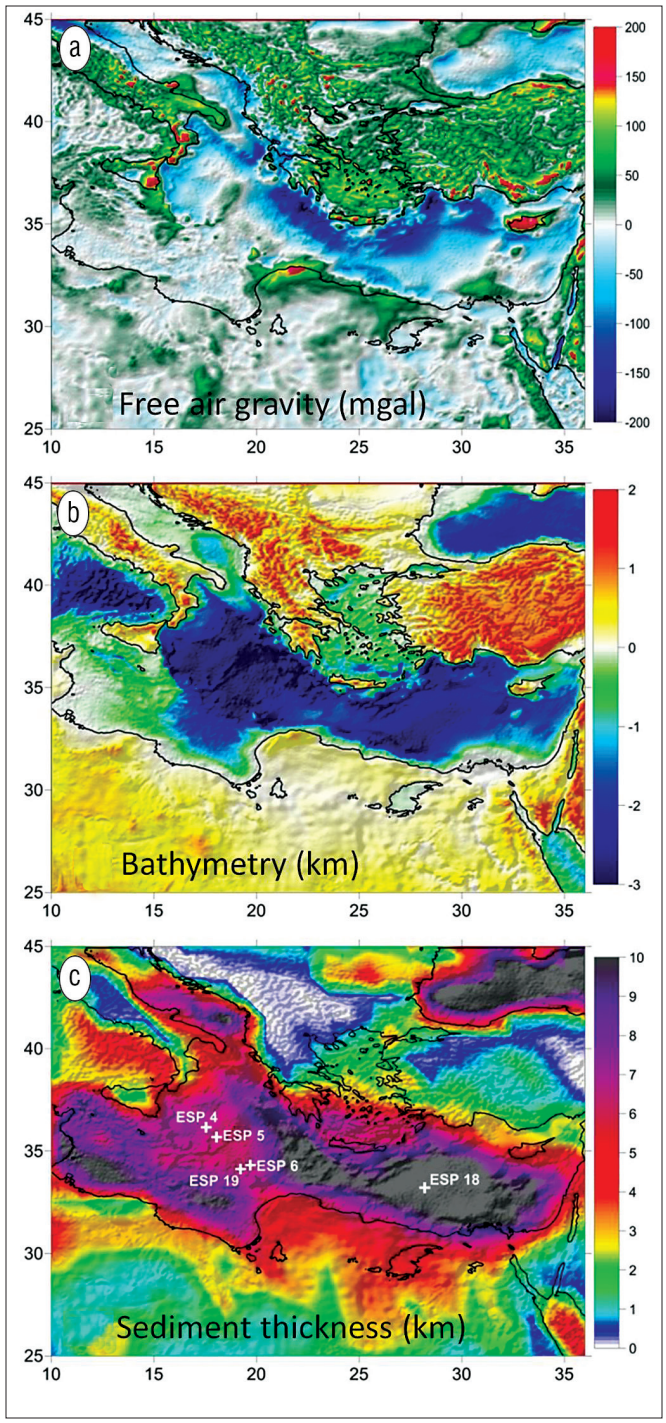

Figure 2. *Raw data used in the gravity inversion for the eastern Mediterranean. (a) Free-air gravity (Sandwell and Smith, 2009). (b) Bathymetry (topography) (Amante and Eakins, 2009). (c) Sediment thickness (Laske and Masters 1997). Locations of the ESP seismic observations (de Voogd et al., 1992) used for calibration are also shown.*

Basin to the east of the Herodotus Basin (Figure 4) most probably indicates that this is a rifted continental margin.

While the predicted Moho depth and crustal basement thickness from gravity inversion are dependent on the continental breakup age used to calculate the lithosphere thermal gravity anomaly correction, it is not possible to distinguish

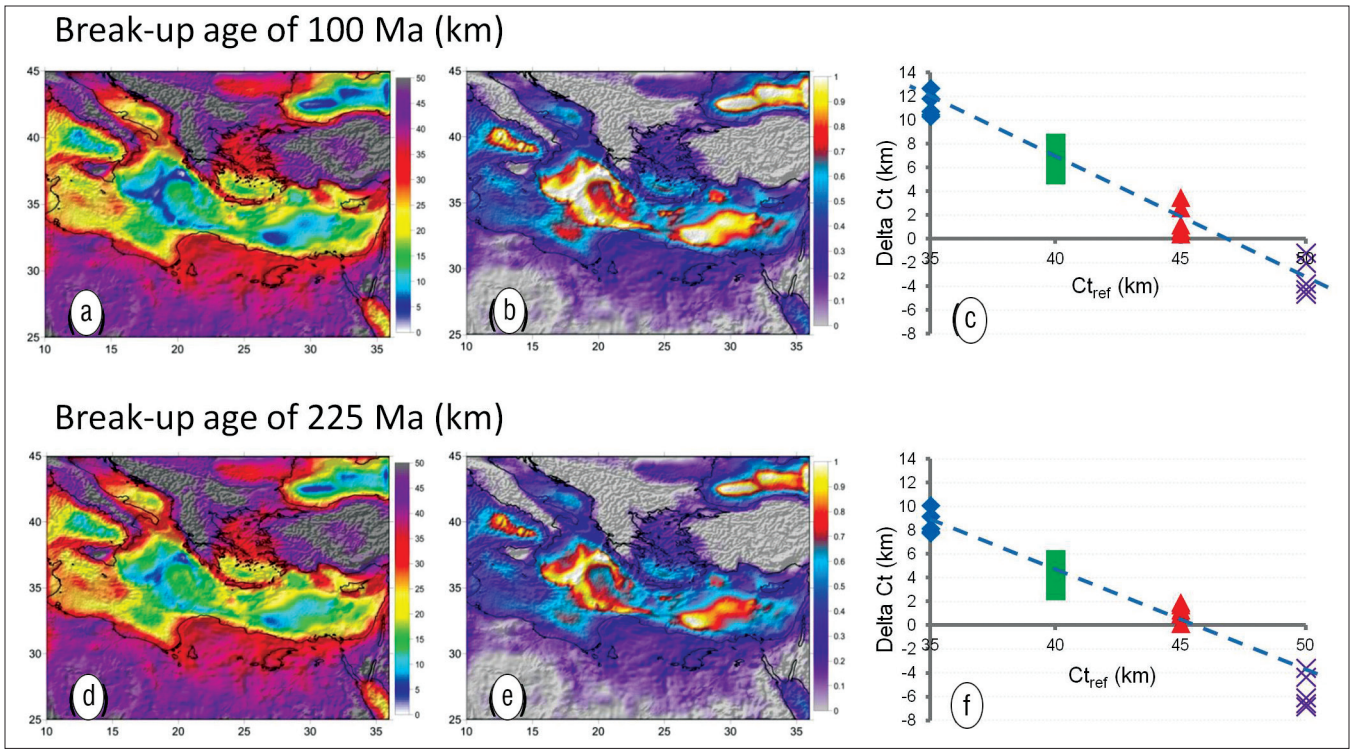

Figure 3. *Crustal thickness (Ct) and continental lithosphere thinning factor (1-1/β) maps, determined from gravity inversion, showing sensitivity to reference crustal thickness (Ct_{ref}), breakup age, and calibration. (a) Crustal thickness map for a breakup age of 100 Ma and a Ct_{ref} of 45 km. (b) Continental lithosphere thinning map for a breakup age of 100 Ma and a Ct_{ref} of 45 km. (c) Calibration of the reference crustal thickness (Ct_{ref}) used in the gravity inversion for a break-up age of 100 Ma. A Ct_{ref} of 47 km is indicated. (d) Crustal thickness map for a breakup age of 225 Ma and a Ct_{ref} of 45 km. (e) Continental lithosphere thinning map for a breakup age of 225 Ma and a Ct_{ref} of 45 km. (f) Calibration of the reference crustal thickness (Ct_{ref}) used in the gravity inversion for a breakup age of 225 Ma. A Ct_{ref} of 45 km is indicated.*

between mid-Cretaceous (100 Ma) and late Triassic (225 Ma) formation ages for the Ionian Sea and the Herodotus Basin using the gravity inversion results.

Offshore Sirte Basin and the Ionian Sea

The crustal thickness under the offshore Sirte Basin, while much thinner than on land, is significantly thicker than that within the Ionian Sea Basin. A cross section through the Ionian Sea, line C-C' in Figure 5, shows a broad region of highly thinned continental crust of 200 km width which lies between the continental margin hinge to the SW near the coast and the interpreted continental-ocean boundary with the Ionian ocean basin to the NE. The broad region of highly thinned continental crust underlying the offshore Sirte Basin is similar to that observed on the northern Angolan margin (Contrucci et al., 2004) and on many other rifted continental margins. The prebreakup sag basins that lie above these broad regions of thinned continental crust at rifted continental margins often contain significant petroleum systems.

Application to heat flow predictions

The prediction of top basement heat flow within the ocean-continent transition at deep-water frontier, rifted continental margins is of great importance for hydrocarbon maturation and other basin modelling predictions. Present-day top basement heat flow is dependent on not only the transient post-breakup heat-flow component but also the contribution from the remaining continental crust radiogenic heat-productivity. Continental lithosphere thinning derived from gravity inversion may be used to predict the preservation of continental crustal radiogenic heat productivity and the transient lithosphere heat-flow contribution for thermally equilibrating oceanic and thinned continental margin lithosphere. The application of this to the eastern Mediterranean is shown in Figure 6, where predicted residual crustal radiogenic heat productivity and lithosphere transient heat-flow components, together with base lithosphere background heat-flow, are used to produce regional maps of present-day top basement heat flow. Lithosphere thinning controls the preservation of continental radiogenic heat productivity and the post-thinning lithosphere transient component. The sensitivity to breakup age is shown. A higher lithosphere thinning gives a lower preservation of continental radiogenic heat productivity and a higher transient component. The resultant top basement heat flow is a "trade-off" between these and depends on post-thinning thermal re-equilibration (cooling) time and initial radiogenic heat-productivity. Heat-flow predictions for the eastern Mediterranean suggest that the thinned basin regions are cooler than the surrounding thinned continental crust for an initial continental radiogenic heat productivity of 30 mWm^{-2}. Note that these heat-flow predictions should not be applied to the tectonically much younger Red Sea region.

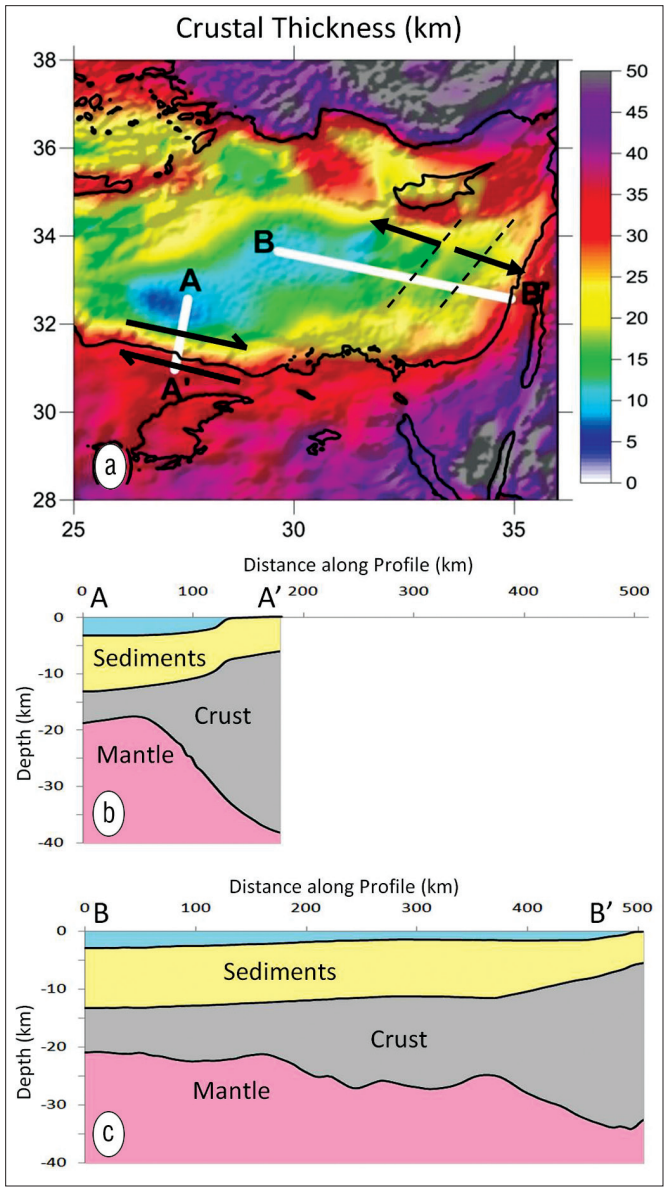

Figure 4. *(a) Predicted crustal thickness map of the eastern Mediterranean determined, using gravity inversion and a late Triassic (225 Ma) breakup age, with interpreted rift and transform margin kinematics. Cross sections A-A' (b) and B-B' (c) show crustal structure through the transform margin and the rift margin, respectively. Dashed lines show NE-SW strike of the Levant margin rifting.*

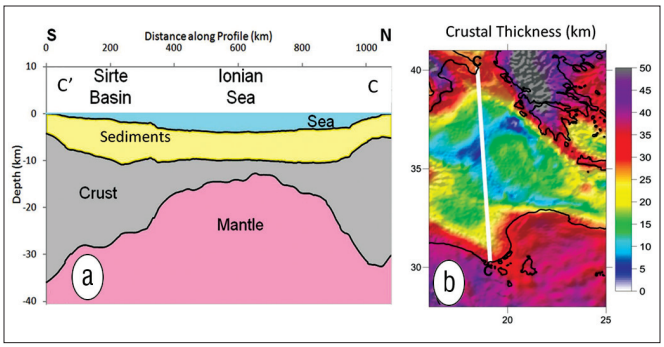

Figure 5. *(a) Crustal cross section along profile C-C' showing bathymetry, sediment thickness, and Moho depth determined from gravity inversion across the Ionian Sea and Sirte Basin. (b) Crustal basement thickness predicted from gravity inversion for the Ionian Sea, Sirte Basin, and Libyan margin.*

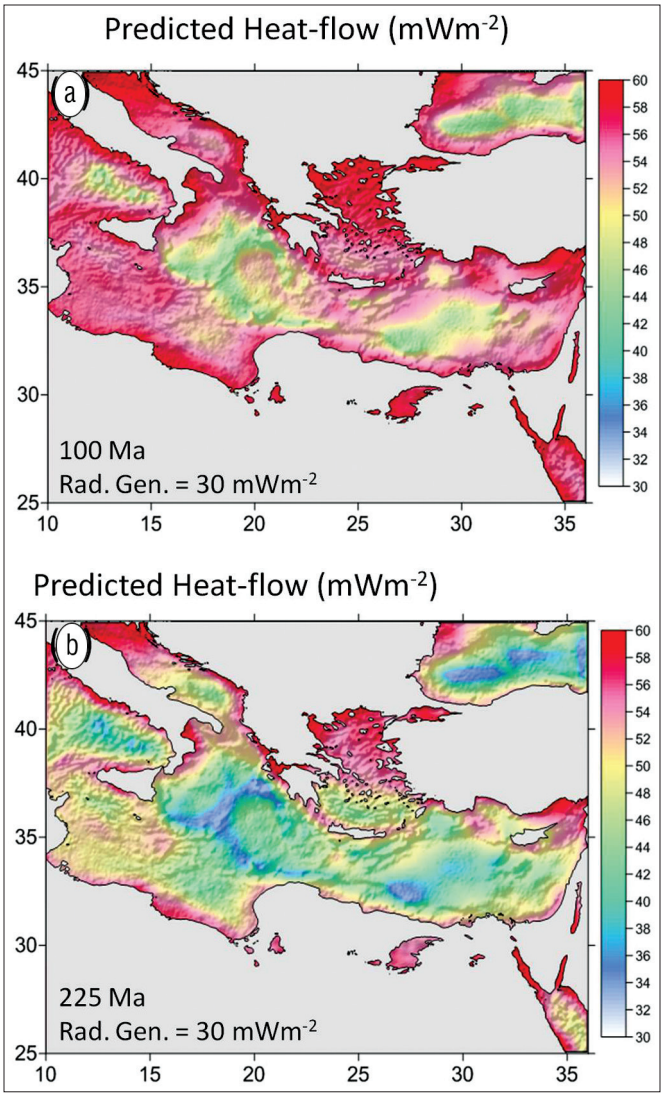

Figure 6. *Present-day top basement heat flow in the eastern Mediterranean predicted from lithosphere thinning factors determined from gravity inversion, (a) using a breakup age of 100 Ma and (b) using a breakup age of 225 Ma.*

Investigating the relationship between the Cretaceous WCARS and the offshore Sirte Basin

Gravity inversion has been used to map crustal thickness and continental lithosphere thinning in order to delineate the geometry of the eastern Mediterranean basins and their possible connectivity to rifting within the Cretaceous West and Central African Rift System (WCARS = Benue Trough, Chad, Central African Shear Zone, commonly known as CASZ, and Sudan basins). Both the onshore and offshore Sirte basins are known to be Cretaceous (Middle Aptian-to-Late Albian) in age (Gumati and Nairn, 1991) and it is often suggested (e.g., Moulin et al., 2010) that these basins are the northern continuation of the Cretaceous WCARS and the South Atlantic opening.

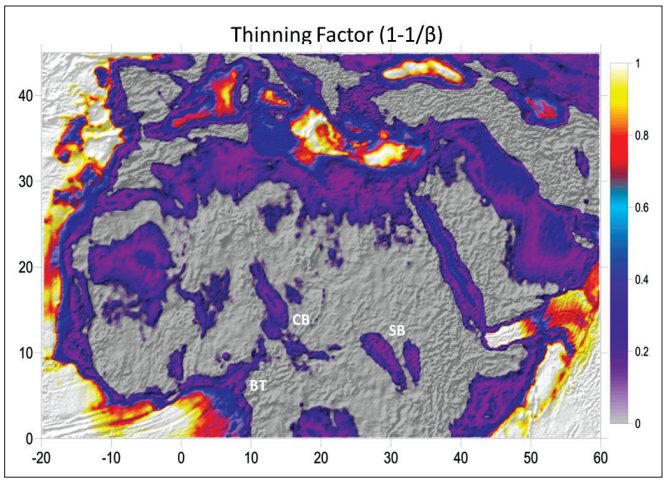

Figure 7. *Continental lithosphere thinning factor map for North Africa determined using gravity inversion and a breakup age of 100 Ma. The West and Central African rift systems show a thinning factor higher than that of the surrounding lithosphere as ds the basin regions and the passive margins to the north. The rift systems of the Benue Trough and Chad do not appear to propagate northward, linking through to the Sirte and Ionian basins of the eastern Mediterranean. BT = Benue Trough. CB = Chad Basin. SB = Sudan Basin.*

The continental lithosphere thinning map for North Africa and the eastern Mediterranean (Figure 7), produced by gravity inversion assuming a 100 Ma rift and breakup age, shows that the Cretaceous West and Central African Rift System does not connect, at least in an obvious way, with the Sirte Basin or other eastern Mediterranean basins. The Cretaceous WCARS propagates as far as 20° north, whereas the southern border of the eastern Mediterranean is at approximately 30° north; there is a lack of continuity of these rift systems which are separated by more than 1000 km. It is therefore concluded that there is no direct linkage between the extensional tectonics of the Cretaceous WCARS and that responsible for the formation of the Cretaceous Sirte Basin.

The continental lithosphere thinning factor predicted from the gravity inversion (Figure 7) shows values of between 0.2 and 0.3 (β = 1.2–1.4) for the onshore Mediterranean border of North Africa. This thinning is of an unknown origin but could correspond to the North African Palaeo-Tethyan continental margin.

Summary

3D gravity inversion, using a new methodology designed specifically for mapping crustal thickness and continental lithosphere thinning at rifted continental margins, has been applied to the eastern Mediterranean in order to determine the distribution of oceanic and continental crust, and ocean-continent transition structure. The new geophysical technique described in this article is of global applicability and has been used on many deep-water frontier, rifted continental margins for the oil and gas industry.

Good quality free-air gravity and bathymetry data are available globally in the public domain for use with this new gravity inversion technique. In this application to the eastern Mediterranean, we use public domain sediment thickness data. The use of industry sediment thickness data with higher resolution and accuracy greatly improves the gravity inversion mapping of margin crustal thickness, ocean-continent transition structure and continent-ocean boundary location. The results using public domain sediment thickness data are still however useful providing valuable regional insights into continental margin structure and breakup kinematics. TLE

References

Amante, C. and B. W. Eakins, 2009, ETOPO1 1 Arc-Minute Global Relief Model: Procedures, Data Sources and Analysis: NOAA Technical Memorandum NESDIS NGDC-24.

Chappell, A. R. and N. J. Kusznir, 2008, Three-dimensional gravity inversion for Moho depth at rifted continental margins incorporating a lithosphere thermal gravity anomaly correction: Geophysical Journal International, **174**, no. 1, 1–13, http://dx.doi.org/10.1111/j.1365-246X.2008.03803.x.

Contrucci, I., L. Matias, M. Moulin, L. Géli, F. Klingelhofer, H. Nouzé, D. Aslanian, J.-L. Olivet, J.-P. Réhault, and J.-C. Sibuet, 2004, Deep structure of the West African continental margin (Congo, Zaïre, Angola), between 5°S and 8°S, from reflection/refraction seismics and gravity data: Geophysical Journal International, **158**, no. 2, 529–553, http://dx.doi.org/10.1111/j.1365-246X.2004.02303.x.

de Voogd, B., C. Truffert, N. Chamot-Rooke, P. Huchon, S. Lallemant, and X. Le Pichon, 1992, Two-ship deep seismic soundings in the basins of the Eastern Mediterranean Sea (Pasiphae cruise): Geophysical Journal International, **109**, no. 3, 536–552, http://dx.doi.org/10.1111/j.1365-246X.1992.tb00116.x.

Dercourt, J., L.-E. Ricou, and B. Vrielynck, 1993, Atlas tethys palaeoenvironmental maps, Paris, France: CCGM.

Greenhalgh, E. E. and N. J. Kusznir, 2007, Evidence for thin oceanic crust on the extinct Aegir Ridge, Norwegian Basin, NE Atlantic derived from satellite gravity inversion: Geophysical Research Letters, **34**, no. 6, L06305, http://dx.doi.org/10.1029/2007GL029440.

Gumati, Y. D., and A. E. M. Nairn, 1991, Tectonic subsidence of the Sirte Basin, Libya: Journal of Petroleum Geology, **14**, no. 1, 93–102, http://dx.doi.org/10.1111/j.1747-5457.1991.tb00301.x.

Laske, G., and G. Masters, 1997, A global digital map of sediment thickness: EOS Transactions, **78**, F483.

Moulin, M., D. Aslanian, and P. Unternehr, 2010, A new starting point for the south and equatorial Atlantic Ocean: Earth-Science Reviews, **98**, no. 1–2, 1–37, http://dx.doi.org/10.1016/j.earscirev.2009.08.001.

Sandwell, D. T., and W. H. F. Smith, 2009, Global marine gravity from retracked Geosat and ERS-1 altimetry: Ridge segmentation versus spreading rate: Journal of Geophysical Research, **114**, no. B1, no. B1, B01411, http://dx.doi.org/10.1029/2008JB006008.

Stampfli, G. M., C. Hochard, C. Wilhem, and J. Raumer,, 2008, Global reconstruction and database Project: Search and Discovery Article 30055.

Acknowledgments: We thank Gabor Tari for his thoughtful and encouraging reviews and also Tim Bevan, Mark Longacre, and Alan Roberts for useful discussions. LC was funded by the MM3 Consortium.

Corresponding author: l.cowie@student.liv.ac.uk